Delineating functional magnetic resonance imaging connectivity states of the old and young during resting-state and sleep

PHILIP DICKINSON

Integrated Program in Neuroscience
McGill University, Montreal
June 2018

A thesis submitted to McGill University in partial fulfillment of the requirements of the degree of Doctor of Philosophy

Abstract

As the population ages, Canada faces a personal, public and financial demand on the health system and society. Heterogeneous health outcomes are notable in older populations. Identifying this diversity is fundamental to understanding age-related health and neuropathology. Magnetic resonance imaging (MRI) is a common non-invasive procedure to study brain aging. Resting-state functional MRI, which places no demands beyond remaining still and awake, effectively measures brain activity in subjects of all ages and capacities. The standard static analysis method identifies functional connectivity differences across cohorts, however, it is ineffective at differentiating within-cohort heterogeneities. We present a data-driven method, with which we identify prototypical *brain states* derived from time-varying functional connectivity, to discriminate sub-populations within cohorts. We analyze a healthy population of young and old subjects for age-related differences, for differential activity during stage 2 non-rapid eye movement sleep (NREM2) and for the impact of differential thought content measured during the resting-state procedure. Finally, in a preliminary, exploratory analysis we used our methods to compare features of sleep and wakefulness across datasets. We demonstrate that our data-driven method derives *brain states* that discriminate between and within cohorts, during both wakefulness and sleep. In both cases, we identify older sub-cohorts that explain almost all the variance, between old and young populations, found in the static analysis. We observed a cross-over interaction effect between thought content scores and age cohort. This may be explained by the middle temporal gyrus acting as a compensatory pathway for past thinking in older subjects. In our final analysis, we found *brain states* most correlated across sleep and wakeful datasets were associated with the younger population. This was expected, since the facility to sleep decreases with age. We also observed less correlation between *brain states* of old and young cohorts during sleep than when awake, highlighting sleep as an

interesting source for age-related research. In sum, our method provides insight into heterogeneities in older populations beyond standard static analysis. This underscores the importance of delineating underlying *brain states* in aging studies. Further, since the method is data-driven, it can be applied to datasets without previous knowledge of pathology. Considering the method can be applied across datasets, it offers a promising tool to identify biomarkers in future studies.

Résumé

À mesure que la population vieillit, le système de santé et la société du Canada font face à des demandes croissantes du public en termes de personnel et de finances. Les populations âgées sont connues pour l'hétérogénéité de leurs états de santé. Caractériser cette diversité de trajectoires de vieillissement est fondamental pour comprendre la santé et les neuropathologies liées à l'âge. L'utilisation de l'imagerie par résonance magnétique (IRM) est une procédure non-invasive typique pour étudier le vieillissement du cerveau. L'IRM fonctionnelle « au repos » mesure efficacement l'activité cérébrale chez des sujets de tous âges et capacités, car elle n'impose aucune exigence au-delà du fait de rester immobile et éveillé. La méthode standard d'analyse statique en IRM fonctionnelle consiste à identifier des différences de connectivité moyenne entre cohortes, mais cette approche est inefficace pour caractériser l'hétérogénéité présente au sein des cohortes. Nous appliquons ici une méthode guidée par les données, avec laquelle nous identifions des *états cérébraux* prototypiques dérivés de la connectivité fonctionnelle variable dans le temps, afin de discriminer des sous-populations au sein des cohortes âgées. Nous analysons une population saine de sujets jeunes et âgés pour les différences liées à l'âge, pour l'activité différentielle pendant le sommeil de mouvement oculaire non-rapide (NREM2) et pour l'impact du contenu des pensées spontanées, mesurées pendant la procédure de repos. Finalement, dans une analyse exploratoire préliminaire, nous avons utilisé nos méthodes pour comparer les caractéristiques du sommeil et de l'éveil. Nous démontrons que notre méthode guidée par les données identifie des *états cérébraux* qui discriminent entre et au sein des cohortes, à la fois pendant l'éveil et le sommeil. Dans les deux cas, nous identifions des sous-cohortes âgées qui expliquent la quasi-totalité de la variance liée à l'âge retrouvée dans l'analyse statique. Nous avons observé un effet d'interaction croisée entre les scores du contenu de la pensée et la cohorte d'âge. Cela peut être expliqué par le gyrus temporal moyen agissant comme une voie de compensation

pour les pensées liées au passé chez les sujets plus âgés. Dans notre dernière analyse, nous avons trouvé que les *états cérébraux* les plus corrélés à travers les bases de données de sommeil et de veille étaient associés à la population plus jeune. Cela était prévu, puisque la facilité à s'endormir diminue avec l'âge. Nous avons également observé moins de corrélation entre les *états cérébraux* des cohortes jeunes et âgées pendant le sommeil que lorsque les participants étaient éveillés, soulignant que le sommeil était une source intéressante pour la recherche liée à l'âge. En somme, notre méthode fournit un aperçu de l'hétérogénéité du vieillissement du cerveau dans les populations âgées, au-delà de ce qui peut être observé au moyen d'une 'analyse standard. Ces résultats soulignent l'importance de délimiter les *états cérébraux* sous-jacents dans les études sur le vieillissement. De plus, puisque la méthode est guidée par les données, elle peut être appliquée à des bases de données sans connaissance préalable de la pathologie, et offre donc un outil prometteur pour identifier les biomarqueurs dans les études futures.

Table of Contents

List of Figures

List of Tables

Acknowledgements

Thank you to Pierre Bellec for contributing to all facets of my doctoral development; for being a real person with passion, honesty and integrity; for patiently giving me space and time to explore, and joyously welcoming my return; for believing in me, even when in doubt; for helping me truly learn, develop and discover, and supporting me throughout. I am deeply grateful.

To Sylvain Baillet, for taking me on as a student and allowing me to get through this all; for being patient, supportive, and positive; for providing insightful feedback and a solid foundation for the work that followed. I truly thank you.

To Josephine Nalbantoglu thank you for accepting me to the Neuroscience and inaugural Rotation Program; for always believing in me; for being there for the students first; for providing leadership, by showing how things can and should be done; for providing feedback and mentorship even when you had no time and likely didn't want to; for allowing me to flourish and enjoy my experience; for giving me confidence that graduate life would be fair knowing I had your support; for being you.

Thank you to the members of the SIMEXP lab: Pierre Orban, Christian Dansereau, Yassine Benhajali, Angela Tam, Sebastian Urchs, AmanPreet Badhwar and Pierre-Olivier Quirion for providing feedback and enjoyment at all times. A special thank you to Julie Carrier for allowing me access to her incredible sleep dataset, along with feedback I have received from her and her former students Nicolas Martin and Veronique Daneault. Thank you as well to Bratislav Misic for your valuable reflections and input as member of my committee. Thank you also to Beth Bock for coordinating computer access, office

space and everything else to allow me to work effectively. Thank you to Francine Bélanger for maintaining RBIQ and helping me where possible.

I would also like to acknowledge the CIHR Vanier Graduate Scholarship Program for their financial support. In addition, for the opportunity this provided me to receive the Michael Smith Travel Award and pursue research at the NIH, where my exploration of dynamic connectivity began in earnest. In as much I would like to thank Peter Bandettini, Javier Gonzalez-Castillo, Daniel Handwerker and Catie Chang for much guidance and feedback in those early investigations.

Most importantly, I want to thank my family; Therese for allowing me the time and space to advance in what seemed like an endless endeavour; all while providing widespread feedback and assistance; keeping our two young, beautiful children happy and amazed; Maurice for challenging me in every way and providing me with endless joy; and Emmanuelle for being the sweetest little thing, learning to walk and talk as I struggled to simply write sentences. Thank you my precious loves.

"Papa, when are you going to finish your effing PhD?"

"When you do finish your PhD; give it to me and I'll fix it for you."

Maurice, 3-years old

Contribution to original knowledge

In this work I present a novel data-driven, dynamic method to analyze resting-state fMRI data. The majority of fMRI resting-state studies are analyzed using static functional connectivity. The static approach is of limited value in populations that are heterogeneous in nature. Of the studies that utilize a dynamic windowing approach, a k-means method is almost exclusively chosen for clustering, with network-based discriminating features. By contrast the method I present is based on a hierarchical clustering method (Ward's criterion) and is spatially discriminated using voxel-based connectivity values. Unlike k-means, hierarchical clustering is unconstrained by the spatial size of the clusters and provides deterministic results. Further, the voxel-based analysis permits a more precise and interpretable result.

In Study#1, I present the analysis method as a proof of concept, and confirm age-related functional connectivity differences described in the resting-state literature [1, 2]. Beyond this, however, I identify a *brain state*, derived from the medial prefrontal cortex seed region that discriminates *successful* from *normal* aging. As a result, almost all the variance between the age groups are explained by only half the older sample. The remaining half show no significant effects of aging, as compared to the young. Although heterogeneity is expected, this result has not been demonstrated from a data-driven approach. This also highlights the importance of accounting for heterogeneity in the design and interpretation of age-related research.

In Study#2, I identify a significant age-related reduction in fMRI functional connectivity, between the thalamus-caudate seed region and parts of the cerebellum, during NREM2 sleep. Age-related fMRI functional connectivity differences during sleep have not been

described previously. As in the previous study, I delineate a *brain state* associated to a sub-cohort of older subjects that explain the age-related variance.

In Study#3, I explore age-related differences in the thought content during the resting-state procedure. Here, I describe a cross-over interaction effect, between the thought content scores and age cohort, on functional connectivity. Further, the related *brain states*, derived from the middle temporal gyrus seed region, associate differentially by age and thought content scores. The younger subjects retain greater default-mode connectivity, while older subjects do not. These unique results suggest the middle temporal gyrus may act as a compensatory pathway for older subjects when thinking of the past.

In Study#4, in a preliminary exploratory analysis, I identify a correspondence between *brain states* primarily associated with young subjects and their correlation across resting-state and sleep datasets. These initial observations may form a diagnostic basis to correlate prototypical *brain states* to individuals and cohorts across disparate datasets.

As a whole, I also delineated sub-significant connectivity profiles that nonetheless showed significant association by age. Thus, the method may be more sensitive to population differences than standard methods. In addition to differentiating cohort level heterogeneity and potential outliers in the data, this is key to early biomarker identification. Overall the results also highlight the importance of measuring thought content, and assessing and controlling for sleep, during age-related resting-state procedures.

Contribution of Authors

In all studies I wrote the code for the dynamic analysis (supplemental to existing NIAK procedures [3]), performed all data analysis, statistics, visualization, interpretation of the results and writing of the text. I received important and invaluable assistance, as follows:

- Pierre Bellec: method design; analysis design; general guidance; edits and feedback on the methods, results and writing; access to NKI-e dataset; enabling access to the Sleep dataset.
- Sylvain Baillet: analysis design; general guidance; edits and feedback on the methods, results and writing
- Julie Carrier (Lab): permitting access to the Sleep dataset; data collection; EEG preprocessing, sleep staging, processing slow-wave sleep densities
- Nicolas Martin: data collection (sleep dataset); feedback on the structure and challenges of the dataset
- Véronique Daneault: feedback on the sleep dataset and slow-wave sleep results
- Pierre Orban: fMRI preprocessing (sleep dataset)
- Michael Milham (Child Mind Institute): data collection and providing open-access to the enhanced Nathan Kline Institute – Rockland Sample dataset
- AmanPreet Badhwar: preprocessing and quality control (NKI-e dataset)

Chapter 1

1 Introduction

1.1. Literature Review

1.1.1. Background

With an aging population there is increased interest in understanding the basis for maintaining health throughout the lifespan. This demographic change has resulted in ever increasing precedence of neurodegenerative related disorders [4]. The personal, social and financial burden is a major concern for society. Even without a pathological association, healthy aging can lead to manifestations of cognitive decline, affecting individuals at different rates and severities [5].

Differentiating healthy aging from neurodegeneration, and by extension those at risk for severe forms of pathology is of heightened interest. Consequently, a better understanding of the neural basis for healthy aging may highlight pathways to explore neurodegenerative illness. A current focus in aging research has been on patient populations that already demonstrate some cognitive impairment. The goal is to identify features that predict which subjects will transition to more serious illness [6, 7], with the intent to identify key bio-markers for the illness. In doing so, heterogeneity in the healthy older population may be overlooked. Thus, a challenge that faces researchers exploring the heterogeneous nature of aging are the diverse health outcomes, ubiquitous even in healthy older populations [8]. Delineating the heterogeneity in healthy populations may

provide insight into early disease development that may otherwise be missed [9]. Thus, understanding the diversity in healthy aging is fundamental to better understand diverse manifestations in pathological aging and neurodegeneration [10].

A common challenge facing research involving older populations is the ability of subjects to comprehend and properly complete the research tasks. In recent years, a frequently applied procedure that limits this potential confound is the resting-state protocol. The resting-state procedure employs magnetic resonance imaging (MRI), a routine approach to studying healthy aging throughout the lifespan, to assess functional variations in brain activity over time (fMRI). Unlike most fMRI procedures (or even psychometric batteries), resting-state protocols are not task-based. Subjects are simply asked to remain still and awake in the MRI scanner and allow their minds to wander for a duration of generally 5 to 20 minutes. Due to the simplicity of the approach and the absence of specific cognitive demands placed on the subject, this is well-suited for older subjects. In particular, for subjects that may be suffering from known or unknown cognitive deficits a more complex task-based approach would be untenable.

To measure the functional (fMRI) activity in the brain over time, changes in the magnetic properties of hemoglobin in the blood (when oxygenated or deoxygenated) that result in signal variations are detected by the MRI scanner [11]. This is referred to as the blood oxygenation level contrast (BOLD) signal. The technique is non-invasive and allows researchers to acquire functional images of the brain with high spatial resolution. It is important to note that this is an indirect measure of neural activity. Generally, an interpretation of fMRI presumes that neural activity leads to energy demands, resulting in an increased cerebral blood flow (hemodynamic response) to that brain region [12]. Although the specific relationship between neural activity and BOLD measures has not been fully elucidated, fMRI is an extremely important tool to investigate brain regions involved in cognition and other activities [13].

Studies that incorporate resting-state driven paradigms make it possible to assess the inter-regional correlations of brain activity across brain regions [14]. The idea that spontaneous fluctuations at rest provided insight into underlying relationships between brain regions was first demonstrated by Biswal et al. [15]. They found that during rest, BOLD measures from one region of the motor cortex correlated with the BOLD activity in other motor regions [15]. The method is also well-suited suited for studying heterogeneities that impact distributed brain regions [16]. This eventually led to the identification of numerous brain networks that often fluctuate in synchrony while an individual is at rest [17]. A good test-retest reliability has likewise been demonstrated [18].

Traditionally when analysing resting-state data, the correlation coefficient across the time series of distinct regions is calculated to provide a measure referred to as functional connectivity. Brain regions that demonstrate stronger correlations with one another and fluctuate in a coherent fashion can be referred to as networks. A characteristic network found during resting-state procedures is the default-mode network (DMN). It is most active during periods of rest, consisting of non-task driven activity and thought. The DMN comprises regions including the posterior cingulate cortex (PCC), the medial prefrontal cortex (mPFC), the precuneus, the angular gyrus (lateral parietal cortex – inferior parietal lobule) and lateral portions of the temporal lobe [19]. The hippocampal complex is also often considered a part of the network [20]. The DMN has been implicated in measures of healthy aging, autobiographical memory, imagining the future, self-referential thinking, sleep, as well as neurodegeneration [21]. As such, the exploration of resting-state with this network and how it varies with age, has become a fundamental aspect of aging research. Using these analytic methods to explore heterogeneity in populations, as well as at the individual level, are directions within the field both now and in the future [22].

1.1.2. Functional neuroimaging research in aging

In early functional neuroimaging studies on aging Damoiseaux et al. found a reduction in connectivity between ten different brain networks, with significant changes observed in the DMN [23]. This was supported by findings from Andrews-Hanna et al. (2007) in which they found a reduction in connectivity between the posterior and anterior regions of the brain in older cohorts of subjects [1]. The regions in which they observed the reduced connectivity, the PCC and the mPFC, comprise integral portions of the DMN. In fact, some of the earliest observed tissue deterioration and pathogenesis associated with cognitive decline and memory deficits occurs in these DMN brain regions, where one finds the highest levels of activity during rest [24].

Although much of the research on aging using resting-state procedures has focused on the DMN, other networks have also been implicated in age-related changes. The dorsal attention network (DAN), most active during goal directed tasks, is anti-correlated with the DMN [25]. A deterioration of long-range connectivity within the DAN has also been observed as a result of aging processes [26]. In contrast, within the visual and somatosensory networks researchers have found no significant deterioration [27]. In our own previous research, we have found that significant changes occur throughout the brain in aging, which are likewise not limited to the DMN [28]. Similar results in aging studies have been found using network modeling [29], topology [30], and co-activation models [2].

Age has been identified as a significant factor that effects the variability of functional connectivity measures during resting-state [31]. Correspondingly, resting-state has been a successful tool for comparing old and young cohorts to identify age-related functional changes [32]. To elucidate group differences, studies to date have largely relied on an assumption of underlying homogeneity within each given cohort [33]. This, however, is not representative of the heterogeneity found in an aging population, even when healthy

[5]. As it stands, when there is heterogeneity among subgroupings of subjects within a cohort, the differences may not be effectively characterized with the standard connectivity analysis.

To capture this heterogeneity, other analytic methods are required [32]. For example, data-driven methods that cluster subjects within a cohort or across the dataset, independent of group labeling, are better suited to address challenges in characterizing heterogeneity within healthy or neurodegenerative older populations [6]. This is becoming the focus of current studies that examine neurodegeneration [6, 7]. There is, however, very little research combining the heterogeneity of healthy aging, with resting-state functional connectivity measures.

1.1.3. Sleep

A well-known, but little studied consideration in resting-state fMRI is the possibility of people sleeping in the scanner and how that might affect the analysis and results. This may be of particular concern in aging studies with differences in sleep quality of old and young subjects. For example older subjects, as compared to younger subjects, tend to sleep less, and less deeply, have less physiologic activity (such as sleep spindles and k-complexes), less slow-wave sleep and an overall lower quality of sleep [34-36]. If subjects sleep in the scanner, these differential sleep qualities could impact the results [37]. Heterogeneous sleep qualities within the older population may likewise play a factor. Notably, in a study from Horowitz et al. a loss of connectivity between the anterior and posterior regions of the brain were observed during sleep [38]. These are important DMN regions which have shown similar reduced connectivity in previous resting-state aging studies. Such overlapping results underline the importance of considering sleep in any resting-state study, particularly when subjects and cohorts comprise different sleep profiles.

In research that has addressed subject vigilance during resting-state scans, sleep appears to be ubiquitous [39]. Using a machine learning classifier able to predict sleep stages in the scanner with over 80% accuracy [40], Tagliazucchi et al. estimated, based on over 1000 resting-state scans, that 30% of subjects fall asleep within 3 minutes of beginning the scan [39]. Further, they also found that subjects were not reliable in their subjective assessment of whether they slept in the scanner, compared to results validated through electroencephalography (EEG) sleep staging. The type of resting-state protocol did influence vigilance, with only 10% of subjects falling asleep when the instructions included a request to keep the eyes open while focusing on a fixation cross [39].

To reliably measure sleep in the scanner, however, there needs to be a combined EEG/fMRI protocol. The combined EEG/fMRI procedure can be time-consuming and present other technical and analytic challenges that make it less common. Recently, Wang et al explored test-retest reliability of resting-state data, while taking sleep into consideration [41]. Rather than an EEG/fMRI protocol, the researchers relied on heart rate variability to assess periods in which subjects were more alert, or when they were less alert and correspondingly sleepy or potentially sleeping. This transition between wakefulness and sleep is a period that has been characterized by changes in brain activity and network connectivity [42]. Following removal of these periods, identified as less vigilant phases that may involve sleep, they found that the reliability and reproducibility of the results was significantly improved [41].

The impact sleep may have on resting-state analysis is an open question. The impact is likely amplified when cohorts show fundamentally different sleep patterns, or likewise heterogeneity within a given cohort. Notably, in all of the sleep studies discussed above, the subjects were comprised of young adults. The impact of sleep during resting-state in older adults has not been examined, for classification, frequency, nor reliability of the results. Since the qualities of sleep are different between older and younger individuals,

there remain many questions regarding the differential impact of sleep during resting-state in aging studies. An important consideration to address these issues is the dynamic aspect of sleep and the variability this presents during a resting-state scan. Subjects can sleep at variable times within a scan, with variable lengths, depths and characteristics. Accordingly, the analysis method must allow for such variations over time.

1.1.4. Thought content

Functional connectivity measures from resting-state procedures are well established and robust [18]; yet interpreting and assessing the results while considering the unconstrained spontaneous nature of the thoughts that drive the outcome is unclear [43, 44]. In particular, when performing a contrast between groups that have heterogeneous mental states or thought content, an analysis may be impacted by these differences [43]. Interpretation of the results is potentially further complicated by the dynamic nature of resting-state measures and the resultant heterogeneity of thought even at the individual level [43].

Older adults tend to retrieve less episodic detail when thinking about memories from the past [45]. Those that display a deficit that corresponds to a lack of detail from the past thoughts show a diminished ability to imagine the future [46]. In task-based neuroimaging studies, older subjects show less activation in the medial temporal lobe and precuneus, when mentally elaborating on past thoughts, and similarly differential activation in the medial and temporal regions, including the superior temporal gyrus [47]. Studies that report the content of spontaneous thought have found younger subjects focus predominantly on future thought [48, 49]. From this perspective, when we consider the resting-state procedure as a method to identify age-related differences, the quality and content of the underlying thoughts may differ strongly between young and old cohorts.

There is an overlap that has been identified between past and future thought content [50]. Much of the research has found self-referential thought largely intersects regions of the DMN network. As Buckner et al. (2007) outlined these regions are associated with autobiographical memory, imagining the future, theory of mind, and moral decision-making [21]. Follow up studies found that the DMN could be broken down into more specific subsystems that would activate differentially based on the type of self-referential thinking [51]. In particular, they found that one subset of the DMN was more active for self-relevant thoughts, while another set of regions was more prevalent during imagery with memory. These regions were seen to combine in activity when participants were involved in future thinking and imagining [51].

To address these issues and explore the inner experience of subjects in the scanner during resting-state, distinct approaches to measure thought content have been proposed. These methods include sampling throughout the scan [49, 52] and post-scan questionnaires [53-55].

Using descriptive experience sampling during the scan, Kuhn et al. observed brain activation complementary to the described inner events of individual subjects [56]. Since the sampling occurred throughout the scan a method of analysis that allows for time-varying connectivity measures is necessary. Unlike static connectivity, such dynamic methods of connectivity analysis can successfully track thought content during resting-state [57]. Sampling inner thoughts during the scan, however, may raise a conscious awareness of the experience, potentially reducing activation levels as compared to being left undisturbed and unaware of the mind-wandering [58]. Sampling methods during the scan can be biased by the questions asked, which tend to be more limited and less rich than is possible when less constrained by time and physical space [59]. Accordingly, although sampling thoughts and experience during the scanning session may increase

precision, it may also inevitably distort the experience of uninterrupted rest and free flowing thought, the core premise of the resting-state procedure.

The benefit of a retrospective post-scan questionnaire is that it allows the spontaneous thought to continue uninterrupted. The inclusion in a resting-state protocol also benefits from the simplicity of use. By contrast, with post-scan questionnaires there are questions of the reliability of subjects' recollection after sufficient time-delay [44]. There are likewise potential biases towards positivity that may arise [60]. In contrast to sampling methods, there would also be a loss of temporal precision [59]. The dynamic character of the resting-state may still be better characterized in relation to the thought content, than a static measure, however, it would no longer be possible to relate specific periods of thought to specific time periods during the scan.

Despite the limitations, studies incorporating different post-scan questionnaires have reported associations between aspects of the thought content and measures of brain activity [53, 61]. In a study from Andrews-Hanna, by varying peripheral stimuli with periods of spontaneous thought, a relationship between the DMN and the spontaneous fluctuations was confirmed [62]. Results from a post-scan questionnaire could explain a significant portion of the variance of connectivity between the medial temporal lobe and other brain regions [62]. Recently, a study that incorporated post-scan questionnaires, explored thought content during the resting-state scan in relation to aging [63]. In this study from Mevel et al., they found the expected functional connectivity changes in the DMN as a result of age, however, they did not find a relationship between these changes and the inner experience of the subjects in the scanner [63]. A notable limitation of this study was the fact the connectivity values were based on an assumption of stationarity, and the dynamic variability was not explored.

Ultimately, the impact variations in thought content may have on resting-state measures remains unclear. Despite the strengths and limitations of methods to measure mentation during and after resting-state procedures, the inclusion of some type of thought content analysis during resting-state procedures is very relevant. The differential thought content between old and young, along with heterogeneity in the old population are factors that may impact the results [37, 64]. Thus, particularly when employing resting-state procedures that include older populations, both clinical and healthy, measuring and potentially controlling for variations in thought content may be pivotal for a better interpretation of some of the variance [59].

1.1.5. Dynamic Connectivity

There are limitations and challenges that we currently face in resting-state studies. At present the vast majority of analysis of resting-state data assumes stationarity. As a result, a number of variables may be lost in the analysis. Of importance when differentiating healthy and pathological aging, the heterogeneity of older populations may be poorly characterized, or lost, when analytic methods assume stationarity.

The assumption of stationarity was first questioned in the literature, in a paper from Chang et al. in 2010 [65]. In it, by breaking the calculations of connectivity into 2 to 4 minute segments, they found notable variation in the connectivity measures over the entire time series [65]. A paper from Allen et al. in 2014 raised general awareness of the issues and detailed a sliding-window method, similar to Chang et al., that is most commonly used in current dynamic connectivity studies [66]. In their paper, Allen et al. measured connectivity across a given window of time, sliding the measurement a specified number of volumes and repeating, across the entire time-series. The connectivity matrices were then clustering using a k-means clustering algorithm, from which they identified 7 distinct clusters, representative of *brain states*. This allowed the authors to better characterize the data and infer various states and stages of activity

throughout the resting-state procedure. Although these results were notable, original, and garnered much interest in the neuroimaging field, they lacked clarity as to what the variations and *brain states* actually meant. Lacking independent measures, such as electrophysiological or psychometric data, or other tests to associate the findings, the validity of the interpretations were unclear [67].

This led to a number of published articles questioning whether the measured dynamics arose as much from noise as it might from signal [68]. In 2012, using simulation methods, Handwerker et al. found that noise could evoke the dynamics attributed to signal [68]. Similarly, Leonardi et al. showed through simulated data that if the window length chosen was too short the data would be susceptible to spurious autocorrelations [69]. Although these studies were based on simulated data, the results reinforced the need to interpret time-varying connectivity results with caution and to develop statistical methods to support the interpretations [67].

Bolstering dynamic connectivity as a viable analytic procedure, other studies using experimental data, have highlighted supporting evidence. For example, in 2015, Gonzalez-Castillo et al, used various sliding window parameters and clustering techniques to identify the mental tasks of subjects from fMRI data [70]. The subjects were given 4 mental tasks throughout the scan, including a standard resting-state, a memorization task, a math task and watching a video. Data-driven techniques used to identify the task in the given window included clustering via k-means or hierarchical clustering methods, different sizing of the windows, and varying the number of regions of interest (ROIs) used in the analysis. Overall, the results showed at least 70% accuracy, but when the number of ROIs were increased along with the size of the window, this increased to ~95% accuracy. Although differences in accuracy were seen between k-means and hierarchical clustering, when the pre-processed high-pass filter (HPF) value

was adjusted to keep the window length greater than the value's reciprocal (i.e.: 1/HPF), as proposed by Leonardi et al. [69] and described above, those differences disappeared.

A relationship between dynamic functional connectivity from fMRI, and EEG measures of electrical brain activity has also been demonstrated. In a 2013 study, Chang et al. observed an association between the alpha power band and functional connectivity measures between and within the DMN and the dorsal attention network [71]. Likewise, Tagliazucchi et al. demonstrated a correlation between EEG power bands and dynamically derived functional connectivity measures between numerous brain regions [72].

Exploring illness classification using a data-driven dynamic connectivity method, Damaraju et al., found that the resulting clusters associated significantly to either the healthy controls or schizophrenia patients [73]. Using a sliding window analysis and k-means clustering procedure, subjects in a given cohort would spend significantly more or less time in the corresponding cluster [73]. Further, when comparing the dynamic with static connectivity analysis, they uncovered differences in connectivity they would not have been able to identify in the static analysis alone.

In 2014, Kucyi et al. found a correlation between self-reported mind-wandering and functional connectivity, when it was measured dynamically [57]. They did not observe this relationship when using a static functional connectivity analysis. As described earlier, Taglizucchi et al. used a dynamic sliding window procedure as the basis for their support vector machine classifier [40]. The fact they could successfully identify not only sleep or wakefulness, but specific sleep stages as well, further supports the application of dynamic analysis on fMRI data. None of this would be possible through standard stationary methods. In our own previous research, we found an association between sleep stages and *brain states* [74]. Sleeping subjects were analysed, and we clustered the

brain data into 24 different *brain states* using a whole brain connectome and a k-means clustering algorithm. We similarly found that *brain states* specifically associated with a given sleep stage, which we observed from wakefulness through to NREM3 sleep.

In a very recent aging study, the authors looked at the development of the brain during childhood up to early adulthood [75]. Using dynamic methods on resting-state data that incorporated a sliding winding and k-means clustering procedure, they were able to characterize age through *brain states* most associated with subjects in a given developmental period [75]. In another study that likewise examined the brain from childhood to adulthood, the mean dwell time and connectivity strength within given *brain states* varied with age [76]. There is only one study that we are familiar with that has applied dynamic techniques on resting-state data for the study of healthy aging in an older population [32]. In this study, Eavani et al. employed a classifier utilizing both supervised and unsupervised learning to successfully isolate two subgroups with different connectivity patterns in the older cohort [32]. The older cohort consisted only of subjects over 85 years of age, while the younger cohort consisted of subjects less than 60 years of age.

Analysis of resting-state data with dynamic connectivity methods is still at a nascent stage. Initial observations, however, demonstrate that it is a method with considerable potential to illuminate the impact of time-varying factors, such as sleep and thought content, on the analysis, while characterizing heterogeneous differences between and within populations.

1.1.6. Summary

The overall goal of my research is to better determine age-related heterogeneity in resting-state fMRI data, both by comparing healthy young to old cohorts, as well as

within the older cohort itself. To capture the heterogeneity, we will be utilizing dynamic connectivity techniques that cluster the results across the entire dataset.

There is one study that has touched on these questions [32]. Aside from methodological differences in the analysis, compared to this study, we will be examining different age groupings [32]. In that study, the older cohort incorporated was very old (>85 years), whereas all our older subjects will be less than 85 years. This is an important distinction since the rate of cognitive decline already increases markedly in individuals over 70 years [77]. We hope to identify group differences at a much earlier time frame that will have more relevance when trying to transfer knowledge from our findings in healthy older adults to clinical populations with pathological aging.

Other factors influencing the analysis of resting-state results arise due to the unconstrained nature of the procedure. This includes the thought content and the potential for sleep in the scanner. These are pertinent factors for any resting-state study, but even more so when the cohorts under investigation display differential sleep and thought patterns. This is the case in studies of aging. As before, these factors display an impact that is variable over time. Thus, in order to better determine age-related heterogeneity in resting-state fMRI data, we need to apply dynamic analysis methods that account for variable thought content and vigilance throughout the entire acquisition. We are unaware of any study that combines the examination of thought content during resting-state through dynamic connectivity methods, while considering age-related differences. Likewise, we are unaware of any fMRI study that compares differential functional connectivity in old and young adults during sleep, and in particular, utilizing dynamic connectivity methods.

To explore these questions and identify heterogeneity in the populations, we present a data-driven method to identify representative *brain states*, simplify the analysis and allow for inter-dataset comparison.

Numerous methods have been proposed to examine dynamic connectivity, however, there is a paucity of results on non-simulated data to effectively evaluate their validity and appropriateness for our objectives [78]. Although some other methods are more sophisticated, the sliding window technique is the most common approach to derive connectivity maps [78]. It has been effective in delineating *brain states* and clinical from healthy populations [70, 73]. Our analysis will involve the use of a sliding window connectivity analysis method that is complementary in many ways to that described by Allen et al. [66].

We will, however, employ a hierarchical clustering method over the k-means clustering method used by Allen et al. [66] and the vast majority of other dynamic connectivity studies. This is a key modification, since in contrast to k-means clustering, the hierarchical clustering method allows for spatially variable cluster sizes, variable cluster scales (the number of clusters does not need to be defined *a priori*) and provides a deterministic result. Imposing spatially equal-sized spherical clusters, as with k-means, causes the method to break down with different cluster densities [79]. There is no such assumption with hierarchical clustering and it makes little sense to impose this limitation on the data. Of the studies that have used hierarchical clustering, one focused on hidden Markov models [80], one on a task-based analysis [70], and the other on graph theory [81]. No studies have explored hierarchical clustering in relation to fMRI functional connectivity values in resting-state of healthy individuals.

We will also pursue a voxel-wise seed-based analysis, rather than the more common network analyses in dynamic connectivity studies. The main advantage in doing so is the

analysis will not be constrained to predetermined functional regions, since these are not always representative in older populations [82]. We likewise anticipate the visualization of voxel-wise brain maps will provide us with more tangible and biologically interpretable results. Finally, we will use the voxel-wise result to correlate a spatial similarity score between window maps across the dataset, and in relation to the representative *brain states*. This will allow us to statistically assess our results within the dataset, and permit comparison across datasets. For this purpose, we will specifically target a comparison between a dataset containing resting-state data and a dataset comprised of sleep data confirmed through EEG measures. This is also made possible by using the same network atlas to derive seed regions across each dataset.

This analytic approach will permit us to address our research questions (see Research Studies) and further our understanding of healthy aging, heterogeneity and resting-state analysis. Combining these analyses, we hope to identify and characterize potential age-related differences that can have an impact on resting-state results. The result of these studies may establish a foundation that will be of significant benefit and importance for future studies in aging.

1.2. Research Studies

1.2.1. Study#1 – Aging

In the first study our objective is to apply our method as a proof-of-concept. We intend to analyze resting-state data of old and young subjects to identify age-related differences using both a static and dynamic analysis approach. The static analysis will provide a benchmark for the dynamic analysis, and insight for any interpretation of the data. There has been sufficient literature in this area that this study will serve to support our method. Additionally, we hope to identify heterogeneity in the older population that may convey biological relevance. We will utilize posterior and anterior regions of the brain as seeds of interest (PCC and mPFC). These seed regions will best serve to confirm our results in relation to the literature, where a reduction in connectivity between the regions in healthy older subjects, as compared to young subjects, has been consistently observed [1]. In this study we have three basic objectives.

- Compare and analyze resting-state data of young and old subjects.
- Assess the outcomes using static analysis as a benchmark.
- Apply dynamic analysis methods to delineate *brain states* and compare with the static results.

Since the dynamic analysis is data-driven, it involves pooling all the data without differentiating cohorts. Through the clustering method we will derive representative mean clusters, which we will refer to as *brain states*. These states will characterize a mean of connectivity patterns that we most-frequently observe across all subjects. We nonetheless expect the heterogeneity between the age cohorts to emerge from our analysis. Thus, we hypothesize the following:

Hypotheses:

- Individual *brain states* will associate with young and old subjects, respectively.
- A *brain state* that typifies DMN connectivity found in the literature [21] will be identified.
- A *brain state* will associate with only a subset of the older population, differentiating it from old subjects not associated with the state.
- This *brain state* will be characterized by the reduced posterior-anterior connectivity described in the literature [1].

The importance of this analysis is to confirm that we will uncover results consistent with what is observed through static analysis. Further, it is important that we are able to delineate heterogeneity in the older population through *brain states* driven by the data. Such results will support the added value of this method, as compared to the benchmark static analytic procedures. This will support the method for further application to other studies.

1.2.2. Study#2 – Sleep

For the second study we will apply our analytic methods to data derived from cohorts of young and older subjects while they sleep in the scanner. Once again, we intend to identify age-related differences using both a static and dynamic analysis approach, whereby the static analysis serves as a baseline analytic benchmark. We will look specifically at non rapid eye movement stage 2 sleep (NREM2). During this sleep stage electrophysiological events that include k-complexes, sleep spindles and some slow-wave sleep activity are prevalent [34]. The k-complex, identified using EEG, results from synchronous neural excitation [83]. Sleep spindles often follow k-complexes and are characterized by short periods of oscillatory activity as observed with EEG, and originate in the reticular nucleus of the thalamus [84]. During slow-wave sleep, the EEG-measured activity reflects slow synchronous wave activity up to 4Hz [85]. As a result of differential age-related activity during these processes [36], we anticipate measurable outcomes using our dynamic method. We will utilize the thalamus and insula as seed regions. The thalamus serves as an important seed region due to its strong association with sleep regulation [86, 87], k-complex activity [83] and sleep spindles [84], while the insula region has been implicated in the origin of slow-waves during sleep [85]. These sleep oscillations are also altered with age [85]. Our objectives are as follows:

- Relate the fMRI data to the NREM2 sleep stage.
- Assess the age-related differences using static analysis.
- Dynamically delineate *brain states* during NREM2 sleep.
- Assess the age-related differences in NREM2 *brain states* and compare with the static results.

Due to age-related differences in electrophysiological measures of sleep qualities (quantity and quality of k-complexes, sleep spindles, slow-wave sleep) that have been observed in EEG-related and other MRI studies, described above, we anticipate observing

differences in the fMRI analysis. We also anticipate a different connectivity pattern in older subjects due their difficulty entering and maintaining deeper stages of sleep [36]. Specifically, we hypothesize the following:

Hypotheses:

- An individual *brain state* will be associated with the older cohort during NREM2 sleep.
- The older population will display *brain state* heterogeneity during NREM2 sleep (i.e. divergent sub-cohorts across multiple *brain states*).
- A *brain state* associated with the older population will be characterized by greater connectivity to the DMN during NREM2, found typically in awake subjects.

This study raises important questions in regards to the interpretation of resting-state data. If we consider sleep an ubiquitous event in resting-state procedures, then any analysis of resting-state inevitably includes periods of sleep. If the qualities of sleep are consistent across cohorts, the impact may be limited to dampening or modulating results with no sleep. However, if there are cohort wide differences that may include length or quality, this could impact the results. Thus, we hope to better determine whether there are distinguishable age-related differences in sleep under fMRI. Likewise, the heterogeneity within a cohort, in this case our interest lies in the older cohort, may impart important effects on an overall analysis. This is not limited to studies in aging, as there may be strong differences in sleep between many healthy and clinical populations. If we determine there are significant age-effects, or heterogeneous effects, this would highlight the importance of controlling for sleep, when exploring age-related studies using resting-state procedures.

1.2.3. Study#3 – Thought Content

In the third study our objective is to apply our analytic methods to measure the relationship between thought content and *brain states*, and its association to the young and old age cohorts. We will apply a static analysis as a baseline analysis, and then apply data-driven clustering to establish representative *brain states* found across all subjects. We hypothesize that certain *brain states* may reflect more or less detailed thought content, and seek to determine if these states differentiate by age, or subgroups within the cohorts. For this purpose, we will use the middle temporal gyrus and superior temporal gyrus as seed regions. In previous studies both the middle temporal gyrus and superior temporal gyrus have been implicated in remembering the past and imagining the future in both young and old subjects [46, 50]. In addition to mediating thoughts about the past and imagining the future [46, 88], compensatory activity has been observed in these regions in older adults, to counteract age-related memory deficits [89]. In addition, the superior temporal gyrus has been associated with though content variations in a previous preliminary study [61]. These seed regions, with their relationship to thinking about the past and imagining the future, are well-suited for this analysis. Our objectives are as follows:

- Assess correspondence between thought content scores and static connectivity results.
- Identify *brain states* that correlate with high or low thought content scores.
- Explore interaction between thought content scores, connectivity, and age (using both static connectivity and *brain states*)

Due to age-related differences during the elaboration of past and future thoughts, we do expect to find corresponding differences in the resting-state analysis. In particular, we anticipate that the clustering analysis will better highlight age and thought related differences than we would otherwise find with a static analysis alone. We would

additionally anticipate a heterogeneity within the older population that will be identifiable in the dynamic analysis. Specifically, we hypothesize the following:

Hypotheses:

- Identify connectivity differences, from the seed regions, with thought content as the variable of interest, in the static analysis
- A *brain state* will be associated with higher or lower thought content scores.
- An interaction between age and thought content scores in relation to connectivity and *brain states*. (Due to compensatory activity found in these regions during past and future thought [89], we hypothesize greater connectivity in older subjects as a compensatory mechanism.)

We anticipate that older subjects will have lower thought content scores for both past and future thought, as has been found in the literature [45-47]. This is particularly relevant if we find a significant difference in connectivity measures across cohorts, or sub-cohorts. This would highlight the importance of controlling for thought content, when cohort-related differences in content may be determining factors in connectivity. On the other hand, compensatory mechanisms that allow for similar content scores across cohorts, while otherwise hiding brain alterations are of particular interest. Although we anticipate an interaction between age and thought content scores, this has not been demonstrated in the literature using resting-state procedures. In both cases, the results may confirm the need to control for thought content scores within the analysis of future resting-state studies.

1.2.4. Study#4 – Dataset Comparison

As a final study we propose an exploratory, preliminary analysis to compare *brain states* derived from our analytic method across datasets. In particular, we will compare data from an independent resting-state dataset to the imaging data from the sleep study in Study#2. We will focus again on sleep stage NREM2. During this sleep stage subjects are falling in a deeper sleep that is easier to differentiate than NREM1 [40]. The deeper NREM3 sleep stage requires more time for subjects to enter, and would be less common in typical short resting-state scans [39]. To address the impact population differences can have on the data, we match the cohorts for age and sex. To maintain continuity with our earlier studies, we will focus our attention on one seed region from each of the first studies (PCC and MTG), respectively; and on both seed regions from our sleep study (thalamus and insula). The PCC seed region displays a reduction of connectivity to the DMN with increasing sleep depth, in particular to the anterior regions of the DMN [90]. The MTG region is most associated with past and future thought in both young and old subjects [46]. Aside from responding to unexpected and meaningful auditory events during sleep, the MTG has not known for specific sleep-related activity [91, 92]. We will use this seed region as a control, and accordingly expect to find less notable observations. Along with an association with sleep, the thalamus also displays alterations in activity related to periods of wakefulness and brief sleep [93]. Since we conjecture this is common during resting-state procedures, the thalamus is a relevant seed region for both sleep and resting-state studies. We also include the insula as a seed region, as, along with the thalamus, activity in this region increases during resting wakefulness with eyes closed [94]. This may capture periods of the resting-state scan where subjects are unable to maintain eyes open while fixated on the cross-hair. Since this is an exploratory analysis, we have selected broad seed regions from each study. Our objectives are as follows:

- Assess the feasibility of comparing *brain states* across datasets
- Explore correlational relationships between sleep and resting-state *brain states*.

- Evaluate the characteristics of inter-dataset *brain states* that show an association (i.e.: an association between NREM2 sleep and apparent wakefulness *brain states*).

Since it is estimated that during resting-state procedures 10 – 30% of subjects will sleep in the first 3 minutes [39], we expect to find some resting-state *brain states* that correlate strongly to *brain states* delineated during NREM2 sleep. Likewise, due to age-related sleep differences we anticipate age to be a factor in correlating the *brain states* across the sleep and resting-state datasets. Specifically, we hypothesize the following:

Hypotheses:

- A *brain state* from the resting-state analysis will be associated with an inter-dataset NREM2 sleep *brain state*.
- These *brain state* will correspond according to age.
  (i.e.: a *brain state* associated with older subjects in resting-state will associate to NREM2 sleep *brain states* that likewise associates more with older subjects.)
- The associations across datasets will be lower in the MTG seed region.

Despite the preliminary nature of the analysis, the implications from this study are of great importance. First, we are presenting a simple method of comparing results across datasets. This may be of immense benefit for vast research in aging, as well as other areas of study that incorporate resting-state. If we find a correlation across datasets of a *brain state* in resting-state with an NREM2 sleep *brain state*, it supports our conjecture that a brain-state derived from resting-state data may show characteristics of sleep. Likewise, this would suggest that through data-driven methods alone we may be able to delineate sleep influenced *brain states* in resting-state data. Further, this would align with previous research that has found sleep to be ubiquitous in resting-state research.

If *brain states* correlated across the sleep and resting-state datasets retain age associations, this would support our proposition that age-related heterogeneity in sleep is of fundamental importance when researching age with resting-state analysis. Such age-related differences in sleep measurements may impact the outcomes of research that does not take this into account.

Chapter 2

2 Methodology

2.1 Datasets

2.1.1 Enhanced Nathan Kline Institute Rockland Sample

Subjects

The enhanced Nathan Kline Institute Rockland (NKI-e) sample is a publicly available dataset that consists of multiple measures per participant, including neuroimaging data [95]. The data collection is ongoing and the community sample currently consists of over 1000 participants across the lifespan [96]. For this work, we pre-processed and analysed the first five releases of data (n=418). Participants who reported or tested positive for medical, neurological or psychiatric disorders, severe head injury (one or more concussions), anxiety, depression and obesity (body mass index >29) were excluded (n=201). We then identified the participants that satisfied the age criteria for the older and younger cohorts, specific to each study. The ages and composition of the cohorts varied based on the constraints and objectives of each study.

In the aging study, our objective in part was to establish a proof of concept for our analytic methods. To accentuate age-related changes, we selected a higher age range for the older cohort than the other studies. This study comprised 116 subjects (Old: 38 subjects (37% male), 65-85yrs, 72.6±5.97yrs; Young: 78 subjects (50% male), 18-35yrs, 23.8±4.61yrs). In the thought content study, only participants that completed the post-scan questionnaire

were included. To balance the cohort size, we included older participants as of age 56 years. This study comprised 145 subjects (Old: 68 subjects (31% male), 56-85yrs, 66.4±7.86yrs; Young: 77 subjects (49% male), 18-35yrs, 23.8±4.61yrs). In the cross-dataset study, we matched the NKI-e participants to those of the sleep dataset. For the resting-state component, this study comprised 153 subjects (Old: 75 subjects (29% male), 50-69yrs, 58.4±5.85yrs; Young: 78 subjects (50% male), 18-35yrs, 23.8±4.61yrs); see also Table 2.1.

fMRI Acquisition:

The fMRI resting-state data was acquired using a 3.0-Tesla scanner (Magnetom TrioTim, Siemens) with an echo planar imaging sequence (voxel size = 3.0 x 3.0 x 3.0 mm^3; 38 transversal slices; repetition time [TR] = 2500 ms; echo time [TE] = 30 ms; flip angle = 80°; field of view [FOV] = 216 mm; delay = 0 ms, TA = 5:05). The structural T1-weighted image was acquired with a magnetization-prepared rapid gradient echo sequence (voxel size = 1.0 x 1.0 x 1.0 mm^3; 176 sagittal slices; TR = 1900 ms; TE = 2.52 ms; flip angle = 9°; FOV = 250 mm, TA = 4:18).

The NKI-e protocol included two other multi-band resting-state sequences (TR=645ms, TR=1400ms), enabled through simultaneous multiple-slice acquisition techniques. For our studies, we selected the standard imaging sequence (TR=2.5s) to provide a complementary sequence for analysis and comparison across the datasets (NKI-e: TR=2500ms vs Sleep: TR=2460ms).

Psychometric Measures:

The NKI-e study includes a wide range of assessments and cognitive batteries [95]. This comprises tests for cognitive and executive functioning, short-term memory and working memory. Many of the tests, however, were not completed by all subjects and were excluded from the analysis. To determine if any characteristics measured from the remaining tests associated with our results, we ran Student's t-tests with Bonferroni

corrections. This included testing against results from the Wechsler Abbreviated Scale of Intelligence, the NEO Five Factor Inventory, the Pittsburgh Sleep Quality Index, along with physiological measures (age, sex, handedness, blood pressure, pulse, and body-mass index).

In the thought content study, a post-scan questionnaire – the New York Cognition Questionnaire (NYC-Q) – was utilized to measure a subject's thought content while in the scanner. Previously, this measure has been used in conjunction with other analytic methods to identify relationships between the thought content of mind wandering and brain activity (fractional amplitude of low frequency fluctuations, regional homogeneity, and degree centrality) [53].

Immediately following MRI, the NYC-Q self-report questionnaire was given to each participant. It consisted of 31 questions, of which 30 have been retained (one questions was inadvertently included and deemed redundant) [53]. The questionnaire expands on aspects of the Dundee Stress State Questionnaire that investigates self-generated thought [97] and has previously been used to identify neural processes related to thought content [53]. Participants responded to questions about what they were thinking and how they felt during the scan, and the degree to which the questions describe their internal experience. The questionnaire is divided into two sections. The first section explores questions that break down the content of thoughts the participant had while in the scanner (e.g.: Q#7: *I thought about an interaction with somebody that took place in the past*; Q#12: *I thought about something that happened a long time ago in the past*). The second part of the questionnaire surveys the manner in which the content is articulated in the mind of the individual (e.g.: Q30: *Vague and non-specific*) (see [53], for a complete list of all questions). The questionnaire is defined by 8 data-driven factors that best describe the self-generated thought [53]. In our study, we focused on the first section (22 questions) that examine thought content. From the five factors that best describe the results from

this section, we selected past and future thought as our factors of interest [53]. The three remaining factors that we did not include in this study comprised positive and negative thoughts, along with thoughts of close social relationships.

2.1.2. Sleep dataset

Subjects

The sleep dataset comprised thirty older and younger subjects. The participants were divided into two groups: an older cohort (n=14 (36% male), 52-69yrs, 59.5±5.9yrs) and a young cohort (n=16 (50% male), 20–30yrs, 23.3±3.3yrs); see also Table 2.1. Participants who reported sleep, medical, neurological or psychiatric disorders or suffered from extreme sleeping or waking times [98], excessive sleepiness (during the day) [99], consistently poor sleep quality [100], anxiety [101], depression [102] and obesity (body mass index >27) had been excluded. Medication that could affect the nervous system, working night shifts (in the previous year) and travel across more than one time-zone (in the previous 3 months) were likewise exclusion criteria. All participants were right-handed, non-smokers and consumed only a moderate quantity of caffeine or alcohol. Preceding acquisition, all participants were tested to rule out sleep apnea, periodic leg movements or other relevant medical conditions.

There was no significant difference between the younger and older cohorts for sleep quality, anxiety, depression, or body mass index. The older participants, however, went to bed and woke earlier, and slept less than the younger participants. Likewise, the older participants scored higher on measures of morning alertness. The study received ethics approval from the Regroupement Neuroimagerie Québec (RNQ) and all participants provided written informed consent.

Pre-acquisition

In the week prior to scanning, participants maintained a regular bedtime and waking schedule that remained no more than ±30 minutes within their usual sleep and wake times. Participants arrived at the laboratory the day before the scanning, 12 hours after their waking time. Participants were instructed to avoid naps, engaging in intense physical activity, and beverages that contained caffeine or alcohol for that entire day. After arrival, the participants remained awake in dim light (<15 lux) for the next 14 hours. In total, the participants sustained 26 hours of sleep deprivation before entering the scanner (2 hours after their usual waking time). In the scanner, the participants were instructed to relax and allow themselves to sleep. The data was acquired simultaneously with EEG-fMRI.

EEG Acquisition

Scalp-surface EEG was recorded using a 64-electrode cap (BrainCap MR; Brain Products; referenced to FCz) while electrocardiography was recorded using 3 bipolar electrodes (Brain Products). Electrode-skin impedance was maintained at a level below 5 kΩ (plus 10 kΩ built-in resistors) using an abrasive paste (Nuprep; Weaver and Company) and an electrode gel (Electro-gel; Electro-cap International). These steps stabilized the data acquisition throughout the longer than typical acquisition time. Two 32-channel amplifiers (BrainAmp MR plus, Brain Products) were utilized to record the EEG signals, while one 16-channel amplifier (BrainAmp ExG MR, Brain Products) was incorporated to record the ECG signals. The signal information from both the EEG and ECG was transmitted via fiber-optic cable to a computer outside the scanning room. The scanner clock was used to synchronize the EEG/ECG acquisition. The data was analog-filtered (0.016-250 Hz) and digitized (5 kHz sampling rate; 500 nV resolution) using a BrainVision Recorder 1.20 (Brain Products). The participant's sleep was simultaneously monitored online with BrainVision RecView (Brain Products).

fMRI Acquisition

The head was immobilized to minimize movement and the resultant artifacts. This was achieved using a vacuum pad in the head coil. To minimize scanner gradient artifacts that could impact EEG measures, the participant's axial position was shifted 40 mm (relative to the standard iso-center position) in the direction of the feet [103]. The fMRI data was acquired using a 3.0-Tesla scanner (Magnetom Trio, Siemens) with an echo planar imaging sequence (voxel size = 3.4 x 3.4 x 3.0 mm^3; 32 transversal slices; repetition time [TR] = 2460 ms; echo time [TE] = 40 ms; flip angle = 90°; field of view [FOV] = 220 mm; delay = 0 ms). The structural T1-weighted image was acquired with a magnetization-prepared rapid gradient echo sequence (voxel size = 1.0 x 1.0 x 1.0 mm^3; 176 sagittal slices; TR = 2300 ms; TE = 2.91 ms; flip angle = 9°; FOV = 256 mm) at a previous visit. The EEG-fMRI acquisition time varied from subject to subject, but did not exceed 100 minutes

2.2 Pre-processing

The EEG data was analyzed using BrainVision Analyzer (Brain Products) [104] and a commercial software (Harmonie, Stellate System). The fMRI data was processed using the NeuroImaging Analysis Kit version 0.12.18 [105], (NIAK release: [3]), under CentOS with Octave (http://gnu.octave.org) version 3.6.1 and the Minc toolkit [106] version 0.3.18. The analyses were implemented on a network supercomputer (Guillimin) [107], using the pipeline system for Octave and Matlab (PSOM 1.0) [105].

2.2.1 EEG data

In order to remove scanner gradient artifacts from the EEG recordings, the adaptive subtraction function from BrainVision Analyzer [104] was applied. The residual gradient artifacts were removed with independent component analysis (ICA). An algorithm from

the FAST toolbox based on constrained independent component analysis (cICA) [108], was incorporated for ballistocardiographic artifact correction. An automatic algorithm was used to detect movement artifacts [109]. Finally, visual inspection identified any other artifacts. The EEG data was downsampled to 250Hz. It was then low-pass filtered using an infinite impulse response filter (-48dB at 0.3-50Hz), and then re-referenced from FCz to linked mastoids (i.e.: TP9 and TP10). An experienced technician visually scored the sleep stages in 20-second epochs. Standard criteria [110] and commercial software (Harmonie, Stellate System) were applied.

In addition to sleep staging, the density of slow-wave sleep (SWS) was assessed during NREM2 and NREM3 sleep. The SWS was determined by an automatic algorithm on periods of uninterrupted NREM2 and NREM3 sleep. This detection process took place through left parasagittal derivations: Fp1, F3, C3, P3, and O1. A bandpass filter between 0.3 and 4.0 Hz using a linear phase Finite Impulse Response filter (–3 dB at 0.3 and 4.0 Hz) was applied to the data, as previously published [111-113]. Periods of artifact-free NREM sleep were utilized to detect the SWS. The criteria for detection comprised: a) negative peak <–40 μV; b) peak-to-peak amplitude >75 μV; c) duration of negative deflection >125 ms and <1500 ms; and d) duration of positive deflection <1000 ms. The density of SWS was calculated by the number of SWS per minute of either NREM2 or NREM3 sleep.

2.2.2 fMRI data

The fMRI datasets underwent correction for slice timing and rigid-body motion. The rigid-body motion was estimated for each time frame of the functional run, as well as between functional data and the T1 scan for each subject [114]. The T1 scan was non-linearly co-registered to the Montreal Neurological Institute ICBM152 stereotaxic symmetric template [115] using the CIVET pipeline [116]. The rigid-body, fMRI-to-T1 and T1-to-stereotaxic transformations were combined to resample the fMRI in MNI space at

3 mm isotropic resolution. To minimize motion artifacts, volumes showing a frame displacement (FD) of greater than 0.5-mm were censored, along with adjacent volumes [117]. Nuisance covariates were regressed out from fMRI time series. This comprised slow time drifts (basis of discrete cosines with a 0.01 Hz high-pass filter cut-off), average signals in conservative masks of the white matter and the lateral ventricles, along with the first principal components (accounting for 95% variance) of the six rigid-body motion parameters and their squares [118]. Lastly, the fMRI volumes were spatially smoothed with a 6-mm isotropic Gaussian kernel. A detailed description of the pipeline can be found on the NIAK website [119].

There was a statistical difference between the number of volumes by subject in each cohort subsequent to the censoring (scrubbing) process in the NKI-e dataset (Table 2.1) however, there was no significant difference between the number of windows between cohorts (see Dynamic Connectivity). In the sleep dataset neither the number of volumes (Table 2.1), nor the number of windows by subject (see Table 2.2) were significantly different between cohorts. In both datasets, there was significantly more motion in the older cohorts across the entire scan. In the sleep dataset, this observation remained independent of sleep stage. Likewise, following the removal (censoring) of volumes with high degrees of motion, older subjects still moved significantly more than the younger subjects in both datasets (Table 2.1).

Study	Cohort	N	N Cohort	N Male (%)	Age Range	Mean Age (sd)	FD (sd)	Volumes (sd)
Study#1: Aging (NKI-e)	**Older**	116	38	14 (37%)	65 - 85	72.6 (6.0)	0.208 (0.044)	100.53 (15.45)
	Young		78	39 (50%)	18 - 35	23.8 (4.6)	0.168 (0.051)	106.90 (14.64)
	t-test						p<0.001	p<0.05
Study#2 & 4: Sleep / Cross-Dataset (NREM2)	**Older**	30	14	5 (36%)	52 - 69	59.5 (5.9)	0.23 (0.05)	1449 (518)
	Young		16	8 (50%)	20 - 30	23.3 (3.3)	0.18 (0.05)	1583 (448)
	t-test						p<0.001	p>0.4
Study#3: Thought Content (NKI-e)	**Older**	145	68	21 (31%)	56 - 85	66.4 (7.9)	0.207 (0.051)	100.38 (16.43)
	Young		77	38 (49%)	18 - 35	23.8 (4.6)	0.167 (0.050)	107.17 (14.56)
	t-test						p<0.001	p<0.01
Study#4: Cross-Dataset (NKI-e)	**Older**	153	75	22 (29%)	50 - 69	58.4 (5.9)	0.207 (0.051)	100.65 (16.89)
	Young		78	39 (50%)	18 - 35	23.8 (4.6)	0.168 (0.051)	106.90 (14.64)
	t-test						p<0.001	p<0.05

Table 2.1. Demographic information for all studies after censoring. (sd = standard deviation, FD=frame displacement in mm after censoring)

2.3 Analysis

Brain Parcellation Atlas

To analyze the functional data, we utilized the MIST brain atlas derived from the publicly available Cambridge sample, part of the 1000 Functional Connectome Project [120] (Figure 2.1). The brain atlas was generated from the resting-state fMRI data of 198 young healthy subjects (75M, 18-30yrs) using a bootstrap analysis of stable clusters (BASC, [121]). Through BASC, the Cambridge network atlas provides a functionally derived parcellation, which can improve upon anatomically delineated atlases [122].

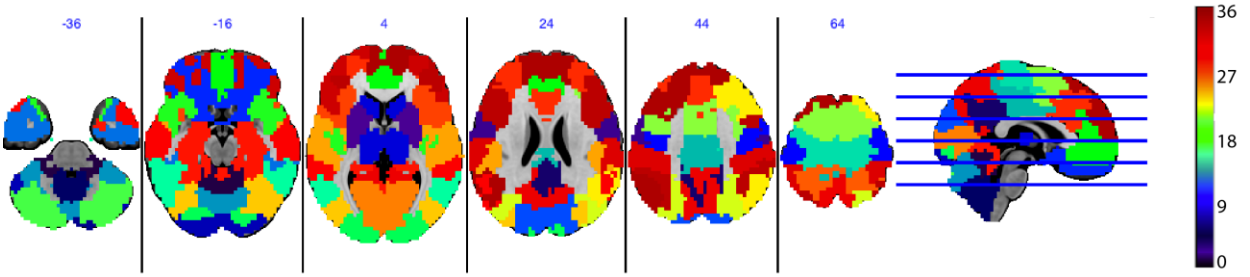

Figure 2.1. Axial view of the MIST-36 sample brain atlas showing each region of interest.

We chose specific seed regions for each aspect of our investigation. We described the basis for these selections in detail in the Introduction (see Research Studies). In our study investigating age-related differences in brain connectivity, the seed regions of interest comprised the posterior cingulate cortex (PCC, region#4 [120]) and the medial prefrontal cortex (mPFC, region#18 [120]; see Figure 3.1). In our study investigating age-related differences in functional brain connectivity during NREM2 sleep, we considered the thalamus-caudate seed region (TC, #8) and the insula (INS, #28; see Figure 3.12). In the study we examined age-related associations of thought content and brain connectivity, we included the middle temporal gyrus (MTG, region#31, [120]) and the superior temporal gyrus (STG, region#25, [120]) as seed regions (see Figure 3.25). Finally, for the

cross-dataset comparison, we included both seed regions from the sleep study (TC and INS), and one region each from the other studies (PCC and MTG).

2.3.1 Static Connectivity

Connectome-wide association and network analysis

For all participants, we calculated the connectivity between networks (MIST-36 brain atlas [120]) by first averaging the time series across voxels in each network. We calculated the Pearson's correlation between the average time series for each network pair, and then a Fisher transform was applied on the coefficient to reduce its variance and make its distribution across individuals more normal [123]. The within-network connectivity was calculated by taking the average of the Fisher-transformed pairwise correlations between all voxel time series inside the network. Thus, with the MIST-36 brain atlas, individual subject-level connectomes comprised 36 x 36 symmetrical matrices, with 36x35/2=630 distinct inter-network connectivity measures, and 36 distinct intra-network connectivity measures.

We evaluated network connectivity with the seed regions (networks selected for this study) for significant age-cohort differences. To provide a stringent threshold for statistical significance, the p-values were corrected for multiple comparisons at the level of the full connectome, i.e. 666 tests for each distinct connectivity measure.

Statistics

For each inter- and intra-network connectivity measure, a group-level general linear model (GLM) was used to assess age associations. The age cohort was the variable of interest, while sex was considered a confounding covariate in the model. Movement, defined by the average residual frame displacement (subsequent to censoring) was not included in this model. There is a strong association between age and movement [124],

which was also present in our samples (see Table 2.1). Thus, including movement as a covariate may have undermined detection of age-related variation.

For the GLM analysis, we utilized the GLM-connectome pipeline available in NIAK package11 [125]. The parameters of the model were estimated through minimum least-squares. A t-test with associated p-value was derived under a Gaussian, independent and identically distributed assumption on the residuals. A Benjamini-Hochberg false discovery rate (FDR) correction for multiple comparisons [126] ($q < 0.05$) tested the significance of the number of discoveries against the global null hypothesis of no association (permutation test with family wise error, $p<0.05$; [125]). The connectome-wide association analysis provided an overview of age-related differences in static connectivity.

2.3.2 Dynamic Connectivity

2.3.2.1 Sliding windows

We studied the temporal variability of functional connectivity with a sliding time window approach [66]. The window size was set to 40 volumes (~100seconds). The minimum window length was calculated as the multiplicative inverse (reciprocal) of the high-pass filter cut-off applied during preprocessing (i.e. 1/0.01 sec). We chose this value to limit spurious fluctuations and autocorrelation that may occur in window lengths that fall below this cut-off frequency [69]. The window was advanced 4 volumes for every new measure (90% overlap between consecutive connectivity measures). This step size was selected to match half the length of the epoch used to determine sleep stages in the sleep analysis (20-second epochs). Since we planned for eventually running analyses across datasets, we also applied this step size for the NKI-e analyses. For windows that comprised volumes censored due to excessive motion, we discarded those with less than

20 uncensored volumes (i.e.: windows were discarded if <50sec of measures). In previous published reports, a window length of 45 seconds is common [66, 70, 78]. The maximum number of windows per subject in the NKI-enhanced dataset was 21, with a minimum of 5 for the few subjects that had time series with extensive censoring (20.26 ± 2.49). There was no significant difference between cohorts for the number of windows in all studies (All, $p>0.3$, T-test).

In the sleep dataset, the duration of each participant's acquisition was variable. As a result, the number of windows incorporated in the analysis varied from subject to subject. The total number of windows that comprised exclusively one sleep stage are listed in Table 2.2. Since only the NREM2 sleep stage provided both a sufficient and balanced numbers of windows between the younger and older cohorts, we performed all analyses exclusively on the NREM2 sleep stage.

	Awake	NREM1	NREM2	NREM3
Older	236	14	1900	58
Young	99	19	1893	1622

Table 2.2. Number of 100s time windows for each sleep stage, by cohort. Only time windows that contain volumes exclusively from the indicated sleep stage, are counted.

For each time window, we calculated the Pearson correlation coefficient voxel-wise between the average time series of the seed region and every other voxel in the grey matter mask, and Fisher transformed the results. This provided a representative connectivity map for each time window, with >50,000 measures between the seed region and all voxels across the brain. We repeated this computation for all windows across the time-series for each participant. The connectivity maps provide a measure of temporal

variability in every participant and across the dataset. We calculated this for each seed region specific to the dataset and analysis.

2.3.2.2 Clustering

We generated pairwise spatial similarity scores (Pearson's correlation) across all connectivity maps in the dataset. The resultant matrix represented the spatial similarity of each connectivity map to one another, corresponding to all the time points of the windows across all subjects. This defined a (W_{tot} x W_{tot}) square similarity matrix, where (W_{tot} = total time windows) and which varied in size in each study.

Using a hierarchical clustering procedure with Ward's criterion (as implemented in NIAK; [3]) the maps were organized into a series of nested homogeneous subgroups. We cut the resultant branching of the hierarchy to generate a parcellation of maps representing four clusters. Our rationale for selecting four clusters was based on the relatively short duration of the time-series in the NKI dataset (5:05 minutes, providing a maximum of 21 sliding windows per subject), as well as our exclusive focus on NREM2 in the sleep study. We anticipated variations due to brain activity associated with the NREM2 sleep stage, however, we did not expect a large number of *brain states*. For more detail, see also the Discussion (section: 4.7. Limitations).

Partitioning the hierarchically clustered connectivity maps into *brain states* involved assigning a State ordinal to each map. Thus, a prototypical connectivity map representative of each *brain state* was calculated the mean of all maps assigned to the given State. The nomenclature we use in this text to identify the *brain states* is prefixed by the acronym for the seed region, followed by the cluster (or state) number (i.e.: PCC#4 refers to the 4th *brain state* derived from the posterior cingulate cortex seed region).

For each connectivity map – corresponding to the time windows across all subjects – we computed the spatial Pearson correlation coefficient with each *brain state*. We used this matrix, of size (W_{tot}) x (number of *brain states*), as a weighted measure to statistically test the variability of the *brain states* over time, and across subjects and cohorts.

To better visualize the *brain states* and how they differ from the average across all subjects, we calculated a z-map for each State. We displayed the z-maps in each results section for both *brain states* and average cohort maps. By construction, z-maps for two cohorts are symmetrical with one another in relation to the average connectivity across all subjects.

2.3.3 *Brain state* transitions

The probability of transitioning between *brain states*, or remaining in the same State, was measured for each time window in all subjects. We measured both the likelihood of a transition in general, as well as to between specific states (e.g. PCC#1 → PCC#1, PCC#1 → PCC#2 … PCC#4 → PCC#3, PCC#4 → PCC#4). The average transition probability between given states was evaluated across all subjects. This analysis was performed on each cohort (young and old) independently. We measured significance of observed differences using a z-test on two population proportions [127]. In the two proportion z-test, we test the null hypothesis that the proportion of older subjects that transition is equal to the transition probability of the younger cohort, against the alternative hypothesis that they are not equal.

In addition, we measured the probability of simply switching states. The cohorts were examined independently and we again measured the significance of any cohort differences with a two proportion z-test, as described above [127].

Finally, in order to determine whether mean connectivity higher than average would increase the likelihood of remaining in (or transitioning from) a given *brain state*, we

assessed the relationship between connectivity and transition probabilities. For every time window, we assessed whether there was a change of state. We averaged the connectivity across subjects and cohorts that remained in a *brain state*, as well as for those that transitioned to a different *brain state*. We ran a GLM on these values using age cohort as the variable of interest, while controlling for sex as a covariate.

2.3.4 Statistics

To assess whether a *brain state* was significantly associated by age cohort we applied two main methods of analysis: permutation testing and a general linear model.

2.3.4.1 Permutation Tests:

For each of the *brain states*, we performed a permutation test to assess whether the proportion of older and younger subjects associated with the given *brain state* was significantly different than what we would expect by chance.

In this analysis, we test the null hypothesis that the proportion of time spent by subjects from the older cohort in a given *brain state* is equal to that of the younger cohort. We test this against the alternative hypothesis that these proportions are not equal. We permuted the cohort assignments randomly across subjects, n=100,000. This provided us with a p-value for the observed value in each *brain state* representing the proportion of time spent in the given *brain state*. We performed this test with regards to age cohort in each study, as well as with high and low thought content groupings in the Thought Content study.

2.3.4.2 General Linear Modelling

Weight scores

A general linear model [125] was applied to the weight scores (the spatial Pearson correlation coefficient of each time window's connectivity map to each *brain state*). The age cohort was the variable of interest, with sex included as a covariate.

As previously, the parameters of the model were estimated through minimum least-squares, and a t-test with an associated p-value that was derived under a Gaussian, independent and identically distributed assumption on the residuals. A Benjamini-Hochberg false discovery rate (FDR) correction for multiple comparisons on each of the states [126] ($q< 0.05$) tested the significance of the number of discoveries against the global null hypothesis of no association (permutation test with family wise error, $p<0.05$, [125]).

2.3.4.3. Z-Test for Two Population Proportions

In order to assess the significance of measures that involved proportions, or transition probabilities, a two proportion z-test was applied [127]. This determined the significance of the difference in proportions measured. Significance was applied at $p<0.05$.

2.4 Study–specific Methods

2.4.1 Aging

In order to determine the impact *brain states* significantly associated with the older cohort may have on connectivity, we performed a post-hoc analysis. We determined the association of each subject to given *brain states* by their weight scores. We delineated high and low association by the median value of the weight scores to the given *brain state*. To test the relationship of high or low association to a *brain state* with connectivity, we

repeated the static analysis twice, excluding either the high or low association groups for each run alternately.

2.4.2 Sleep

The sleep recordings were acquired in the morning 2 hours after the usual waking time and a total of 26 hours of sleep deprivation. Although sleeping in the scanner is well documented [39], it can be difficult to enter deeper stages of sleep, in particular for older subjects [111]. Thus, sleep deprivation helped participants falling asleep and augmented their sleep duration in the scanner.

After excluding windows with excessive movement (censoring of more than 20 volumes), the windows were categorized by sleep stage. Each volume was assigned a sleep stage label consisting of Awake, NREM1, NREM2 or NREM3. A window was defined exclusively by one of these sleep stages, or a mixture thereof. Only windows that comprised volumes scored exclusively as NREM2 sleep were utilized. This selection was governed by the equal distribution of windows between the older and younger subjects, and the time spent in NREM2, which was greater than any other sleep stage (see Table 2.2).

In addition, we explored the relationship of slow-wave sleep (SWS) density to the *brain states* for each network in the sleep dataset. We utilized linear regression for this purpose. We associated the proportion of time each subject spent in the given *brain state*, to the density of SWS during NREM2.

The transition calculations described in the general methods section took into account transitions in and out of each state, as observed in each dataset. In the sleep dataset, the transitions also included those that went out of the sleep stage studied (NREM2) to other sleep stages and mixed sleep stages. Thus, in the transition analysis for the sleep dataset

we addressed the probability of switching from a state to another state, of staying in the same state, as well as transitioning into or out of NREM2 sleep completely. We quantified both specific *brain state* and sleep stage transitions, as well as the overall total transitions to other *brain states* or out of NREM2 sleep, in general.

As with the aging analysis (see above), we performed a post-hoc analysis to measure the impact sub-cohorts of subjects may have on the analysis. In this instance, we repeated the static analysis while excluding subjects from one of the older cohorts, and again while removing an equal number of subjects that most closely resembled these subjects – by age, sex and movement in the scanner.

2.4.3 Thought Content

To measure thought content, the NYC-Q – a self-report questionnaire – was administered following the MRI sequence [53]. To quantify the results, we multiplied the individual response scores to each question by a weighting-matrix that was computed to measure the relevance of each question to each of the factors that defined the thought content [53]. In this study, the factors of interest were past and future thought content. Thus, for each question the corresponding relevance (weight) to past and future thought was multiplied by the respondent's numerical assessment. The sum of these weighted-scores provided a total score for past and future thought content by subject.

In the static connectivity general linear model analysis, we included these content scores (past, and future) as variables of interest, with sex as a covariate to test for the relationship between observed connectivity and thought content scores. Further, we tested the interaction between thought content scores and age as variables of interest, with sex as a covariate. We used these models to test for an interaction between thought content and age on the functional connectivity of the networks.

For the dynamic analysis, a general linear model was likewise applied with the content scores as the variable of interest, along with the interaction between age and thought content, with sex as a covariate. We explored the effect of these variables on the mean-weighted scores by subject (i.e. the mean of the weighted scores of each window specific to the subject). For each subject, there were four weighted scores, each corresponding to one of the State maps.

To better identify the relationship between thought content and age, we performed additional post-hoc analysis. We delineated each cohort into sub-cohorts with high or low thought content scores, in both past and future measures. We defined the high or low classification by scoring above or below the median scores across the sample and by cohort, respectively. We determined the time spent in each *brain state*, by the high and low content score groups across the sample and by cohorts. As described previously, we assessed the significance of this distribution using permutations tests ($q<0.05$, FDR corrected). We ran the tests across the sample and by cohort. In addition to testing *brain state* transitions by age cohort, we also performed the tests by high and low thought content sub-groupings, with respect to the entire sample and age cohort.

2.4.4 Cross-dataset Analysis

To provide an overview of the relationship between *brain states* across datasets, we calculated the pairwise Pearson correlation coefficient for all *brain state* maps and group average maps across and within two datasets. This comprised the NKI-e resting-state dataset, with awake subjects, and the sleep dataset of subjects in NREM2 sleep.

Chapter 3

3 Results

3.1. Aging

3.1.1. Introduction

In this study our objective is to analyze resting-state data of old and young subjects, largely as a proof of concept to our methods. We apply both a static and dynamic analysis. We expect to replicate a reduction in connectivity between the posterior and anterior regions of the brain (PCC and mPFC), which has reliably been observed in the literature [1]. To recap, our objectives are as follows:

- Compare and analyze resting-state data of young and old subjects.
- Assess the outcomes using static analysis as a benchmark.
- Apply dynamic analysis methods to delineate *brain states* and compare with the static results.

We expect the dynamic analysis to be consistent with common static analysis results. Likewise, since the dynamic method involves pooling of all the data indiscriminate of age group, we anticipate we will identify heterogeneity in the older cohort. This result would demonstrate the importance of including a dynamic analysis in resting-state studies. To recap, our hypotheses are as follows:

Hypotheses:

- Individual *brain states* will associate with young and old subjects, respectively.
- A *brain state* that typifies DMN connectivity found in the literature [21] will be identified.
- A *brain state* will associate with only a subset of the older population, differentiating it from old subjects not associated with the state.
- This *brain state* will be characterized by the reduced posterior-anterior connectivity described in the literature [1].

We analyzed the standard acquisition resting-state data from the NKI-e dataset using two different ROIs from the Cambridge-36 functional network atlas [120], representative of anterior and posterior regions of the default-mode network. These seeds, selected as described above to replicate past results, comprised the posterior cingulate cortex (PCC, region#4) and the medial prefrontal cortex (mPFC, region#18) (Figure 3.1).

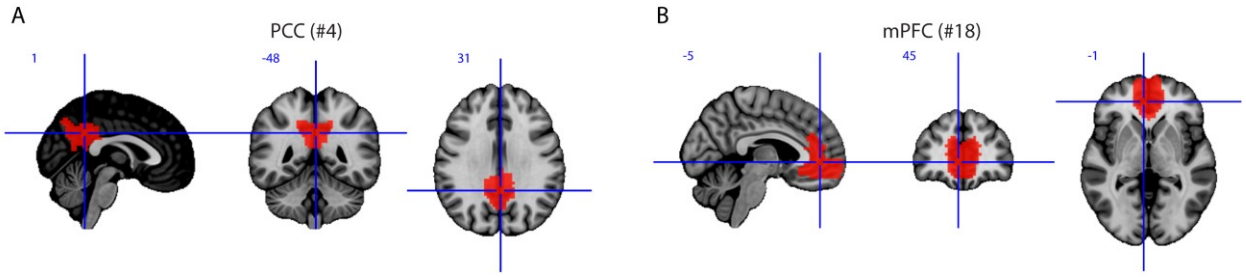

Figure 3.1. MIST-36 regions of interest. A) The posterior cingulate cortex seed (region of interest #4). B) The medial prefrontal cortex seed (region of interest #18).

We analyzed 116 subjects (Old: 38 subjects (37% male), 65-85yrs, 72.6±5.97yrs; Young: 78 subjects (50% male), 18-35yrs, 23.8±4.61yrs) from the NKI-e dataset.

3.1.2. Results

3.1.2.1. Static Connectivity

We applied a general linear model to assess the significance of age to connectivity variations from the two seed regions (Figure 3.2). The age cohort was the variable of interest and sex was used as a covariate. From the PCC seed region, we found a significant (FDR, $q<0.05$) reduction in connectivity to the superior temporal pole, the superior temporal gyrus, medial orbitofrontal cortex, the medial prefrontal cortex, the anterior cingulate, the hippocampal complex and the fusiform gyrus in the older cohort, as compared to the young (Figure 3.2.A. *Top panel*).

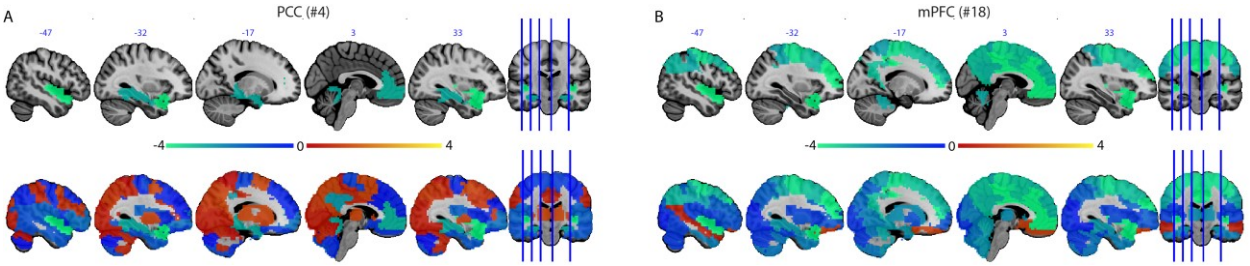

Figure 3.2. Age-related changes in connectivity between (A) posterior cingulate cortex seed and (B) medial prefrontal cortex and the entire brain, during resting-state. The general linear model was run on the MIST-36 network atlas comparing network connectivity with the age cohort as the variable of interest, while controlling for sex as a covariate. (Upper panels) Significant differences between cohorts (FDR, $q<0.05$). (Bottom panels) The map of the t-statistic.

From the mPFC seed region, we observed a significant reduction in connectivity to the frontal and parietal lobes, including to the posterior cingulate cortex, as well as to the superior temporal pole, and the superior temporal gyrus, in older, as compared to younger subjects ($q<0.05$, Figure 3.2.B. *Top panel*). The t-maps (*bottom panels*) highlight areas that showed increases and decreases in connectivity albeit not all significant under $q<0.05$.

3.1.2.2. Dynamic Connectivity

To examine the connectivity from the seed regions using a dynamic perspective, we first computed the mean connectivity of our ROIs with all other regions across all windows, to determine the voxel-wise connectivity of each ROI with the rest of the brain (Figure 3.3. *Top panel*). The same procedure was applied to each age cohort separately. We then calculated the corresponding z-maps for each cohort (Figure 3.3. *Middle and bottom panels*). With the PCC seed, the older cohort showed a reduced connectivity to anterior regions of the brain, namely in the medial prefrontal cortex, anterior cingulate and the orbital frontal cortex; along with diminished connectivity to the posterior regions themselves, including within the PCC (i.e.: seed region average in a voxel-wise comparison); and likewise the superior temporal gyrus, the middle temporal gyrus and the hippocampal complex, as compared to the average connectivity across all subjects. The younger cohort showed the opposite connectivity differences.

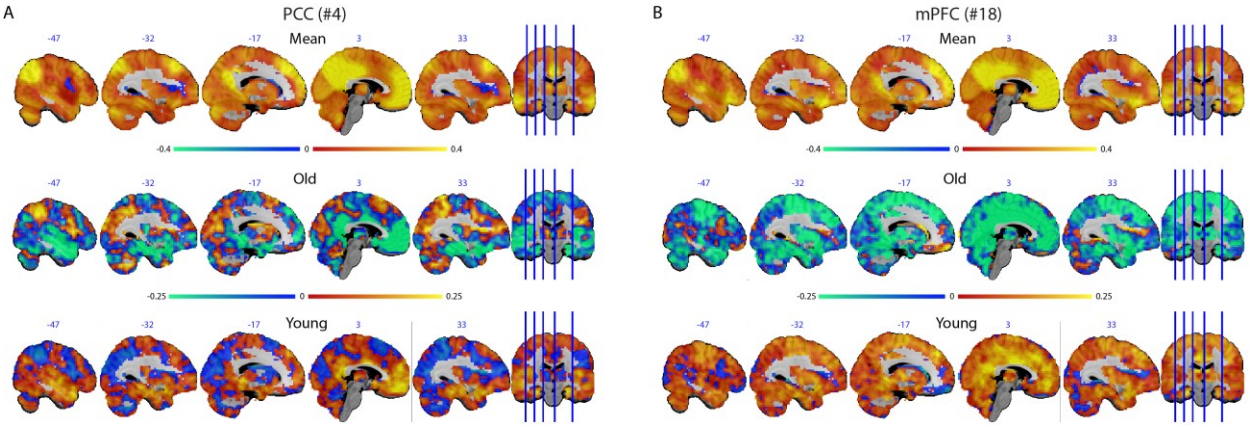

Figure 3.3. Voxel-wise connectivity from the (A) posterior cingulate cortex seed and medial prefrontal cortex seed during resting-state. The overall connectivity (top panels) is the mean connectivity of all windows across all subjects. The Old cohort (middle panels) section represents the Z-map of the connectivity in the older cohort relative to the mean connectivity across all subjects. The Young cohort (bottom panels) section represents the Z-map of the connectivity in the younger cohort relative to the mean connectivity across all subjects.

In the mPFC seed the diminished connectivity seen in older subjects, as compared to the average connectivity across all subjects, extended beyond the typical anterior and posterior regions to most regions throughout the brain. Regions that showed increased connectivity included the orbital section of the superior frontal gyrus, opercular regions of the inferior frontal gyrus, and some cerebellar regions.

To identify *brain states* to which the subjects converged, we performed a hierarchical clustering procedure (Ward's criterion) on the correlation between each window map with all the other window maps (Figure 3.4. *Left panels*). This procedure assigned an associated cluster or state (n=4) to each given window map (Figure 3.4. *Right panels*).

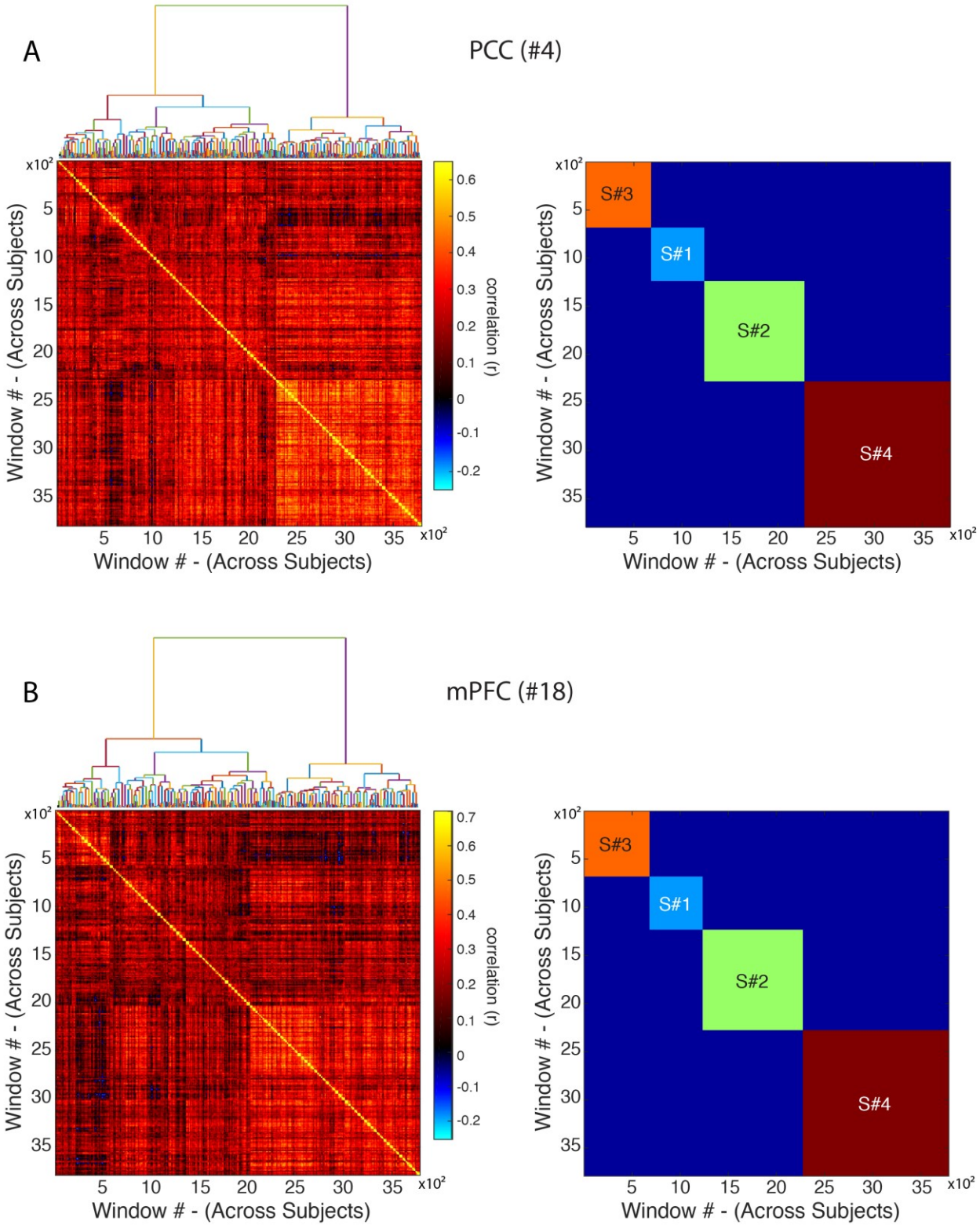

Figure 3.4. Hierarchical clustering of the correlation of each window map to all other window maps across all subjects. Each window map represents the connectivity between the (A) posterior

cingulate cortex (#4) seed to the entire brain and (B) medial prefrontal cortex (#18) to the entire brain. (Left panels) The similarity matrix ordered with hierarchical clustering of the correlation of all window maps to one another under Ward's criteria. The dendogram is shown above the similarity matrix. (Right panels) The clusters defined by the selection of four States. The numbers listed (i.e.: S#3, S#2, etc.) refer to the State numbers referenced in the text.

After clustering, the window maps associated with each state were averaged to provide mean *brain state* maps. To reiterate, in this text we use the acronym for the seed region, followed by the cluster (or state) number, to identify the *brain states* (i.e.: PCC#4 refers to the 4th mean *brain state* derived from the PCC seed region). To visualize the difference of each map with the average connectivity map across all subjects and windows, a z-map was calculated from the *brain state* maps (Figure 3.5). In the *brain state* PCC#3 (Figure 3.5.A.), we found less correlation to the default mode network, while we observed greater correlation to other regions, as compared to the average map. In contrast, the opposite correlation map was observed in PCC#4, where there was increased connectivity to the DMN and diminished connectivity to other regions, as compared to the average map across all subjects. In PCC#1, we observed a similar pattern of connectivity as with PCC#3. In PCC#1, we observed low connectivity to the medial prefrontal cortex region, and high connectivity to the cerebellar areas and the thalamus caudate region, as compared to the average map. In PCC#2, we observed a moderate reduction of connectivity to the PCC region itself, as well as to the occipital lobe and cerebellum, while there was a mild increase in connectivity to most other regions, as compared to the average connectivity across all subjects.

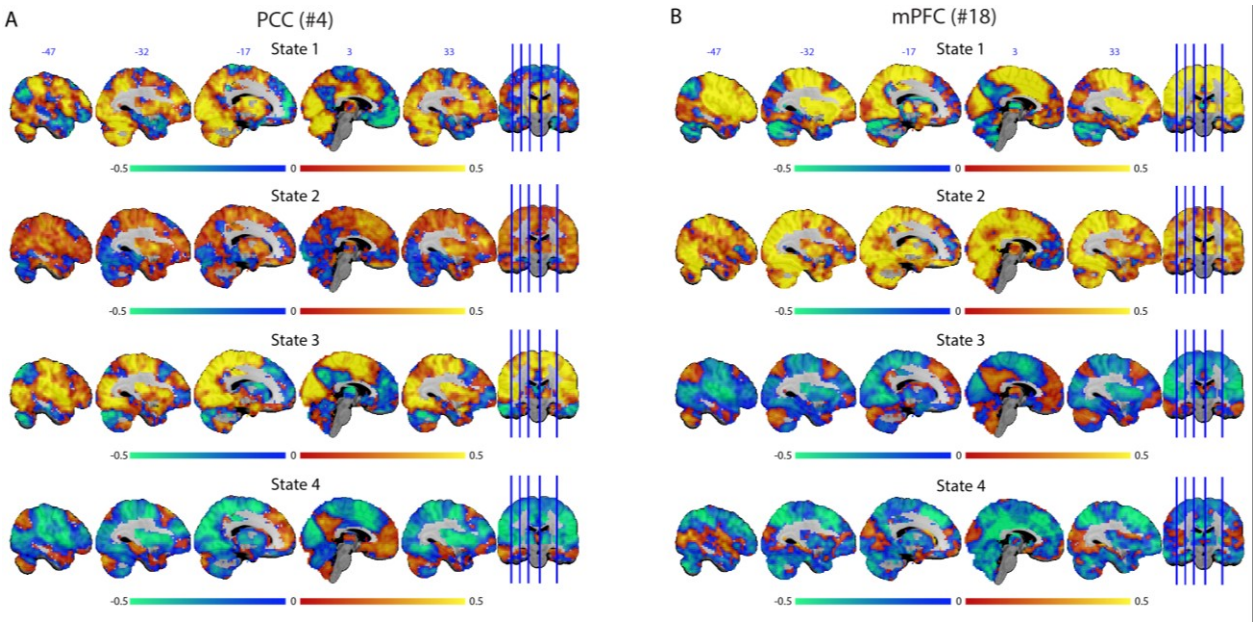

Figure 3.5. Z-maps of each *brain state* relative to the average voxel-wise connectivity between (A) the posterior cingulate cortex seed and the entire brain (B) the medial prefrontal cortex seed and the entire brain. State-wise connectivity is calculated as the average of the voxel-wise connectivity within all windows that correlate most with the given *brain state* of interest.

From the mPFC seed region (Figure 3.5.B.), in the *brain state* mPFC#3 we found an increase in connectivity to the DMN and a reduced connectivity to other regions, as compared to the average map across all subjects. This resembled our observations in PCC#4, and best describes the anticipated connectivity patterns observed from DMN seed regions during resting-state acquisition. In mPFC#1 we observed reduced connectivity to regions of the DMN, and increases in connectivity to other brain areas; however, the reduction in connectivity to the DMN was less pronounced to the mPFC region itself. The connectivity map for mPFC#1 bore a resemblance to a pattern of connectivity observed in PCC#3. In mPFC#2, we observed an increase in connectivity throughout the brain, excluding the mPFC region itself, as compared to the average connectivity map across all subjects. This mPFC *brain state* shows little resemblance to any *brain states* from the PCC. In mPFC#4 there is an extensive reduction in connectivity to most regions, except in areas of the occipital lobe, the cuneus, and the middle temporal gyrus.

The *brain state* maps provide insight into how the connectivity varies from the given seed region to the rest of the brain over the dataset, but does not provide information about the distribution of time spent in the *brain state*, by subject or cohort. In order to determine how the window maps were distributed across subjects, cohorts and time-series for each state, we differentiated the information in the following two figures. In Figure 3.6, the windows across subjects for each *brain state* are represented both as a bar graph and a boxplot. In Figure 3.7, the distribution of windows by cohort and *brain state* are shown.

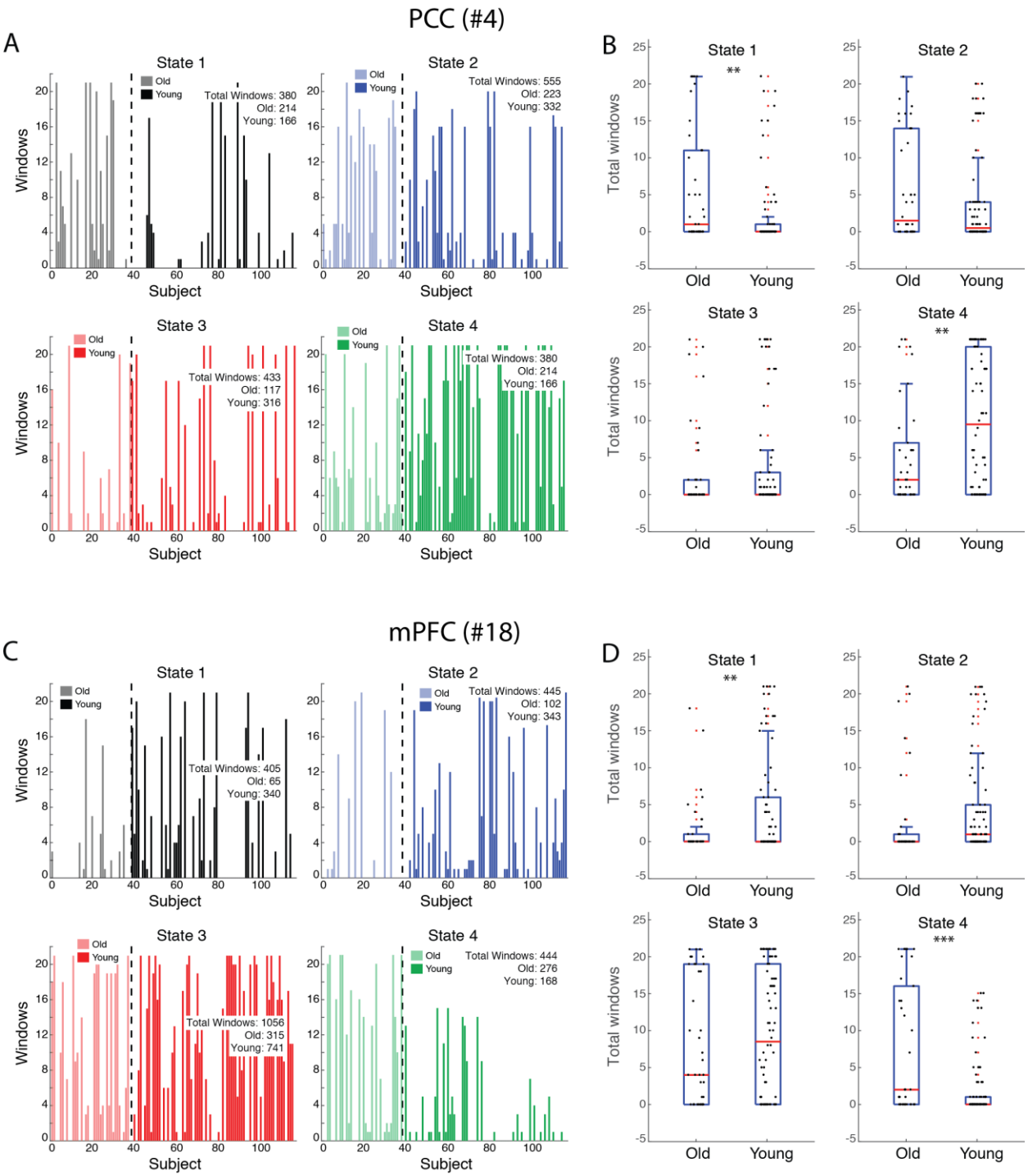

Figure 3.6. Distribution of window maps by *brain state* and cohort. The upper panels (A & B) represent the posterior cingulate cortex seed and the lower panels (C & D) the medial prefrontal cortex seed. In (A) & (C) the number of window maps that are most correlated to the given *brain state* by subject. The dashed line demarcates the older and younger cohorts, with the older cohort to the left of the dashed line. In (B) & (D) boxplots show the distribution of the number of windows for each subject associated with the given *brain state*, by cohort. Permutation testing on the proportion of windows distributed across subjects and cohorts (n=100,000) determined the

brain states that had a significant tendency to associate preferentially to either older or younger subjects (Posterior cingulate cortex: PCC#1 & PCC#4: $p<0.01$; Medial prefrontal cortex: mPFC#1: $p<0.01$, mPFC #4: $p<0.001$).

We ran permutation tests to determine the significance ($p<0.05$, n=100,000) of the age-related differences in state composition we observed. For the PCC seed region, the association of the subject windows to the *brain states* PCC#1 and PCC#4 were significantly different between the old and young cohorts (both, $p<0.01$). The *brain state* PCC#1 was comprised largely by older subjects, while PCC#4 was associated predominantly with younger subjects (Figure 3.7.A). From the mPFC seed region, there was a significant association by age cohort of subject windows to mPFC#1 and mPFC#4 ($p<0.01$ and $p<0.001$, respectively). The mPFC#1 *brain state* was comprised primarily of younger subjects, while mPFC#4 was largely associated with the older subjects (Figure 3.7.B). These results show that differences in the connectivity profiles of certain *brain states* are sufficient to be distinguished significantly by age cohort.

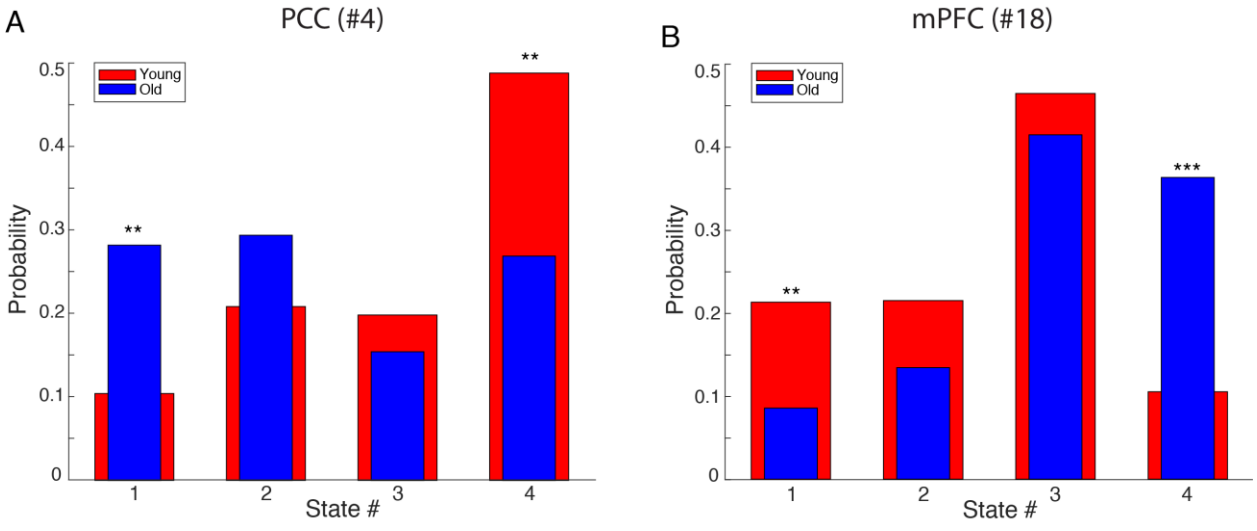

Figure 3.7. Proportional distribution of windows by *brain state* for (A) the posterior cingulate cortex seed and (B) the medial prefrontal cortex seed. The proportion of time spent in each window by cohort (this is equivalent to the probability of spending time in the given state, by cohort). The significance of the results is based on permutation testing the proportion of windows distributed across subjects and cohorts (n=100,000; * $p<0.05$, ** $p<0.01$, *** $p<0.001$).

Each time window was assigned to a given *brain state* following the clustering procedure. Despite this a given window may maintain similar, albeit slightly less, correlation to other *brain states* as to the assigned *brain state*. In order to better understand the relationship between the window map and its association to the mean state maps, we computed the correlation between the window map and each of the *brain state* maps. This provided a weight, measuring the strength of association to each of the *brain states* from each window map.

The strength of the weight scores varied over time, yet revealed consistently greater scores for one *brain state* over another in most subjects. The weight scores obtained from PCC and mPFC, are displayed across all windows and *brain states*, for each cohort in Figure 3.8 (*Left panels*). The distribution of weight scores by *brain state* and cohort is displayed on the right panels.

We ran a general linear model (GLM) on the mean weight values computed from each subject for each *brain state*. The variable of interest was age cohort, while sex was controlled for as a covariate. In the PCC seed region, weight values were similar between age cohorts for all *brain states*, however we observed a trend identifying age-related differences in PCC#3 and PCC#4 ($p<0.1$). For the mPFC seed region, we found a significant difference between weight values by age cohort in mPFC#1 and mPFC#2 ($p<0.01$ and $p<0.001$, respectively), but no difference in the other *brain states*. In both seed regions, we found the *brain states* that were significantly associated with the older, but not the younger, cohort did not differentiate significantly when comparing weight scores. This may be a result of the different sample sizes of young and old subjects in this analysis.

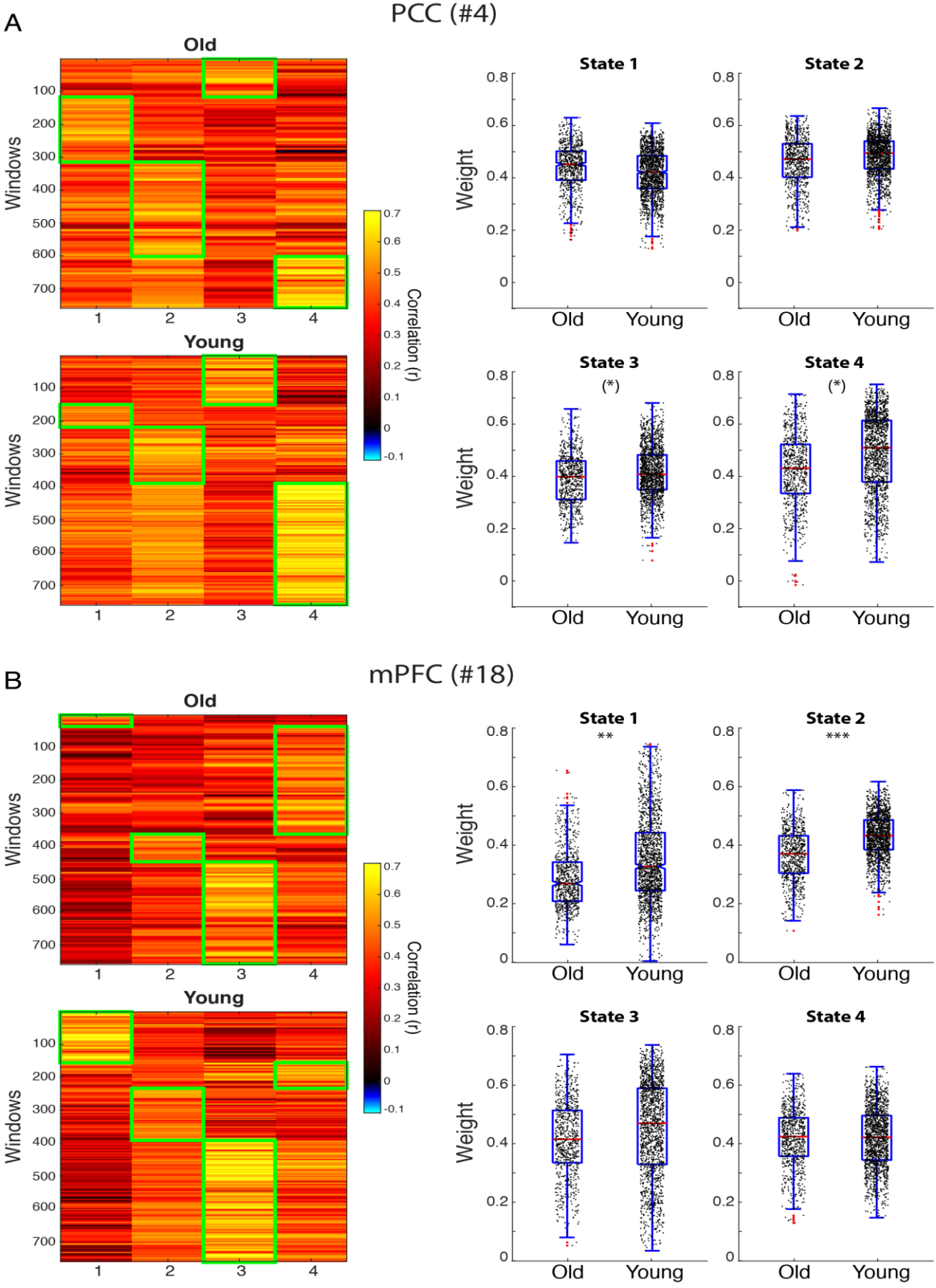
A
PCC (#4)
Old
Young
Windows
Correlation (r)
State 1
State 2
State 3
State 4
Weight
(*)
B
mPFC (#18)
**
***

Figure 3.8. Correlation of each *brain state* across windows and cohorts (i.e.: weight) for both (A) the posterior cingulate cortex seed and (B) the medial prefrontal cortex seed. The left panels show a visual representation of each state (columns) and the correlation to all windows (rows), by cohort. This is ordered by State, with the bright green line demarcating areas where the given State shows the greatest correlation to the respective windows as compared to the other States. The right panels show boxplots of the distribution of the weights for each State across cohorts. We analyzed the weight scores using a general linear model with the age cohort as the variable of interest, and sex as a confounding factor, where (*) q<0.1, * q<0.05, ** q<0.01, *** q<0.001.

The relationship (correlation) of each *brain state* map to one another is listed in Figure 3.9. The mean of the correlations was lower for the mPFC seed region than the PCC seed region (0.675 vs 0.743), but not significant (p=0.27).

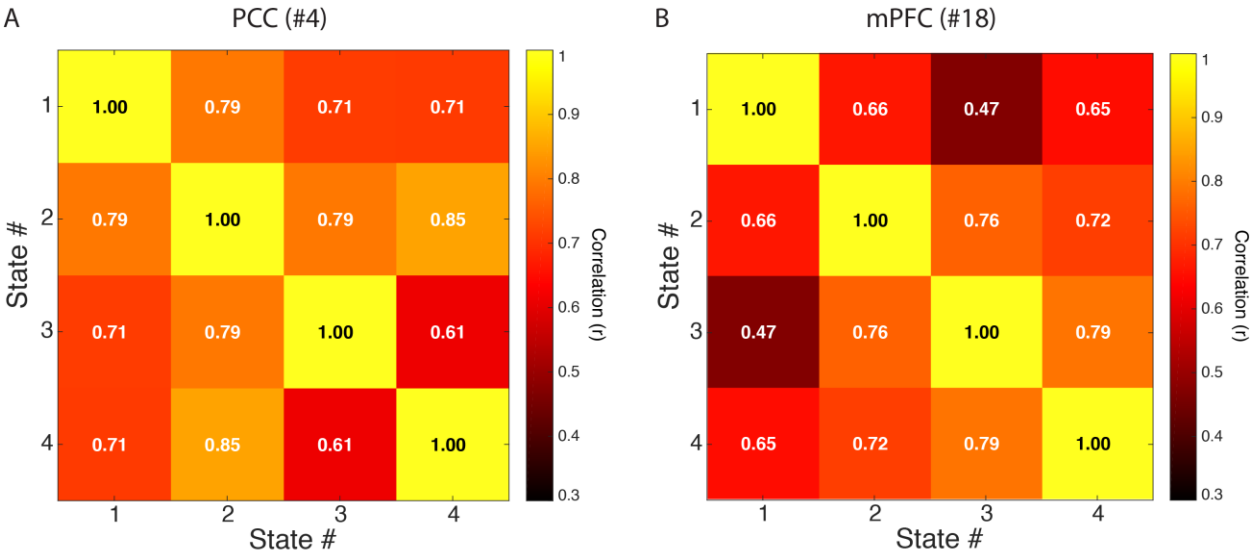

Figure 3.9. The correlation of each of the *brain states* with one another.

We assessed the relevance the association of *brain states* to time windows, across subject and cohorts, may have on our original static GLM analysis with age as the variable of interest. We identified mPFC#4 as the *brain state* that most significantly differentiated (p<0.001) between the old and young subjects (Figure 3.7.B). We then removed half of the older subjects that were most associated with the mPFC#4 *brain state* (i.e. weight value

greater than the median) and repeated the static analysis. We hypothesized these subjects would explain more of the variance we found between age groups from the initial static analysis, than those whose weight values were less than the median.

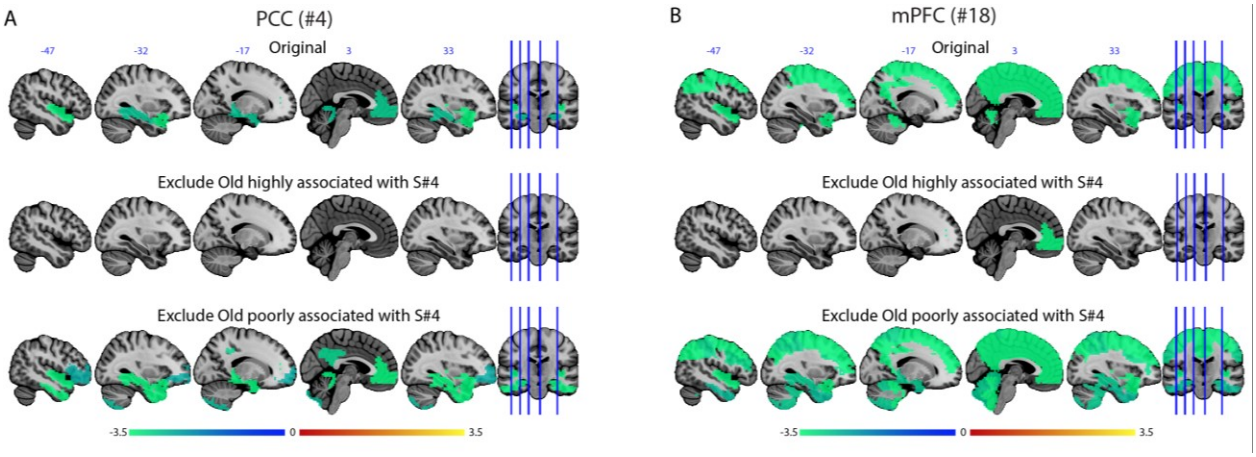

Figure 3.10. Post-hoc GLM analysis of age-related changes in connectivity when excluding sub-groups of old subjects that are highly or poorly associated with mPFC#4. Connectivity is measured between the seed-region (A) posterior cingulate cortex (#4) and (B) medial prefrontal cortex (#18) and the entire brain, during resting-state. The general linear model is run on the MIST-36 network atlas comparing network connectivity with the age cohort as the variable of interest, while controlling for sex as a covariate. (Upper panels) The original GLM analysis included all subjects. (Middle panels) The GLM analysis excluding the sub-group of older subjects that has a greater association to mPFC#4 than the median value. (Bottom panels) The GLM analysis excluding the sub-group of older subjects that has less association to mPFC#4 than the median value. Significant differences between cohorts (FDR, $q<0.05$).

Following the removal of the older subjects most associated with the mPFC#4 *brain state*, we noted fewer significant differences in connectivity between the old and young subjects in the GLM analysis (Figure 3.10, Middle row). From the PCC seed region there were no longer any significant age-related differences in connectivity ($q<0.05$; Figure 3.10.A, middle row). Likewise, from the mPFC seed region only connectivity within the region itself remained significantly different between old and young subjects ($q<0.05$; Figure 3.10.B, middle row). The age-related differences we observed across the majority of the frontal and parietal lobes in the original analysis (Figure 3.10.B., upper row), were no longer significant ($q<0.05$).

To confirm that these observations did not simply arise from a reduced sample size, we repeated the analysis by removing the same number of old subjects with weight values that fell below the median for mPFC#4.

By contrast with the previous test, there was an increase of significant age-related findings ($q<0.05$; Figure 3.10, Bottom row) from both the PCC and mPFC seed regions, as compared to the original GLM assessment with all subjects ($q<0.05$; Figure 3.10, Top row). From the PCC seed region, we observed a significant difference within the region itself that we did not previously find (Figure 3.10.A, Bottom row), while from the mPFC seed region, we identified significant age-related connectivity differences in all brain regions, including the cerebellum, but excluding the occipital lobe (Figure 3.10.B, Bottom row).

To determine if any psychometric or physiologic characteristics might significantly associate with either of the excluded older groups, we ran a Student's t-test with a Bonferroni correction for multiple samples. The NKI-e dataset is a rich dataset that provides many psychometric measures, including tests for cognitive and executive functioning, short-term memory and working memory. Despite this, many of these tests were not complete for all subjects and we needed to exclude a number of them from the analysis. This included the Rey Auditory Verbal Learning Test, the Digit Span test and the Delis-Kaplan Executive Functioning System battery. We were able to include results from the Wechsler Abbreviated Scale of Intelligence, the NEO Five Factor Inventory, the Pittsburgh Sleep Quality Index and physiological measures that included age, sex, handedness, blood pressure, pulse, and body-mass index.

Even before multiple comparison correction, however, we did not find any significant relationship between any of these variables and the sub-groups of older subjects that were either highly or weakly associated to mPFC#4 (All, $p>0.188$, uncorrected). We

likewise found no association between movement in the scanner (measured as average frame displacement after censoring) and these older sub-groups (p= 0.915).

3.1.2.3. Transitions:

To explore the dynamics of the functional connectivity measures, we computed the state transition probabilities for each cohort (Figure 3.11). Transition probabilities that showed significant age-related differences ('Old' minus 'Young') are highlighted in the bottom panels ($p<0.05$). Negative values (blue background) indicate higher transition probabilities for the young cohort, while positive values (white background) indicate more transitions for the old cohort. The *brain state* PCC#4 was significantly associated with the younger cohort, and we found a significantly greater likelihood of younger subjects remaining in this state than older subjects. By contrast, mPFC#4 was significantly associated with the older cohort, and correspondingly we found a significantly greater likelihood that older subjects remained in this state as compared to younger subjects. Further, we found there was a significantly greater likelihood that younger subjects would transition from mPFC#4 to mPFC#1, as compared to the older subjects. The *brain state* mPFC#1 was associated significantly with the younger cohort of subjects, as compared to the older cohort. We also observed trends ($p<0.1$), whereby older subjects transitioned more frequently from mPFC#1 to mPFC#4, and younger subjects were more likely to remain in mPFC#1, as compared to the older subjects.

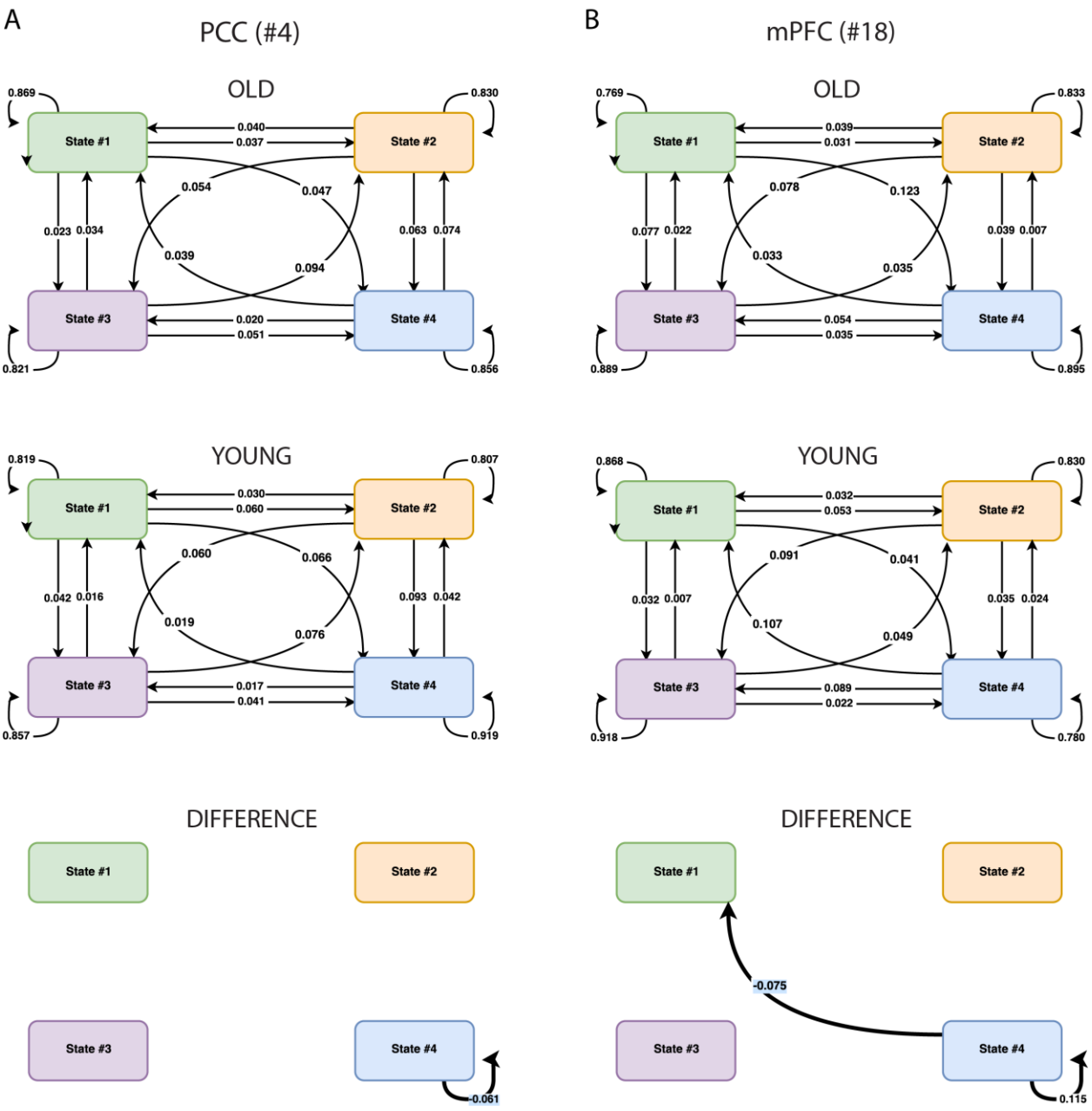

Figure 3.11. Transition probabilities between *brain states* for older, younger and the difference between cohorts, for (A) the posterior cingulate cortex seed and (B) the medial prefrontal cortex seed. In the top panels the transition probabilities between *brain states* for the older cohort are listed. In the middle panels the transition probabilities between *brain states* for the younger cohort are shown. The bottom panels show the difference in transition probabilities between cohorts (Older minus Younger; thus the negative values highlighted in blue depict a higher value for the younger cohort and vice-versa for the older cohort). Only significant differences are shown ($p<0.05$).

In Figure 3.11, we only displayed transitions between *brain states*. We did not include periods that were censored from the time-series due to excessive movement. This accounted for only 0.85% of the transitions in the NKI-dataset. In the PCC seed region, none of these transitions differed significantly by the age cohort. In the mPFC seed region, however, younger subjects were significantly more likely to transition from periods of movement into mPFC#1 ($p<0.05$), while older subjects were significantly more likely to transition into mPFC#3 ($p<0.05$) from periods of movement, than were the younger subjects. There was no significant difference in terms of age group in regards to the transition frequencies from a given State to periods of movement (All, $p>0.05$).

We next investigated the overall frequency each cohort switched states. In the PCC seed region, switches between states were not significantly different between the old and young cohorts (13.8% vs 12.0%, $p=0.22$). Similarly, in the mPFC seed region, there was no significant difference for the frequency of transitions between states between the old and young cohorts (11.2% vs 11.9%, $p=0.61$).

We then assessed the impact that remaining in a *brain state* and transitioning from a *brain state* would have on mean connectivity for each of the seeds. In the PCC, there was no significant difference in overall mean connectivity for transitions out of or remaining in a *brain state*, in either cohort (All, $p>0.1$). When looking at individual *brain states*, we found greater mean connectivity in PCC#1 for the older cohort for remaining in, rather than transitioning out of the *brain state* (0.224 vs 0.186, $p=0.037$). Likewise, for PCC#3, we found a greater mean connectivity in younger subjects and overall for those subjects that remained in the *brain state*, than the subjects that transitioned to another *brain state* (Young: 0.276 vs 0.235, $p<0.001$, All: 0.263 vs 0.220, $p<0.001$).

In the mPFC, we did not observe any significant difference in overall mean connectivity for transitions out of or remaining in a *brain state*, across subjects and cohorts (all, $p>0.4$).

When looking at individual *brain states*, we found a significantly greater mean connectivity in older subjects that remained, rather than transitioned from mPFC#2 (0.330 vs 0.272, p=0.017).

3.1.2.4. Summary:

In this study, we analyzed the resting-state data of young and old subjects using static and dynamic methods. We identified the expected age-related reduction in connectivity between the posterior and anterior regions of the brain using both methods. With the dynamic methods, we were able to identify *brain states* that were significantly associated to one of the age cohorts. We also identified *brain states* from each seed region that displayed typical DMN activity (PCC#4, mPFC#3), as we anticipated. The *brain state* mPFC#4 was most associated with older subjects that explained the age-related variance from the static analysis. As compared to the average across all subjects, this *brain state* was characterized by a diminished connectivity throughout the brain, except in areas of the occipital lobe, the cuneus, and the middle temporal gyrus. These results are consistent with our original hypotheses.

3.2. Sleep

3.2.1. Introduction

For this study, we analyse fMRI data from young and older subjects sleeping in the scanner. Our goal is to identify age-related differences using both static and dynamic analyses. The static analysis will again serve as a baseline analytic benchmark. Our focus will be on EEG-confirmed non rapid eye movement stage 2 (NREM2) sleep. To recap, our objectives are as follows:

- Relate the fMRI data to the NREM2 sleep stage.
- Assess the age-related differences using static analysis.
- Dynamically delineate *brain states* during NREM2 sleep.
- Assess the age-related differences in NREM2 *brain states* and compare with the static results

Due to differential age-related activity (k-complexes, sleep spindles, slow-wave sleep) during NREM2 [36], we anticipate measurable differences in our analyses. Older subjects also have greater difficulty entering and remaining in deeper stages of sleep [36], which we anticipate will impact connectivity patterns. Such a result would highlight the importance of measuring and controlling for sleep in age-related resting-state studies, and in general. To recap, our hypotheses are as follows:

Hypotheses:

- An individual *brain state* will be associated with the older cohort.
- The older population will display *brain state* heterogeneity (i.e. divergent sub-cohorts across multiple *brain states*).

- A *brain state* associated with the older population will be characterized by greater connectivity to the DMN, found typically in awake subjects.

The data from the sleep stage NREM2 will be analyzed from two different ROIs from the Cambridge-36 functional network atlas [120]. These seeds comprised the thalamus-caudate (TC, region#8) and the insula (INS, region#28) (Figure 3.12). The thalamus is associated with sleep regulation [86, 87], k-complex activity [83] and sleep spindles [84]. The insula region is believed to be a region of origin for slow-wave sleep [85].

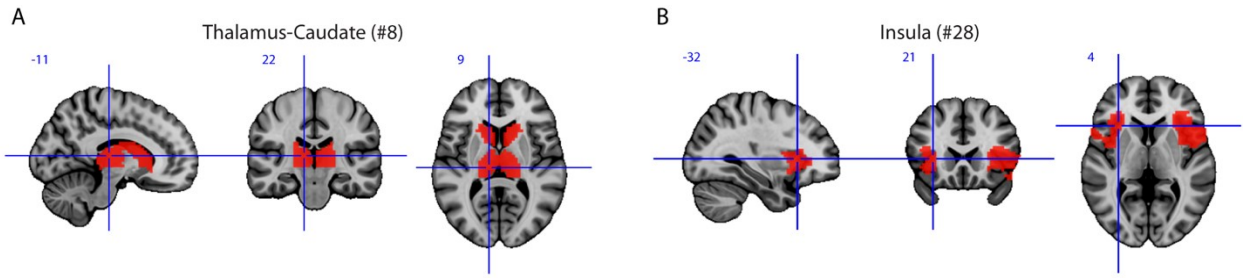

Figure 3.12. MIST-36 regions of interest. A) The thalamus-caudate seed (region of interest #8). B) The insula seed (region of interest #28).

We analyzed 30 subjects (Old: 14 subjects (36% male), 52-69 years, 59.5±5.9yrs; Young: 16 subjects (50% male), 20-30 years, 23.3±3.3yrs) during NREM2 sleep.

3.2.2. Results

3.2.2.1. Static Connectivity

We applied a general linear model to assess the significance of age to connectivity variations within the ROIs (Figure 3.13). The age cohort was the variable of interest and sex was used as a covariate. In the TC a significant (FDR, $q<0.05$) reduction in connectivity to the cerebellum was observed in the older cohort, as compared to the young cohort

(Figure 3.13,A, *Top panel*). No significant differences in connectivity due to age cohort differences were found between the INS and other brain regions (q<0.05, Figure 3.13.B. *Top panel*). The t-maps (*bottom panels*) highlight areas that showed differences albeit not significant under q<0.05.

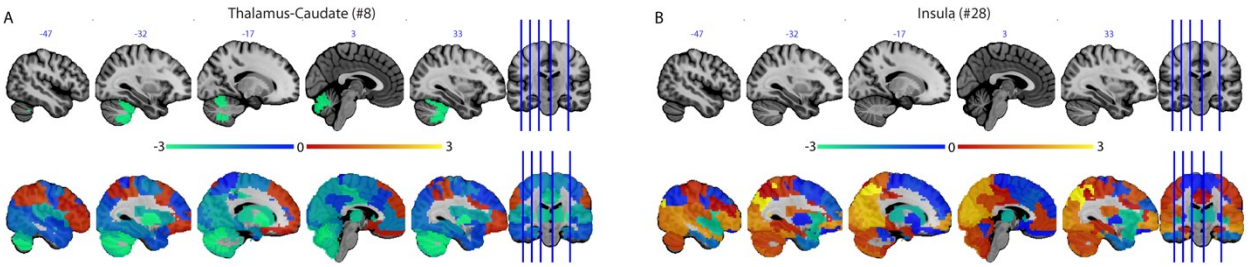

Figure 3.13. Age-related changes in connectivity between (A) the thalamus-caudate seed and (B) the insula seed, and the entire brain, during NREM2 sleep. The general linear model was run on the MIST-36 network atlas comparing network connectivity with the age cohort as the variable of interest, while controlling for sex as a covariate. (Upper panels) Significant differences between cohorts (FDR, q<0.05). (Bottom panels) The map of the t-statistic.

3.2.2.2. Dynamic Connectivity

To first examine the ROIs from a dynamic perspective during NREM2, we computed the mean pairwise connectivity of the selected ROIs from the MIST-36 brain atlas to all the voxels within the functional brain mask, across time windows. This provided us with the voxel-wise connectivity of each ROI with the rest of the brain (Figure 3.14, *Top panel*). The same procedure was applied to each age cohort separately. To visualize these results, we calculated the corresponding z-maps for each cohort (Figure 3.14, *Middle and bottom panels*). In the older cohort we generally observed low connectivity between the thalamus-caudate and the rest of the brain, excluding the orbital frontal cortex and the angular gyrus in which higher connectivity was observed, as compared to the mean connectivity across all subjects. The younger cohort showed the opposite connectivity differences. In contrast, the INS seed generally showed high connectivity to the rest of

the brain in older subjects as compared to the mean connectivity across all subjects. Specifically, the older cohort showed high connectivity from the insula seed to the parietal lobe, as well as areas of the default mode network. The younger cohort by contrast maintained high connectivity between the insula and the cerebellum, along with the thalamic region during NREM2 sleep, as compared to the average across all subjects.

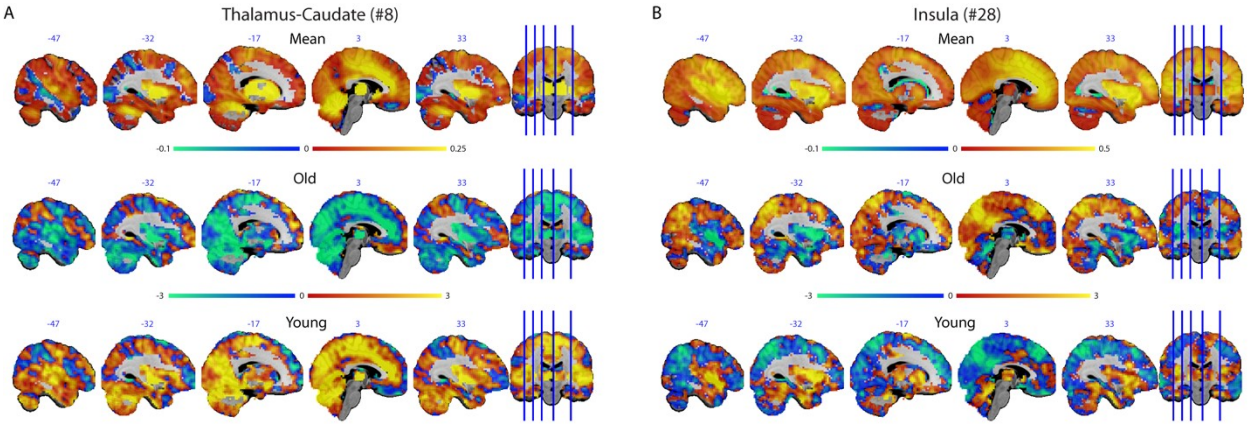

Figure 3.14. Voxel-wise connectivity from the (A) thalamus-caudate seed and (B) insula seed during NREM2. The overall connectivity (top panels) is the mean connectivity of all NREM2 windows across all subjects. The Old cohort (middle panels) section represents the Z-map of the connectivity in the older cohort relative to the mean connectivity across all subjects. The Young cohort (bottom panels) section represents the Z-map of the connectivity in the younger cohort relative to the mean connectivity across all subjects.

To identify *brain states* to which the subjects converged, we performed a hierarchical clustering procedure (Ward's criterion) on the correlation between each window map with all the other window maps (Figure 3.15, *Left panels*). This procedure assigned an associated cluster or state (n=4) to each given window map (Figure 3.15, *Right panels*).

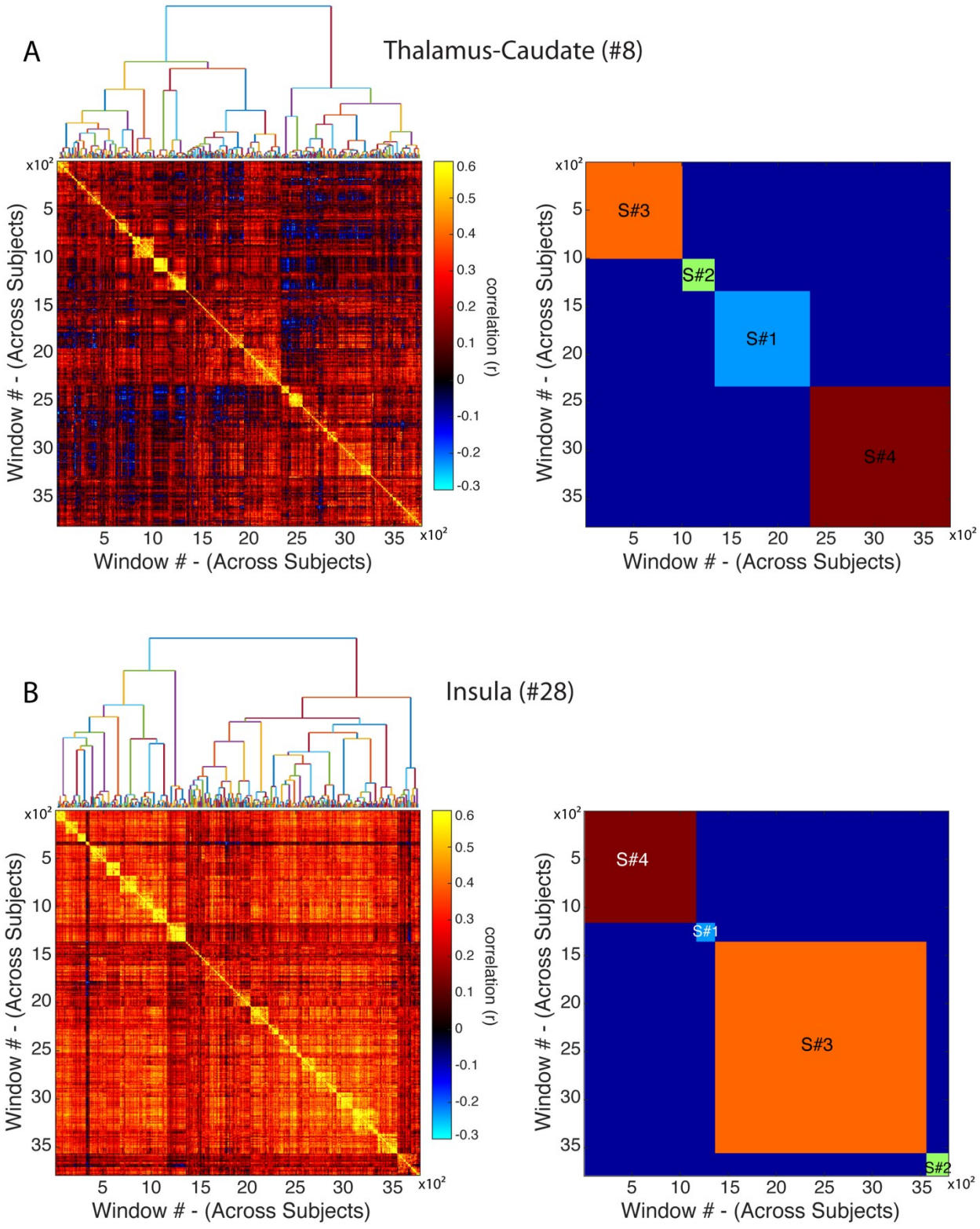
A
Thalamus-Caudate (#8)
x10²
Window # - (Across Subjects)
Window # - (Across Subjects)
correlation (r)
0.6
0.5
0.4
0.3
0.2
0.1
0
-0.1
-0.2
-0.3
S#3
S#2
S#1
S#4
B
Insula (#28)
S#4
S#1
S#3
S#2

Figure 3.15. Hierarchical clustering of the correlation of each window map to all other window maps across all subjects. Each window map represents the connectivity between (A) the thalamus-caudate seed to the entire brain and (B) the insula seed to the entire brain. (Left panels) The similarity matrix ordered with hierarchical clustering of the correlation of all window maps to one another under Ward's criteria. The dendogram is shown above the similarity matrix. (Right panels) The clusters defined by the selection of four States. The numbers listed (i.e.: S#3, S#2, etc.) refer to the State numbers referenced in the text.

After clustering, the window maps, associated with each state, were averaged to provide *brain state* maps. To visualize the difference of each map from the average connectivity map across all subjects and windows, a z-map was calculated from the *brain state* maps (Figure 3.16). In the TC seed (Figure 3.16.A.) the TC#2 and TC#4, respectively, showed maps of broadly less and more correlated regions with the ROI seed, as compared to the average map. The *brain state* TC#3, although largely uncorrelated with the parietal lobe, tended to be more correlated in regions of the default-mode network. In TC#1, areas of the occipital lobe and cerebellum showed greater connectivity, whereas other regions tended to show less connectivity, as compared to the average connectivity map.

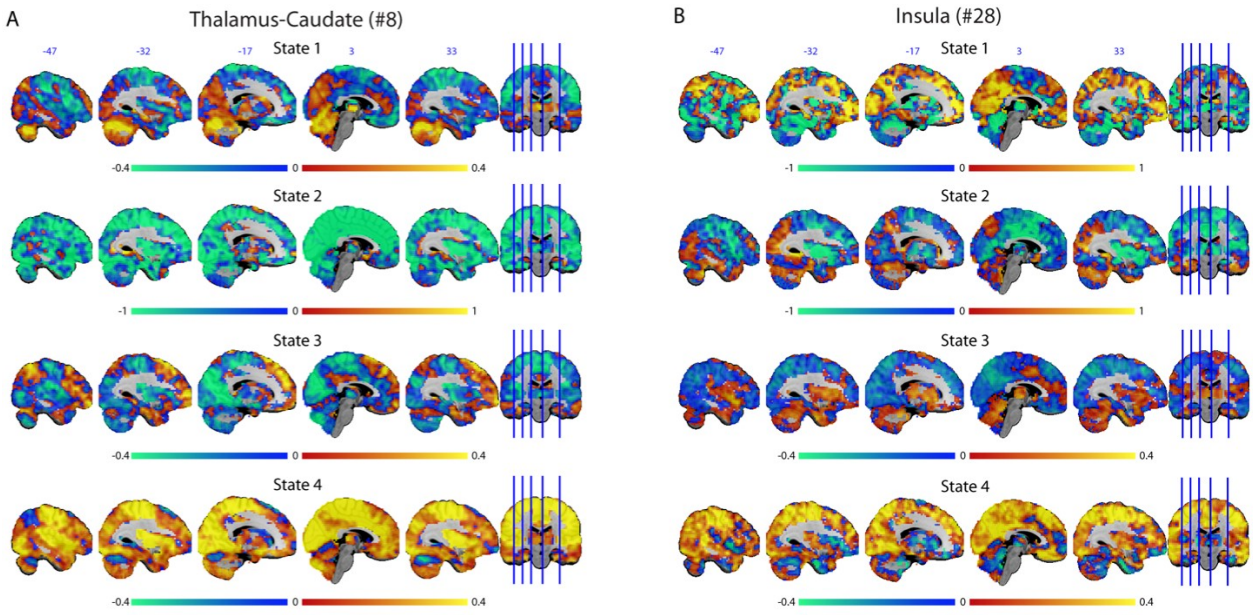

Figure 3.16. Z-maps of each *brain state* relative to the average voxel-wise connectivity between (A) the thalamus-caudate seed and (B) the insula seed, and the entire brain, during NREM2 sleep.

State-wise connectivity is calculated as the average of the voxel-wise connectivity within all windows that correlate most with the given *brain state* of interest.

In INS#1, from the insula seed region, we found greater correlation with most other parts of the brain, excluding the cerebellum, motor areas and the thalamus, as compared to the mean connectivity across all subjects (Figure 3.16.B). The *brain state* INS#2 generally showed less correlation than the average, except to areas of the precuneus, occipital lobe and the cerebellum. The INS#3 *brain state* showed a small increase in correlation between the insula and the cerebellum, the thalamic region and within the insula area itself, as compared to the average. Otherwise, we observed a decreased connectivity to other areas. This map resembles the average connectivity maps across young subjects (Figure 3.14.B, *Bottom panel*). In INS#4, aside from the connectivity to the cerebellum and insula itself, we observed an overall increase in connectivity between the insula and the rest of the brain, as compared to the average connectivity across all subjects.

The *brain state* maps provide insight into how the connectivity varies from the given ROI with the rest of the brain over the dataset, but does not provide information as to the subject composition of each State. In order to determine how the window maps were distributed across subjects, cohorts and time-series for each state, we differentiated the information in the following two figures. In Figure 3.17, the windows across subjects for each state are represented both as a bar graph and boxplot. In Figure 3.18, the distribution of windows by subject and state, along with the proportional distribution of State by subject are shown. Of note, TC#2, INS#1 and INS#2 were driven mainly by two, one and one subjects respectively (Figure 3.17.A and C.). As a result, different color scales were applied to the corresponding displays in Figure 3.16, due to the increased variance from single subjects.

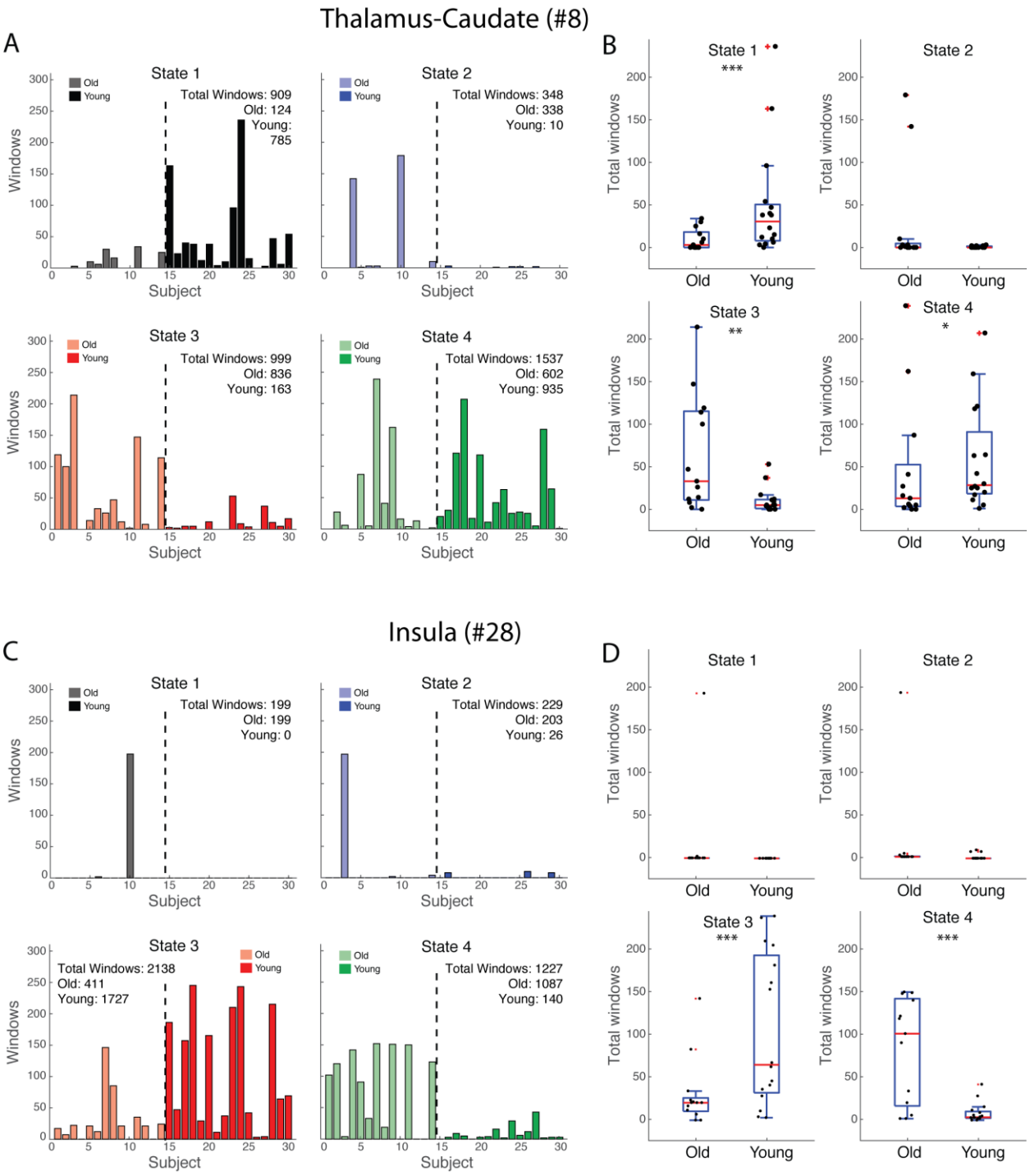

Figure 3.17. Distribution of window maps by *brain state* and cohort. The upper panels (A & B) represent the thalamus-caudate seed and the lower panels (C & D) the insula seed. In (A) & (C) the number of window maps that are most correlated to the given State by subject. The dashed line demarcates the older and younger cohorts, with the older cohort to the left of the dashed line. In (B) & (D) boxplots show the distribution of the number of windows for each subject associated with the given state, by cohort. Permutation testing the proportion of windows distributed across subjects and cohorts (n=100,000, * $p<0.05$, ** $p<0.01$, *** $p<0.001$) showed all *brain states* had a

significant tendency to associate preferentially to either older or younger subjects, except the *brain states* driven by only one or two subjects (TC#2; INS#1, INS#2).

Permutation testing on the likelihood of observing these age-related differences by chance showed that all *brain states*, excluding those driven by only one or two subjects were significantly against the null hypothesis. For the TC seed, average window map associations to TC#1, TC#3, and TC#4 were significantly different between the old and young cohorts (#1: $p<0.001$, #3: $p<0.01$, #4: $p<0.05$). For INS, the window maps were differentially associated to INS#3 and INS#4 by cohort ($p=0.001$, in both cases). These results demonstrate that young and old cohorts differ significantly in the amount of time they spent in the different States.

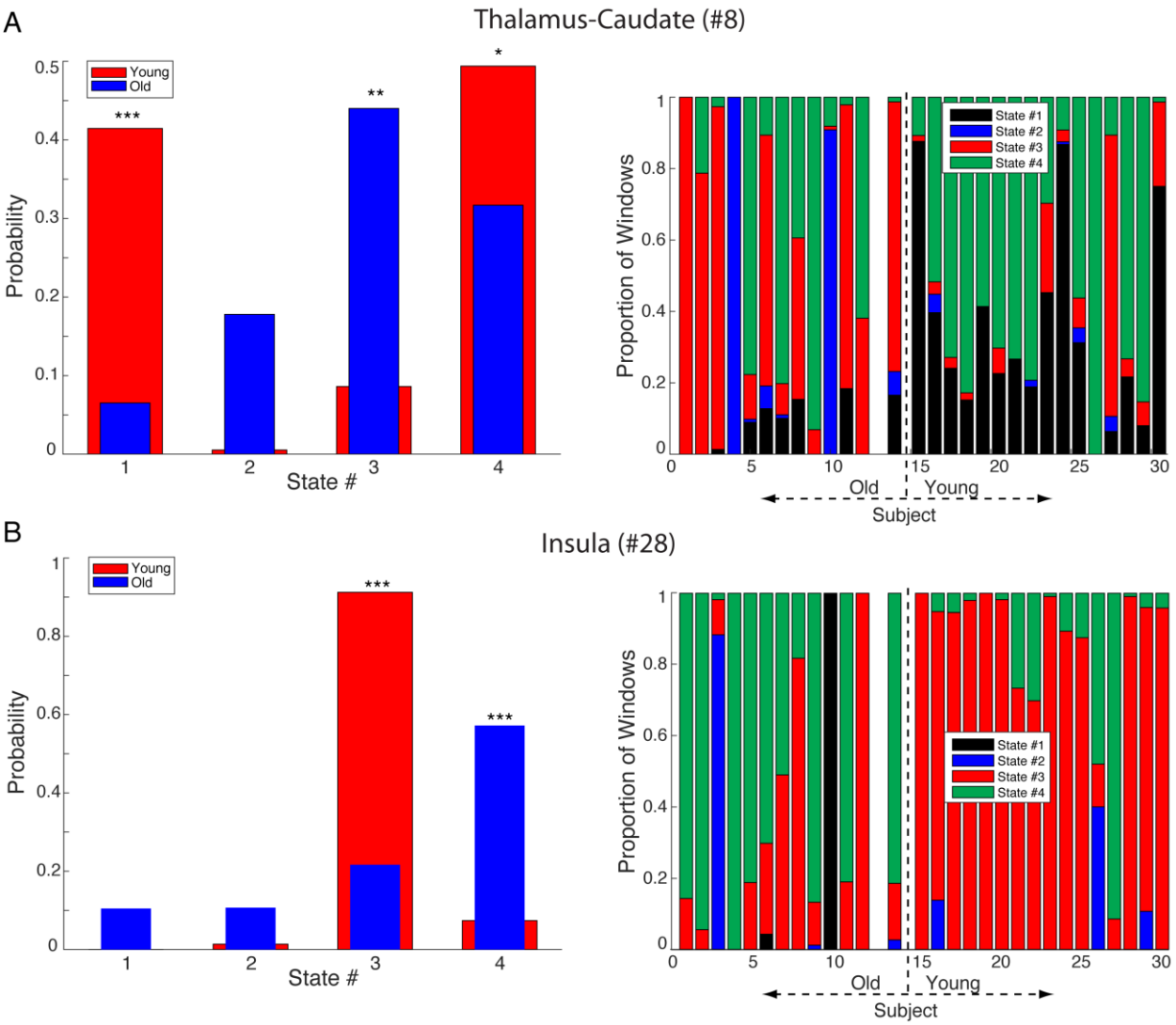

Figure 3.18. Proportional distribution of windows by state and subject for (A) the thalamus-caudate and (B) the insula seed. The (left panels) represent the proportion of time spent in each window by cohort (this is equivalent to the probability of spending time in the given state, by cohort). The (right panels) represent the proportion of time spent in each state by subject. The older and younger cohorts are demarcated by the dashed line. The significance of the results is based on permutation testing the proportion of windows distributed across subjects and cohorts (n=100,000; * p<0.05, ** p<0.01, *** p<0.001).

Every window was assigned to a given state following the clustering procedure. Despite this a given window may maintain similar, albeit slightly less, correlation values to other states as to the assigned state. In order to better understand the relationship between the window map and its association to the mean state maps, we computed the correlation

between the window map and each of the state maps. This provided a weight measure of the strength of this relationship. An example of how this window-state correlation varied over time within subjects is shown in Figure 3.19.

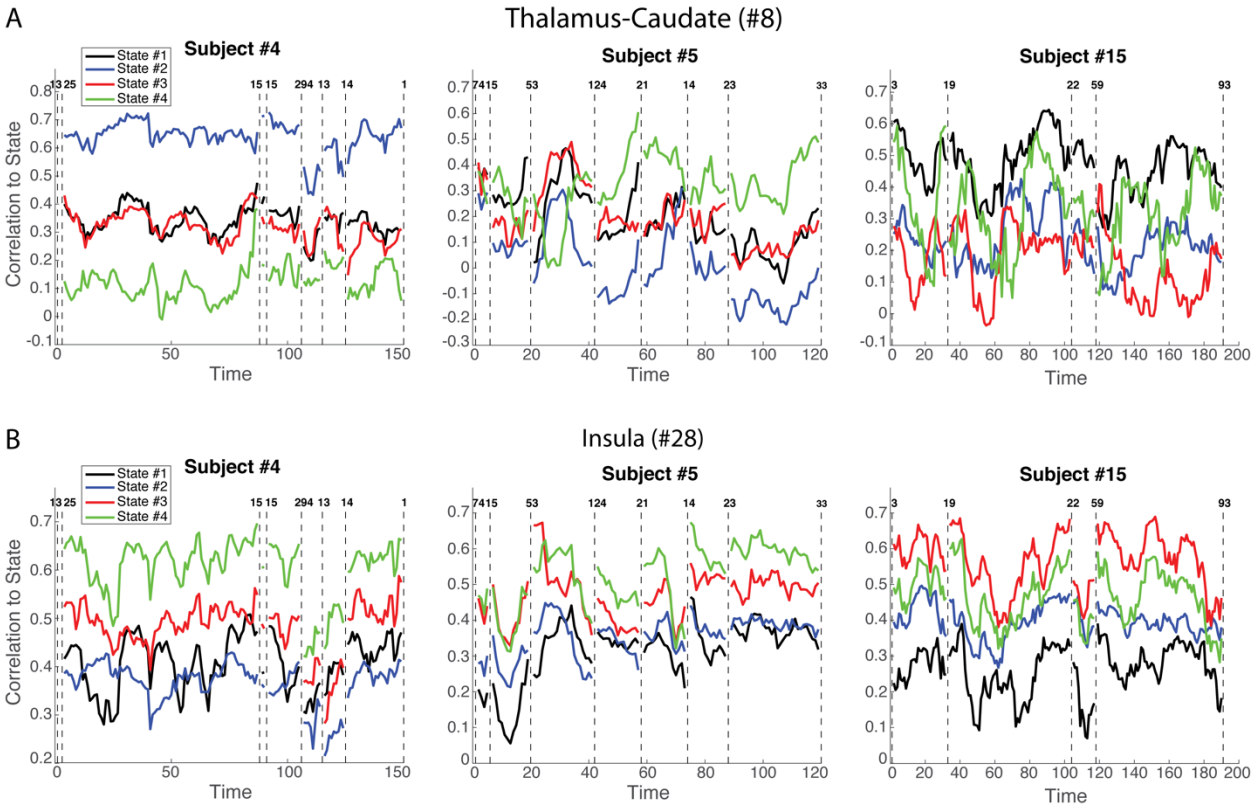

Figure 3.19. The correlation of each State to the window maps measured across time by subject. Each time iteration represents 9.84sec; whereby each window of time advances 4 volumes with a repetition time of 2.46s between each volume. The same three example subjects are chosen for both the (A) thalamus-caudate seed and (B) the insula seed. The dashed line signifies periods in which the subject no longer is in NREM2 sleep, while the number above the line denotes the number of windows the subject spent outside NREM2 during this period. The subjects provide a sample of some the variability seen over time, both in terms of how the association to each State can show consistency and unevenness over time, as well as, the impact of leaving and entering NREM2.

The strength of these weight scores (correlation to *brain state*) varied over time, yet revealed one dominant state in time in most subjects (albeit the dominant state differed across subjects). The weight scores obtained from TC and INS, are displayed across all

windows and states, for each cohort in Figure 3.20 (*Left panels*). The distribution of weight scores by State and cohort is displayed on the right panels.

A general linear model was run on the mean weight values computed from each subject. The variable of interest was age cohort, while sex was controlled for as a covariate. The GLM revealed a significant difference between the TC connectivity weight values of the old and young cohorts for TC#1 and TC#4 ($p<0.001$ and $p<0.01$, respectively), while TC#3 showed a trend ($p=0.055$). In contrast, weight values for INS connectivity were similar between age cohorts for all the States.

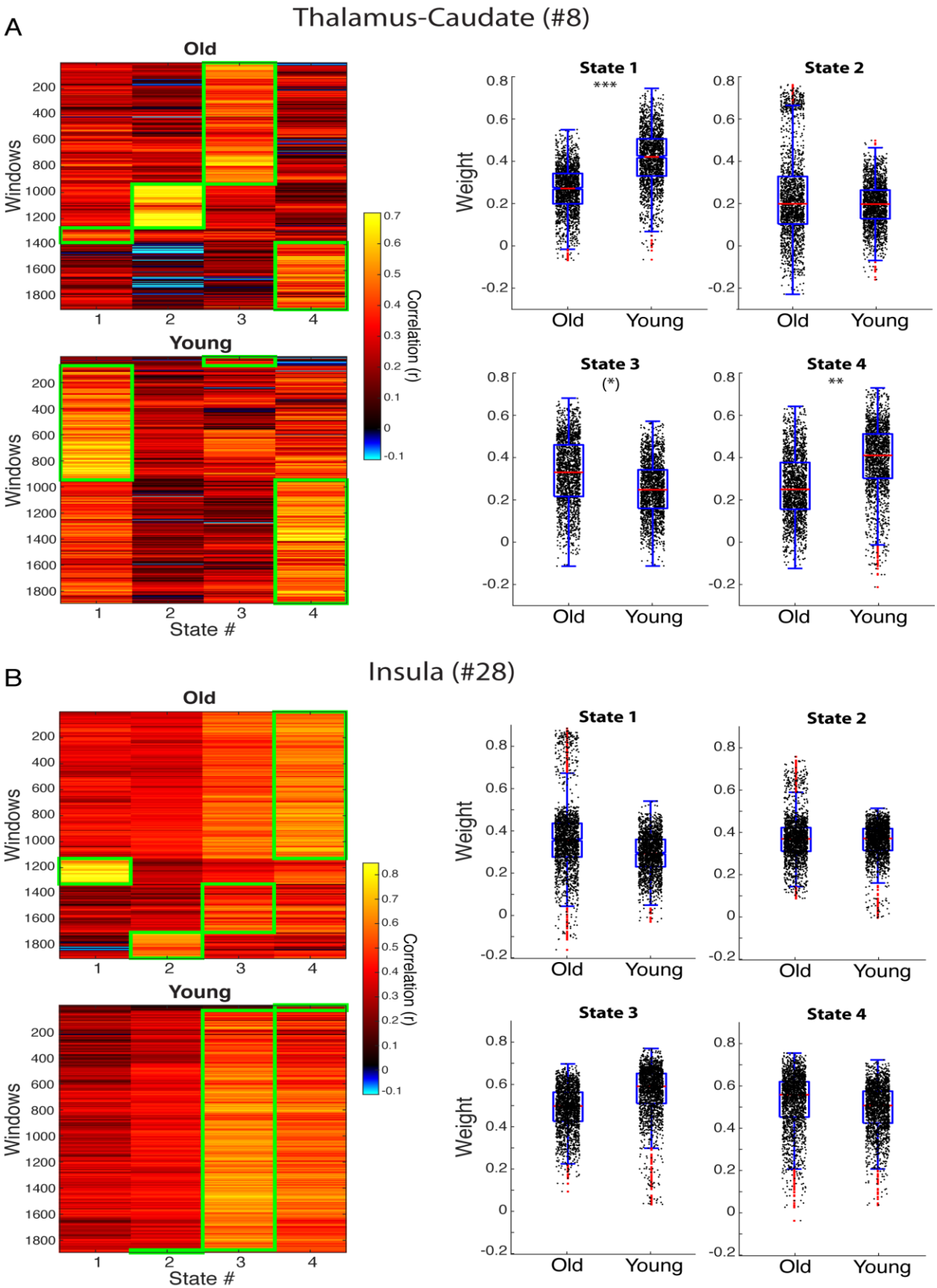
A
Thalamus-Caudate (#8)
Old
Young
Windows
State #
Correlation (r)
State 1
State 2
State 3
State 4
Weight
Old
Young
***
(*)
**
B
Insula (#28)

Figure 3.20. Correlation of each *brain state* across windows and cohorts (i.e.: weight) for both (A) the thalamus-caudate seed and (B) the insula seed. The left panels show a visual representation of each state (columns) and the correlation to all windows (rows), by cohort. This is ordered by *brain state*, with the bright green line demarcating areas where the given *brain state* shows the greatest correlation to the respective windows as compared to the other *brain states*. The right panels show boxplots of the distribution of the weights for each *brain state* across cohorts. A general linear model using the age cohort as the variable of interest, while maintaining sex as a confounding factor, where (*) q<0.1, * q<0.05, ** q<0.01, *** q<0.001.

The relationship (correlation) of each mean state map to one another is listed in Figure 3.21. In line with these GLM results the mean of the correlation between the States was greater in the INS than in the TC seed (0.6 vs 0.49), however, this difference was not significant (p=0.32).

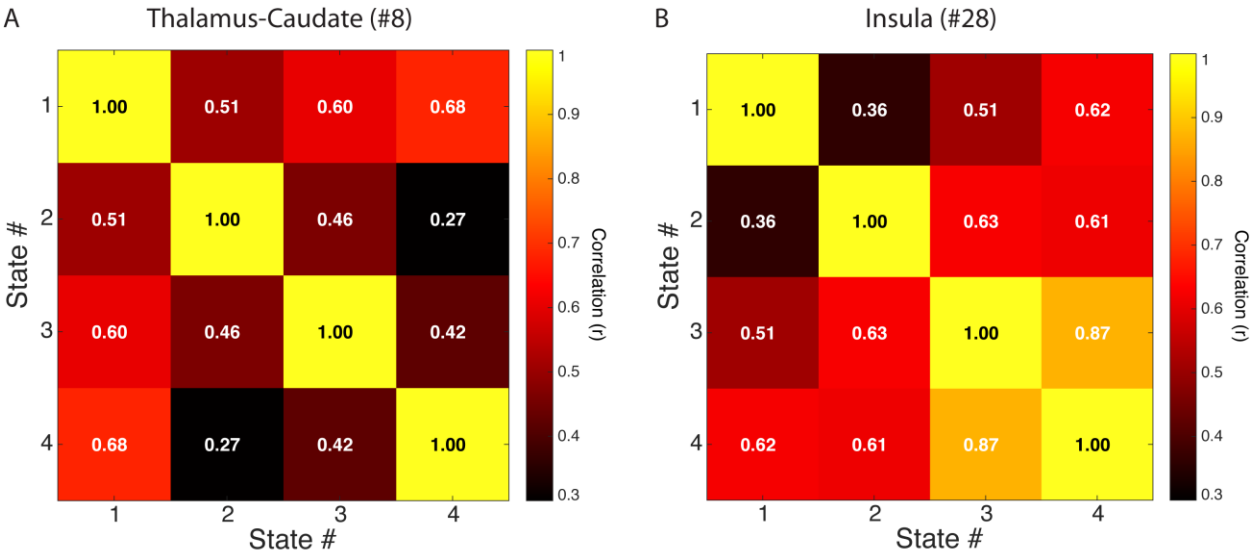

Figure 3.21. The correlation of each of the *brain states* with one another.

3.2.2.3. Slow-Wave Sleep

We assessed the relationship between State and other measures of sleep beyond sleep stage. We used linear regression analysis to evaluate slow-wave sleep (SWS) density and its relationship to the time spent in each state (Figure 3.22). We only analyzed the *brain*

states TC#4, and INS#3, as data in the other states were insufficient for analysis. When the cohorts were combined, we found significant positive correlations emerged (TC: $p<0.01$; INS: $p<0.05$) suggesting that the time spent in these *brain states* increased as SWS density increased. When we analyzed these findings by cohort, however, we found only a non-significant trend in TC#4 for the older cohort ($p=0.055$) and less so with the younger cohort ($p=0.139$; Figure 3.22.A.). For INS#3, we did not observe any significant linear relationship between the time spent in *brain state* and SWS density ($p>0.1$; Figure 3.22.B.). The result from the TC#4 cohort analysis may be influenced by the relatively small sample size. Likewise, the cohort-level results in INS#3, and potentially TC#4, may be confounded by the relationship between SWS and age, whereby SWS density decreases with age. In both of these *brain states* younger subjects spent significantly more time in the state, than subjects from the older cohort (Figure 3.18).

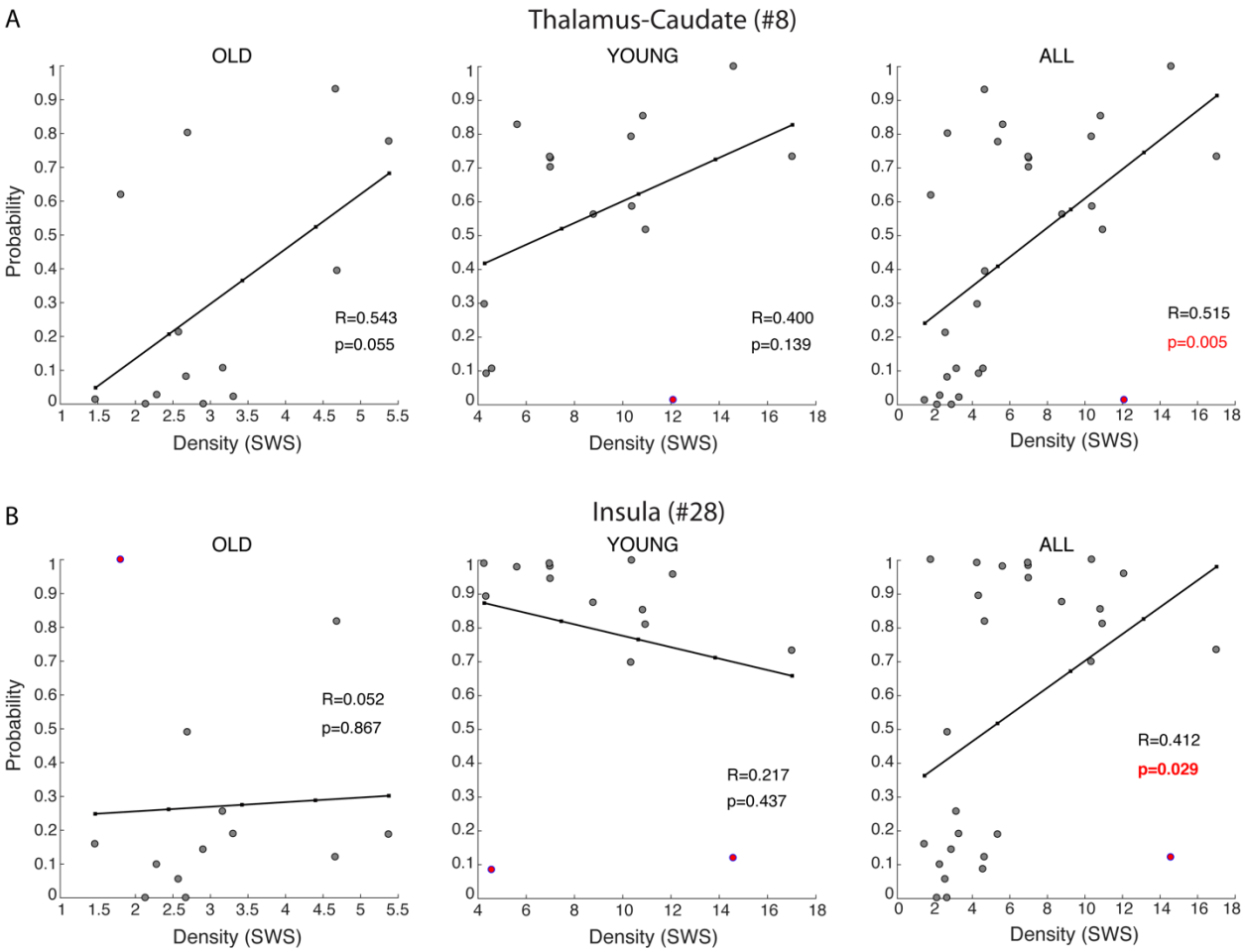

Figure 3.22. Linear regression of the probability of spending time in the given state versus the density of slow-wave sleep during NREM2. In (A) applied with TC#4 and in (B) applied with INS#3.

3.2.2.4. Transitions:

To explore the dynamics of the functional connectivity measures, we computed the between-state transition probabilities within NREM2 for each cohort (Figure 3.23). Transition probabilities that showed significant age-related differences (Old minus Young) are highlighted in the bottom panels ($p<0.05$). Negative values (blue background) indicate higher transition probabilities for the young cohort, while positive values (white background) indicate more transitions for the old cohort.

When we explored the transitions between *brain states* derived from TC connectivity, we found TC#1 strongly associated with the younger cohort. Young subjects were significantly more likely to remain in the state than older subjects. On the contrary, older subjects were more strongly associated with TC#2 and TC#3 and more likely to remain in these states compared to the young cohort. Further, there was a significantly greater probability that younger subjects will transition to TC#1 from all other States, as compared to the older cohort. Likewise, younger subjects were significantly more likely to transition from TC#3 to TC#4. This transition was consistent with TC#3 being comprised of a significantly greater number of older subjects that spend more time in the state, and TC#4 being comprised with a significantly greater number of younger subjects.

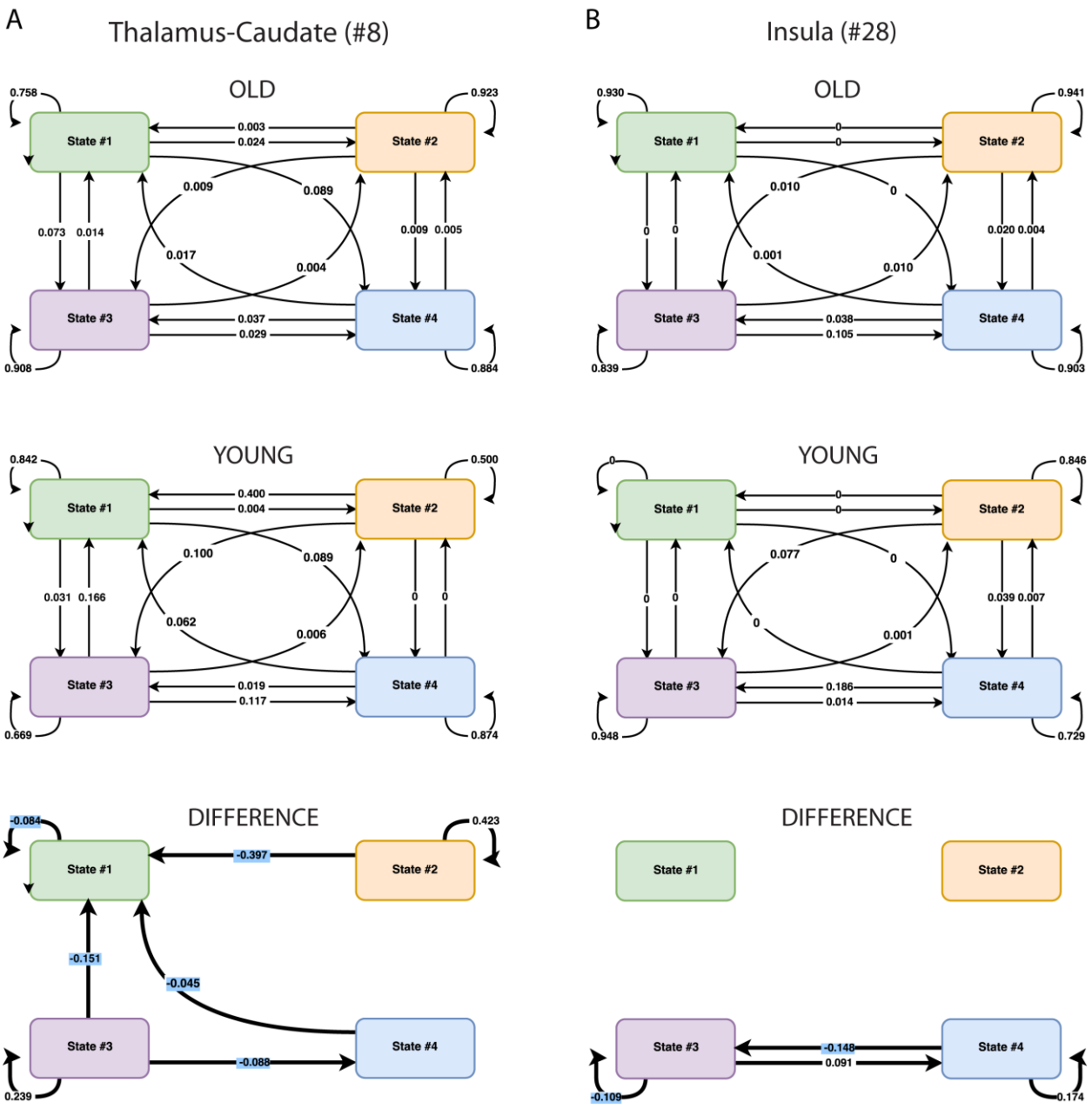

Figure 3.23. Transition probabilities between States for older, younger and the difference between cohorts, for (A) the thalamus-caudate seed and (B) the insula seed. In the top panels the transition probabilities between *brain states* for the older cohort are listed. In the middle panels the transition probabilities between *brain states* for the younger cohort are shown. The bottom panels show the difference in transition probabilities between cohorts (Older minus Younger; thus the negative values highlighted in blue depict a higher value for the younger cohort and vice-versa for the older cohort). Only differences that are significant are shown ($p<0.05$).

From the INS seed region, we observed very few transitions in and out of INS#1 and INS#2. This is likely due to differences in connectivity from both INS#1 and INS#2 that were driven by a single subject, respectively (see Figure 3.17.C.). Accordingly, none of the transitions to or from either of these states showed significant age-related differences. The *brain state* INS#3 was associated more strongly with the younger cohort and showed a significantly greater likelihood of younger subjects remaining in the state with older subjects significantly more likely to transition out of the *brain state* to INS#4. Conversely, in INS#4, a *brain state* associated more with older subjects (Figure 3.18.B.), there was a significantly greater likelihood the older subjects would remain in this *brain state*, as compared to the younger cohort. Further, the younger subjects were significantly more likely to transition out of the state to INS#3, as compared to the older cohort (Figure 3.23).

Since the focus of this analysis was on NREM2, some transitions entered other sleep stages, a mixture of sleep stages (over the period of the window) and periods of movement. Likewise, transitions into NREM2 may have originated from any of these periods. A chart of all observed transitions is shown in Figure 3.24.A. The difference in transition probabilities that were significantly different between cohorts are shown (Figure 3.24.B. and C.) for both ROIs.

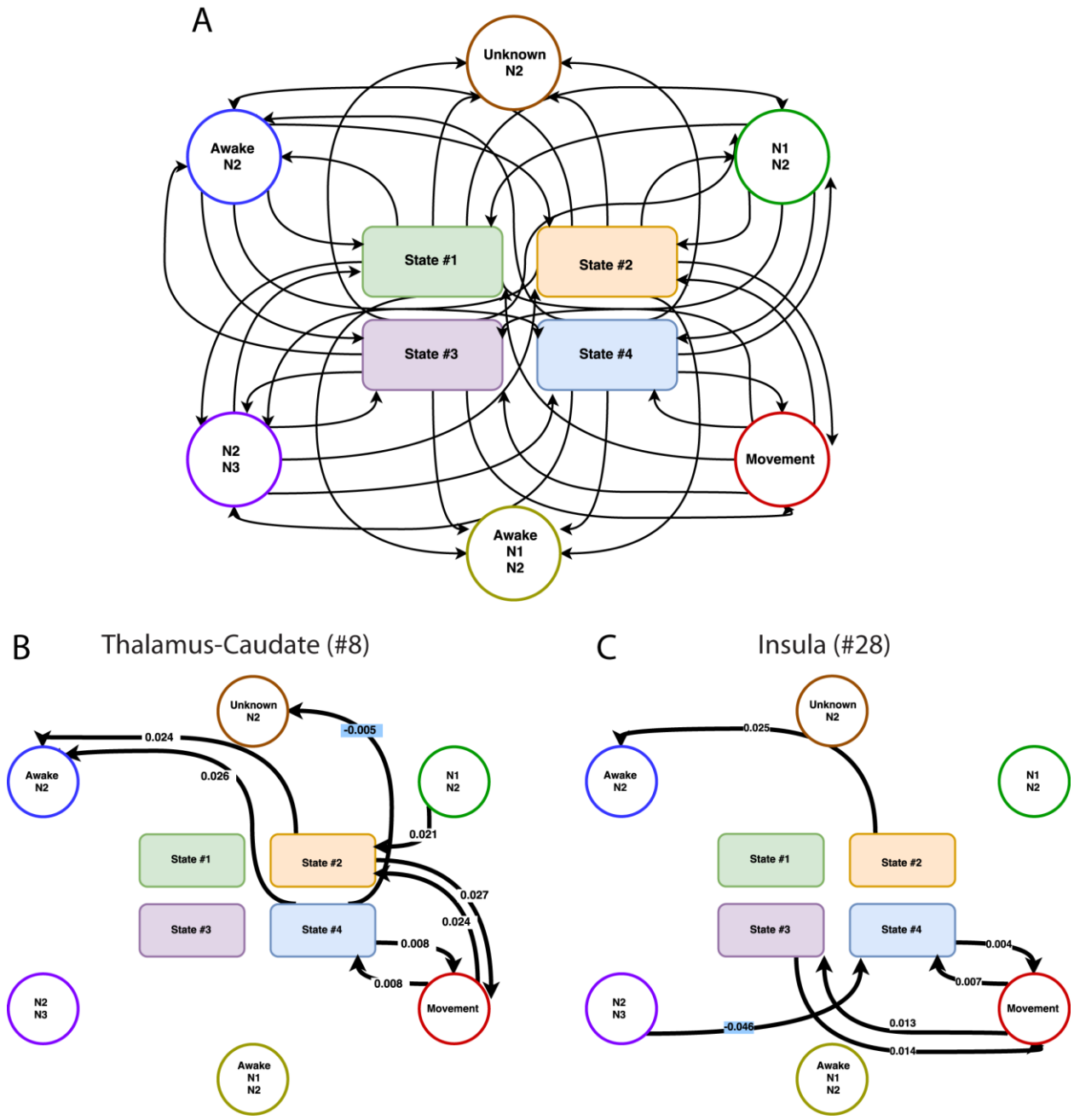

Figure 3.24. Transition probabilities entering and exiting NREM2 to and from other sleep stages or periods of movement removed during pre-processing. A) The overall map of all possible transitions that were observed entering or exiting NREM2. The windows referenced all contained mixed staging assignments, such that through sleep staging different volumes in the same window were assigned a different sleep stage. Unknown refers to windows where the sleep staging could not be assessed. Movement refers to periods that were removed due to excessive frame displacement. B) The left panel shows the results from the thalamus-caudate seed and the right panel from the insula seed. The difference (Older minus Younger) in transition probabilities between cohorts is shown in both panels. A negative value (highlighted in blue) denotes a greater

transition probability of the younger cohort. Only statistically significant differences are listed ($p<0.05$).

In TC connectivity, there were numerous transitions from TC#4 out of NREM2 completely, that significantly differed by age cohort. For the older cohort, this included significantly more transitions to periods of wakefulness mixed with NREM2 and to periods of movement that had been censored from the data. Younger subjects on the other hand had a greater probability of transitioning to undetermined sleep stages mixed with NREM2. The transitions from periods of movement showed a significantly greater probability that older subjects, as compared to younger subjects, enter NREM2 in TC#4. In TC#2, older subjects were significantly more likely to transition out of NREM2 to wakefulness mixed with NREM2, as well as to periods of excessive movement, as compared to the younger cohort. Likewise, older subjects were significantly more likely to transition into NREM2 in TC#2 from periods of NREM1 mixed with NREM2, and from periods of excessive movement, as compared to the younger subjects. The *brain states* TC#1 and TC#3 showed no significant difference between cohorts for transitions into and out of NREM2.

INS connectivity showed that older subjects were significantly more likely to transition into both INS#3 and INS#4 from periods of movement and vice-versa, as compared to the younger cohort. Although INS#4 was more associated with older subjects there were still significantly more young subjects that transitioned from NREM2/NREM3 into the state than older subjects. Despite a single subject driving INS#2, there were significantly more transitions into Awake/NREM2 from the older cohort, as compared to the young.

We next investigated the overall frequency each cohort switched states. In the TC seed, NREM2 switches between states were significantly greater in the young, as compared to the older cohort (11.4% vs 5.2%, $p<0.001$). Switches from one of the states out of NREM2

to a different or mixed sleep stage were not significantly different between cohorts (3.9% vs 4.9%, p=0.126). Combining all transitions within and external to NREM2 revealed a significantly greater frequency of switching in the younger cohort, as compared to the older cohort (15.3% vs 10.2%, p<0.01).

In the INS seed, we found overall fewer transitions compared to the TC. The frequency of switches between states within NREM2 was significantly different between the young and old (2.8% vs 4.9%, p<0.001), and likewise for all switches in and out of NREM2 (6.7% vs 9.9%, p<0.001). Thus, in contrast to the TC, the younger cohort transitioned significantly less than the older cohort. The *brain states* INS#1 and INS#2 were driven by single subjects from the older cohort. Of the remaining states only INS#3 was associated with the younger cohort, resulting in a relative reduction of transitions in the younger group. The older cohort maintained comparable transition probabilities to the TC seed. Similar to the TC seed, when measured from the INS switches that transitioned into or out of the sleep stage were not significantly different between cohorts (p=0.126).

We then assessed the impact that remaining in a state and transitioning from a state would have on mean connectivity for each of the seeds. In the TC, there was no significant difference in overall mean connectivity for transitions out of or remaining in state, in either cohort (p=0.164). When looking at individual states, we found greater mean connectivity for TC#4 in both cohorts for remaining in, rather than transitioning out of the state (Young: 0.165 vs 0.143, p=0.011; Old: 0.177 vs 0.146, p=0.020; Combined: 0.170 vs 0.144, p=0.0005). For TC#3, the opposite was observed, whereby younger subjects that remained had a significantly lower mean connectivity compared to those that transitioned to other states (0.043 vs 0.100, p=0.0037). Older subjects revealed similar mean connectivity (p=0.182). In TC#1 no significant differences were observed for either cohort (all p>0.2), while in TC#2 data was driven by only two older subjects and hence insufficient to analyze.

In the INS, there was a significant difference in overall mean connectivity for transitions out of or remaining in state found in the older cohort (0.249 vs 0.218, $p<0.001$), but not in the young ($p=0.1444$). In INS#1 and INS#2 the data was essentially driven by only one older subject in each state, thus it was deemed insufficient to analyze. In INS#3 no significant differences were observed for either cohort (all, $p>0.3$). In INS#4 the older cohort revealed a significant difference between the mean connectivity of subjects that remained in the state and those that transitioned from the state (0.284 vs 0.246, $p<0.001$). This indicates that older subjects with a higher connectivity were significantly more likely to remain in the state. By contrast, although younger subjects were less likely to spend time in INS#4 than the older subjects the younger subjects that remained showed a trend towards a lower mean connectivity than those that transitioned to a different state (0.242 vs 0.278, $p=0.0517$). Overall, INS#4 shows a higher connectivity seen in their z-maps, as compared to the average (see Figure 3.16.B.).

Finally, using linear regression analysis, we assessed the relationship between mean connectivity and the consecutive time spent in a given state, which was based on the duration of the time period without transitions. In the TC, overall there was no significant relationship between connectivity and consecutive time that either cohort spent in a state ($p=0.246$). At the state level, this relationship varied according to the level of connectivity associated with the given state. For example, in TC#2, where the z-maps show lower connectivity, we observed a significant negative correlation between mean connectivity and time spent in the state ($p=0.019$). In contrast, in TC#4, where overall connectivity is high, we observed a significant positive correlation between connectivity and consecutive time spent in the state ($p=0.020$). In the INS seed, there were no significant associations between mean connectivity and time spent in a given state. This was true for all states individually, as well as combined (all, $p>0.05$).

3.2.2.5. Summary

In this study, we analyzed NREM2 sleep data of young and old subjects using static and dynamic methods. We identified a significant reduction in connectivity between the TC seed region and regions of the cerebellum in the older cohorts, as compared to younger subjects. With the dynamic methods, we were able to identify *brain states* that were significantly associated by age cohort. Essentially, all *brain states* that comprised more than two subjects differentiated significantly by cohort. We also identified a *brain state* (TC#2) primarily associated with two subjects that explained the age-related variance in connectivity that we observed from the static analysis. The *brain state* TC#3 displayed more connectivity to the DMN than other *brain states*, while older subjects spent significantly more time than younger subjects in this *brain state*. We observed an association between SWS and the *brain states*.

3.3. Thought Content

3.3.1. Introduction

In this study our objective is to analyze the relationship between thought content and connectivity, and to identify any age-related associations from these findings. As in the other studies, we apply both a static and dynamic analysis, with the static analysis serving as a benchmark. We do anticipate that through clustering we will be better able to discern the effects of an interaction between age and thought on connectivity, than with a static analysis alone. To recap, our objectives are as follows:

- Assess correspondence between thought content scores and static connectivity results.
- Identify *brain states* that correlate with high or low thought content scores.
- Explore interaction between thought content scores, connectivity, and age (using both static connectivity and *brain states*)

Since elaborating past and future thoughts may differ by age, we anticipate identifying associated connectivity differences in this analysis [46, 50]. We are similarly motivated by possible compensatory mechanisms that may account for comparable content scores across cohorts. Despite the potential interaction between age and thought content scores, this has not been reported in the literature in association with resting-state analysis. To recap, our hypotheses are as follows:

Hypotheses:

- Identify connectivity differences, from the seed regions, with thought content as the variable of interest, in the static analysis
- A *brain state* will be associated with higher or lower thought content scores.

- An interaction between age and thought content scores in relation to connectivity and *brain states*. (Due to compensatory activity found in these regions during past and future thought [89], we hypothesize greater connectivity in older subjects as a compensatory mechanism.)

We analyzed the standard acquisition resting-state data from the NKI-e dataset using two different ROIs from the Cambridge-36 functional network atlas [120]. The seed regions comprise the middle temporal gyrus (MTG, region#31) and the superior temporal gyrus (STG, region#25) (Figure 3.25). These regions have been associated with past and future thought elucidation [46, 50, 61, 88], as well as compensatory activity in older adults [89].

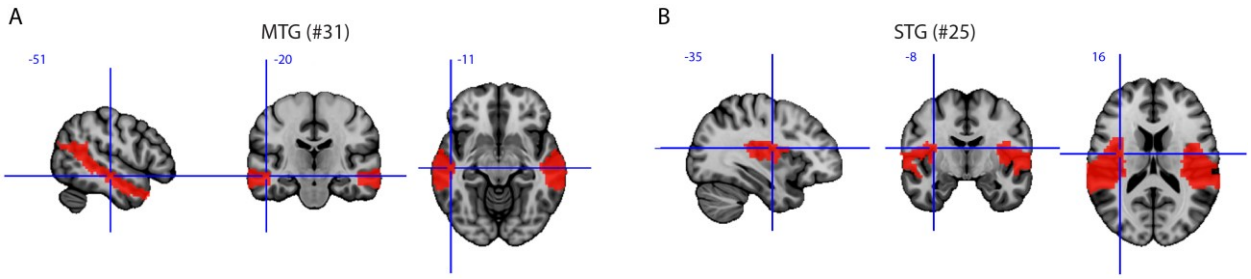

Figure 3.25. MIST-36 regions of interest. A) The middle temporal gyrus seed (region of interest #31). B) The superior temporal gyrus seed (region of interest #25).

For this analysis we analyzed subjects from the NKI-e dataset, for which complete thought content score data existed. We focused on past and future thought content scoring. We analyzed 145 subjects (Old: 68 subjects (31% male), 56-85yrs, 66.4±7.86yrs; Young: 77 subjects (49% male), 18-35yrs, 23.8±4.61yrs).

3.3.2. Results

3.3.2.1. Thought Content Scoring

To derive a specific subject-level score for thought content we utilised the participant's subjective responses to the post-scan questionnaire and weighted it according to values established for each question and theme [53]. We found a significant difference with future thought content scores, but no difference for past thought content scores between age cohorts (Figure 3.26.A; p=0.157 (past) and p<0.01 (future), controlling for sex, respectively).

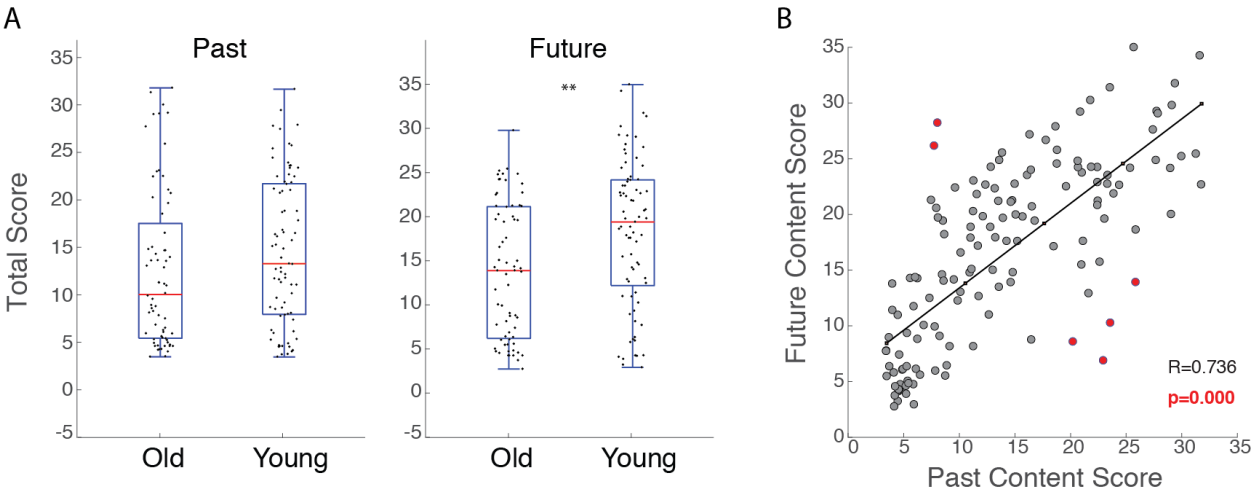

Figure 3.26. Thought content scores. A) Distribution of thought content scores by age cohort for past and future thought. B) Linear relationship between scores for past and future thought content across all subjects. (In (A), ** p<0.01).

We also observed a strong relationship between the scores from the past and future content measures (Figure 3.26.B). This relationship between past and future content scores was maintained for each cohort when examined separately (not shown).

3.3.2.2. Static Connectivity

We applied a general linear model to assess the significance of age, scores for the past and future content of thoughts, and the interaction between them to connectivity variations from the two seed regions (Figure 3.27). In each model sex was used as a covariate. From the MTG seed region, using age as the variable of interest we found a significant (FDR, $q<0.05$) reduction in connectivity to the inferior parietal lobule and angular gyrus, the posterior region of the middle frontal gyrus and the superior frontal gyrus, the temporal pole and to the middle temporal gyrus itself. (Figure 3.27.A. Top panel). From the STG seed region, we found a significant (FDR, $q<0.05$) reduction in connectivity to the temporal pole, to the precentral gyrus and the posterior region of the superior frontal gyrus, along with posterior portions of the insula. We found a significant increase in connectivity with age as the variable of interest in to the middle occipital gyrus and the anterior portion of the insula (Figure 3.27.B. Top panel).

We did not find any significant differences from either seed region, when using the scores for past or future content as the variable of interest (Figure 3.27, Middle panels).

We explored the relationship between the interaction of age and content scores to connectivity variations, and found significant findings in both seed regions for past content scores. In the MTG, we found much of the occipital and parietal lobes, excluding DMN related structures – the inferior parietal lobule and the posterior cingulate cortex – displayed significant interactions ($q<0.05$, Figure 3.27.A. Third and fourth panels from the bottom). From the STG seed region, we observed a significant positive interaction to the calcarine ($q<0.05$, Figure 3.27.B. Third and fourth panels from the bottom); as we likewise observed from the MTG seed region.

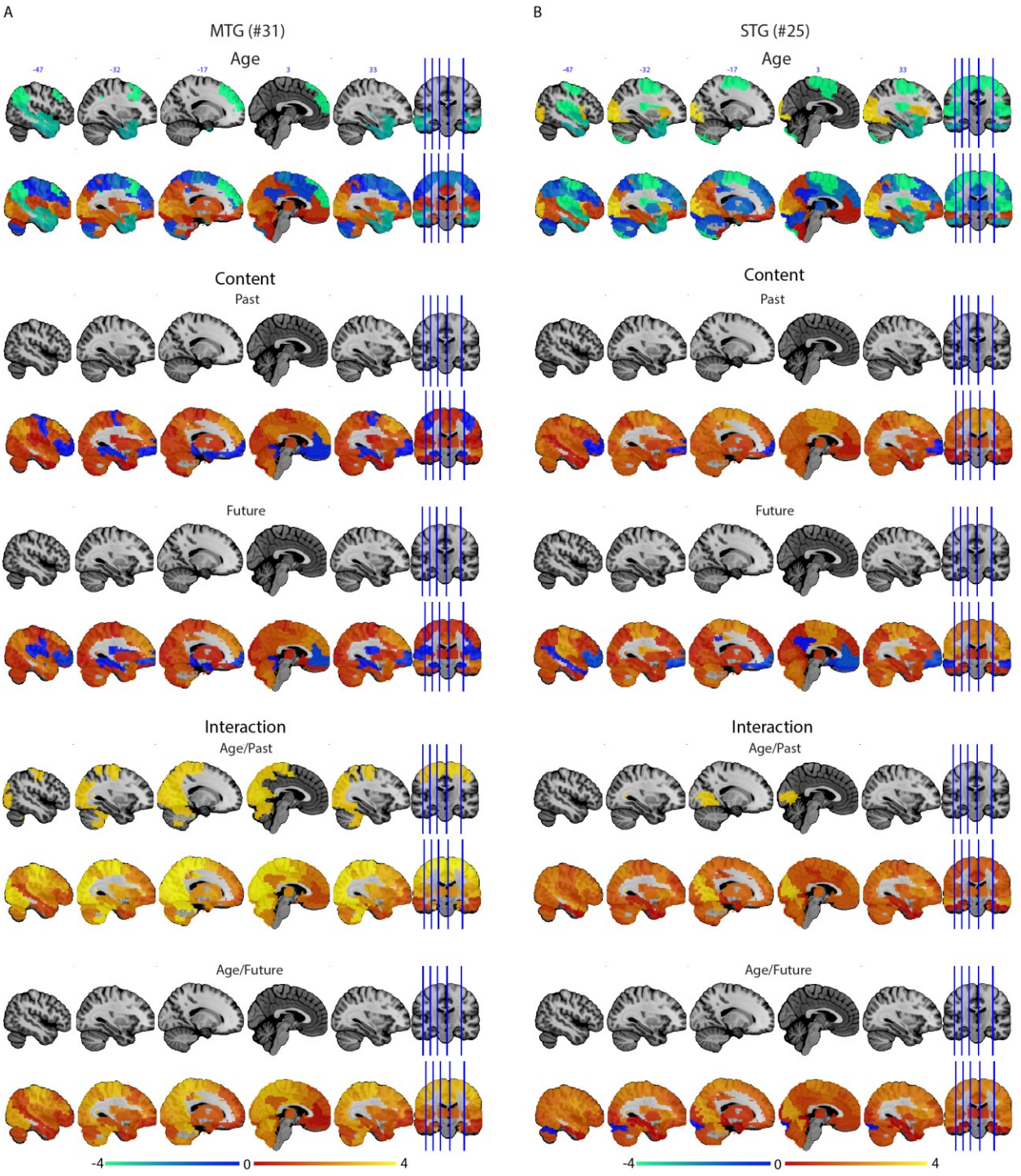

Figure 3.27. General linear model of age and thought content related changes in connectivity between (A) middle temporal gyrus and (B) superior temporal gyrus seed and the entire brain, during resting-state (top two panels). Significant age-related differences between cohorts (Top panel, FDR, $q<0.05$). The map of the t-statistic (second panel). Thought content related changes in connectivity (third to sixth panels). The significant differences are followed by the t-statistic maps for past and future content. The interaction between age and thought content scores

(bottom four panels). The significant differences followed by the t-statistic map for interactions between age-past content and age-future content scores.

We did not find any significant interactions between age and thought content scores on connectivity for future thought ($q<0.05$, Figure 3.27, Bottom two panels). This is in contrast to the future content scores alone, in which we found a significant difference between age cohorts. In each of the GLM tests we show the t-maps below the maps of significant findings to highlight areas that show increases and decreases in connectivity despite not passing significance under $q<0.05$.

3.3.2.3. Dynamic Connectivity

To examine the seed regions from a dynamic perspective, we first computed the mean connectivity of our ROIs with all voxels within the functional brain mask, across all windows. This provided us with the voxel-wise connectivity of each ROI with the rest of the brain (Figure 3.28, Top panel). The same procedure was applied to each age cohort separately. The corresponding z-maps for each cohort was then calculated (Figure 3.28, Middle and bottom panels). In the MTG seed, the older cohort showed a reduced connectivity to most regions of the brain, including the MTG region itself, along with the mid- and frontal superior gyrus. We observed high connectivity to regions that included the occipital lobe and anterior regions of the parietal lobe, as compared to the average across all subjects. This included a high connectivity, relative to the average connectivity across the entire sample, to the inferior parietal lobule, portions of the inferior frontal gyrus and the thalamus. The younger cohort accordingly showed opposite connectivity differences, relative to the average across all subjects.

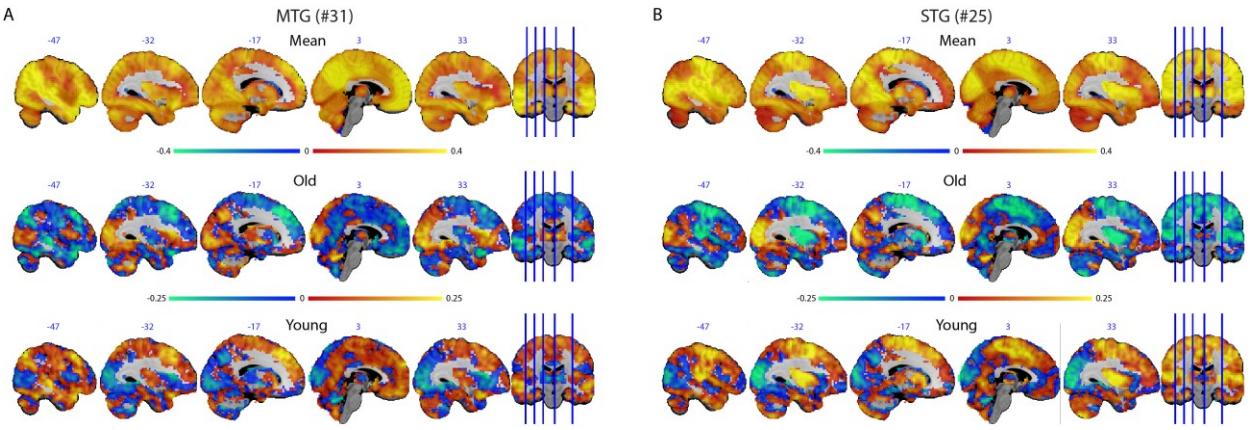

Figure 3.28. Voxel-wise connectivity from the (A) middle temporal gyrus and (B) superior temporal gyrus seed during resting-state. The overall connectivity (top panels) is the mean connectivity of all windows across all subjects. The Old cohort (middle panels) section represents the Z-map of the connectivity in the older cohort relative to the mean connectivity across all subjects. The Young cohort (bottom panels) section represents the Z-map of the connectivity in the younger cohort relative to the mean connectivity across all subjects.

In the STG seed, we also found increased connectivity to the occipital lobe and portions of the parietal lobe in the older cohort, as compared to the average across the sample. We observed diminished connectivity to the putamen, motor regions, the superior frontal gyrus and most regions of the frontal lobe. Correspondingly, we observed the opposite connectivity patterns in the younger cohort, as compared to the average.

To better interpret the role thought content scores may play on the interaction effect between age cohort and content scores on connectivity, observed in the static analysis, we differentiated groups that had higher and lower content scores. We did this for the entire sample, as well as separately within each cohort. In each case, subjects that scored above the median thought content score were assigned to the high content group, and those that scored lower than the median were assigned to the low content group. We repeated this for past, as well as future content scores (Figure 3.29: MTG seed region; Figure 3.30: STG seed region).

We found similar connectivity patterns between past and future brain maps at both high and low content scores, which is consistent with the strong relationship we observed between the past and future content scores (Figure 3.26.B). This was observed in both seed regions.

From the MTG seed region, in the older cohort we found high connectivity within the group with higher content scores, as compared to the average. We found generally low connectivity in the lower content score group, as compared to the average. The opposite was seen in the younger cohort. These observations suggest that the variation in connectivity we found in the static analysis as part of the interaction between age cohort and content scores is explained through a cross-over (qualitative) interaction. Thereby, younger subjects with high content scores have low connectivity from the seed regions to other brain regions as compared to high content scoring older subjects; with the reverse finding for low content scores across cohorts.

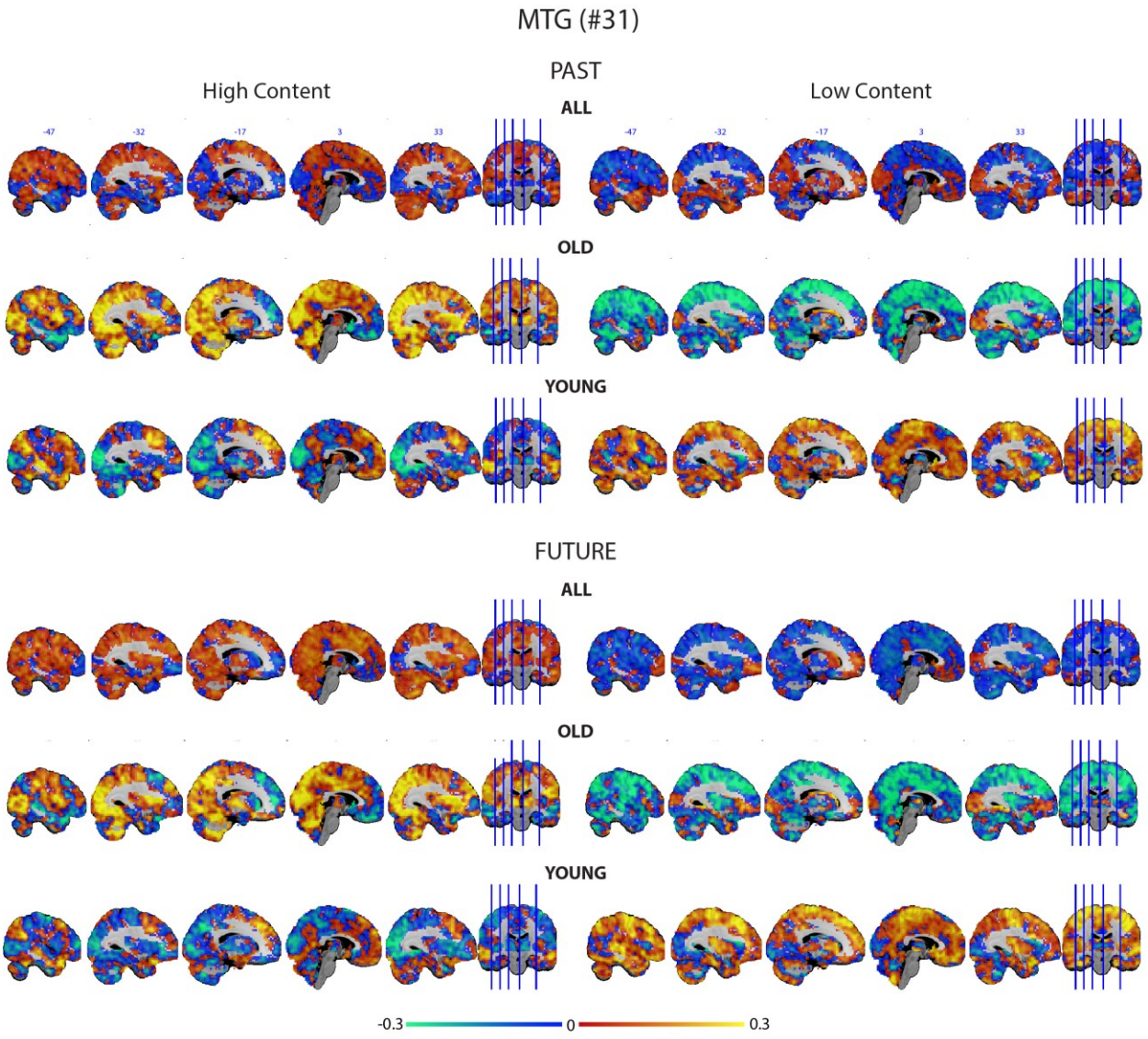

Figure 3.29. Z-maps of voxel-wise connectivity, from the middle temporal gyrus seed during resting-state, of thought content groups. The high content (left panels) and low content (right panels) groups show the Z-map of the connectivity in the given content group relative to the mean connectivity across all subjects. The subjects are assigned to the content group based on the median of the cohort examined (All, Old or Young). The groups are separated by Past and Future thought content scores.

In the older cohort, the middle and superior occipital gyrus, the calcarine and the lingual gyrus, maintain a greater correlation with the MTG seed region in both high and low content groups, as compared to the average or the younger cohort. By contrast we found

connectivity to the thalamus from the older cohort was diminished, while it was increased in the younger cohort as compared to the average overall connectivity.

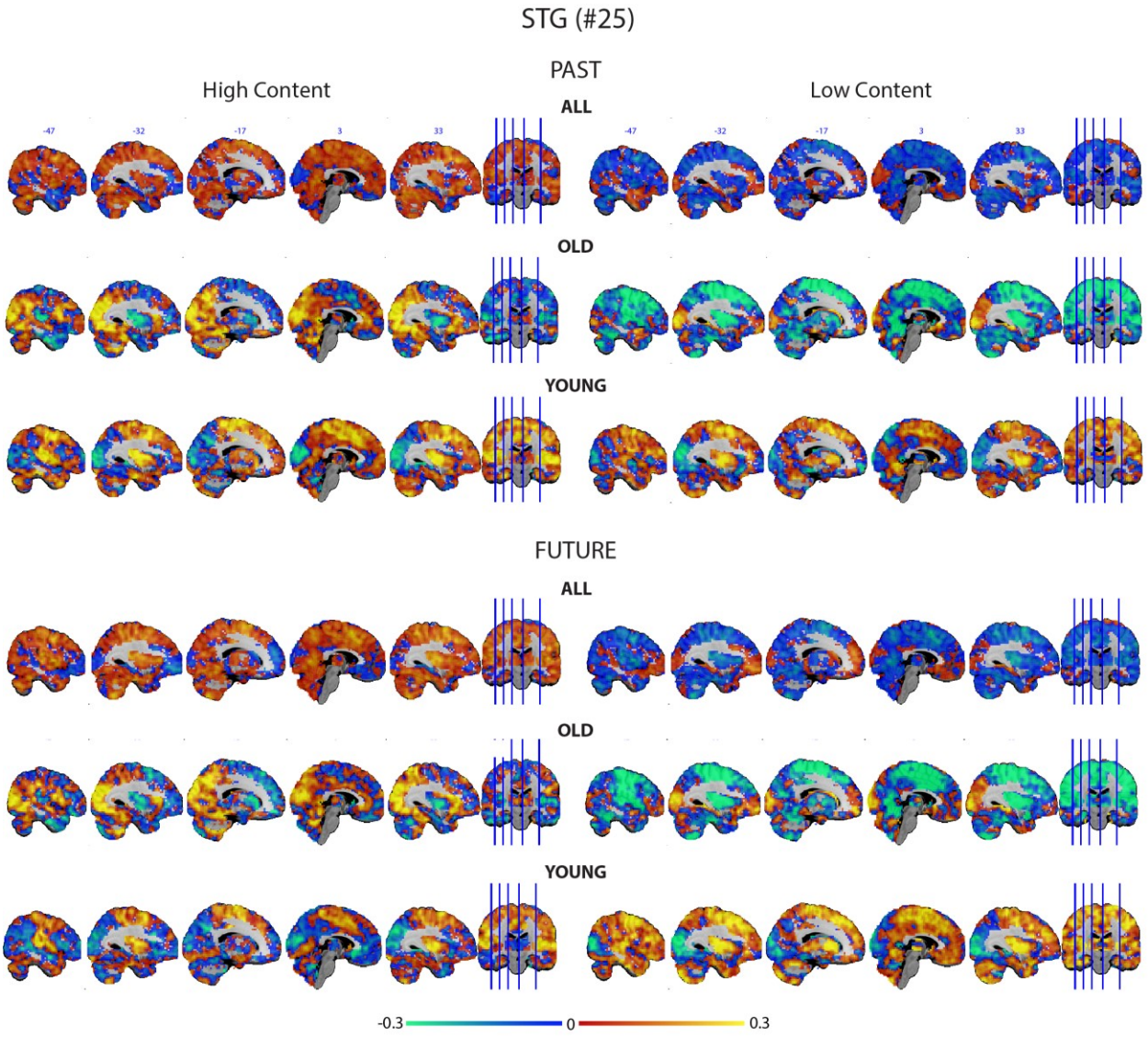

Figure 3.30. Z-maps of voxel-wise connectivity, from the superior temporal gyrus seed during resting-state, of thought content groups. The high content (left panels) and low content (right panels) groups show the Z-map of the connectivity in the given content group relative to the mean connectivity across all subjects. The subjects are assigned to the content group based on the median of the cohort examined (All, Old or Young). The groups are separated by Past and Future thought content scores.

From the STG seed region, in the high content score group we generally observed high correlation to the occipital and parietal lobe regions in older cohorts, and low correlation to the frontal lobe, as compared to the average. By contrast the young cohort displayed opposite correlation patterns in those regions. In the future content group of the younger cohort, however, there was diminished connectivity to the medial prefrontal cortex and the posterior cingulate cortex, as compared to the overall average connectivity to the STG seed region. As we observed with the MTG seed region, connectivity to the STG seed region was low to the thalamus in the older cohort, as compared to the younger cohort, across both high and low content groups; and the connectivity to the occipital gyrus, the calcarine and the lingual gyrus was high across both high and low content in the older cohort, as compared to the young cohort. This corresponds to our observations during the static analysis.

3.3.2.4. Clustering

To identify *brain states* to which the subjects converged, we performed a hierarchical clustering procedure (Ward's criterion) on the correlation between each window map with all the other window maps (Figure 3.31, Left panels). This procedure assigned an associated cluster or state (n=4) to each given window map (Figure 3.31, Right panels).

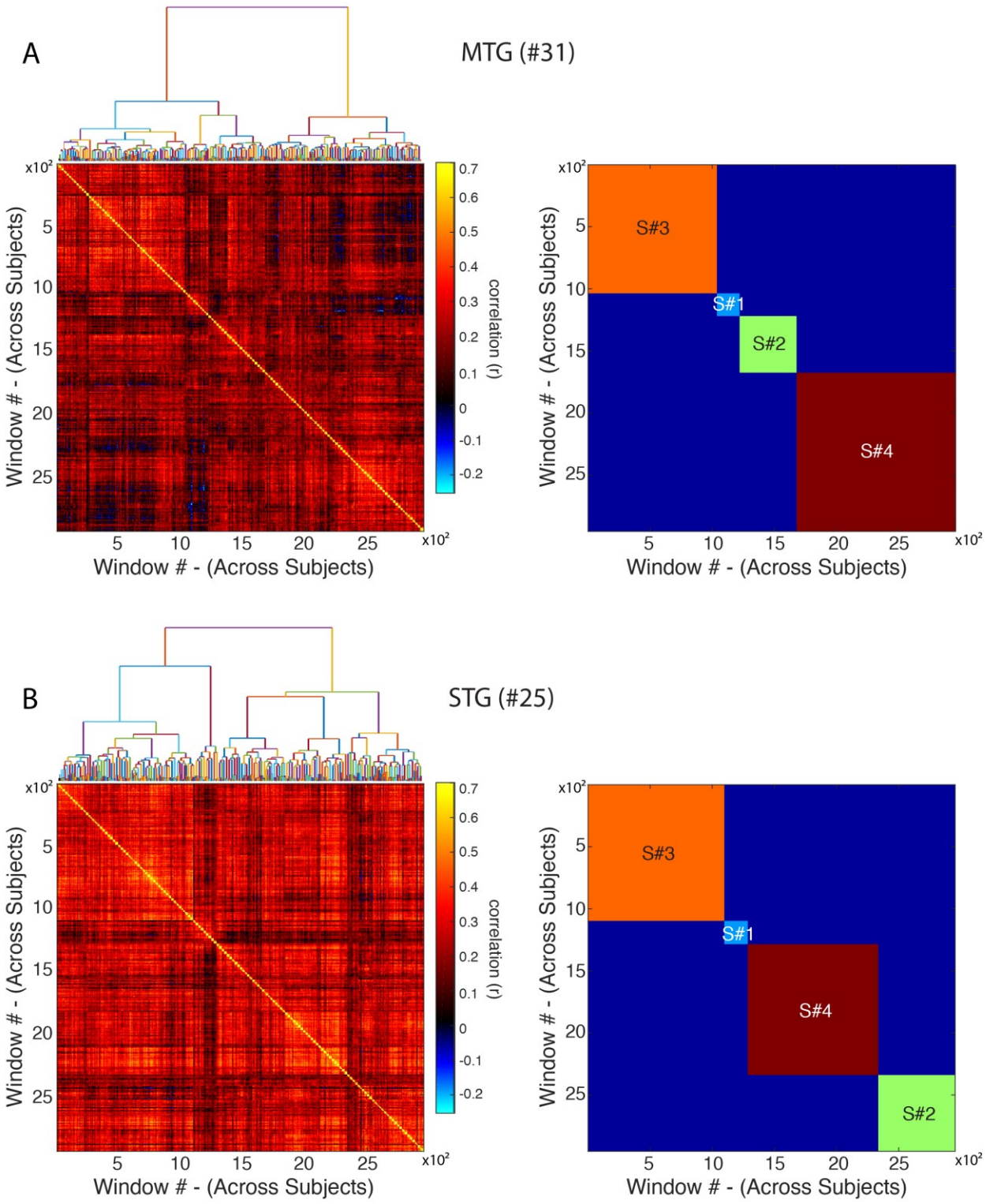

Figure 3.31. Hierarchical clustering of the correlation of each window map to all other window maps across all subjects. Each window map represents the connectivity between the (A) middle temporal gyrus (#31) seed to the entire brain and (B) superior temporal gyrus (#25) to the entire

brain. (Left panels) The similarity matrix ordered with hierarchical clustering of the correlation of all window maps to one another under Ward's criteria. The dendogram is shown above the similarity matrix. (Right panels) The clusters defined by the selection of four States. The numbers listed (i.e.: S#3, S#1, etc.) refer to the State numbers referenced in the text.

After clustering, the window maps associated with each state were averaged to provide mean *brain state* maps. To visualize the difference of each map from the average connectivity map across all subjects and windows, a z-map was calculated from the mean *brain state* maps (Figure 3.32). From the MTG seed region (Figure 3.32.A), in MTG#3, we found a stronger correlation to regions of the default mode network, while we observed less correlation to other brain regions, as compared to the average map. In contrast, the opposite correlation map was observed in MTG#4, where there was decreased connectivity to the DMN and increased connectivity to other regions and a reduced connectivity to the thalamic region, as compared to the average map across all subjects. In the *brain state* MTG#1, we observed an overall reduction in connectivity to the rest of the brain, although with some increased to medial regions of the thalamus; whereas with MTG#2, we found an overall increase in connectivity, except to the middle temporal gyrus itself, the angular gyrus, and the pre- and post-central gyri, as compared to the average connectivity across all subjects.

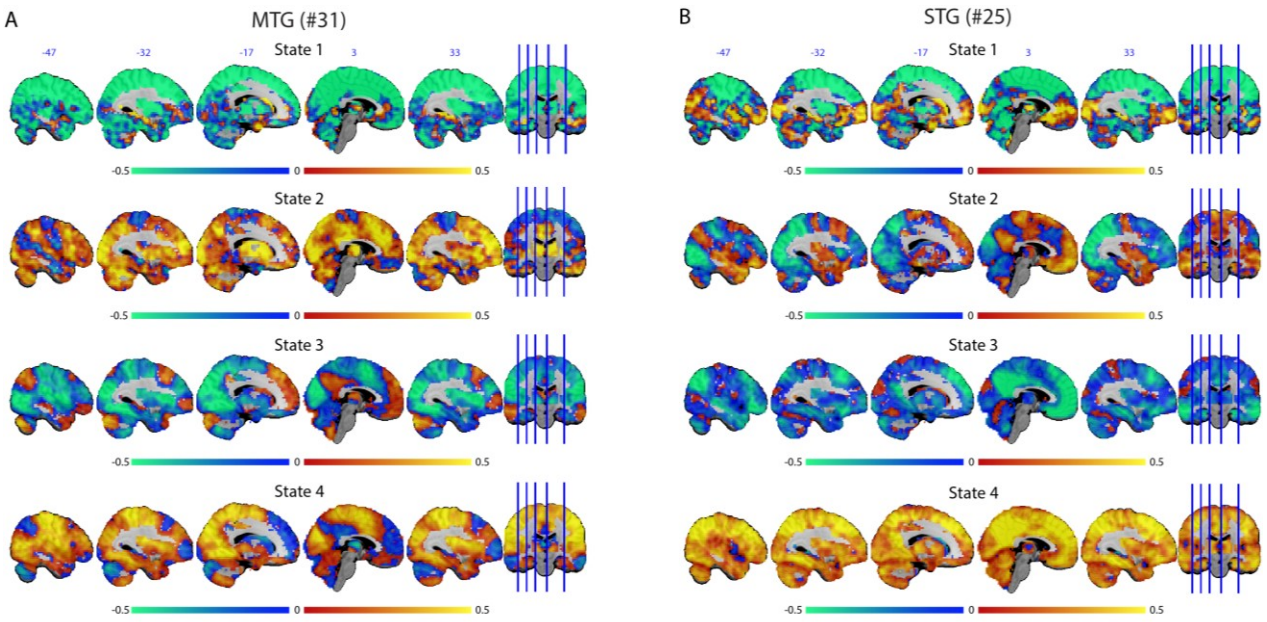

Figure 3.32. Z-maps of each *brain state* relative to the average voxel-wise connectivity between (A) the middle temporal gyrus and (B) the superior temporal gyrus seed and the entire brain, during resting-state. State-wise connectivity is calculated as the average of the voxel-wise connectivity within all windows that correlate most with the given *brain state* of interest.

From the STG seed region (Figure 3.32.B), in STG#3 we found an overall decrease in connectivity to most brain regions and an even greater decrease to the DMN, as compared to the average map across all subjects. By contrast in in STG#4, we found an overall increase in connectivity throughout the brain, as compared to the average. In STG#1 we found an increase in connectivity to the occipital lobe and the prefrontal cortex, while there was diminished connectivity to most other brain regions, when compared to the average across all subjects. In STG#2, we observed a reduced connectivity to most regions of the occipital and parietal lobe, along with lateral regions of the frontal lobe, while excluding regions of the DMN.

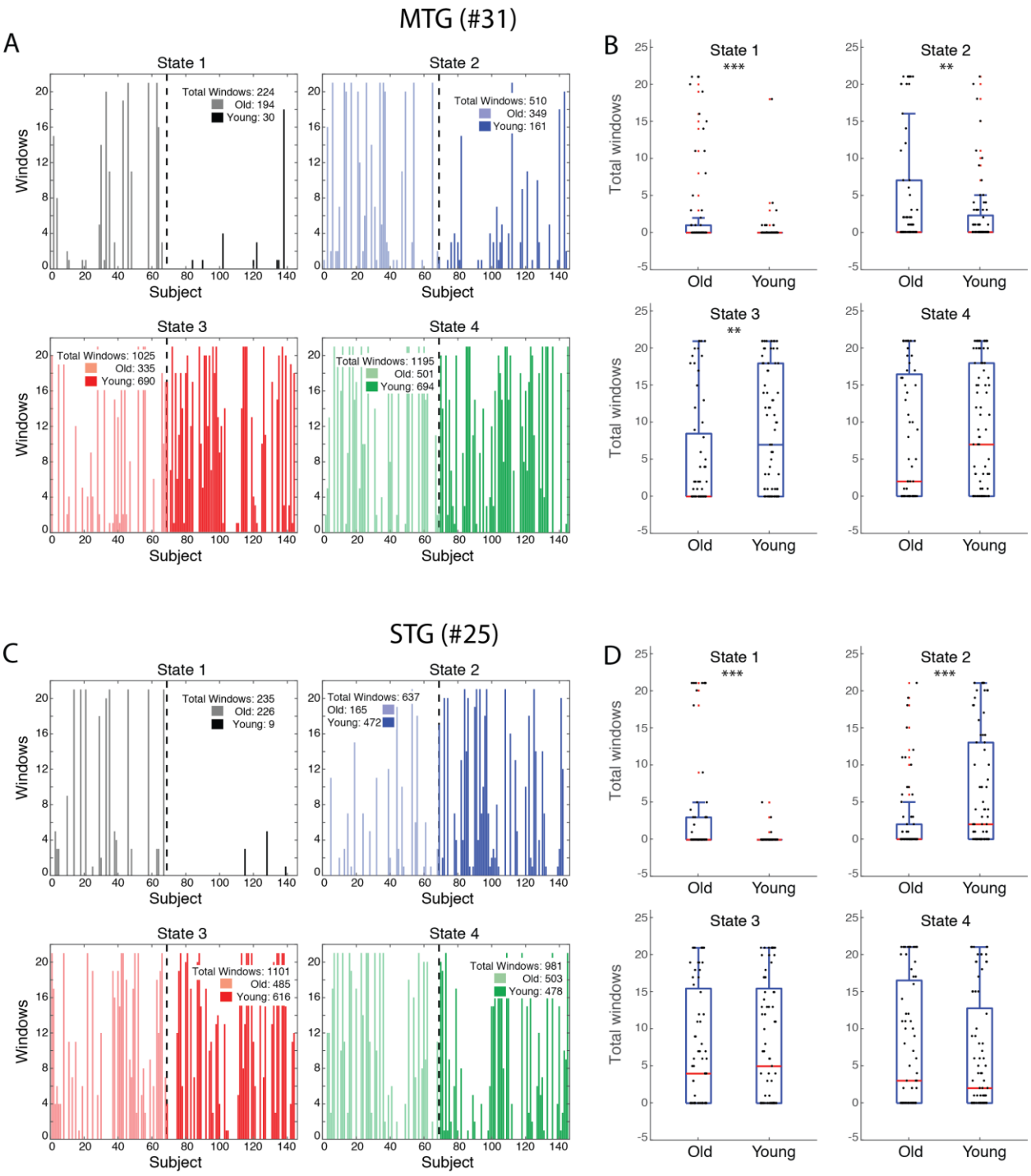

Figure 3.33. Distribution of window maps by *brain state* and cohort. The upper panels (A & B) represent the middle temporal gyrus seed and the lower panels (C & D) the superior temporal gyrus seed. In (A) & (C) the number of window maps that are most correlated to the given *brain state* by subject. The dashed line demarcates the older and younger cohorts, with the older cohort to the left of the dashed line. In (B) & (D) boxplots show the distribution of the number of windows for each subject associated with the given *brain state*, by cohort. Permutation testing on the proportion of windows distributed across subjects and cohorts (n=100,000) determined the

brain states that had a significant tendency to associate preferentially to either older or younger subjects (MTG#1: $q<0.001$; MTG#2 & MTG#3: $q<0.01$; STG#1 & STG#2: $q<0.001$).

The *brain state* maps provide insight into how the connectivity varies from the given seed region to the rest of the brain over the dataset, but does not provide information about any age-related association of each *brain state*. In order to determine how the window maps were distributed across subjects, cohorts and time-series for each state, we differentiated the information in the following two figures. In Figure 3.33, the windows across subjects for each state are represented both as a bar graph and a boxplot. In Figure 3.34, the distribution of windows by cohort and *brain state* are shown.

We ran permutation tests to determine the significance ($q<0.05$, FDR corrected) of the age-related differences in state composition we observed. For the MTG seed region, the association of the subject windows to MTG#1, MTG#2 and MTG#3 were significantly different between the old and young cohorts ($q<0.001$, $q<0.01$ and $q<0.01$, respectively). The *brain states* MTG#1 and MTG#2 were comprised of significantly more older subjects, while MTG#3 was associated with significantly more younger subjects (Figure 3.34.A). In the STG seed region, there was a significant association by age cohort to subject windows in STG#1 and STG#2 (both, $q<0.001$). The *brain state* STG#1 was comprised of significantly more windows from older subjects, while STG#2 was associated with significantly more windows from the younger subjects (Figure 3.34.B).

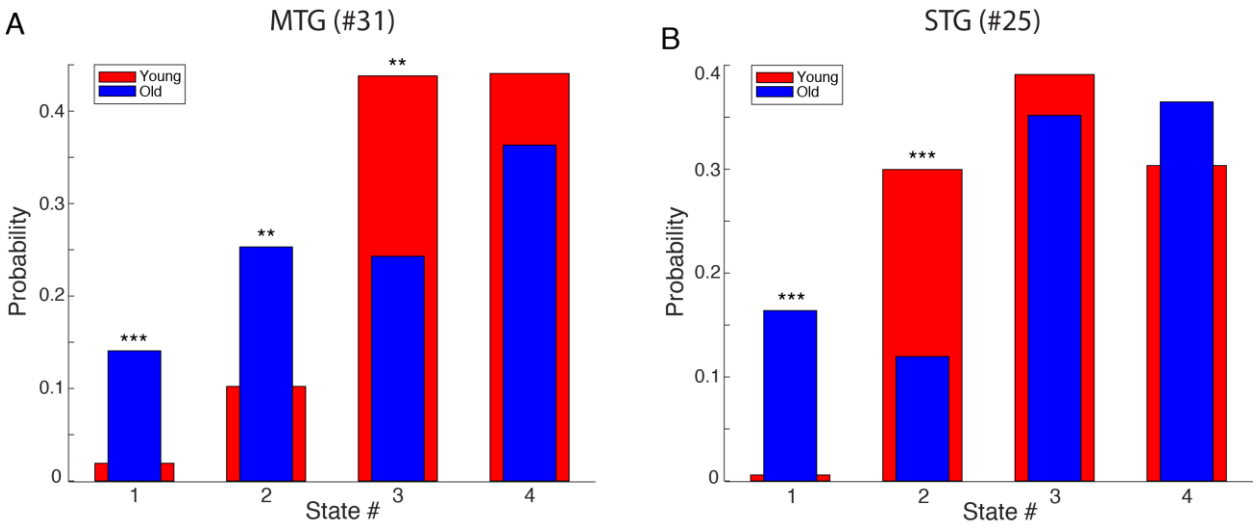

Figure 3.34. Proportional distribution of windows by state for (A) the middle temporal gyrus and (B) the superior temporal gyrus seeds. The proportion of time spent in each window by cohort (this is equivalent to the probability of spending time in the given *brain state*, by cohort). The significance of the results is based on permutation testing the proportion of windows distributed across subjects and cohorts (n=100,000; ** q<0.01, *** q<0.001).

We also investigated the distribution of thought content scores according to *brain state* and cohort. As previously, we divided the sample by those that scored higher or lower than the median thought content score across all subjects, and again separately within each cohort. We repeated this analysis for both past and future thought content scores. We then calculated the proportional distribution of the high and low content score groups across *brain states* and cohorts (Figure 3.35).

To assess the relevance of any differences in high and low content score distribution between the states that we observed, we likewise ran permutation tests to determine significance (q<0.05, FDR corrected). We ran the tests across the sample, as well as within each cohort separately.

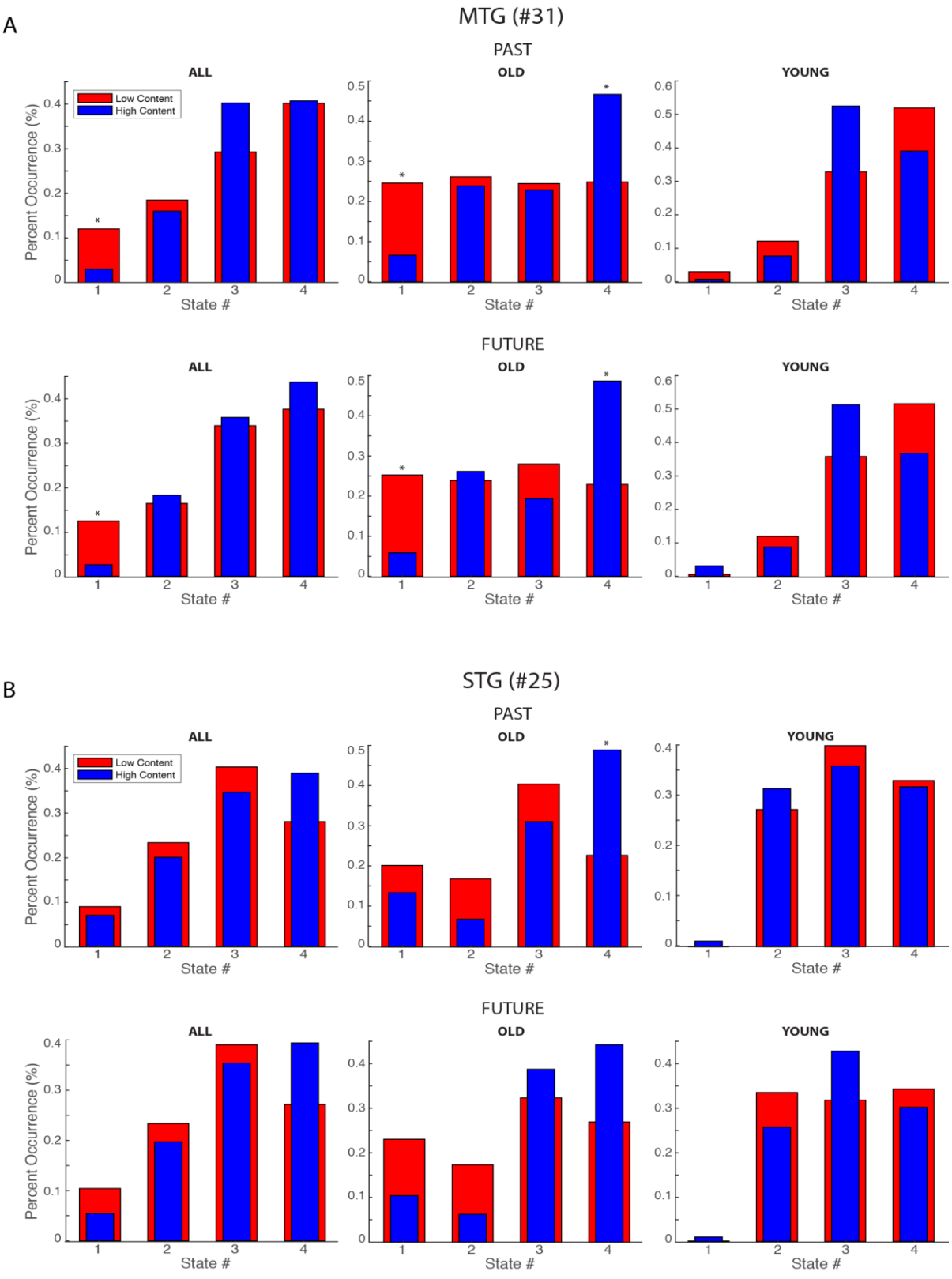

Figure 3.35. Proportional distribution of windows within each *brain state* by content score for (A) the middle temporal gyrus and (B) the superior temporal gyrus seeds. The proportion of time

spent in each window is depicted relative to high or low content scores in either Past or Future thought. The left panels show the results across all subjects, the middle panels for subjects only in the older cohort, and right panels for subjects only in the young cohort. The high or low content groupings are determined by cohort, demarcated by the median content scores for the cohort. We determined significance based on permutation tests on the proportion of windows distributed across subjects and content groups (n=100,000; FDR corrected; * q<0.05).

From the MTG seed region, we found a significant association between the low content group and MTG#1 across the entire sample and within the older cohort (q<0.05; Figure 3.35.A). This was significant for both past and future content scores. Within the older cohort, we found a significant association between high content scores and MTG#4 for both the past and future scores (q<0.05; Figure 3.35.A). In the older cohort, we also observed a relatively consistent distribution of subjects with low content scores across all *brain states*, for both the past and future scores. In the younger cohort, we did not find any significant associations.

From the STG seed region, we only found a significant association when looking at past content scores between the high content group and STG#4, within the older cohort (q<0.05; Figure 3.35.B). We did not observe any other significant associations in the young cohort, nor across the sample as a whole.

Every window was assigned to a given state following the clustering procedure. Despite this a given window may maintain similar, albeit slightly less, correlation values to other states as to the assigned *brain state*. In order to better understand the relationship between the window map and its association to the mean state maps, we computed the correlation between the window map and each of the state maps. This provided a weight to measure the strength of association to each of the states, from each window map.

The strength of the weight scores (correlation to *brain state*) varied over time, yet revealed consistently greater scores for one state over another in most subjects. The weight scores

obtained from MTG and STG, are displayed across all windows and *brain states*, by age cohort in Figure 3.36 (Left panels). The distribution of weight scores by *brain state* and cohort is displayed on the right panels.

We ran a general linear model (GLM) on the mean weight values computed from each subject for each *brain state*. We first ran age cohort as the variable of interest, while sex was controlled for as a covariate. In the MTG seed region, weight values were similar in MTG#1 and MTG#2, however, in MTG#3 and MTG#4 we found significant age-related differences ($q<0.001$ and $q<0.05$, respectively). For the STG seed region, we found a significant difference between weight values by age cohort in all *brain states* (STG#1 and STG#2, $q<0.001$; and State STG#3 and STG#4, $q<0.05$).

When we tested content scores as the variable of interest on the mean weight values, likewise controlling for sex, we did not find any significant effects in either of the seed regions. We came to the same conclusion with the static GLM analysis (Figure 3.27).

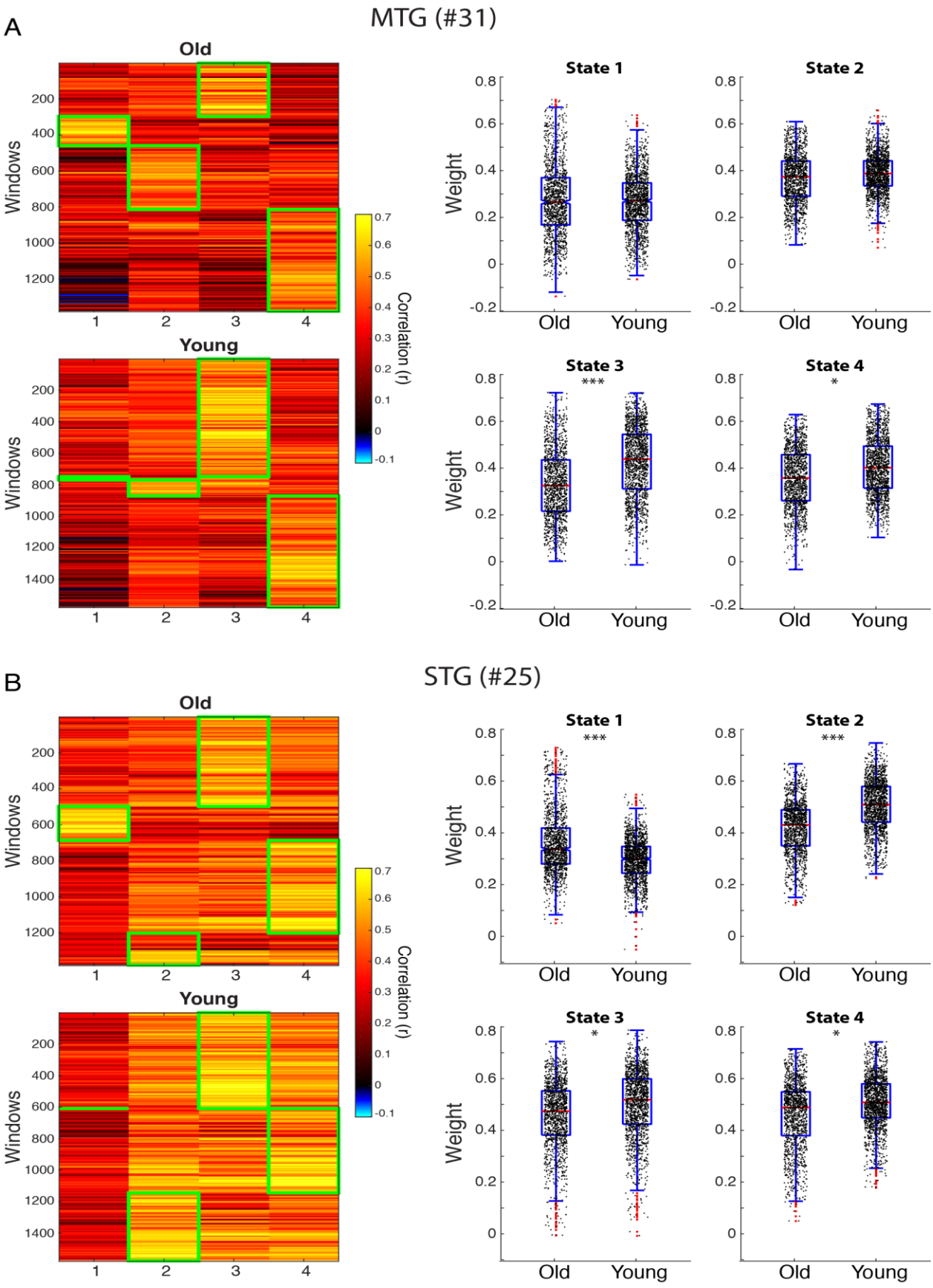
A
MTG (#31)
Old
Young
Windows
Correlation (r)
State 1
State 2
State 3
State 4
Weight
Old
Young
***
*
B
STG (#25)
Old
Young
Windows
Correlation (r)
State 1
State 2
State 3
State 4
Weight
Old
Young
***
*

Figure 3.36. Correlation of each *brain state* across windows and cohorts (i.e.: weight) for both (A) the middle temporal gyrus and (B) the superior temporal gyrus seeds. The left panels show a visual representation of each *brain state* (columns) and the correlation to all windows (rows), by age cohort. This is ordered by *brain state*, with the bright green line demarcating areas where the given *brain state* shows the greatest correlation to the respective windows as compared to the other *brain states*. The right panels show boxplots of the distribution of the weights for each *brain state* across cohorts. In the general linear model analysis on the weight scores, with age as the variable of interest, and sex as a confounding factor, where (*) $q<0.1$, * $q<0.05$, ** $q<0.01$, *** $q<0.001$.

We tested the interaction between age and content (for both past and future thought scores) in the GLM and likewise did not find any significant effects for either seed region, however, we found a trend in MTG#1 and MTG#4 ($q<0.1$) for the interaction between past content scores and age, as well as the interaction between future content scores and age in MTG#1. This overlaps in part with the findings from the permutation testing (Figure 3.35.A). We did not find any association from the superior temporal gyrus between any of the States and the interaction between age and content, in either past or future scores.

Due to the overlapping results from the weight analysis and the permutation analysis, we decided to analyze this further. We took the older subjects most associated with MTG#4 (n=24) and tested them against the remainder of the subjects in the older cohort (n=44) for any psychometric or physiologic characteristics differences. As described in the previous results section, we tested differences in subject results from the Wechsler Abbreviated Scale of Intelligence, the NEO Five Factor Inventory, the Pittsburgh Sleep Quality Index and in physiological measures that included age, sex, handedness, blood pressure, pulse, and body-mass index. We also tested for differences in movement in the scanner.

After correcting for multiple comparisons we did not observe any association between the subjects associated with MTG#4 and the psychometric or physiologic measures and the subjects not associated with MTG#4.

The relationship (correlation) of each mean state map to one another is displayed (Figure 3.37). The mean of the correlations was lower for the MTG seed region than the STG seed region (0.6 vs 0.688), however, this difference was not significant (p=0.299).

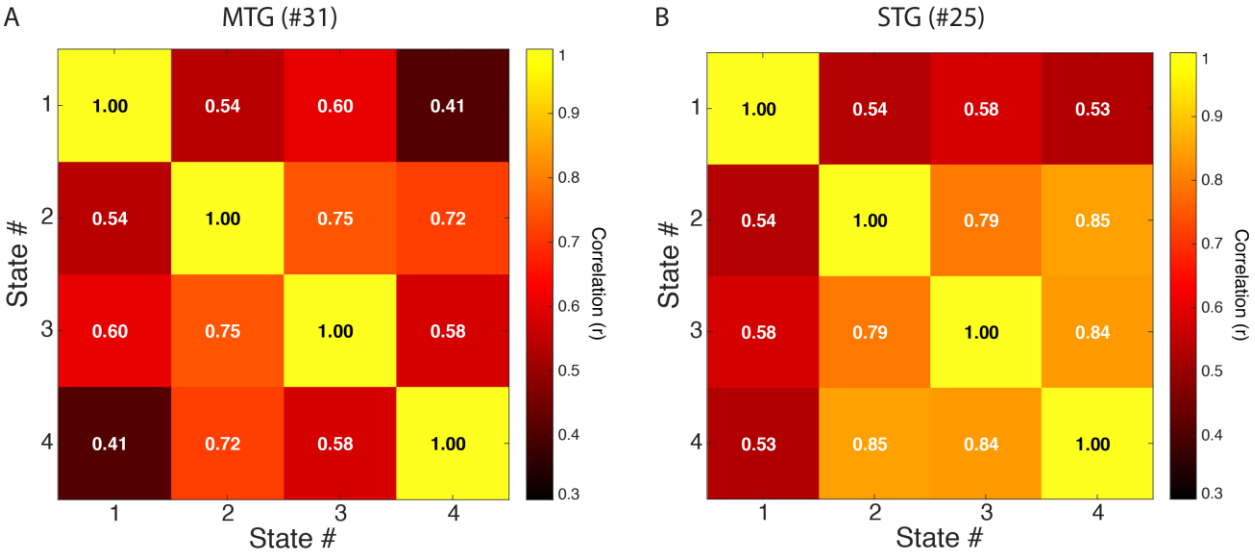

Figure 3.37. The correlation of each of the *brain states* with one another.

3.3.2.5. Transitions:

To explore the dynamics of the functional connectivity measures, we computed the state transition probabilities for each cohort (Figure 3.38). Transition probabilities that show significant age-related differences ('Old' minus 'Young') are highlighted in the bottom panels ($p<0.05$). Negative values (blue background) indicate higher transition

probabilities for the young cohort, while positive values (white background) indicate more transitions for the old cohort.

In the MTG, we found a significantly greater likelihood of older subjects remaining in MTG#1, MTG#2 and MTG#4 than the younger subjects (Figure 3.38.A). Only MTG#1 and MTG#2 were significantly associated with the older cohort, while MTG#4 did not show a significant relationship with either the older or younger cohorts (Figure 3.34.A). Both past and future content scores, however, did show an association with the older cohort in MTG#1 and MTG#4. Younger subjects were significantly more likely to transition from MTG#2 and MTG#4, to MTG#3 than were the older subjects. Similarly, we found younger subjects were significantly more likely to transition from MTG#1 and MTG#2 to MTG#4, than the older subjects (Figure 3.38.A). The *brain state* MTG#3 was significantly more associated with younger subjects than old, and as noted above, we found no significant association with either age-cohort to MTG#4 (Figure 3.34.A).

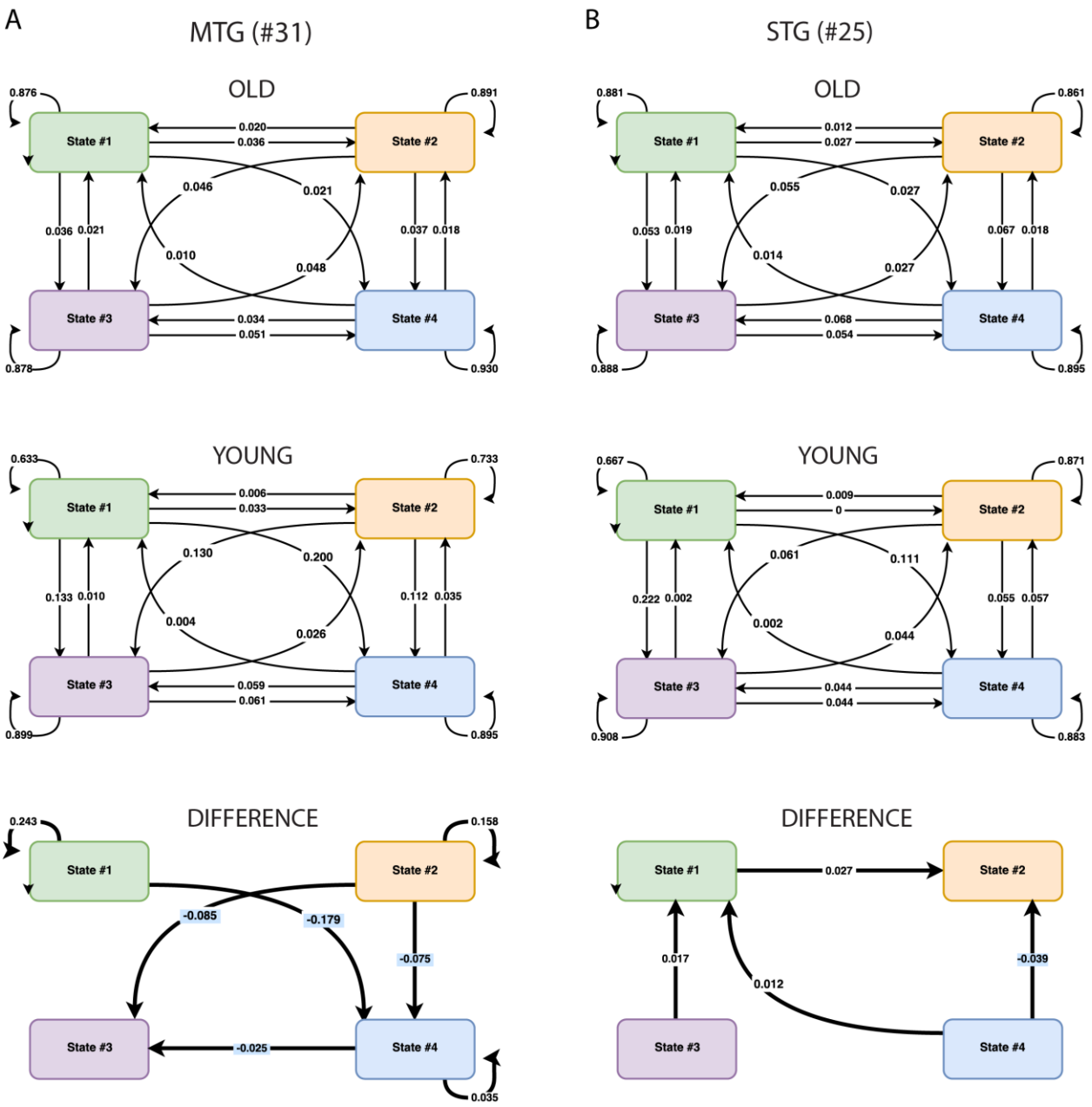

Figure 3.38. Transition probabilities between *brain states* for older, younger and the difference between cohorts, for (A) the middle temporal gyrus and (B) the superior temporal gyrus seeds. In the top panels the transition probabilities between *brain states* for the older cohort are listed. In the middle panels the transition probabilities between *brain states* for the younger cohort are shown. The bottom panels show the difference in transition probabilities between cohorts (Older minus Younger; thus the negative values highlighted in blue depict a higher value for the younger cohort and vice-versa for the older cohort). Only significant differences are shown ($p<0.05$).

For the STG seed region, we found a significantly greater likelihood that older subjects would transition from STG#3 and STG#4 to STG#1, than were younger subjects (Figure 3.38.B). STG#1 was significantly associated with the older cohort (Figure 3.34.B). We also found significantly more of the older subjects transition from STG#1 to STG#2 than younger subjects (Figure 3.38.B), despite STG#2 being significantly associated with the younger cohort (Figure 3.34.B). The *brain state* STG#1, however, consisted of almost no younger subjects (Figure 3.33.B), which may explain this observation. We observed significantly more of the younger subjects transition to STG#2 from STG#4, than older subjects.

In Figure 3.38, we only displayed transitions between *brain states*. We did not include periods that were censored from the time-series due to excessive movement. This accounted for 0.85% of the transitions in the NKI-dataset. In the MTG seed region, we found older subjects were significantly more likely to transition both to and from MTG#1 within periods of movement ($p<0.05$). In the STG seed region, older subjects were significantly more likely to transition from periods of movement into STG#1 ($p<0.05$), as compared to younger subjects.

We extended the transition analysis to explore the relationship grouping by high and low content (as described previously) may have on the results (Figure 3.39). When looking at past content scores in the MTG, we found the high content group tended to stay in MTG#3 significantly more than the low content group across all subjects, and within the young cohort. ($p<0.05$, Figure 3.39.A). Although the difference was not significant, there were more subjects with high content scores associated to MTG#3 in the young cohort and across all subjects. When we compared high and low content scores in the old cohort group, we found the transition from MTG#1 to MTG#4 was significantly higher for low content subjects ($p<0.05$). The lack of subjects with high content scores associated to MTG#1 may be a factor in this result, as we observed this when looking at future content

scores as well. Across all subjects there were significantly more participants with high content that transitioned from MTG#1 to MTG#2. In the older cohort and across all subjects we found that low-content score subjects were significantly more likely to transfer from MTG#1 to periods of movement. In the older cohort, subjects with high-content scores were significantly more likely to transition both to and from MTG#4, within periods of movement ($p<0.05$). These observations were consistent for both past and future content scores. In contrast, subjects with low-content scores in the younger cohort were significantly more likely to transition from MTG#4 to periods of movement ($p<0.05$). All of these significant transitions to and from periods of movement, were replicated when analyzing future content scores as well.

In the STG, when we examined the past content scores, we found the high content group remained in STG#4 with a significantly greater frequency than the low content group across all subjects and in the older cohort ($p<0.05$; Figure 3.39.B). We also observed a significantly higher probability that high content subjects transitioned from STG#2 to STG#3 than low content subjects, again across all subjects and in the older cohort ($p<0.05$). In the younger cohort, we did not find any significant difference between low and high content groups for past content scores.

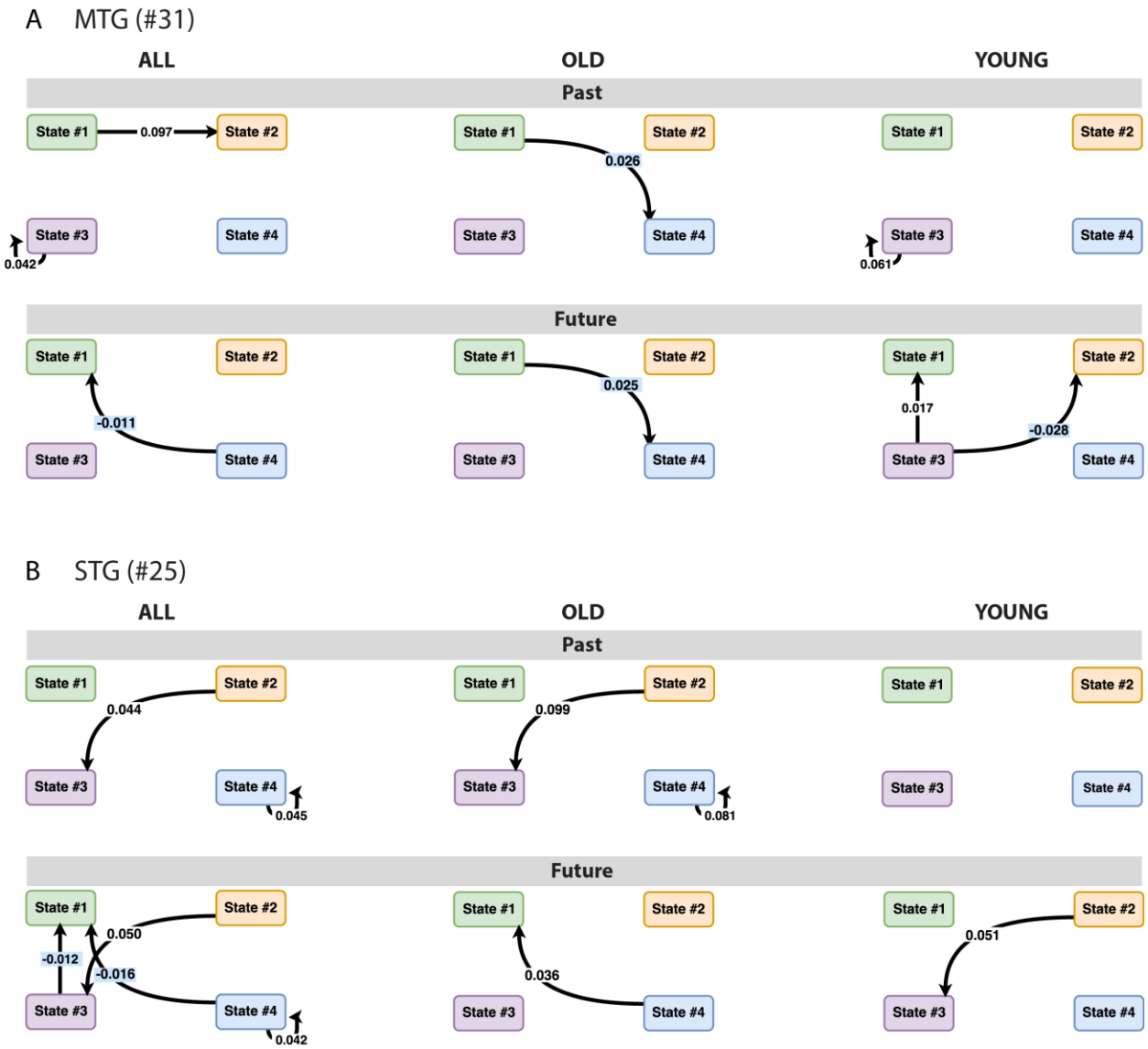

Figure 3.39. Transition probabilities by content group between *brain states* for all, older and younger subjects, for (A) the middle temporal gyrus and (B) the superior temporal gyrus seeds. All panels only show when there is a significant difference ($p<0.05$) in the transition probabilities between higher content score groups and low content score groups. The values are depicted as High vs. Low; thus the negative values highlighted in blue represent a value for the lower content group and vice-versa for the high content group. The results are shown for Past and Future content scores separately, for all subjects, as well as for only subjects in the old or young cohorts.

For the future content scores in the STG, we found significant differences in each cohort and across all subjects. In the younger cohort, subjects in the high content group were significantly more likely to transition from STG#2 to STG#3, than the subjects in the low

content group ($p<0.05$; Figure 3.39.B). In the older cohort, we found subjects in the high content group were significantly more likely to transition from STG#4 to STG#1, than the subjects in the low content group ($p<0.05$). By contrast, we found the opposite across all subjects with those in the low content group significantly more likely to transition from STG#4 to STG#1, than the high content group ($p<0.05$; Figure 3.39.B). Across all subjects, we also found significantly more high content subjects switching from STG#2 to STG#3 than low content subjects, as observed with the younger cohort. In addition, lower content subjects transitioned significantly more from STG#3 to STG#1, and higher content subjects were significantly more likely to remain in STG#4, that the reciprocal groups (all $p<0.05$; Figure 3.39.B).

We next investigated the overall frequency each cohort switched states. In the MTG seed region, we observed subjects from the older cohort switched between states significantly less than did subjects in the young cohort (8.97% vs 11.74%, $p=0.013$). By contrast, in the STG seed region, there was no significant difference for the frequency of transitions between states between the old and young cohorts (10.34% vs 10.48%, $p=0.901$).

Within the MTG, when we explored these relationships broken down into content groups, we found no significant relationship in the past content score group, between either high and low content scores and switching behaviour. This was true across all subjects and within cohorts (All: 10.07% vs 10.83%, $p=0.499$; Old: 8.43% vs 9.52%, $p=0.477$; Young: 10.6% vs 12.18%, $p=0.325$). When we examined high and low scores for future content, we found similar results with no significant differences in switching frequencies between high and low content groups, across all subjects and cohorts (All: 10.15% vs 10.69%, $p=0.631$; Old: 8.12% vs 9.52%, $p=0.357$; Young: 10.69% vs 13.02%, $p=0.154$).

In the STG, except for the old cohort in future content scores we found no significant differences in switching activity between high and low content groups for both past and

future, across all subjects and both cohorts. (Past: All: 10.41% vs 10.36%, p=0.964; Old: 9.57% vs 11.11%, p=0.345; Young: 10.6% vs 10.38%, p=0.887; Future: All: 10.22% vs 10.55%, p=0.769; Young: 10.82% vs 10.16%, p=0.670). In the old cohort, however, when looking at the future content scores, subjects in the low content group transitioned to other *brain states* significantly more than subjects in the high content group (Future: Old: 8.55% vs 12.16%, p=0.027).

We then assessed the impact that remaining in a *brain state* and transitioning from a *brain state* would have on mean connectivity for each of the seeds. In the MTG, we only observed an overall significant difference in mean connectivity for transitions out of or remaining in a given state, in the older cohort (0.255 vs 0.220, p=0.0018). When looking at individual states, we found greater mean connectivity in MTG#4 for both cohorts combined and individually for subjects that remained in, rather than transitioned out of the state (All: 0.313 vs 0.280, p=0.0010; Old: 0.315 vs 0.264, p=0.0146; Young: 0.312 vs 0.287, p=0.0187). In MTG#2, we found an association with the older cohort and across all subjects (All: 0.320 vs 0.292, p=0.0181; Old: 0.315 vs 0.277, p=0.0250). By contrast in MTG#3 we found the reverse, whereby the younger cohort and all subjects combined were significantly more likely to transition out of the *brain state* with a higher connectivity, than if they were to remain (All: 0.192 vs 0.212, p=0.0206; Young: 0.204 vs 0.233, p=0.0101).

When we examined the relationship between mean connectivity and past content scores in the MTG, we found a lower connectivity in high content scoring individuals that remained in MTG#3, than those that switched (High Content: 0.187 vs 0.211, p=0.045); and a higher connectivity in subjects that remained in MTG#4 that had lower content scores, than those that transitioned to a different *brain state* (Low Content: 0.310 vs 0.269, p=0.045). When we examined the impact on mean connectivity within each cohort, we found the high content group in the older cohort had an overall higher connectivity when

subjects remained in a given *brain state*, than those that transitioned to other *brain states* (High Content: 0.289 vs 0.248, p=0.015). We also found a significantly higher mean connectivity in the subjects with high content scores that remained in MTG#4, than those that transitioned to a different *brain state* (High Content: 0.336 vs 0.285, p=0.044). In the younger cohort we did not observe any significant relationship between the mean connectivity when remaining or transitioning from a *brain state* and the past content scores.

For the future content score groups, across all subjects we found a greater mean connectivity in subjects from both high and low content scoring groups that remained in MTG#4, than those that transitioned to a new *brain state* (High: 0.321 vs 0.293, p=0.046; Low: 0.304 vs 0.266, p=0.006). Within the older cohort, subjects with high content scores overall had a significantly higher connectivity mean when they remained in a *brain state*, as opposed to transitioning from it (High: 0.282 vs 0.243, p=0.018). Subjects with scores in the low content group had a significantly higher mean connectivity when they remained in MTG#2, than those that transitioned to a new *brain state* (Low: 0.325 vs 0.276, p=0.018). In the younger cohort, subjects with high content scores had a significantly higher connectivity mean when they remained in MTG#4, as opposed to transitioning from to a different *brain state* (High: 0.309 vs 0.274, p=0.038). By contrast, younger subjects that were in the low content group had a significantly lower mean connectivity when they remained in MTG#3, than if they transitioned to a new *brain state* (Low: 0.207 vs 0.239, p=0.046).

In the STG, we did not observe any significant difference in overall mean connectivity for transitions out of or remaining in state across subjects and age cohorts (all, $p>0.05$). When looking at individual states, we found a significantly greater mean connectivity in older subjects, and for all subjects combined, that remained rather than transitioned from STG#4 (All: 0.351 vs 0.312, $p<0.001$; Old: 0.349 vs 0.290, $p<0.001$). We observed the reverse

patterns in which the older cohort and all subjects combined had a significantly lower mean connectivity when they remained in STG#3, than when they transitioned from the *brain state* (All: 0.198 vs 0.212, p<0.0383; Old: 0.184 vs 0.202, p<0.0486).

When looking at the STG using the high and low content scores for past and future thoughts, we found a significantly lower mean connectivity for subjects with high content scores that remained in STG#3, as compared to those that transition to a different *brain state*. This was observed for both past and future content scores, across all subjects, as well as in the older cohort alone (All-Past: 0.198 vs 0.230, p=0.001; All-Future: 0.200 vs 0.226, p=0.007; Old-Past: 0.184 vs 0.218, p=0.005; Old-Future: 0.191 vs 0.217, p=0.035). By contrast in STG#4 subjects from both low and high content groups, as a whole and in the older cohort alone, had a significantly higher mean connectivity when they remained in the *brain state*, as opposed to when the transitioned to a different *brain state* (High Content Score: All-Past: 0.349 vs 0.312, p=0.005; All-Future: 0.351 vs 0.319, p=0.016; Old-Past: 0.359 vs 0.292, p=0.001; Old-Future: 0.353 vs 0.286, p=0.003; Low Content Score: All-Past: 0.356 vs 0.314, p=0.001; All-Future: 0.350 vs 0.305, p=0.0002; Old-Past: 0.326 vs 0.289, p=0.039; Old-Future: 0.342 vs 0.294, p=0.0035). In the younger cohort, we found no significant relationship between the mean connectivity for remaining or transitioning from a *brain state*, for any content group or *brain state* (all, p>0.05). In the older cohort for past content scores, we found a significantly higher mean connectivity for the subjects in the high content group across all *brain states* that remained, compared to those that transitioned (0.270 vs 0.237, p=0.033).

3.3.2.6. Summary:

In this study, we correlated thought content of young and old subjects to resting state connectivity using static and dynamic methods. We did not find a significant main effect of thought content on connectivity, however, we did find a significant cross-over

interaction between age and past thought content from both seed regions. We identified a significant increase in connectivity the occipital and parietal lobes from the MTG, and a significant increase to the calcarine from the STG seed region. Through the dynamic analysis we observed that older subjects with high content scores displayed high connectivity, while young subjects with high content scores were characterized by lower connectivity than the average across all subjects. We observed the inverse with low-content scores. Older subjects with high content scores were significantly associated with MTG#4. This *brain state* was characterized by diminished connectivity to the DMN and thalamus and increased connectivity to other regions, as compared to the average. By contrast, younger subjects spent significantly more time than older subjects in MTG#3. Younger subjects with higher content scores were more associated to this state, however, this did not reach significance. The *brain state* was characterized by a higher connectivity to the DMN and reduced connectivity to other brain regions, as compared to the average across all subjects. A compensatory pathway via the MTG for older subjects when thinking about the past, may explain these observations. These are encouraging results that offer support for our original hypotheses.

3.4. Cross-Dataset Comparison

3.4.1. Introduction

In this exploratory, preliminary analysis our objective is to compare *brain states* derived from our analytic method across datasets. Since awake subjects may sleep inadvertently during a resting-state procedure, we are interested in associations between the *brain states* of awake (resting-state) subjects and those during NREM2 sleep. We calculate the Pearson correlation coefficient for all possible combinations of *brain state* and average cohort maps, across and within datasets. We anticipate some correspondence between resting-state and NREM2 *brain states*. To recap, our objectives are as follows:

- Assess the feasibility of comparing *brain states* across datasets
- Explore correlational relationships between sleep and resting-state *brain states*.
- Evaluate the characteristics of inter-dataset *brain states* that show an association (i.e.: an association between NREM2 sleep and apparent wakefulness *brain states*).

Due to differential age-related activity during sleep, we expect corresponding associations between *brain states* linked with similar age cohorts, across datasets. This would support our argument that along with sleep, age-related heterogeneous activity during sleep may have an important impact on resting-state results. We present a simple data-driven method to compare *brain states* across datasets. To recap, our hypotheses are as follows:

Hypotheses:

- A *brain state* from the resting-state analysis will be associated with an inter-dataset NREM2 sleep *brain state*.
- These *brain state* will correspond according to age.

(i.e.: a *brain state* associated with older subjects in resting-state will associate to NREM2 sleep *brain states* that likewise associates more with older subjects.)

- The associations across datasets will be lower in the MTG seed region.

To maintain continuity with our earlier studies, we focused our attention on four ROIs from the Cambridge-36 functional network atlas [120]. The posterior cingulate cortex (PCC, region#4), the middle temporal gyrus (MTG, region#31), and both seed regions from the sleep study, comprising the thalamus caudate (TC, region#8) and the insula (INS, region#28).

From the PCC, we expect diminished connectivity to the DMN following sleep [90]. The MTG is not known for specific sleep-related activity [91, 92], and will serve as a control. The TC is sensitive to drifting between wakefulness and sleep, along with sleep activity [93]. The INS has been related to slow-wave sleep activity, as well variations in activity according to eyes open and closed conditions [94]. Excluding the control seed region, we anticipate these regions will provide sufficient variation between wakefulness and sleep to identify corresponding vigilance across *brain states*.

To make this assessment as analogous between datasets, we matched subject cohorts by age and sex. As a result, the cohorts of subjects from the NKI-e dataset differ somewhat from those in previous results sections. For this analysis, from the NKI-e dataset we analyzed 153 subjects (Old: 75 subjects (29% male), 50-69yrs, 58.4±5.85yrs; Young: 78 subjects (50% male), 18-35yrs, 23.8±4.61yrs). This is matched with our previously described Sleep dataset of 30 subjects (Old: 14 subjects (36% male), 52-69 years, 59.5±5.9 years; Young: 16 young subjects (50% male), 20 – 30 years, 23.3±3.3 years).

3.4.2. Results

For readability, the results are organized by seed region. Further, within each section we first present a figure describing the cross-dataset comparison, followed by figures describing the results of the clustering analysis, the composition of the states and a figure that displays the brain maps across datasets. The figures are explained in greater detail in the first section (posterior cingulate cortex), thus the reader may refer to this section for additional information to better read and interpret the figures in subsequent parts of this chapter.

3.4.2.1. Posterior cingulate cortex

For the cross-dataset comparison, we calculated the Pearson correlation coefficient for all *brain state* maps and group average maps across and within the datasets that comprised awake subjects during resting-state and the sleeping subjects during NREM2 (NKI-e and Sleep dataset, respectively; Figure 3.40).

The cross-dataset comparison figure is mirrored along the diagonal. We have divided the figure into four quadrants (demarcated by the green dashed lines) and most easily interpreted by reading across rows. With this in mind, the upper-left quadrant illustrates the intra-dataset relationship of all NKI-e maps to those within the same dataset. Reading across rows, each row then highlights the relationship of one of the NKI-e States or Group Averages across the NKI-e dataset. In the bottom-right quadrant the within-dataset relationship of all Sleep (NREM2) maps is represented, and can be read across rows as in the upper-left quadrant.

The upper-right and lower-left quadrants are mirror images that illustrate the inter-dataset relationship of each map from the NKI-e dataset to each map of the Sleep (NREM2) dataset. When reading across rows, in the upper-right quadrant each row

highlights the relationship of one of the NKI-e States or Group Averages across those from the Sleep (NREM2) dataset, and vice-versa reading across rows in the lower-left quadrant each row represents one of the Sleep (NREM2) States or Group Averages and its relationship to those from the NKI-e dataset.

We present the cross-dataset comparison derived from the posterior cingulate cortex seed for both the NKI-e and Sleep (NREM2) datasets in Figure 3.40.

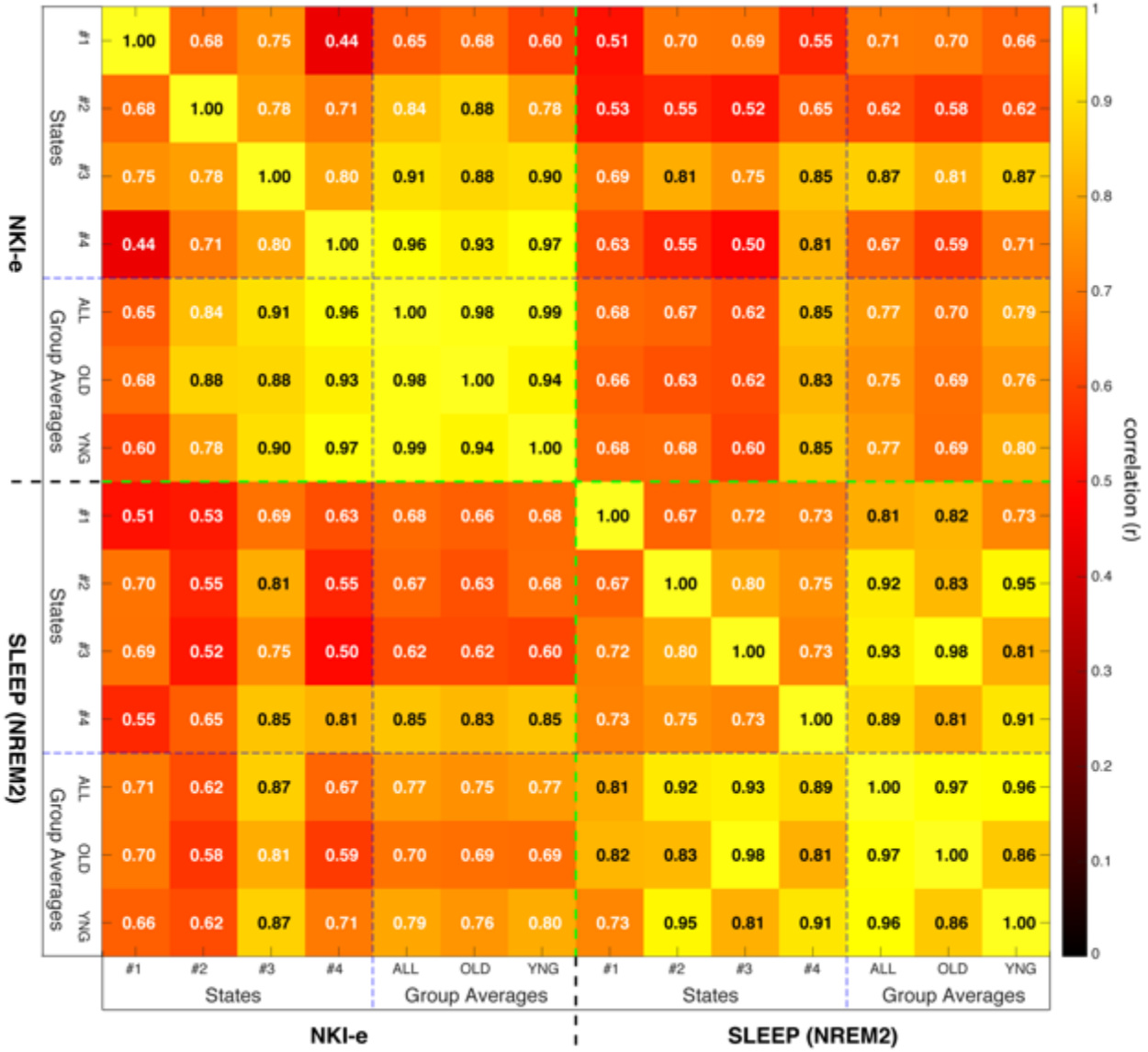

Figure 3.40. Cross-dataset correlation map for the posterior cingulate cortex seed comparing both within and across NKI-e and Sleep (NREM2) datasets. A color-coded, Pearson correlation coefficient is listed for all comparisons between each mean *brain state* map and group average maps for all, old and young subjects. The green dashed lines separate the two datasets and highlight the four quadrants of the correlation map; the black dashed lines divide the *brain state* data from the Group Averages.

In the upper-right quarter (Figure 3.40), we observed that PCC#3 (NKI-e) correlates comparably to the *brain states* across both datasets (Mean: 0.775 vs 0.777, respectively). When comparing PCC#3 (NKI-e) to the group averages, we found a slightly lower mean correlation with the Sleep (NREM2) dataset as compared to the NKI-e dataset (Mean: 0.85 vs 0.897). This *brain state* correlated most with PCC#4 (NREM2) and with the young (NREM2) cohort (0.85 and 0.87, respectively). From the Sleep dataset, we observed that PCC#4 (NREM2) correlates more to PCC#3 (NKI-e) and PCC#4 (NKI-e) (0.85 and 0.81, respectively), than to all other Sleep states (≤0.75 for all; Figure 3.40, lower-left and -right quarters). The *brain state* PCC#4 correlated more to the Sleep (NREM2) group averages for all and young cohorts, but less to the old cohort, as compared to the NKI-e group averages (All: 0.89 vs 0.85; Young: 0.91 vs 0.85; Old: 0.81 vs 0.83).

When we examined the Group Averages, we found a greater correlation between the young and old cohort maps in the awake NKI-e dataset, than from the Sleep (NREM2) dataset (0.94 vs 0.86, respectively).

With both datasets we applied a hierarchical clustering procedure (Ward's criterion) on the correlations between each window map with all the other window maps, resulting in a similarity matrix (Figure 3.41, left panels). Based on these similarity matrices, four states were assigned (Figure 3.41, right panels). In the NKI-e dataset, one cluster comprised over half of all windows, while the remaining three clusters were of comparable size. In the Sleep (NREM2) dataset, the procedure resulted in three comparably sized clusters, with one clusters driven by less data.

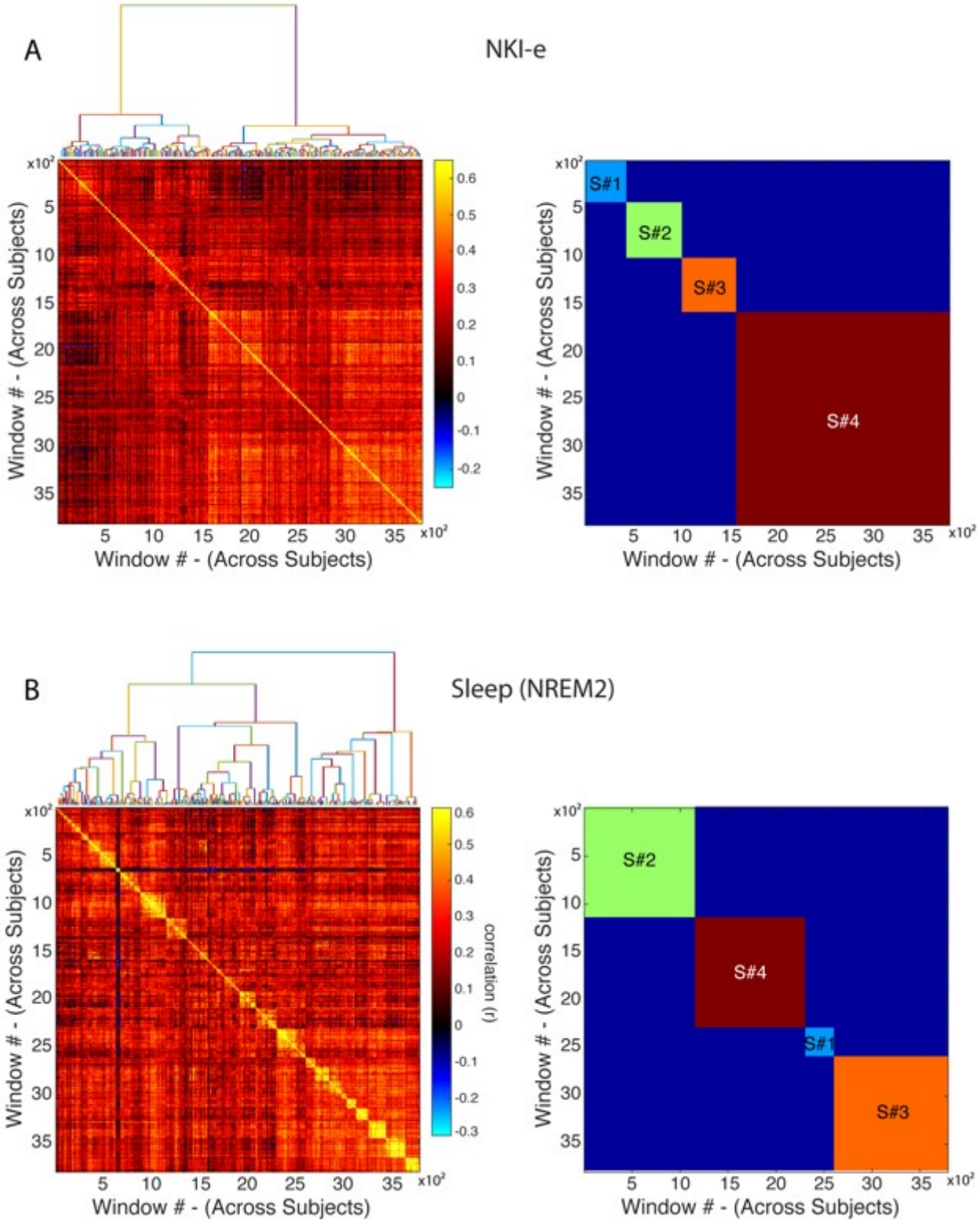
A
NKI-e
Window # - (Across Subjects)
Window # - (Across Subjects)
S#1
S#2
S#3
S#4
B
Sleep (NREM2)
Window # - (Across Subjects)
Window # - (Across Subjects)
correlation (r)
S#2
S#4
S#1
S#3

Figure 3.41. A) Hierarchical clustering in the NKI-e dataset. Left: Similarity matrix: Hierarchical clustering of the correlation of each window map to all other window maps across all subjects under Ward's criteria. Each window map represents the connectivity between the posterior cingulate cortex seed to the entire brain. The dendogram is shown above the similarity matrix. Right: The clusters defined by the selection of four *brain states*. The numbers listed (i.e.: S#1, S#2, etc.) refer to the State numbers referenced in the text. B) Same as in A) for the Sleep dataset during NREM2.

In the NKI-e dataset we observed that the probability of spending time in two of the states was significantly different between cohorts (Figure 3.42, left panel). Old subjects spent more time in State#2 ($p<0.001$), while PCC#3 (NKI-e) had significantly more young subjects than old subjects associated with it ($p<0.01$). We found that PCC#4 (NKI-e) contains approximately half of the windows from both age cohorts, with no significant difference between the presence of the old and young subjects (Figure 3.42), whereas PCC#4 (NREM2) was associated significantly more with younger than older subjects ($p<0.05$).

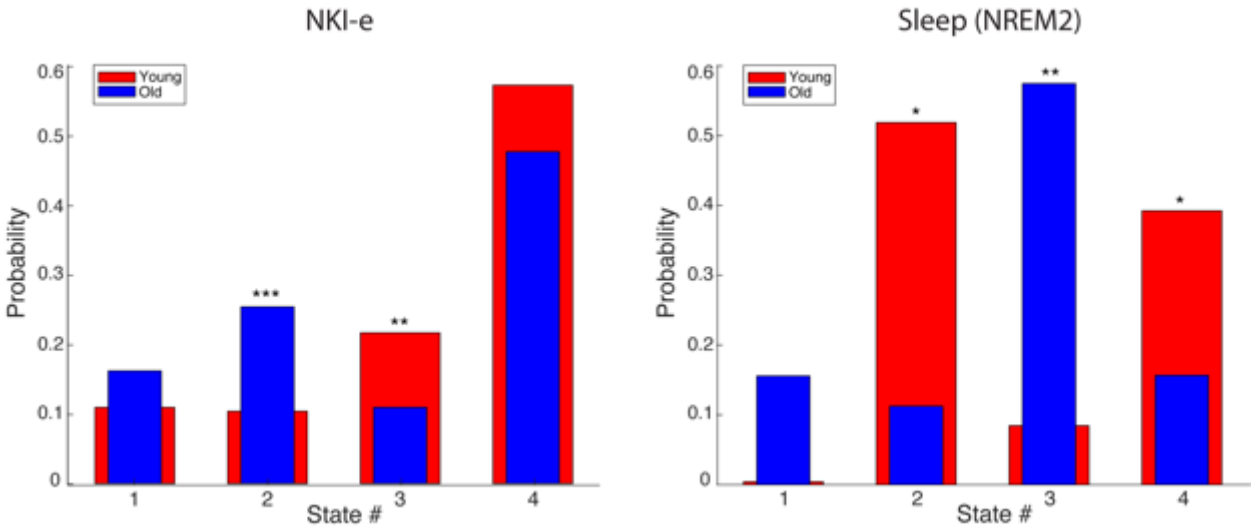

Figure 3.42. Probability of time spent in a *brain state* for young (red) and old (blue) cohorts computed for the posterior cingulate cortex seed in the NKI-e dataset (left) and the Sleep (NREM2) dataset (right). Significance was assessed using permutation tests (n=100,000; * $p<0.05$, ** $p<0.01$, *** $p<0.001$).

In the Sleep dataset, only PCC#1 (NREM2) did not associate significantly with either age cohort (Figure 3.42, right panel). In PCC#2 (NREM2), we observed a greater association to the subjects in the younger cohort ($p<0.05$). In PCC#3 (NREM2) by contrast, we found significantly more of the older subjects associated to the State than young ($p<0.01$), while comprising almost 60% of all windows from the older cohort.

When we examined the distribution of window maps across subjects and cohorts (Figure 3.43), we confirmed that PCC#1 (NREM2) dataset was driven by a single older subject (Figure 3.43.C).

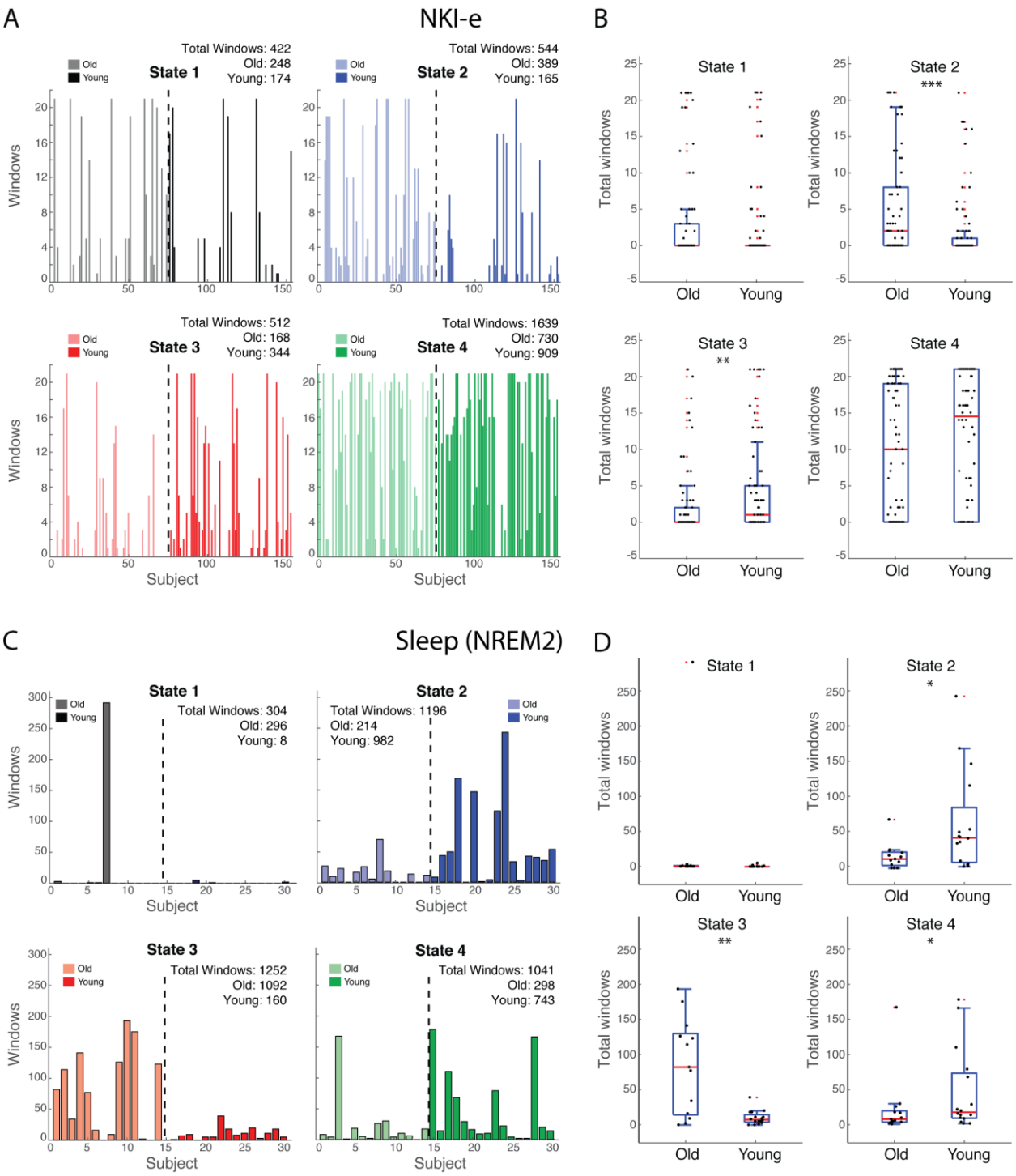

Figure 3.43. Distribution of window maps by *brain state* and cohort in the posterior cingulate cortex seed. A) The number of window maps that are most correlated to the given *brain state* by subject for the NKI-e dataset. The dashed line demarcates the older and younger cohorts, with the older cohort to the left of the dashed line. B) Corresponding boxplots show the distribution of the number of windows for each subject associated with the given *brain state*, by cohort. C) and

D) The same as in A) and B) for the Sleep (NREM2) dataset. Significance was assessed using permutation tests (n=100,000, where * $p<0.05$, ** $p<0.01$, *** $p<0.001$).

In Figure 3.44, we display brain maps resulting from the PCC seed for each of the *brain states* and Group Averages in both datasets. Specifically, we computed the mean of the voxel-wise connectivity across windows and subjects, both while awake in the NKI-e dataset and while sleeping in NREM2 in the sleep dataset (Figure 3.44, row 5: "Mean"). All other maps were then z-standardized in relation to this average map. State-wise connectivity (rows 1-4) was calculated as the average of the voxel-wise connectivity within all windows that correlate most with the given *brain state* of interest. The limits used for the figure were kept constant across the datasets for each row of data, except in cases where a *brain state* was driven by only one or two subjects. *Brain states* that bear similarity to one another across datasets do not necessarily appear adjacent to one another. Finally, we computed the z-maps of the connectivity in the older and younger cohorts relative to the mean connectivity across all subjects in each respective dataset (Figure 3.44, rows 6 and 7).

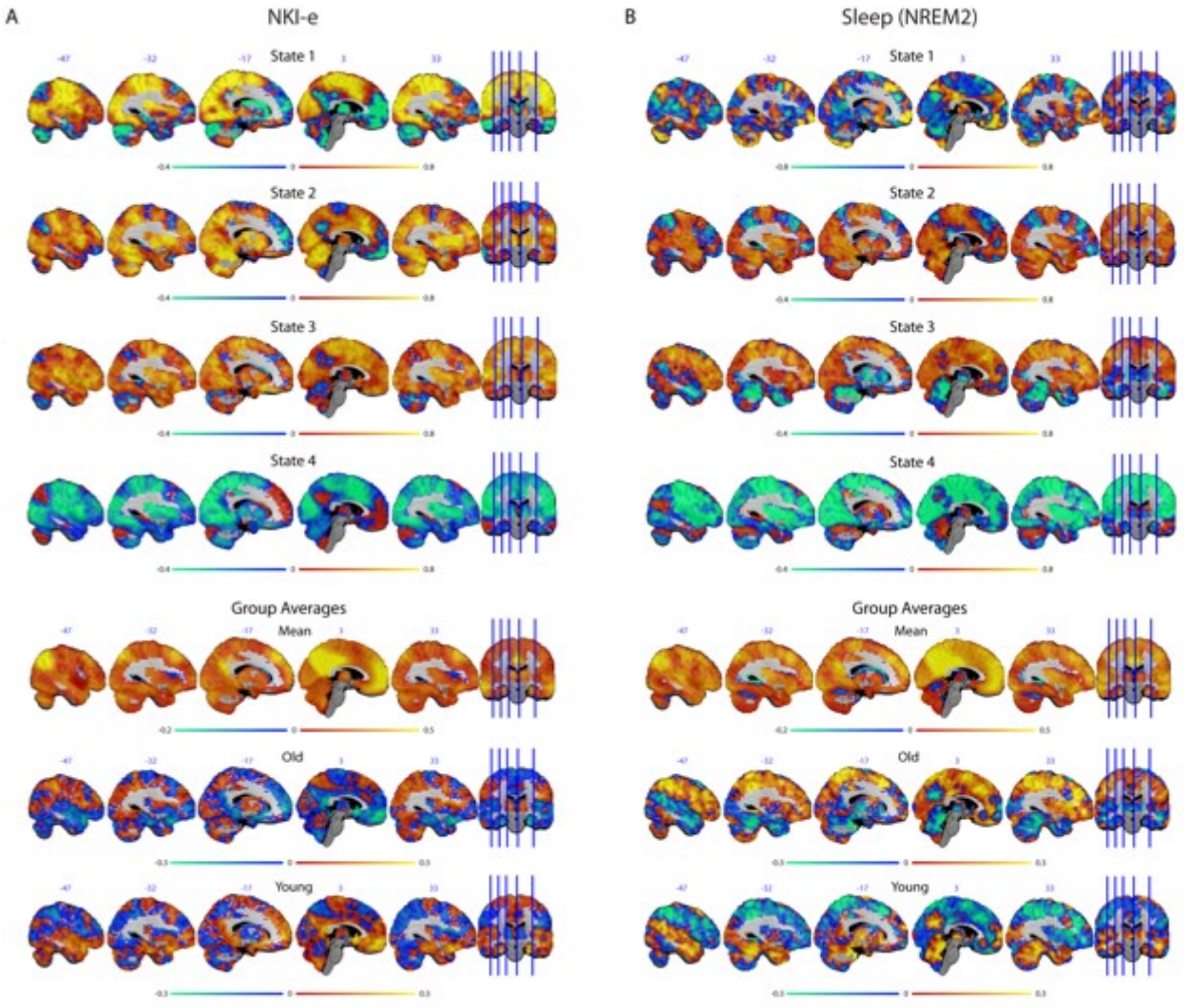

Figure 3.44. Brain connectivity maps between the posterior cingulate cortex seed and the entire brain in (A) the NKI-e dataset and (B) the Sleep (NREM2) dataset. The upper four rows show z-maps of each *brain state* relative to the average voxel-wise connectivity depicted in the fifth row ("Mean"). The bottom two rows illustrate the z-maps of the connectivity in the older and younger cohorts, respectively.

In PCC#3 (NKI-e), a *brain state* significantly associated with younger subjects (Figure 3.42.A.), we observed a lower connectivity to the default-mode network (DMN), whereas a higher connectivity to all other brain regions as compared to the dataset average. The *brain state* PCC#4 (NKI-e) displays typical DMN connectivity expected from a PCC seed. There is generally an increased connectivity to the DMN and a reduction in connectivity to other brain regions, as compared to the average. There is no significant difference in

the number of older or younger subjects in PCC#4 (NKI-e), There is also a reduction of connectivity in PCC#4 (NREM2), but this is observed more extensively throughout the brain, as compared to the average. There are significantly more younger subjects in PCC#4 (NREM2) (Figure 3.42).

Looking at the average connectivity across the NKI-e dataset, there is greater connectivity between the anterior and posterior regions of the brain, from the PCC seed, as compared to the sleep average. The younger population shows this connectivity to a greater degree than the older population, while these apparent age-related differences are more notable during sleep than wakefulness (Figure 3.44. Bottom panels).

In summary, PCC#3 (NKI-e) shows the greatest correspondence to the Sleep (NREM2) data, and most specifically to PCC#4 (NREM2). Both of these *brain states* are significantly associated to younger over older subjects. We observed that both of these *brain states* have a greater inter-state, as opposed to intra-state correspondence, but correlate more to intra-dataset group averages.

3.4.2.2. Thalamus-caudate

In Figure 3.45, we show the results from the cross-dataset comparison with the thalamus-caudate seed region. As in the previous section, we calculate the Pearson correlation coefficient of each mean *brain state* map, along with the average maps across all, old and young subjects from the NKI-e dataset to that of the Sleep (NREM2) dataset. For a more extensive explanation, refer to the analogous figure in the posterior cingulate cortex section (Figure 3.40).

The highest correlation we observed between States (0.65), was found between TC#3 (NKI-e) and TC#4 (NREM2) (Figure 3.45: Upper-right quarter). In TC#2 (NREM2), we

observe almost no correlation to any of the states in NKI-e (Figure 3.45: Bottom-left quarter). We observed the greatest correspondence between the young cohort group average in NKI-e, when compared to the overall and young cohort group averages in the Sleep (NREM2) dataset (0.71 and 0.70, respectively; Figure 3.45: Upper-right quarter).

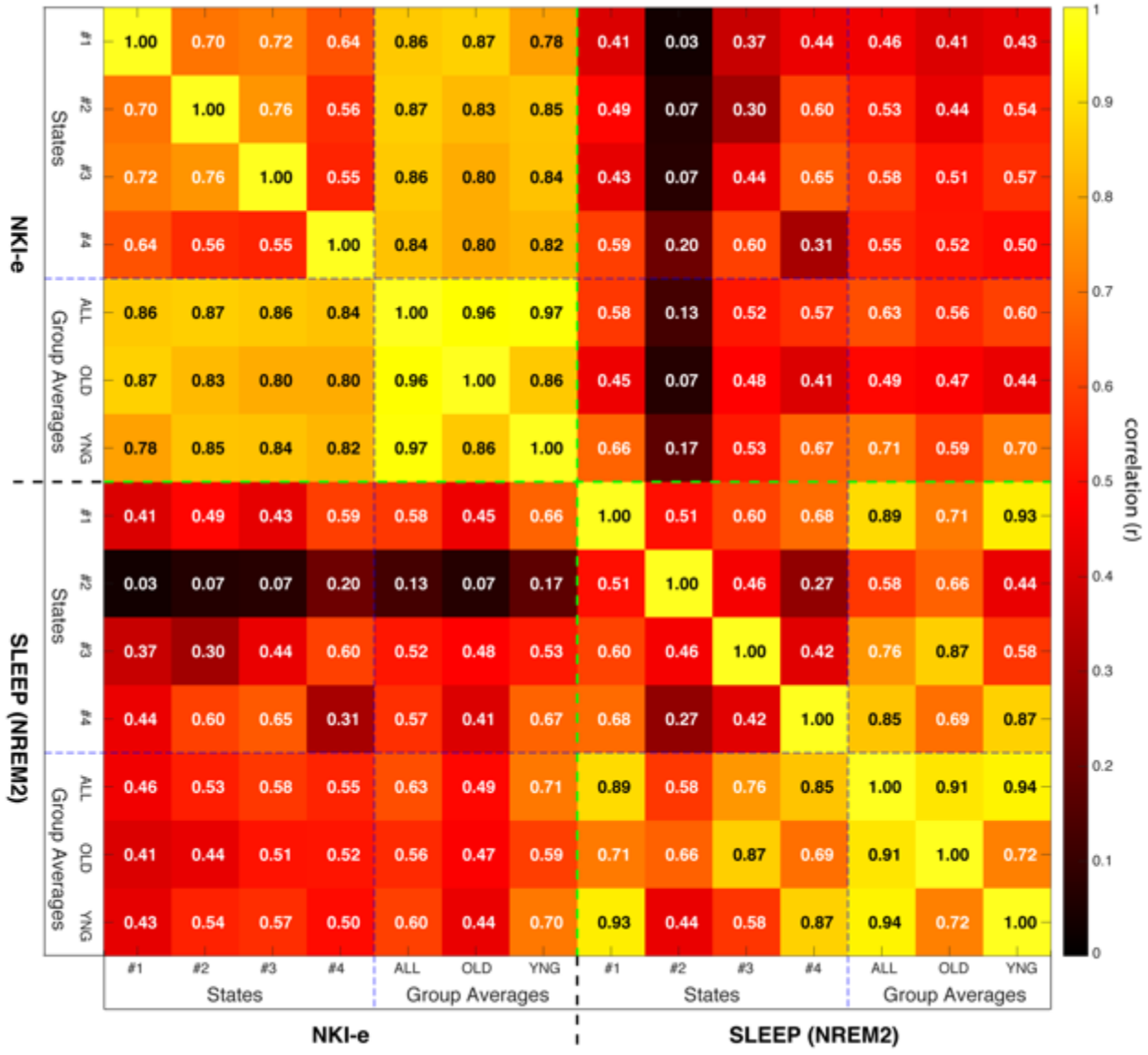

Figure 3.45. Cross-dataset correlation map for the thalamus-caudate seed comparing both within and across NKI-e and Sleep (NREM2) datasets. A color-coded, Pearson correlation coefficient is listed for all comparisons between each mean *brain state* map and group average maps for all, old and young subjects. The green dashed lines separate the two datasets and highlight the four quadrants of the correlation map; the black dashed lines divide the *brain state* data from the Group Averages.

As seen in the PCC seed, the correlation between the older and younger cohort maps is greater in the NKI-e dataset than in the Sleep (NREM2) dataset (0.86 vs 0.72; Figure 3.45: Upper-left and bottom-right quadrants).

As described in the previous section, we applied a hierarchical clustering procedure (Ward's criterion) to both datasets on the correlations between each window map with all the other window maps, resulting in a similarity matrix (Figure 3.46, left panels). We derived the clusters based on the similarity matrix, after we assigned four States to the data (Figure 3.46, right panels). In the NKI-e dataset, the clusters are of comparable size, whereas in the Sleep (NREM2) dataset, the procedure resulted in three main clusters, with one smaller cluster.

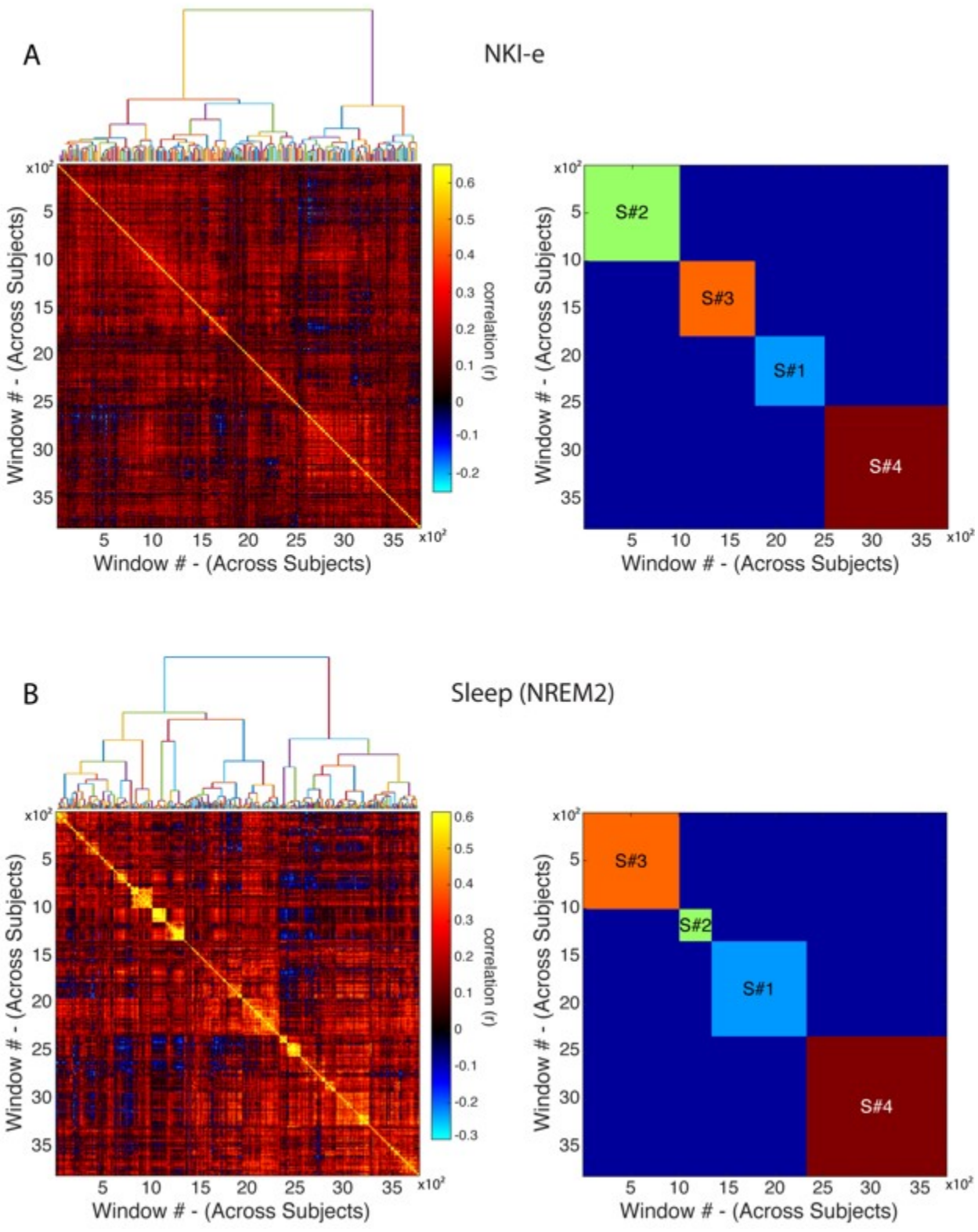

Figure 3.46. A) Hierarchical clustering in the NKI-e dataset. Left: Similarity matrix: Hierarchical clustering of the correlation of each window map to all other window maps across all subjects

under Ward's criteria. Each window map represents the connectivity between the thalamus-caudate seed to the entire brain. The dendogram is shown above the similarity matrix. Right: The clusters defined by the selection of four *brain states*. The numbers listed (i.e.: S#1, S#2, etc.) refer to the State numbers referenced in the text. B) Same as in A) for the Sleep dataset during NREM2.

We assessed the probability of spending time in a given *brain state* for each cohort (Figure 3.47) along with the respective distributions of the window maps by *brain state* across subjects and cohorts (Figure 3.48). In Figure 3.48.A.&C., the window distributions for both datasets are shown, demarcated by a dashed line between the older subjects on the left and younger subjects on the right. The boxplots are shown in Figure 3.48.B.&D.

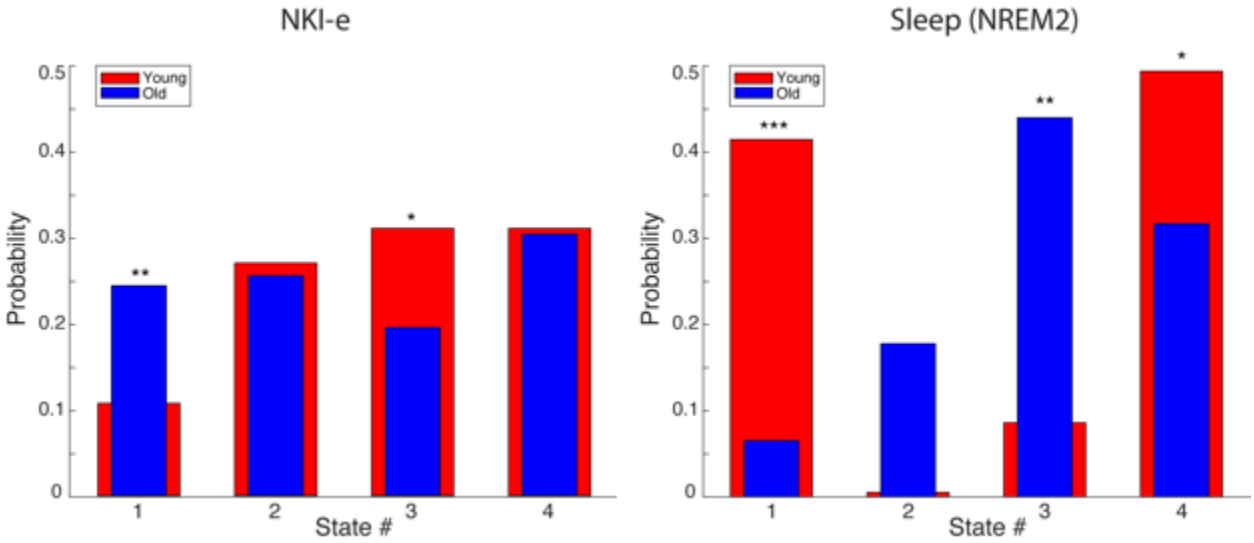

Figure 3.47. Probability of time spent in a *brain state* for young (red) and old (blue) cohorts computed for the thalamus-caudate seed in the NKI-e dataset (left) and the Sleep (NREM2) dataset (right). Significance was assessed using permutation tests (n=100,000; * $p<0.05$, ** $p<0.01$, *** $p<0.001$).

In the NKI-e dataset, we found that age association to TC#1 and TC#3 differed significantly by cohort. The old cohort spent significantly more time than the young cohort in TC#1 ($p<0.01$), while the younger cohort spent significantly more time than the old cohort in TC#3 ($p<0.05$; Figure 3.47). In the Sleep (NREM2) dataset, each state was significantly associated with either the old or young cohort, expect TC#2 (NREM2). When

we examined the distribution of windows by subject we found this state to be driven by only two older subjects and thus did not reach significance (Figure 3.48). In essence the Sleep (NREM2) dataset was characterized by three states, when excluding TC#2 (NREM2).

The *brain state* TC#4 (NREM2) associated significantly with younger subjects than old ($p<0.05$), as did TC#1 (NREM2) ($p<0.001$). We found that TC#3 (NREM2) was significantly associated to older subjects ($p<0.01$), as compared to younger subjects, and these older subjects spent a little less than half the time in this state (Figure 3.47, Right panel).

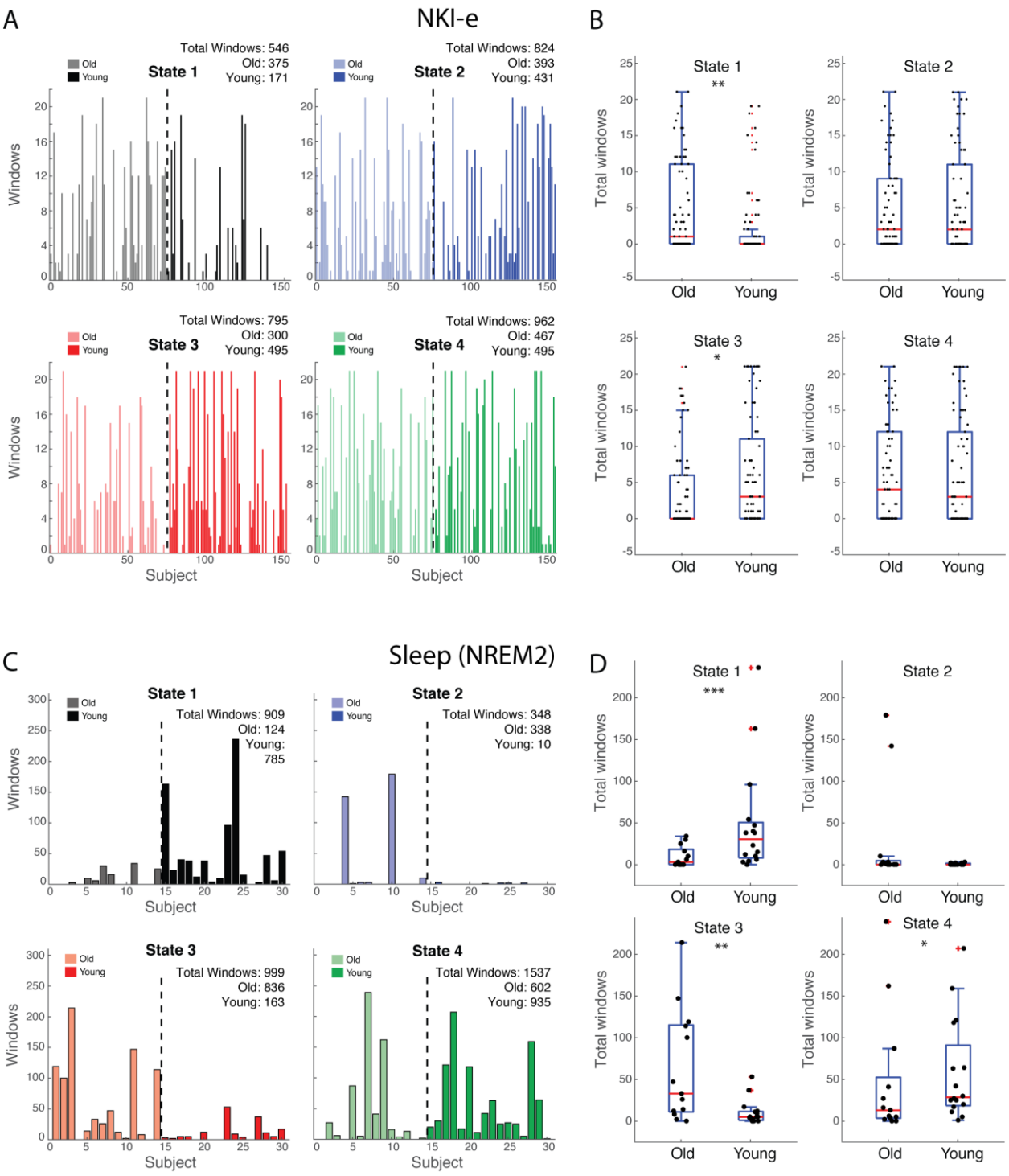

Figure 3.48. Distribution of window maps by *brain state* and cohort in the thalamus-caudate seed. A) The number of window maps that are most correlated to the given *brain state* by subject for the NKI-e dataset. The dashed line demarcates the older and younger cohorts, with the older cohort to the left of the dashed line. B) Corresponding boxplots show the distribution of the number of windows for each subject associated with the given *brain state*, by cohort. C) and D) The same as

in A) and B) for the Sleep (NREM2) dataset. Significance was assessed using permutation tests (n=100,000, * p<0.05, ** p<0.01, *** p<0.001).

In Figure 3.49 we show the maps for the TC seed, of resting-state subjects in the NKI-e dataset and sleeping subjects (NREM2) in the Sleep dataset. Figure 3.49 is organized, and described more extensively, as in the previous section (Figure 3.44).

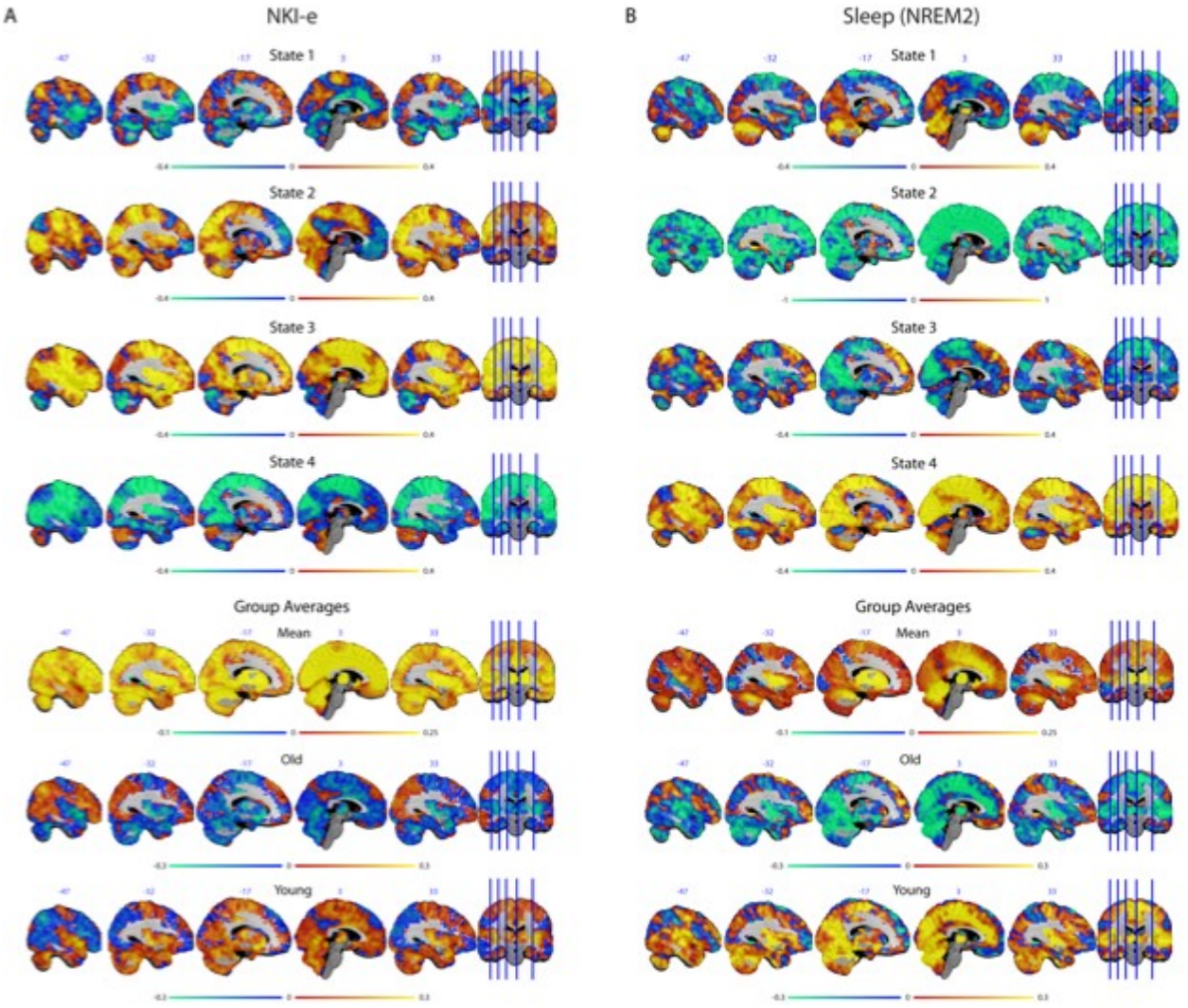

Figure 3.49. Brain connectivity maps between the thalamus-caudate seed and the entire brain in (A) the NKI-e dataset and (B) the Sleep (NREM2) dataset. The upper four rows show z-maps of each *brain state* relative to the average voxel-wise connectivity depicted in the fifth row ("Mean"). The bottom two rows illustrate the z-maps of the connectivity in the older and younger cohorts, respectively.

In TC#3 (NKI-e), in which younger subjects spend significantly more time than the subjects from the old cohort (Figure 3.47), there is a general increase in connectivity throughout most regions of the brain, as compared to the average. This increase is less in regions of the DMN, while there is a reduced connectivity to the cerebellum Figure 3.49.

As we observed in TC#3 (NKI-e), there is a general increase in connectivity to the rest of the brain in TC#4 (NREM2), as compared to the average during NREM2 sleep. This increase is less pronounced to regions of the DMN and slightly reduced to the angular gyri. As with TC#3 (NKI-e) there are significantly more young subjects that spend time in TC#4 (NREM2) as compared to the older cohort. (Figure 3.47).

There was a small increase in connectivity from the TC seed across the brain in the younger cohort of the awake (NKI-e) dataset. This excludes the occipital lobe and PCC which showed slight decreases in connectivity as compared to the average (Figure 3.49). We observed some overlap in how the younger cohort in the Sleep (NREM2) dataset differed from the average, however, the decreases were more focused in the angular gyri region, as opposed to the occipital lobe, and the increases in connectivity were stronger as compared to the NKI-e dataset.

In summary, there was some association between TC#3 (NKI-e) and TC#4 (Sleep), however, the correlation was lower than seen in inter-dataset relationships we observed with the posterior cingulate cortex seed (0.65 vs 0.85). We found both of these *brain states* were significantly associated with younger, rather than old subjects. This was supported by the relatively strong correlation between the group averages of the younger cohorts, as compared to other *brain states* (0.70).

3.4.2.3. Insula

We computed the cross-dataset comparison with the Insula seed region (Figure 3.50). As in each of the previous sections, we preformed this comparison by calculating the Pearson correlation coefficient of each *brain state* map, along with the average maps across all, old and young subjects from the NKI-e dataset to that of the Sleep (NREM2) dataset. For a more extensive explanation, refer to the analogous figure in the posterior cingulate cortex section (Figure 3.40).

From the upper-right quarter of Figure 3.50, we observed that INS#2 (NKI-e) correlated more to INS#3 (NREM2), than any other NKI-e States or Group Averages (0.89 vs ≤0.87, Mean: 0.802). We also found that INS#2 (NKI-e) correlated more to the young and all subject group averages across datasets in the Sleep (NREM2) dataset, than to the group averages within the NKI-e dataset (inter vs. intra: 0.89 vs 0.87 (young) and 0.88 vs. 0.87 (all)).

From the Sleep (NREM2) dataset, we found INS#1 and INS#2 correlated poorly to all *brain states* or Group Averages across both datasets. As observed in the previous analyses, the intra-correlation between the older and younger cohort maps were greater in the NKI-e dataset than in the Sleep (NREM2) dataset (Figure 3.50, Upper-left and bottom-right panels; 0.94 vs 0.88).

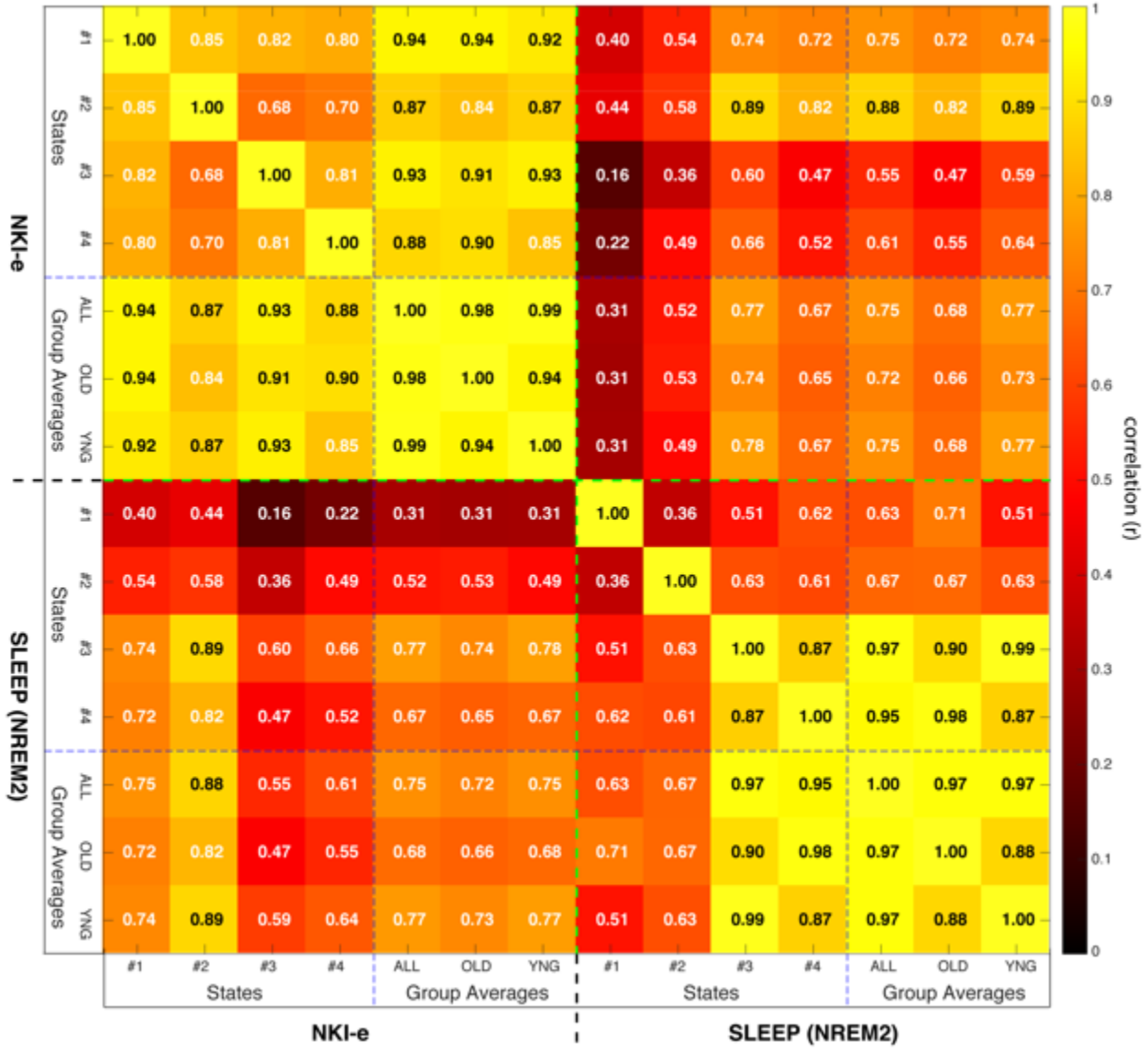

Figure 3.50. Cross-dataset correlation map for the insula seed comparing both within and across NKI-e and Sleep (NREM2) datasets. A color-coded, Pearson correlation coefficient is listed for all comparisons between each mean *brain state* map and group average maps for all, old and young subjects. The green dashed lines separate the two datasets and highlight the four quadrants of the correlation map; the black dashed lines divide the *brain state* data from the Group Averages.

As in the previous sections, we applied a hierarchical clustering procedure (Ward's criterion) to both datasets on the correlations between each window map with all the other window maps, resulting in a similarity matrix (Figure 3.51, left panels). We assigned four States to the data based on the similarity matrix (Figure 3.51, right panels).

In the NKI-e dataset, the clusters were of comparable size with INS#3 the largest and INS#4 the smallest. In the Sleep (NREM2) dataset, the procedure resulted in two main clusters, with the two remaining clusters driven by little data.

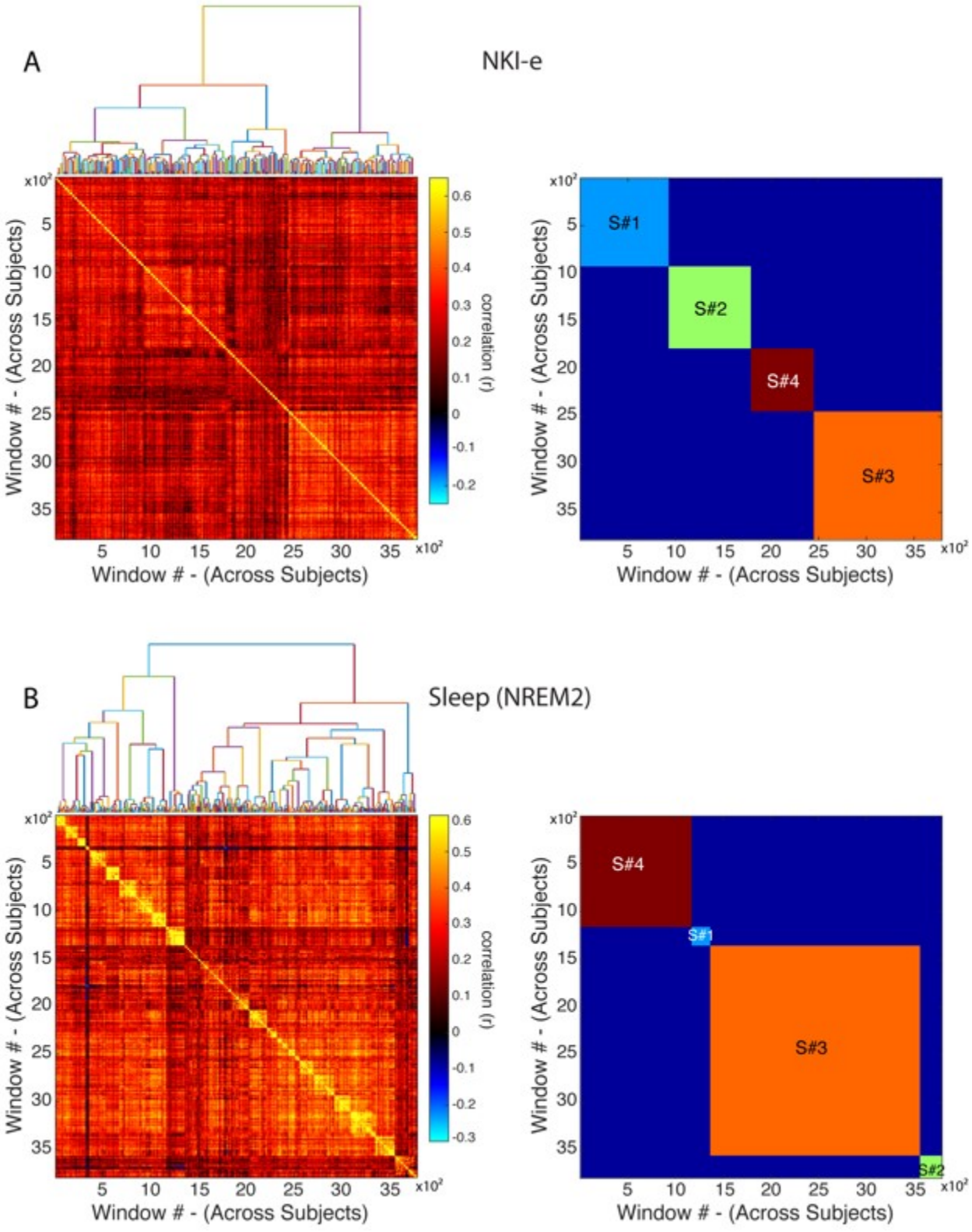

Figure 3.51. A) Hierarchical clustering in the NKI-e dataset. Left: Similarity matrix: Hierarchical clustering of the correlation of each window map to all other window maps across all subjects

under Ward's criteria. Each window map represents the connectivity between the insula seed to the entire brain. The dendogram is shown above the similarity matrix. Right: The clusters defined by the selection of four *brain states*. The numbers listed (i.e.: S#1, S#2, etc.) refer to the State numbers referenced in the text. B) Same as in A) for the Sleep dataset during NREM2.

As in the previous sections, we assessed the probability of spending time in a given state for each cohort (Figure 3.52). In addition we explored the respective distributions of window maps by *brain state* across subjects and cohorts (Figure 3.53).

In both datasets, we found the probability of time spent in INS#3 and INS#4 was significantly different between cohorts. The *brain states* INS#3 (NKI-e and NREM2) had significantly more young than old subjects associated with it, and vice-versa in INS#4 *brain states* (all, $p<0.001$). In INS#3, both datasets comprised more of the young subjects, with >90% of all windows from young subjects associated with this *brain state* in the Sleep (NREM2) dataset.

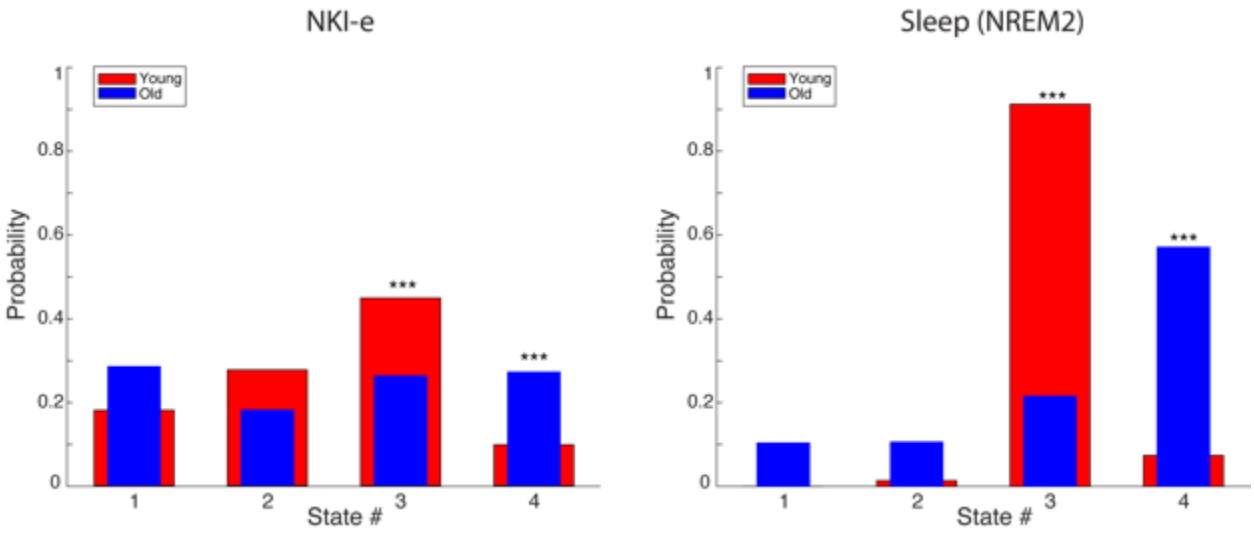

Figure 3.52. Probability of time spent in a *brain state* for young (red) and old (blue) cohorts computed for the insula seed in the NKI-e dataset (left) and the Sleep (NREM2) dataset (right). Significance was assessed using permutation tests (n=100,000; * $p<0.05$, ** $p<0.01$, *** $p<0.001$).

Due to the limited data that was associated with INS#1 and INS#2 of the Sleep (NREM2) dataset, we verified the distribution of windows to those states. We found that in both cases essentially only one subject from the old cohort (Figure 3.53) drove this finding. This explains the limited correlation of these two states to the other maps across the datasets. As a result, the Sleep (NREM2) dataset was essentially clustered into two main groups (see Figure 3.51.B.).

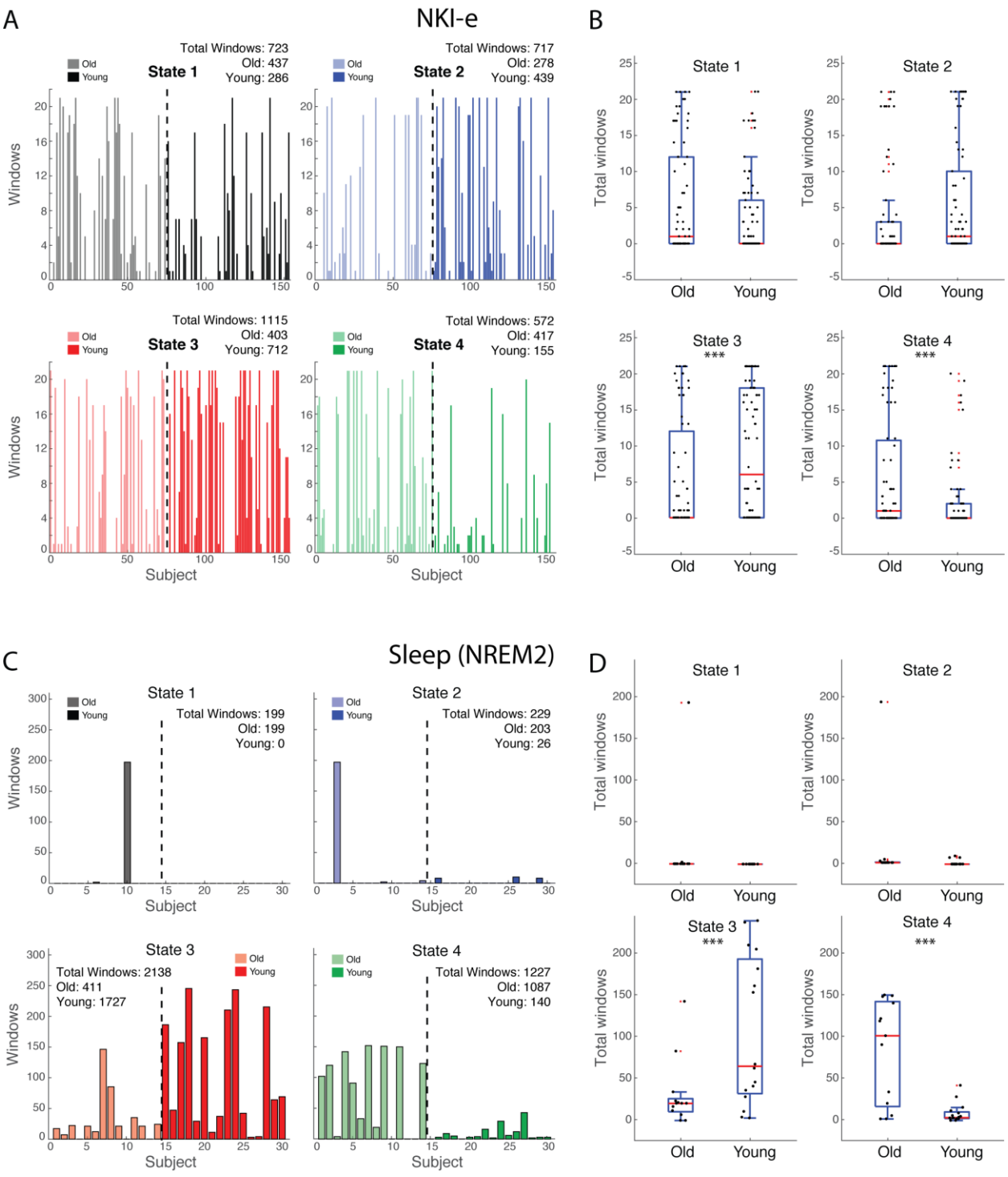

Figure 3.53. Distribution of window maps by *brain state* and cohort in the insula seed. A) The number of window maps that are most correlated to the given *brain state* by subject for the NKI-e dataset. The dashed line demarcates the older and younger cohorts, with the older cohort to the left of the dashed line. B) Corresponding boxplots show the distribution of the number of windows for each subject associated with the given *brain state*, by cohort. C) and D) The same as

in A) and B) for the Sleep (NREM2) dataset. Significance was assessed using permutation tests (n=100,000; * p<0.05, ** p<0.01, *** p<0.001).

We determined the brain maps for the Insula seed, of resting-state subjects in the NKI-e dataset and sleeping subjects (NREM2) in the Sleep dataset (Figure 3.54). The organization of the figure is described more extensively in the posterior cingulate cortex section (Figure 3.44).

In INS#2 (NKI-e) we observed stronger connectivity from the insula seed to the DMN, in particular to the posterior cingulate cortex and the medial prefrontal cortex, when compared to the average connectivity. We also observed a reduced association to the occipital lobe and cerebellum (Figure 3.54). The analysis also revealed greater voxel-wise connectivity to the insula seed region itself and to the superior temporal gyrus as compared to the average, which was also evident in the younger cohort of the Sleep (NREM2) dataset (Figure 3.54). In INS#3 (NREM2), we observed a slight reduction in connectivity to the DMN areas described, as compared to the average. The average connectivity during Sleep (NREM2), however, appears to be greater to these regions than during resting-state wakefulness in the NKI-e dataset (Figure 3.54, Mean: fifth row).

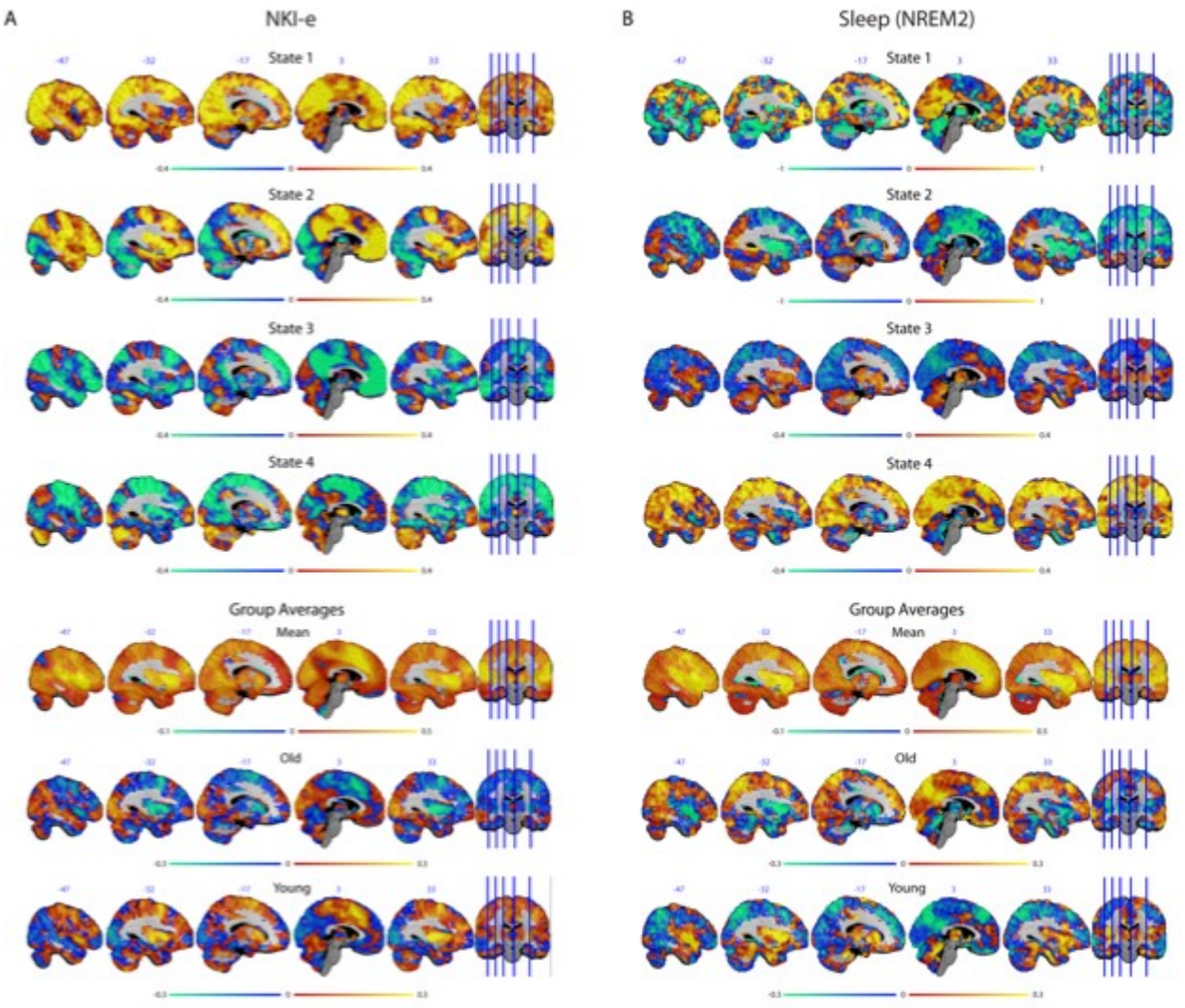

Figure 3.54. Brain connectivity maps between the insula seed and the entire brain in (A) the NKI-e dataset and (B) the Sleep (NREM2) dataset. The upper four rows show z-maps of each *brain state* relative to the average voxel-wise connectivity depicted in the fifth row ("Mean"). The bottom two rows illustrate the z-maps of the connectivity in the older and younger cohorts, respectively.

In summary, INS#2 (NKI-e) of awake subjects showed a strong correlation across the Sleep (NREM2) dataset, and a strong correlation to the All and Young Group Averages. In particular, the correlation of this *brain state* to INS#3 (NREM2) was greater than the within *brain state* comparisons in the NKI-e dataset. The *brain state* did show a trend toward comprising more young than old subjects (Figure 3.52, Left panel; p=0.0664),

which may explain the greater correlation to the young sleep cohort (0.89) as compared to that of the older sleep cohort (0.82; see Figure 3.50).

3.4.2.4. Middle temporal gyrus

In Figure 3.55 we show the results from the cross-dataset comparison with the middle temporal gyrus as the seed region. As described in the first section (posterior cingulate cortex seed, see Figure 3.40) for the cross-dataset comparison we calculated the Pearson correlation coefficient from each *brain state* and group average maps across all, old and young subjects to the equivalent maps across and within both datasets.

For the NKI-e dataset, we observed that MTG#4 was most correlated to the Sleep (NREM2) dataset than the other NKI-e states (Figure 3.55, Upper-right quarter). The *brain state* MTG#4 (NKI-e) revealed particularly high correlations to the young cohort group (0.80), to MTG#2 (0.77) and MTG#4 (0.79) of the Sleep (NREM2) dataset. The *brain state* MTG#2 (NKI-e), likewise, showed a stronger relationship to MTG#3 (NREM2) than other states (0.78), but less to the Sleep (NREM2) dataset group averages (Mean: 0.653). Overall, the young cohort group from the NKI-e dataset showed the highest correlations across all states and groups of the Sleep (NREM2) dataset (Mean: 0.78).

Of the states from the Sleep (NREM2) dataset, MTG#1 showed little correlation across both datasets (Mean: 0.536 for NKI-e and 0.655 for Sleep (NREM2)), whereas MTG#3 (NREM2) overall had the greatest average correlation across all NKI-e states and group averages (Mean: 0.726; Figure 3.55, Bottom-left quarter).

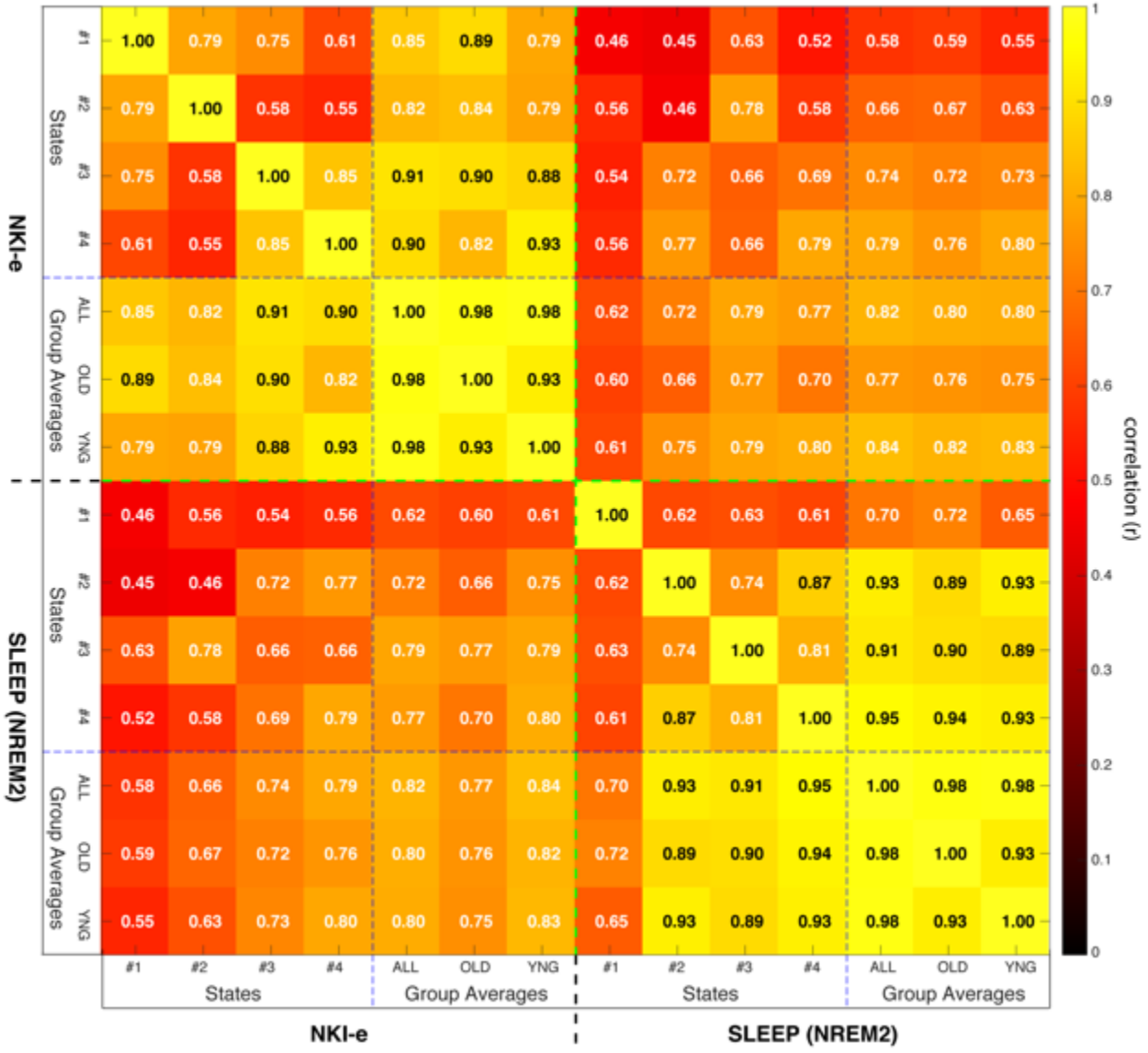

Figure 3.55. Cross-dataset correlation map for the middle temporal gyrus seed comparing both within and across NKI-e and Sleep (NREM2) datasets. A color-coded, Pearson correlation coefficient is listed for all comparisons between each mean *brain state* map and group average maps for all, old and young subjects. The green dashed lines separate the two datasets and highlight the four quadrants of the correlation map; the black dashed lines divide the *brain state* data from the Group Averages.

Unlike the other seed regions, we did not observe a greater correlation between the older and younger cohort group average maps in the NKI-e dataset as compared to the Sleep (NREM2) dataset (0.93 vs 0.93; Figure 3.55, Upper-left and bottom-right panels).

Following the hierarchical clustering procedure (Ward's criterion) to both datasets on the correlations between each window map and all the other window maps, we established a similarity matrix (Figure 3.56, left panel). We assigned four States from this procedure (Figure 3.56, right panel). We found the cluster for MTG#1 (NKI-e) dataset to be smaller than the other comparably sized clusters, while in the Sleep (NREM2) dataset, we observed three main clusters, with one additional cluster (MTG#1) driven by little data.

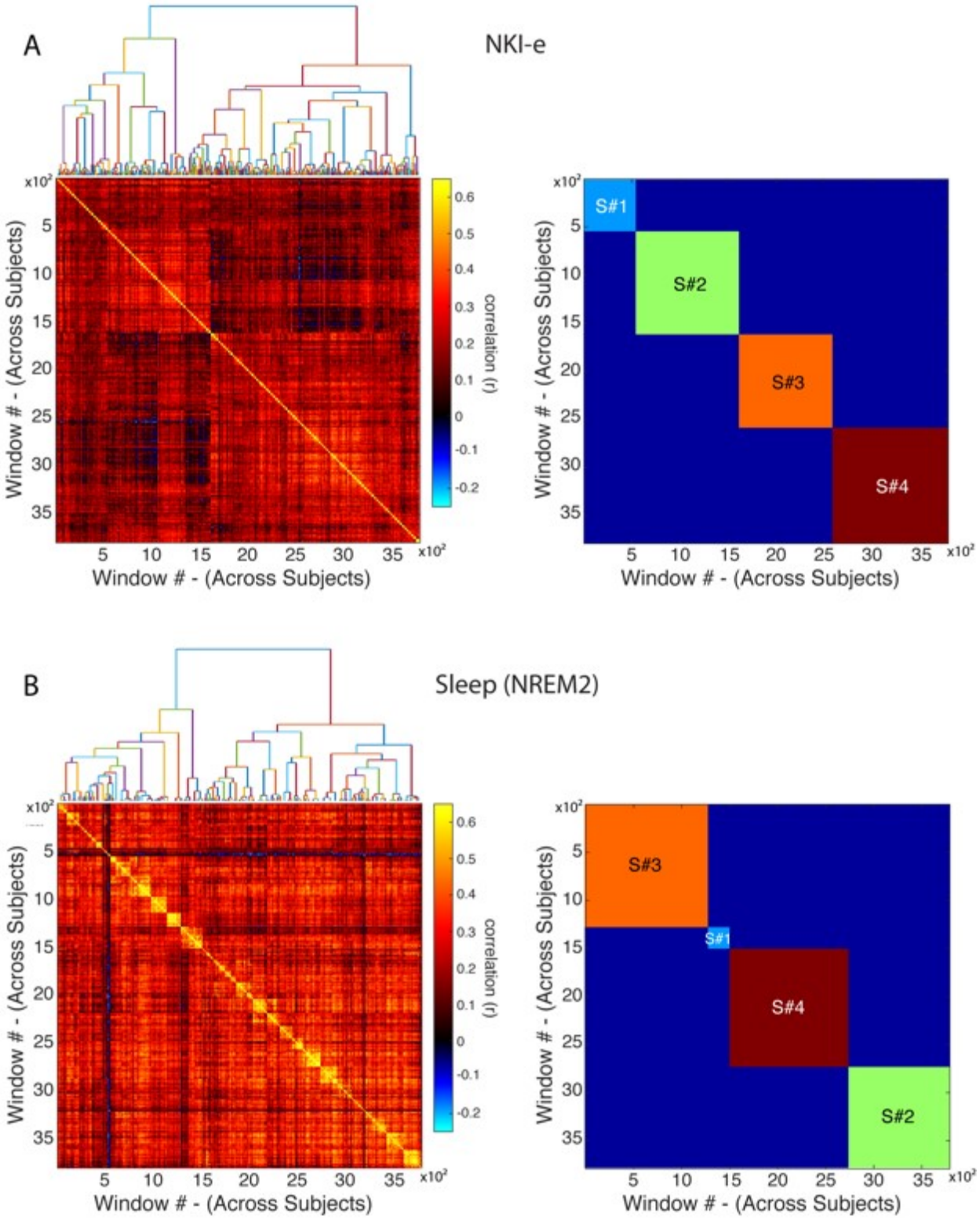

Figure 3.56. A) Hierarchical clustering in the NKI-e dataset. Left: Similarity matrix: Hierarchical clustering of the correlation of each window map to all other window maps across all subjects

under Ward's criteria. Each window map represents the connectivity between the middle temporal gyrus seed to the entire brain. The dendogram is shown above the similarity matrix. Right: The clusters defined by the selection of four *brain states*. The numbers listed (i.e.: S#1, S#2, etc.) refer to the State numbers referenced in the text. B) Same as in A) for the Sleep dataset during NREM2.

As previously described, we computed the probability of spending time in a given state for each cohort (Figure 3.57), followed by evaluating the distribution of the window maps by *brain state*, across subjects and cohorts (Figure 3.58).

In the NKI-e dataset we observed that the probability of spending time in three of the *brain states* was significantly different between cohorts (Figure 3.57, left panel). Old subjects spent more time in MTG#1 (NKI-e) and MTG#3 (NKI-e) ($p<0.05$ and $p<0.01$, respectively), while MTG#4 (NKI-e) had significantly more young subjects than old subjects associated with it ($p<0.001$).

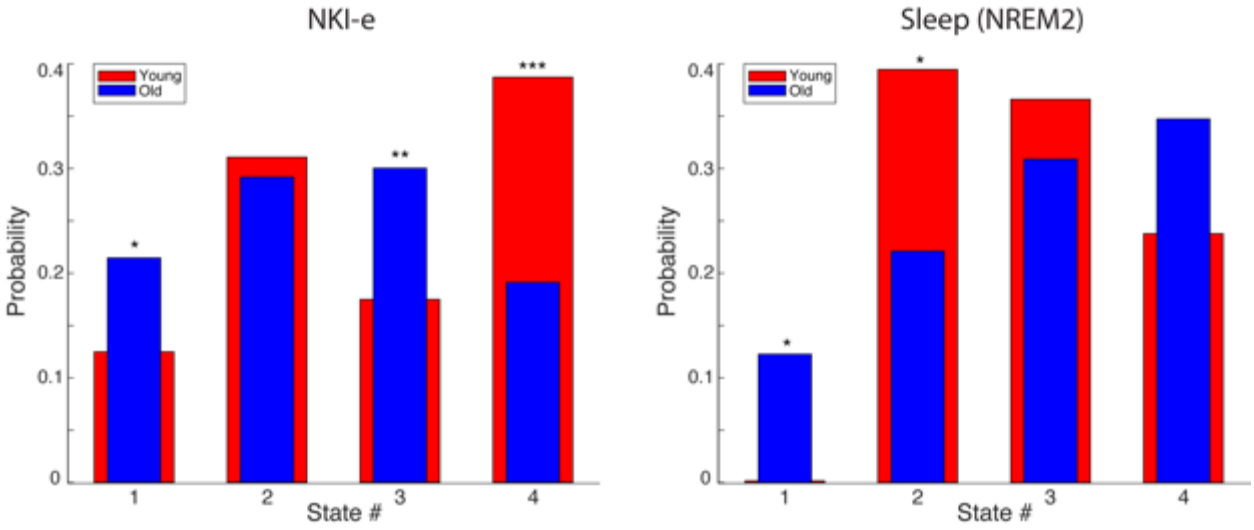

Figure 3.57. Probability of time spent in a *brain state* for young (red) and old (blue) cohorts computed for the middle temporal gyrus seed in the NKI-e dataset (left) and the Sleep (NREM2) dataset (right). Significance was assessed using permutation tests (n=100,000; * $p<0.05$, ** $p<0.01$, *** $p<0.001$).

In the Sleep (NREM2) dataset, although MTG#1 was associated significantly more with old subjects than younger subjects ($p<0.05$, Figure 3.57, right panel), it was driven by a single older subject (Figure 3.58.C and D) and was not representative of other older subjects when comparing states (Figure 3.55). The clustering of the Sleep (NREM2) dataset fell essentially into three States. Of these three remaining States, we only observed a significant association in MTG#2 (NREM2) to young subjects ($p<0.05$).

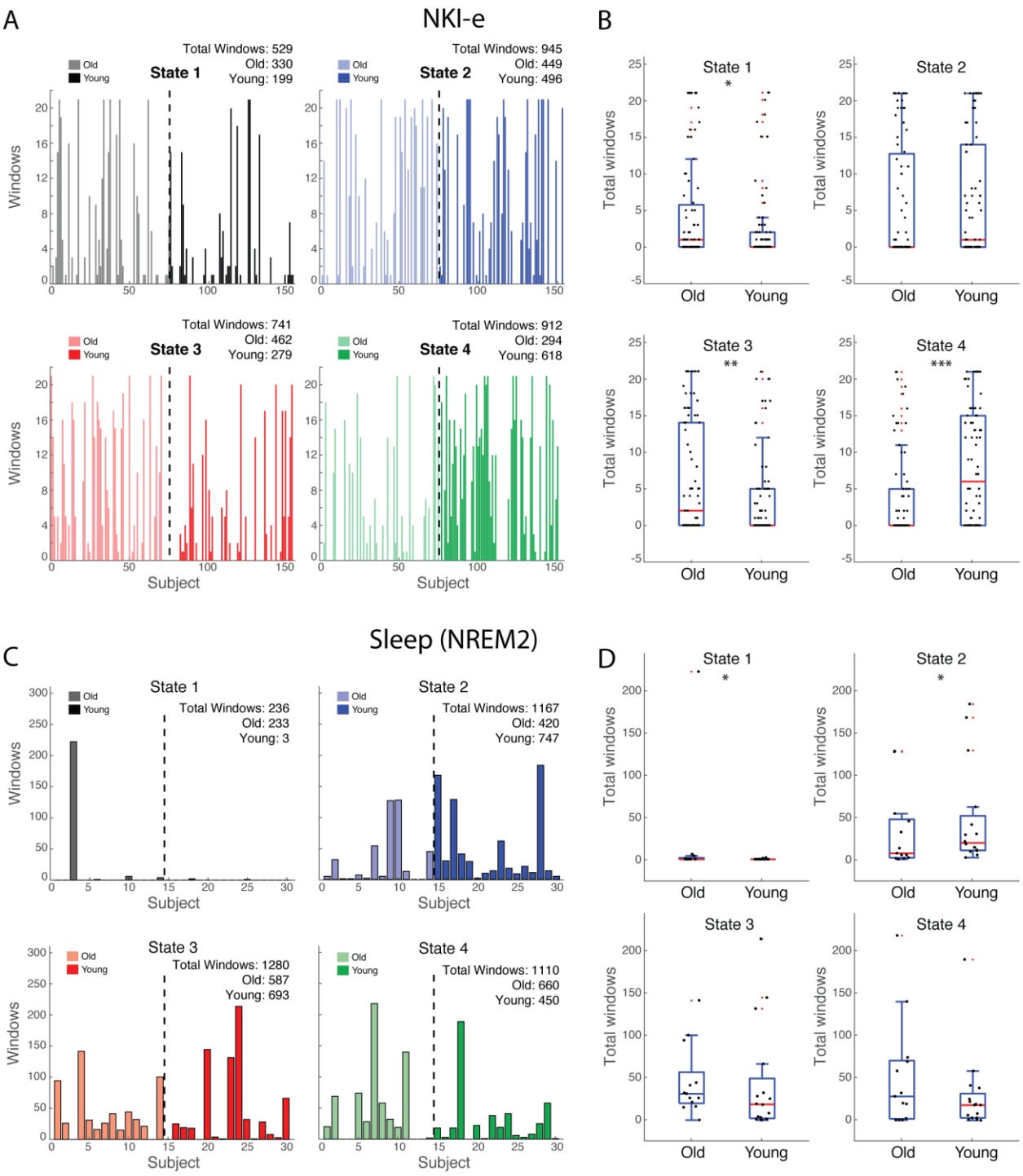

Figure 3.58. Distribution of window maps by *brain state* and cohort in the middle temporal gyrus seed. A) The number of window maps that are most correlated to the given *brain state* by subject for the NKI-e dataset. The dashed line demarcates the older and younger cohorts, with the older cohort to the left of the dashed line. B) Corresponding boxplots show the distribution of the number of windows for each subject associated with the given *brain state*, by cohort. C) and D)

The same as in A) and B) for the Sleep (NREM2) dataset. Significance was assessed using permutation tests (n=100,000; * $p<0.05$, ** $p<0.01$, *** $p<0.001$).

We show the brain maps derived from the middle temporal gyrus seed, for the resting-state subjects in the NKI-e dataset and the sleeping subjects (NREM2) in the Sleep dataset in Figure 3.59. A more extensive explanation of organization of the figure is described in the posterior cingulate cortex section (Figure 3.44).

In MTG#4 (NKI-e), we found reduced correlation to most brain regions, however, there was a higher correlation to the DMN, and within the middle temporal gyrus itself, as compared to the average correlation across all subjects in the NKI-e dataset (Figure 3.59). We likewise observed an increase in connectivity within the middle temporal gyrus, as compared to the group average, in the young cohort of the Sleep (NREM2) dataset as compared to the average correlation across all subjects in the Sleep dataset. Further, in MTG#2 (NREM2), we observed comparable reductions in correlation to most brain regions, but with smaller increases in connectivity to some DMN regions, as compared to the average.

In MTG#2 (NKI-e), we found a slightly reduced correlation to the DMN as compared to the average across all subjects, while there was an increase to other regions, excluding the cerebellum, which showed a greater reduction in correlation as compared to the average. In MTG#3 (NREM2), there was a similar pattern, however, there was only a slightly reduced correlation to the cerebellum, as compared to the average across subjects in the Sleep (NREM2) dataset. The correlation to the DMN was slightly greater than the average, but less than to the other regions.

In summary, we observed the greatest correlation to the Sleep (NREM2) dataset from MTG#4 (NKI-e). The *brain state* was comprised of significantly more young than old subjects ($p<0.05$). The strongest inter-dataset correlation we found from MTG#4 (NKI-e)

was with the young sleep cohort (0.80) in the Sleep (NREM2) dataset. We also observed a higher correlation to MTG#2 (NREM2) (0.77), which comprised significantly more young subjects ($p<0.05$) and MTG#4 (NREM2) (0.79), which had no significant difference in cohort composition ($p=0.142$), than the other state comparisons.

In MTG#2 (NKI-e) and MTG#3 (NREM2), in which we found a greater correlation to one another than in other inter-State comparisons, we observed no difference in the distribution by cohort ($p=0.653$ and $p=0.316$, respectively).

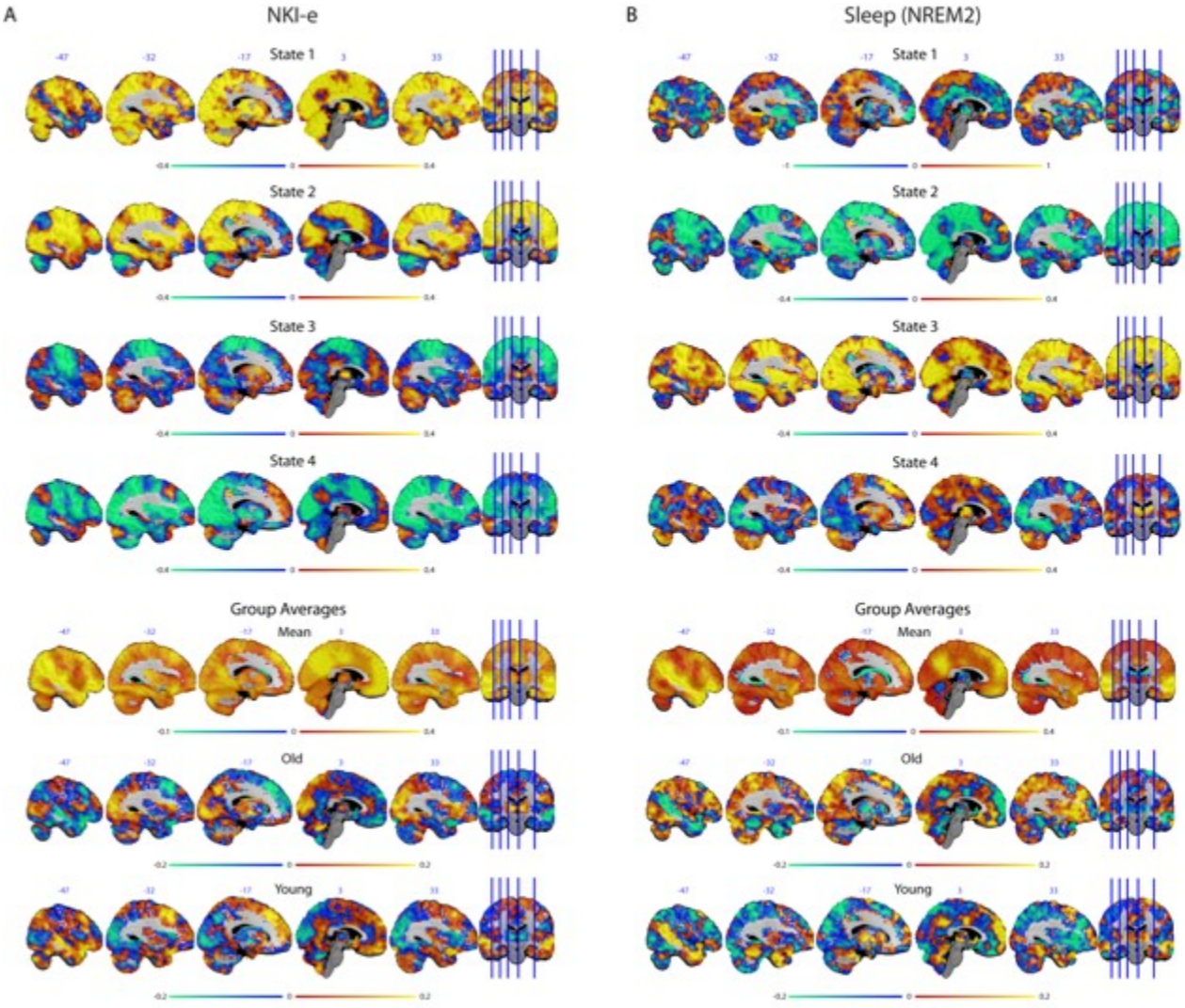

Figure 3.59. Brain connectivity maps between the middle temporal gyrus seed and the entire brain in (A) the NKI-e dataset and (B) the Sleep (NREM2) dataset. The upper four rows show z-maps

of each *brain state* relative to the average voxel-wise connectivity depicted in the fifth row ("Mean"). The bottom two rows illustrate the z-maps of the connectivity in the older and younger cohorts, respectively.

Finally, we observed a relatively high correlation in the inter-dataset comparison of Group Averages (Mean from each NKI-e dataset group average across all Sleep (NREM2) dataset group averages: NKI-e, All – 0.807; Old – 0.76; Young – 0.83).

3.4.2.5. Summary:

In this preliminary, exploratory analysis we compared *brain states* across datasets. Age and sex were matched in cohorts across datasets, from an eyes-open resting-state procedure and an EEG-validated NREM2 sleep procedure in the scanner. There were *brain states* from the resting-state scan that correlated to the sleep data more than others. These tended to be associated with the younger cohort. The *brain state* PCC#3 (NKI-e) correlated most with PCC#4 (NREM2), while young subjects spent significantly more time in both these *brain states*, than did the older subjects. The relationship across datasets was difficult to discern from the MTG seed region. The TC#3 (NREM2) *brain state* was significantly associated with older subjects. It displayed greater connectivity to DMN regions than the rest of the brain. In the resting-state procedure this *brain state* was most associated with TC#4 (NKI-e), likewise characterized by more connectivity to DMN regions than the rest of the brain. We observed a pattern of equal or more correlation between old and young group average connectivity profiles during wakefulness, than during sleep. This raises the possibility more age-related differences may be detected during sleep. This analysis is preliminary and requires further investigation with EEG-monitoring during the resting-state. Despite numerous limitations our basic hypotheses were satisfied.

Chapter 4

4 Discussion

We explored functional connectivity differences in resting-state and sleep data between young and old subjects, using both static and dynamic analysis of fMRI brain networks. Through the dynamic approach, we were able to identify heterogeneity within cohorts. The data-driven method allowed us to delineate subgroups of older subjects that explained essentially all of the significant functional connectivity variability between the old and young cohorts in both the resting-state and sleep dataset. We identified possible compensatory pathways, to explain high thought content scores of older subjects. We also observed sub-significant connectivity profiles that associated significantly with either old or young subjects. These observations may provide a basis to identify new imaging biomarkers of heterogeneous aging pathways that previously would be overlooked. Finally, we demonstrated that our methods are transferable across datasets, to relate different *brain states* to cohort connectivity patterns.

4.1. Heterogeneity and aging

In the resting-state and aging study, we centred our attention on establishing a suitable approach to questions of aging and heterogeneity. Our focus was on two seed regions (PCC and mPFC) sensitive to age-related changes in connectivity [2]. The overall decrease in connectivity we observed from these seed regions (Figure 3.2), when comparing young and old cohorts with static connectivity, is consistent with other studies in aging [2]. We

then applied a data-driven dynamic analysis based on hierarchical clustering of data, and discovered *brain states* that preferentially associated with older or younger subjects. Further, we delineated subgroups within the older cohort by connectivity profiles that displayed contrasting aging effects. One subgroup of older subjects presented almost no significant aging effect compared to young subjects, whereas from the other equal-sized subgroup we found significant aging effects that were more widespread than described in the literature [1].

It has been consistently shown and understood that there is a significant deterioration in connectivity in older populations, as compared to young [2, 23]. The fact that we could explain essentially all the variability between the age cohorts, by delineating the older cohort into two equally sized subgroups was more profound than we anticipated. This meant that approximately half the older sample displayed no significant connectivity differences with the younger cohort. To explain this type of heterogeneity, two overlapping concepts have commonly been described in the literature: successful aging and cognitive reserve.

The concept of successful aging, as opposed to usual aging, has been discussed in the literature for decades [128]. Within this framework, the effects of aging are less impactful when factors under a person's control, such as diet, exercise and other lifestyle habits are cultivated effectively. Poor diet and nutrition are believed to lead to a decline in cognitive performance [129], in particular when there is an insufficient intake of vitamins [130, 131]. That exercise may have an impact on cognitive performance has been observed in studies in aging for both short and long-term exercise regimens [132, 133]. This relationship has likewise been observed between aerobic exercise and resting-state connectivity, with significant increases in connectivity seen in older subjects that exercise [134]. As a result, according to this theory, aging leads to strong heterogeneous outcomes impacted by controllable factors governed largely by life choices [128]. Based on this, we would

conclude that the delineation we observed between those showing no significant connectivity differences with the younger cohort, and those with widespread significant connectivity differences would follow different behavioral or life habits. Due to the structure of the study, we could not correlate measures of life choices with our results, thus we can make no definitive claim how representative the theory is of our observations. Likewise, there is currently insufficient epidemiological data to estimate the prevalence of successful aging in the population [135], thus we cannot confirm whether the distribution of our results is consistent with this model for aging. We would propose that measures that focus on these factors be included in future studies.

This concept has led to recent interest in studies of neurodegeneration [136]. The objective of these studies is to identify neural characteristics of so-called superagers that differentiate them from characteristics of normal (or usual) aging. Superagers in this case, however, have been defined as older subjects that perform on par with younger subjects in memory and cognitive testing [135], meaning a direct link to lifestyle behaviours is left unexplored. For example, studies have found brain areas of superagers show significant differences in connectivity within the DMN and salience network (SN) during resting-state to subjects that age normally, while no significant differences were observed within these networks when compared to younger subjects [137]. Although these results are compatible to our own, the basis for these observations is unclear. Other studies have extended the use of successful aging to include subjects that suffer from MCI and AD to further differentiate the neural characteristics specific to superagers [136-139].

The issue in these studies is whether the continued youthful cognitive performance observed in superagers (or successful aging) is a result of a brain that maintains its structure and function through life choices, hereditary or other means; or rather better performance results through effective compensatory brain mechanisms that hide underlying deterioration [140]. This latter concept of compensatory brain mechanism is

often referred to as cognitive reserve. It was first introduced to account for older individuals that were found to have significant neurodegeneration typical of Alzheimer's disease post-mortem, without showing any clinical symptoms before death [141]. The idea of cognitive reserve has been explored in the course of normal aging, as well as in relation to neurodegeneration. This has been performed using various methods (global connectivity, network topology, EEG, etc.) to characterize cognitive reserve in older subjects [140, 142, 143] and through resting-state measures [140, 144].

If a compensatory model better captures the basis for successful aging, we would expect connectivity differences between successfully aging older subjects and younger subjects that reflect the development and utilization of different pathways of cognition [144]. This is complicated by the need for a post-mortem examination to fully account for possible deterioration, in relation to possible cognitive reserve [145]. Despite extensive research, no studies have effectively established the relationship between theorized cognitive reserve and an improved brain efficiency [146]. In our results (see 3.3. Thought Content), however, we do observe age-related differences in the lateral temporal lobe that may underlie a compensatory pathway. Older subjects with high thought content scores displayed higher connectivity from this brain region than the younger subjects, potentially supporting a cognitive reserve theory.

In contrast to this possible example of cognitive reserve we found no specific relationship with the subgroups of older subjects, to scores measuring intelligence using the Wechsler Abbreviated Scale of Intelligence (WASI-II, [147]). Overlapping somewhat with successful aging, an individual's capacity to develop cognitive reserve is believed to be impacted by education, occupational status and the Intelligence Quotient (IQ), among other factors [146].

Another factor that could be linked to our observations through the BOLD measures and perhaps underlying the concepts of successful aging or compensatory reserve, is cardiovascular health. This comprises variations in cerebral blood flow and cerebrovascular reactivity with age [82]. Cerebral blood flow (CBF) is an important factor in resting-state, since the measure of activity is directly related to deoxygenated hemoglobin in the blood. It is wholly possible that the divisions we are finding between age groups may bear some relationship to differential CBF and the resultant levels of connectivity and activity. The impact of differential CBF on connectivity and performance has previously been observed [148, 149]. A differential cerebral blood flow due to age [150] is also potentially associated with cognitive decline and neurodegeneration [151]. A relationship between cerebral blood flow changes in aging appear to depend in part on vascular factors [150], along with other factors that may be related to neurodegeneration [152]. Supporting these heterogeneous aging concepts (successful aging), exercise notably has an impact on cerebral blood flow as measured by arterial spin labelling [153]. To investigate the relationship of cerebral blood flow to our results, we propose future studies to include arterial spin labelling flow as an appropriate measure [150].

4.2. Characterization of *brain states*

The PCC and mPFC are primary hubs of the DMN. Based on past studies, we expected a significant connectivity difference between these posterior and anterior regions [1, 2, 23]. As we also expected, through both clustering analyses a *brain state* (PCC#4 and mPFC#3) emerged that largely characterized the connectivity associated with the DMN. This featured higher connectivity to DMN regions and lower connectivity to other brain regions as compared to the average connectivity throughout the scan. During the resting-state scan individuals spent about 40% of the time in this *brain state*; measured from both the PCC and mPFC seeds. Young subjects, however, spent more time in the DMN state

compared to older subjects measured from both seeds. When computed from the PCC seed region this difference was significant. The time spent in the DMN may be a reasonable indicator of aging effects at both a group and an individual level.

It was, however, through the connectivity profile of *brain state* mPFC#4 that we could effectively delineate the older cohort into successful and usual aging categories. The subjects' connectivity profiles that most highly correlated with mPFC#4 displayed the greatest loss in DMN connectivity, as compared to the young. We found that overall older subjects spent significantly more time in the mPFC#4 *brain state*, as compared to younger subjects. This represented slightly less than 40% of the total time spent by older subjects in all states, while younger subjects spent only 10% of their time in this state. This *brain state* most notably showed a reduced connectivity relative to the default-mode network activity usually found during resting-state procedures and an increase, relative to the average connectivity across all subjects, between the occipital lobe and the mPFC seed region (see Figure 3.5.B.).

These observations are consistent both with decline expected through natural aging [1], as well as in studies of neurodegeneration [154]. Less has been examined in relation to the visual cortex and the increase in connectivity we observed there. Small age-related decreases in connectivity from the visual cortex, however, have previously been noted [37]. Studies that have found increases in connectivity in relation to aging have explained these results through compensatory activity [37]. Compliance may also be a factor in our observations. We will discuss this further (see 4.4. Thought content and aging), however, simply closing the eyes can cause variations in brain activity and connectivity with the visual cortex and other regions [155-158]. Since this resting-state procedure included asking subjects to keep their eyes open while focusing on a fixation cross [95], any cohort-wide difference in compliance may have resulted in connectivity differences to the visual cortex.

The discrepancy found between time spent in the DMN (mPFC#3) as compared to in mPFC#4 – the *brain state* associated with subjects that drove the age-related differences – may provide a potential marker for successful aging. This, and simply identifying time spent in the DMN state, as potential markers is a notable improvement over standard static connectivity analysis, where no heterogeneity can be identified. It is plausible, that even before there is a significant decline in connectivity that is measurable through static methods, a decrease in time spent in a typical DMN *brain state* (mPFC#3), or other potentially pathological state (e.g. mPFC#4), may be assessed at a subject level. This is viewed as key to future aging and clinical studies [22]. Notably, this may also allow us to identify sub-significant connectivity differences as potential bio-markers. A connectivity profile may be significantly associated with a given cohort, even when the differences between connectivity profiles are not significant. Thus, by using specific *brain states*, or prototypical connectivity profiles for a given quality (e.g. age-related decline, neuropathologies, other clinical measures), we can correlate a subject's connectivity patterns to a set of connectivity profiles. This underscores a subtle yet important difference in the future for potentially identifying early subject-level bio-markers for diagnostic purposes.

Here too, our findings may be explained through concepts of cognitive reserve, or successful aging, or an intersection of both. We observed the preservation of connectivity pathways in an older sub-cohort that does not differ significantly from the younger subjects that could support a successful aging explanation. By contrast, in a subsequent section on thought content (see 4.4. Thought content and aging) we observe a potential compensatory pathway in older subjects with high thought content scores that could support cognitive reserve as an underlying mechanism. There are not, however, sufficient measures related to either theory to confirm their applicability to our observations. We did attempt to identify factors that may explain the differences we found in the older sub-

cohorts. Of these, we explored age, sex, intelligence, emotional measures, and movement in the scanner. Even before correction for multiple comparisons, we found no significant impact from any of these factors.

Previous work has delineated heterogeneity in older populations over 85 years [32], but our study is the first to use a dynamic method of analysis to successfully delineate the heterogeneity in an old population beginning at a relatively younger age (>65 years). This confirms that heterogeneity can be observed already at this age, and likely younger still. This work naturally lends itself to expand on current work focused on identifying early biomarkers of neurodegeneration [6, 7]. Confirmatory studies, along with additional psychometric analysis (cognitive based studies), behavioural measures and cerebral blood flow assessment, are necessary to validate our findings and explore other factors that may characterize the basis for the important connectivity differences we identified.

4.3. Sleep and aging

When we examined data from old and young subjects during NREM2 sleep, we discovered important age-related differences in both our static and dynamic connectivity analyses. In the static analysis, we observed significantly lower connectivity from the thalamus-caudate seed to regions of the cerebellum in the older cohort, as compared to the young (Figure 3.13). This supports our hypothesis that there are significant connectivity differences between older and young adult subjects during sleep. To our knowledge this has not previously been measured using fMRI connectivity analyses. This observation is important in relation to resting-state analysis. It reinforces our premise that not only does sleep need to be a consideration during the procedure, but also the age of the participants. This is in addition to different age-related propensities to sleep, and the duration and sleep-stage variations within sleep.

The reduced connectivity in older subjects between the cerebellum and the thalamus-caudate seed region is consistent with the literature that exists. The cerebellum does play a role in sleep, although it is poorly understood [159]. When the cerebellum does not function as expected, sleep-wake cycle perturbations [159] and other sleep disorders may arise [160]. The cerebellum has also been identified as an important source of activity during slow-wave sleep [161]. As part of the dynamic analysis, we found a relationship between some *brain states* and slow-wave sleep density. When cohorts were combined we found a correlation between time spent in the *brain state* TC#4 and slow-wave sleep density (Figure 3.22.A). Younger subjects likewise spent significantly more time in this *brain state*. The connectivity to the cerebellum in this *brain state* is generally more than the average across all subjects, based on the static connectivity results. There are, however, inherent differences in slow-wave sleep densities observable between old and young populations, with greater densities found in younger subjects, as compared to older subjects [111]. As a result, the relationship between slow-wave sleep and TC#4 may in part arise due to the distribution of subjects in the state, or vice-versa the distribution of subjects in the state may be a result of slow-wave sleep. It is therefore unclear whether the reduced connectivity between thalamus-caudate seed region and the cerebellum is ultimately related to the slow-wave sleep seen in the TC#4 *brain state*.

In our dynamic analysis, we discovered a *brain state* from the thalamus-caudate seed region that essentially only comprised two older subjects who spent time in the state. Notably, when we removed these subjects from the static analysis, we no longer observed any age-related significant differences in connectivity. By contrast, removing two other older subjects that best matched the sleep and movement characteristics of these subjects maintained the significant age-related differences we previously observed. Although the sample size of this dataset was much smaller than that used in our resting-state analysis, in both cases we were able to identify a sub-group of older subjects that explained the variation in age-related connectivity differences we observed in the static connectivity

analysis. As in our previous resting-state analysis, exploring the dynamic connectivity changes using our data-driven method we were able to delineate the sleep results into *brain states* that were associated significantly with either old or young subjects, and sub-cohorts thereof. This demarcation into age-related *brain states* was more pronounced in the NREM2 sleep data.

In contrast to resting-state, while in NREM2 it was the older subjects that spent significantly more time in a *brain state* (TC#3) that displayed the most connectivity to the DMN network. In fact, from the TC seed region older subjects spent over 40% of their time in this state, while younger subjects spent less than 10% of their time in this state. Although this result is perhaps unsurprising considering older subjects have been described as sleeping less deeply than younger subjects [35], and more likely to switch between sleep stages [36], it is important to note that our analysis is exclusive to NREM2. Thus, this result implies that even while exclusively in a verified NREM2 sleep stage, significantly more of the older subjects display traits more typical of wakeful-rest than do younger subjects.

Supporting this observation, we found a similar result as part of the cross-dataset comparison (see 3.4.2.1. Posterior cingulate cortex) from the PCC seed region. During NREM2 sleep, one *brain state* that significantly associated with the older subjects was characterized by patterns that most resembled DMN association (PCC#1), as compared to the other *brain states*. The other *brain state* significantly associated with the older cohort was characterized by a higher connectivity throughout the brain (PCC#3; see Figure 3.5.A). These *brain states* were most correlated with *brain states* during wakeful rest that were significantly associated with the younger cohort (PCC#3 in NKI-e), and one (PCC#4 in NKI-e) that most resembled a typical DMN connectivity profile (see Figure 3.44). Together, this supports the premise that not only do the older subjects sleep less deeply (enter deeper sleep stages less than younger subjects), but within a given sleep stage,

comparatively, may experience it less deeply. In the case of NREM2, this may underlie differences that are seen in the quantity of sleep-related activity, such as k-complexes, sleep spindles and some slow-wave sleep densities [36]. This raises the interesting prospect that the connectivity differences observed between wakefulness and NREM2 sleep, may largely be a function of these sleep-related dynamics and activity. Thus, older subjects may experience NREM2 more closely to wakefulness – in the context of brain dynamics – than a younger subject that experiences a greater density of typical sleep-related activity (i.e. k-complexes, sleep spindles, etc.).

In the INS#4 *brain state*, in which widespread higher connectivity was observed from the insula seed region throughout the brain, older subjects spent a significantly greater amount of time (just under 60%) in this state than did the younger subjects (just over 5%). In the awake brain widespread high connectivity has been related to lower levels of arousal [162]. The dispersion of connectivity may in the future be an interesting measure to differentiate low arousal and activity from brain dynamics in the sleeping brain. The *brain state* (TC#4) that showed a correlation with slow-wave density, generally had a higher connectivity throughout the brain than the average. This was particularly observed in the parietal and occipital lobes, including the motor cortex. In TC#2, the *brain state* representative of the two older subjects that drove the significant differences, for the most part we observed the inverse connectivity relationships to TC#4.

An important result from our analysis of the sleep data, is that we did not find any significant differences between the old and young subjects during NREM2 utilizing the insula seed region. During the dynamic analysis, however, we did identify *brain states* (INS#3 and INS#4) which were associated more with young or old cohort subjects respectively. To highlight this, younger subjects spent approximately 90% of their time in INS#3, whereas older subjects only spent a little over 20% of their time in this *brain state*. By contrast, older subjects spent almost 60% of their time in INS#4, while in younger

subjects it only accounted for less than 10% of their time. As we noted in our analysis of the resting-state data, this type of sub-threshold connectivity observations may nonetheless represent important group differences that have practical application in early identification of biomarkers of illness or other group differences.

There are various limitations in this study. The sample size limits our ability to generalize beyond our observations. To appreciate whether reduced cerebellar connectivity is a consistent age-related result, a greater sample size would be necessary. Further investigation and confirmatory studies would be of benefit. The subjects were sleep deprived before entering the scanner. This permits subjects to sleep more readily in the scanning environment, however, this can have an impact on neural activity [163] and connectivity measures [164], as compared to baseline. This, or likewise the sample size, may have an impact on the increased age-related differences we observed, as compared to the resting-state study. Our older cohort may realistically be considered middle-aged, thus the degree of identifiable age-related differences is notable. Due to the technical challenges of competing measuring systems (EEG and fMRI), however, we were unable to acquire reliable k-complex or sleep spindle activity. In future studies technical adjustments to avoid confounds in these frequency bands would be of interest to link this activity to the derived *brain states*.

Age-related sleep differences have been described using different methods, yet to our knowledge this is the first time they have been characterized using an EEG/fMRI procedure. We found significant differences in connectivity and different characteristic *brain states* between the old and young. We did anticipate this finding due to different densities of activity during NREM2 sleep, however, the demarcations were stronger than we expected. These findings will be of particular importance for age-related resting-state studies. In this regard, any techniques designed to automatically identify sleep in resting-state [40], age-related parameters, features of interest and heterogeneity would require

special attention. A relationship between electrical activity has been shown in some studies, but the relationship between EEG activity and fMRI has only begun to be established [71, 72]. The fact that we identified *brain states* that were specific to old and young subjects, as we found in the resting state analysis supports the premise that coupling exists between EEG and fMRI measures, as previously noted in EEG [36]. Likewise, the possible relationship we observed between slow-wave sleep densities and the TC#4 *brain state*, derived through our dynamic analysis, suggests this method can provide a more comprehensive characterization of such associations. The distinct age-related demarcations we observed between *brain states* supports the use of fMRI sleep studies as an alternative strategy to identify biomarkers sensitive to early connectivity variations in aging populations.

4.4. Thought content and aging

When we investigated the thought content of spontaneous mind wandering during the scan procedure, we observed a strong, albeit expected [46] relationship between scores for past and future thought content. We found significantly higher future thought content scores in the young cohort, than in the older subjects. Higher past thought content scores were similarly observed in the younger subjects than in the older cohort, however, this was not significant (Figure 3.26.A). Despite a previous non-finding in the literature [63], due to the age-related thought content score differences, we had anticipated a possible main effect of past or future thought content scores on connectivity. From our static analysis on our seed regions (MTG and STG), however, we found no significant main effect (Figure 3.27). By contrast, when we examined the interaction effect of age and thought content on connectivity through static analysis, we did find significant differences from both seed regions in relation to past content, but not future thought content scores (Figure 3.27). From the MTG, we observed significant increases in connectivity to the occipital and parietal cortices. We likewise observed a significant

increase in connectivity to the visual cortex – in the calcarine sulcus and the lingual gyrus – from the STG seed region.

To explore further. we performed a dynamic analysis and found an association between thought content scores and the MTG#1 *brain state*, along with an interaction between age and thought content associated with additional *brain states*. When we differentiated high and low past content scores, we observed significantly more subjects with low- than high-content scores in MTG#1. Older subjects, however, spent significantly more time (~12%) than younger subjects (<3%) in this *brain state*. When we considered the interaction between age cohort and thought content scores, we found that older subjects with high content, in both past and future thought, spent significantly more time in MTG#4 and significantly less time in MTG#1. There was no significant difference between thought content scores in MTG#1 for the younger subjects, suggesting the original association with content scores was driven by the older cohort. Notably, older subjects with low content scores were evenly distributed for the time spent in each MTG *brain state*. This implies the differences we observed were driven by older subjects that maintained high thought content scores. The MTG#4 *brain state* was characterized by a lower connectivity to the DMN regions, but higher connectivity to other regions including the occipital lobe, when compared to the average across all subjects.

By contrast, younger subjects with high content scores spent the most time in MTG#3, in which there was a more typical DMN profile, with high connectivity to the DMN and lower connectivity to other regions. The younger cohort spent significantly more time in this *brain state* than did subjects from the older cohort. In MTG#1, the *brain state* significantly associated with older subjects with low content scores, there was a reduced connectivity throughout the brain. When we analysed the data from the STG seed region, older subjects with high past content scores spent significantly more time in the STG#4 *brain state* than did older subjects with low past content scores (Figure 3.35.B). This *brain*

state was characterized by a higher connectivity throughout the brain, as compared to the average (Figure 3.32.B).

By considering the dynamic results and the connectivity differences when averaged across age and high or low content scores, we found the variance in connectivity was explained through a cross-over (qualitative) interaction between age and the thought content scores. Thereby, the younger cohorts displayed comparatively lower connectivity from the seed regions to other brain regions than the older subjects when they scored highly for past and future thoughts and vice-versa for low content scores. Thus, in older subjects, when thought content scores were higher, the connectivity also increased.

There are a few possibilities that may explain these results. One is that older subjects compensate locally, requiring more effort to maintain equivalent thought content, and thus maintain higher connectivity to achieve the same result. In a study using near-infrared spectroscopy to measure hemodynamic effects of tasks on old and young adults, the authors likewise observed opposing effects in young versus older adults and compensation by older adults to attain similar performance outcomes [149]. Our observations from the STG#4 that displayed a higher connectivity throughout the brain for older subjects could support this interpretation. Yet, this does not fully explain our finding that younger subjects have a higher connectivity associated with lower thought content scores and vice-versa for low connectivity.

An intriguing possibility to explain the inverted results we found in the old and young could result from compensatory pathways. In other words, it could be related to differential recruitment of these regions for processing past or future thinking. In previous studies, older subjects were found to incorporate the medial and lateral regions of the temporal lobe more than younger subjects when mentally elaborating autobiographical memories [47]. The premise that older subjects may use this as a

compensatory pathway is also supported by our observation that older subjects with high content scores displayed a lower connectivity to the DMN and higher connectivity to other brain regions, while younger subjects with high content scores tended to maintain the expected connectivity to the DMN. Hence, this observation may underlie, and be indicative of cognitive reserve, whereby subjects that age successfully are recruiting these different brain pathways to achieve the same or similar scores as the younger subjects. The younger subjects by contrast utilize the expected DMN pathway, explaining the apparently contradictory cross-over interaction. Thus, it is not that younger subjects are necessarily accessing memories with less neural activity, rather, the focus of the neural underpinnings of their mentation may be elsewhere, following different pathways in the brain.

Questions of compliance to the scan instructions and vigilance are likewise important considerations. Compliance in this context is specific to keeping the eyes open while focused on a fixation cross, as requested during the procedure. Even though resting state is considered to be task-free, an eyes open or eyes closed instruction, along with the compliance to it, can have an impact on connectivity [157]. This is particularly the case if simple compliance to the instructions may vary between cohorts. Numerous studies have found different connectivity patterns based on whether the eyes are open, or closed [155-158], which may have an unintended effect on this analysis.

Beyond eye closures, drifting between wakefulness and sleep can likewise have an effect on connectivity for subjects that are rested, as well as sleep deprived [42]. As we have described sleep can also lead to differential connectivity profiles. Young subjects sleep more easily than older subjects [35], and when asleep we have already found that younger and older subjects appear to display significantly different connectivity patterns. A portion of subjects (10 – 30% by published estimates) will experience a loss of vigilance and drift in and out of sleep during the scan [39].

A direct connection from the temporal to the occipital lobe has been described [165], which may account for the significant age-related connectivity differences found between the visual cortex and both temporal lobe seeds. Little in the literature describes how the connectivity between these regions may vary based on eyes open or closed, however, studies have looked at variations between the visual cortex and the thalamus. For example, the eyes open on a fixation cross condition, as compared to eyes closed, leads to reduced BOLD activity in both the visual cortex and thalamus [156, 166], and likewise overall lower connectivity between the two regions [158]. This, however, can vary depending on the specific visual and thalamic regions [156]. Measures of alpha power through EEG, associated to the thalamus and visual cortex, likewise show an increase in the alpha band [167] and in connectivity with eyes closed [158].

As part of our cross-dataset analysis we examined the results from the thalamus seed region. Utilizing these results to compare connectivity to that described in eyes open or closed scenarios, we found an equivocal impact. Wang et al. linked connectivity states in fMRI to the state of vigilance, using degree of eyelid closure as a proxy measure [168]. They found that changes in functional connectivity were associated with arousal; an observation that has been recently outlined [162]. In contrast to other studies that measured connectivity to the thalamus, there was a reduced connectivity (when interpreting anti-correlation as described here [169]) between the visual network and the DMN when eyes were closed, as compared to when open [168]. In our analysis, this would support younger subjects having their eyes closed more than the old.

Without combined EEG measures in the resting-state study, however, we are not in a position to confidently assess vigilance or compliance. Since older subjects generally have a more difficult time sleeping the scanner, and different connectivity profiles when they do sleep, as a minimum a video camera should be installed to observe the subject for

compliance. An interesting consideration, beyond variations in connectivity that may result from compliance is how light sleep may impact self-reported thought content. As subjects may not even realize they have slept in the scanner, the thought content may unexpectedly be rich in detail, or similarly less detailed due to forgetfulness. There are no studies to our knowledge that have characterized these possible differences, however, dream-like thoughts, while not actually asleep as confirmed by EEG recordings, have been characterized [170]. Relating wakefulness and vigilance to spontaneous thought generation by age may prove a fruitful avenue of research.

In a study that looked at the relationship between connectivity and spontaneous mind-wandering measured with a post-scan questionnaire, a decrease in connectivity between the superior temporal gyrus and the right-caudate was found for subjects that spent more time in a thought domain [61]. This is complementary to our observations, however, it is unclear how their thought content measures correspond to our scores of past and future thought. An earlier study with the NKI-e dataset, utilizing subjects between 18 and 60 years, explored spontaneous mind-wandering during the resting-state scan using other methods [53]. The study was not focused on age-related differences, but they did find that older subjects reported greater specificity of thoughts. In addition, they found that greater future thought scores resulted in greater heterogeneity in regions of the occipital lobe. Thoughts that were more vague resulted in greater homogeneous activity in the visual cortex and heterogeneous activity in the medial occipital cortex. Some of the heterogeneity may be age-related, as we have observed in our analysis. In particular, this may result from the strong connectivity differences we observed in the occipital lobe when testing for the interaction between thought content and age. The vague thoughts and homogeneous activity found in the visual cortex, may likewise relate to possible periods of sleep, assuming subjects that sleep would provide less detailed descriptions of their thoughts. This interpretation supports our concern that vigilance and compliance are factors that need to be assessed in future studies.

An important limitation in our analysis is the degree to which subjects, in particular when older, may forget their thoughts when responding to the post-scan questionnaire. This may simply strengthen connectivity differences that we already observe between older subjects with higher and lower thought content scores, but the potential impact requires further investigation. Specific cognitive tests, such as the *Logical Memory* subtest of the Wechsler Memory Scale [171], may serve as an important control measure in this regard. Further, the NYC-Q may not fully reflect important aspects of thought content specific to older subjects. Questions that explore nostalgia and sentimentality [172], along with agency over one's life [173], may align well with preoccupations of older subjects.

Difficulty truly assessing thought content and the corresponding dynamics exist both with probes during the scan that disrupt what one attempts to measure [168], along with post-scan questionnaires that may suffer from distorted memory attributions. Treating thought content as a nuisance factor may allow us to better tease apart the factors impacting changes in connectivity through age [59]. The interaction of age, thought content and possible differences resulting from compensatory pathways in distributed seed regions, however, along with cohort heterogeneity requires a clearer understanding before including thought content as a covariate [64].

Our findings merit further investigation. If the lateral temporal lobe regions form a basis for compensatory pathways, this suggests there is potential to utilize this information to better identify early biomarkers. It remains to be seen whether such biomarkers would best identify early elements of cognitive decline or a basis for successful aging through compensatory pathways. If these temporal pathways are not compensatory in nature, then the increase in connectivity may likewise provide a point of entry to uncover other compensatory regions.

4.5. *Brain state* Transitions

As part of our dynamic analysis, we considered state transition frequencies relative to age and thought content. We also measured the overall frequency of state transitions by cohort and the mean connectivity relative to the transition type. We did find a consistency between the state transitions and the cohorts most associated with the given *brain state*. That is to say, a cohort that spent significantly more time in a given *brain state*, also tended to transition out of the state significantly less than subjects from the other cohort. Likewise, there was a tendency for subjects from the cohort to transition significantly more often to the *brain state* in which they spent significantly more time.

For example, the PCC#4 *brain state* was characterized by connectivity patterns that most closely represents DMN activity. Younger subjects spent significantly more time than older subjects in this state, and accordingly they tended to transition out of the state significantly less than older subjects. Likewise, in mPFC#4, where older subjects spent significantly more time than younger subjects, they also transitioned significantly less from this state than did the younger subjects. The younger subjects transitioned significantly more from this state to mPFC#1, where they spent significantly more time, than did the older subjects. Similar results were found in the sleep dataset analysis.

These observations are noteworthy. A difference in the time spent in a *brain state* may simply be representative of the propensity to enter a *brain state* in the first place. The differing transition frequencies, however, provide support to the underlying dynamic basis for these results, and the dynamic quality of the fMRI data.

The overall frequency of switching, conversely, did not show any particular consistency and seemed largely dependent on the seed region. During wakefulness there was no difference between old and young with the PCC or mPFC and STG as seed regions, while

from the MTG region older subjects switched states significantly less than younger subjects. By contrast, during sleep we found the older subjects transitioned significantly more when measured from the INS seed region and significantly less from the TC region. In an aging study that looked at young populations, there was likewise no association found between the frequency of switching states and age [76]. We would tend to interpret any differences in transition frequency with caution. It appears that the transition frequency had more of a relationship to the underlying *brain states*, than an overall attribute of age. Thus, an association between age and transition frequencies was best observed through the time spent in the *brain states*.

This was also true of cohorts delineated by content score, taking age into consideration, as well as independent of age. We found no significant differences in overall transition frequencies, except in the older group from the STG seed. In this case, the low content score group transitioned significantly more than the high content group.

The relationship between mean connectivity and state transitions, likewise was inconsistent overall. In our results, we did find relationships, however the mean connectivity would often be significantly higher in subjects that remained in a given state, while significantly lower in another state. In an aging study, they did find some associations to dynamic connectivity states [76], however, we found the strength of the mean connectivity for subjects remaining in the state was largely defined by the characteristic connectivity of the *brain state*. Thus, a *brain state* with a generally lower connectivity displayed a greater likelihood of lower mean connectivity for subjects that remained in the state, and vice-versa for higher connectivity. This did not seem to be impacted by the age cohort that spent significantly more time in the given *brain state*. This is an important consideration for studies that look at transitions across the entire time series. It suggests the subgroupings of low and high connectivity may provide more information to the dynamics than overall observations.

Our analysis is limited by the short duration of the resting-state scan and the limited sample size in the sleep dataset. Although there were sufficient datapoints for the analysis, an increased power and number of transition points would help validate our observations.

4.6. Cross-dataset comparison

Lastly, as a preliminary analysis, we compared *brain states* across datasets. We matched age groups and utilized data from the eyes-open resting-state procedure and compared this to data from EEG-validated NREM2 sleep in the scanner. We did find a correspondence between datasets for *brain states* associated with the same age cohort. Likewise, we observed that *brain states* associated with the younger cohort, along with the average *brain state* of the young cohort itself, showed greater correspondence between the resting-state and sleep datasets, than those of older cohorts.

For example, the PCC#3 *brain state* from NKI-e resting-state procedure correlated most with PCC#4 from the NREM2 sleep dataset. Young subjects spent significantly more time in both these states than did the older subjects. The connectivity profile found in PCC#3 (NKI-e) displayed a pattern that may be indicative of periods of sleep, while in resting-state. As compared to the average across all subjects, there was less connectivity to the DMN regions and more connectivity across other regions of the brain, excluding the thalamus. This suggests an overall dispersion of connectivity throughout the brain, as we would anticipate during sleep [90]. Since we expect younger subjects to show a greater facility to sleep in the scanner [34], this result was expected and adds credibility to our analysis.

The relationship between datasets was less differentiable when looking at connectivity from the MTG seed region. Since the MTG is not related to sleep processes, we did not anticipate any specific relationships to be uncovered. From the insula seed region, we did find a stronger relationship between specific *brain states* (INS#2 in NKI-e and INS#3 in NREM2 sleep) across datasets, as compared with other *brain states*. The INS#2 (NKI-e) *brain state* was similarly more correlated with the average young *brain state* from the NREM2 dataset. Although younger subjects spent more time in this *brain state* than the older cohort, the difference was not significant. This *brain state* was characterized by reduced connectivity to the occipital lobe and cerebellum as compared to the average across all subjects. Previously, increased BOLD signal and alpha power to the insula, with reductions to the occipital lobe has been observed [94]. Drowsiness has been proposed as an explanation [94] along with increased alpha power to insular regions during slow-wave sleep [174].

The strongest correlation across datasets from the thalamus-caudate seed regions was found between TC#3 (NKI-e) and TC#4 (NREM2), both *brain states* characterized by higher connectivity throughout the brain excluding portions of the cerebellum and inferior parietal lobule. Both were significantly associated with the younger subjects. Although the correlation is less, this is consistent with our comparisons from other seed regions. By contrast, the TC#3 (NREM2) *brain state* is significantly associated with older subjects. It displays greater connectivity to DMN regions than the rest of the brain (Figure 3.16.A). This *brain state* associated most with TC#4 (NKI-e), which was likewise characterized by more connectivity to DMN regions than the rest of the brain. The TC#4 (NKI-e) *brain state* was, however, associated equally with young and old subjects. Rather than evidence of sleep, this correlation may support our speculation that older subjects in NREM2 sleep display connectivity that constitutes wakeful-rest (see also 4.3. Sleep and aging).

We expected stronger correlations across datasets from the thalamus-caudate seed region to infer sleep or drowsiness during resting-state. This may be moderated, however, by the relatively longer length of the windows we used to derive the *brain states* (100sec). Short duration changes when drifting between wakefulness and sleep would be less detectable with window correlation maps comprised of wakefulness and sleep together. In the sleep analysis, we intentionally left out transition periods, in order to make a distinct NREM2 analysis. A mixed *brain state*, however, may better correlate to the resting-state results than our current analysis allows. A future analysis with a smaller window that allows mixed sleep stages may prove fruitful. Despite possible spurious auto-correlations, the majority of studies have successfully identified relevant *brain states* using shorter time windows [78]. Likewise, we have previously used a 45-second window to successfully delineate different characteristics of NREM sleep stages and mixed stages [74].

As part of the cross-dataset comparison we correlated the connectivity profiles of the old and young cohorts. An interesting pattern began to emerge, whereby the old and young cohort connectivity profiles were either equally or more correlated during wakefulness (the resting-state procedure), than during NREM2 sleep. This suggests there may be more age-related differences that are being detected during sleep, which are not observed during wakeful rest. There are a few possible explanations for this result. It is possible that age-related functional connectivity differences can simply be discerned more readily during sleep. This may also result, or be amplified, from the sleep deprivation aspect of the study procedure. Since sleep deprivation causes variations in connectivity, this may be more pronounced in older subjects [42]. The different sample sizes of the datasets may also be a factor. As a result, a larger sleep dataset would be necessary to help confirm or refute these initial observations. The possibility that connectivity measurements during sleep provide potential biomarkers more sensitive to differential aging is an intriguing consideration. This is even more pertinent considering we observed these differences

with an older cohort that was younger than in our previous analyses, ranging in age from 50 to 69 years.

This analysis is preliminary and suffers from certain limitations. Without additional measures with EEG-monitoring during the resting-state, it is difficult to fully assess and validate the relevance of our observations. Comparing results across sites may result in some error, although test-retest results across multiple sites with older subjects has shown some reliability, with the least error found from the PCC seed region [175]. In this cross-site comparison, the scanners were the same model, but there were small differences in the acquisition parameters. As with resting-state connectivity [164, 176], a lack of sleep impacts connectivity during sleep [42]. Thus, if the non-sleep-deprived subjects in the resting state scan fall asleep, it is possible their connectivity profiles during sleep would be different from those of their sleep deprived counterparts, during the same sleep stage.

4.7. Limitations

There are limitations we have discussed in our analyses that are study specific, while others can have an impact across studies. As we have mentioned, the length of our windows is greater than in most studies using dynamic connectivity and sliding windows [78]. The effectiveness of this window length has been confirmed [70] and it allowed us to avoid spurious autocorrelations [69], but resulted in certain limitations when analyzing sleep and thought content. Alternations between sleep stage or thought content shorter than the window length would result in a mixture of *brain states*. Future studies would benefit from exploring the results with a shorter time window. This would increase the number of datapoints, and likewise allow us to increase the number of *brain states*. Our choice of 4 *brain states*, reflected both the length of the time series we examined and the number of subjects in the study. By increasing the number of *brain states* it might

be possible to characterize finer variations and heterogeneity within the data. Another possible technique to increase the number of datapoints and reliable *brain states* is the sampling rate, or repetition time (TR) during the fMRI data acquisition. In our datasets we used a relatively standard TR length for the acquisition. This allowed us to better compare between datasets, however, when looking at dynamic variability a fast-sequence TR would be of interest.

We approached our analysis with discrete age groupings, rather than across the lifespan. As described above, the limited number of brain states we used to characterize differences in our populations, would be insufficient to capture the variability throughout the lifespan. Although age-related decline has been described as a gradual linear process [177], our own previous results and other studies suggest a step-wise, non-linear deterioration that occurs in middle- and very old-age periods [28, 178]. Future studies spanning young adulthood to old age could complement our results. We would anticipate heterogeneous aging trajectories that nonetheless intersect with corresponding brain states at cross-sections along the lifespan.

As we have discussed it is unclear the impact cerebral blood flow may have on our analyses. In order to address these concerns, we recommend future studies include arterial spin labeling measures [150]. Another age-related confound we did not add as a covariate in our analyses was motion in the scanner. Since motion in the scanner increases with age, it may also limit our ability to detect other factors that explain the age-related variance [82]. To address this limitation, we tested for motion differences between cohorts in each analysis. Although we found this was not a significant factor in the results, it would be of interest to include motion as a covariate in future studies. As with most fMRI studies, and considering the heterogeneity in the older population, a greater sample size will be of benefit. Further, successfully completed cognitive and behavioural measures

are essential for future studies, to ascertain a relationship between those measures and the connectivity profiles we identify.

Chapter 5

5 Conclusion

In this body of work, we identified cohort level heterogeneity using data-driven methods. This allowed us to delineate sub-cohorts that explained the age-related variance we observed during wakeful-rest and NREM2 sleep connectivity. The significant differences in connectivity we found between the age cohorts, during NREM2 sleep, has not been described previously in fMRI studies. Further, we identified possible compensatory pathways that older subjects, who measured highly in thought content scores, utilized during resting-state spontaneous cognition.

The consequential delineation of sub-significant connectivity profiles that nonetheless show significant association by age cohort may equally be of importance. These findings may be representative of important age-related differences before they reach typical significance by other methods. In addition to differentiating cohort level heterogeneity, our methods will allow for an evaluation at the individual level. We can correlate the relationship of an individual's *brain state* connectivity profile to specific group averages or prototypical states. This deserves further investigation, and could have practical use in elucidating underlying disease or neurodegenerative mechanisms, as well as, provide a statistical basis for individual diagnostic profiling of subjects through prototypical connectivity mappings.

Our results further support the use of dynamic connectivity analyses to elucidate the relationship between functional connectivity measures and aging. Despite clear

advantages to using a dynamic connectivity framework to analyze the resting-state data, we did find it advantageous to preserve a static analysis. The static analysis acted as a benchmark for the more extensive dynamic investigation and provided a framework to aid with the interpretation of our results. Our results also highlight the importance of accounting and controlling for sleep during all resting-state procedures.

Based on recent findings, our analysis methods may be transferable to task-based fMRI in addition to resting-state analysis [179]. There is potential to use our methods as a tool with widespread application to identify bio-markers in neurodegeneration, psychiatric and neurological disorders [78]. Neuroimaging data analysed from a data-driven perspective using regions of interest as a primary starting point [180], combined with behavioural and psychometric data to establish subject-level profiles, is the current driving force in the field [22]. Our methods provide a basis to continue to address these questions.

References

1. Andrews-Hanna, J.R., et al., *Disruption of large-scale brain systems in advanced aging.* Neuron, 2007. **56**(5): p. 924-35.

2. Wu, J.T., et al., *Aging-related changes in the default mode network and its anti-correlated networks: a resting-state fMRI study.* Neurosci Lett, 2011. **504**(1): p. 62-7.

3. NIAK. Available from: http://niak.simexp-lab.org/.

4. Smetanin, P., et al., *Rising tide: the impact of dementia in Canada 2008 to 2038.* Alzheimer Society, Canada, 2009.

5. Hedden, T. and J.D. Gabrieli, *Insights into the ageing mind: a view from cognitive neuroscience.* Nat Rev Neurosci, 2004. **5**(2): p. 87-96.

6. Orban, P., et al., *Subtypes of functional brain connectivity as early markers of neurodegeneration in Alzheimer's disease.* bioRxiv, 2017: p. 195164.

7. Dansereau, C., et al., *A brain signature highly predictive of future progression to Alzheimer's dementia.* arXiv preprint arXiv:1712.08058, 2017.

8. Chetelat, G., et al., *Amyloid imaging in cognitively normal individuals, at-risk populations and preclinical Alzheimer's disease.* Neuroimage Clin, 2013. **2**: p. 356-65.

9. Chen, P.Y., et al., *Heterogeneous Aging Effects on Functional Connectivity in Different Cortical Regions: A Resting-State Functional MRI Study Using Functional Data Analysis.* PLoS One, 2016. **11**(9): p. e0162028.

10. Mufson, E.J., et al., *Braak staging, plaque pathology, and APOE status in elderly persons without cognitive impairment.* Neurobiol Aging, 2016. **37**: p. 147-153.

11. Ogawa, S., et al., *Brain magnetic resonance imaging with contrast dependent on blood oxygenation.* Proc Natl Acad Sci U S A, 1990. **87**(24): p. 9868-72.

12. Logothetis, N.K., *The underpinnings of the BOLD functional magnetic resonance imaging signal.* J Neurosci, 2003. **23**(10): p. 3963-71.

13. Ekstrom, A., *How and when the fMRI BOLD signal relates to underlying neural activity: the danger in dissociation.* Brain Res Rev, 2010. **62**(2): p. 233-44.

14. Bellec, P., et al., *Identification of large-scale networks in the brain using fMRI.* Neuroimage, 2006. **29**(4): p. 1231-43.

15. Biswal, B., et al., *Functional connectivity in the motor cortex of resting human brain using echo-planar MRI.* Magn Reson Med, 1995. **34**(4): p. 537-41.

16. Raichle, M.E., *Two views of brain function.* Trends Cogn Sci, 2010. **14**(4): p. 180-90.

17. Yeo, B.T., et al., *The organization of the human cerebral cortex estimated by intrinsic functional connectivity.* J Neurophysiol, 2011. **106**(3): p. 1125-65.

18. Meindl, T., et al., *Test-retest reproducibility of the default-mode network in healthy individuals.* Hum Brain Mapp, 2010. **31**(2): p. 237-46.

19. Raichle, M.E., et al., *A default mode of brain function.* Proc Natl Acad Sci U S A, 2001. **98**(2): p. 676-82.

20. Greicius, M.D., et al., *Default-mode network activity distinguishes Alzheimer's disease from healthy aging: evidence from functional MRI.* Proc Natl Acad Sci U S A, 2004. **101**(13): p. 4637-42.

21. Buckner, R.L., J.R. Andrews-Hanna, and D.L. Schacter, *The brain's default network: anatomy, function, and relevance to disease.* Ann N Y Acad Sci, 2008. **1124**: p. 1-38.

22. Dubois, J. and R. Adolphs, *Building a Science of Individual Differences from fMRI.* Trends Cogn Sci, 2016. **20**(6): p. 425-43.

23. Damoiseaux, J.S., et al., *Reduced resting-state brain activity in the "default network" in normal aging.* Cereb Cortex, 2008. **18**(8): p. 1856-64.

24. Buckner, R.L., et al., *Molecular, structural, and functional characterization of Alzheimer's disease: evidence for a relationship between default activity, amyloid, and memory.* J Neurosci, 2005. **25**(34): p. 7709-17.

25. Fox, M.D., et al., *The human brain is intrinsically organized into dynamic, anticorrelated functional networks.* Proc Natl Acad Sci U S A, 2005. **102**(27): p. 9673-8.

26. Tomasi, D. and N.D. Volkow, *Aging and functional brain networks.* Mol Psychiatry, 2012. **17**(5): p. 471, 549-58.

27. Geerligs, L., et al., *A Brain-Wide Study of Age-Related Changes in Functional Connectivity.* Cereb Cortex, 2015. **25**(7): p. 1987-99.

28. Dickinson, P., et al. *Age related changes in resting-state connectivity: A connectome-wide association study*. in *Organization for Human Brain Mapping*. 2012. Beijing, China.

29. Betzel, R.F., et al., *Changes in structural and functional connectivity among resting-state networks across the human lifespan.* Neuroimage, 2014. **102**: p. 345-357.

30. Betzel, R.F., et al., *Generative models of the human connectome.* Neuroimage, 2016. **124**(Pt A): p. 1054-1064.

31. Biswal, B.B., et al., *Toward discovery science of human brain function.* Proc Natl Acad Sci U S A, 2010. **107**(10): p. 4734-9.

32. Eavani, H., et al., *Capturing heterogeneous group differences using mixture-of-experts: Application to a study of aging.* Neuroimage, 2016. **125**: p. 498-514.

33. Fan, Y. and C. Davatzikos. *Pattern recognition of functional brain networks*. in *Acoustics, Speech and Signal Processing (ICASSP), 2017 IEEE International Conference on*. 2017. IEEE.

34. Carskadon, M.A. and W.C. Dement, *Normal human sleep: an overview.* Principles and practice of sleep medicine, 2005. **4**: p. 13-23.

35. Crowley, K., *Sleep and sleep disorders in older adults.* Neuropsychol Rev, 2011. **21**(1): p. 41-53.

36. Pace-Schott, E.F. and R.M. Spencer, *Age-related changes in the cognitive function of sleep*, in *Progress in brain research*. 2011, Elsevier. p. 75-89.

37. Ferreira, L.K. and G.F. Busatto, *Resting-state functional connectivity in normal brain aging.* Neurosci Biobehav Rev, 2013. **37**(3): p. 384-400.

38. Horovitz, S.G., et al., *Decoupling of the brain's default mode network during deep sleep.* Proc Natl Acad Sci U S A, 2009. **106**(27): p. 11376-81.

39. Tagliazucchi, E. and H. Laufs, *Decoding wakefulness levels from typical fMRI resting-state data reveals reliable drifts between wakefulness and sleep.* Neuron, 2014. **82**(3): p. 695-708.

40. Tagliazucchi, E., et al., *Automatic sleep staging using fMRI functional connectivity data.* Neuroimage, 2012. **63**(1): p. 63-72.

41. Wang, J., et al., *Improving the Test-Retest Reliability of Resting State fMRI by Removing the Impact of Sleep.* Front Neurosci, 2017. **11**: p. 249.

42. Ong, J.L., et al., *Co-activated yet disconnected-Neural correlates of eye closures when trying to stay awake.* Neuroimage, 2015. **118**: p. 553-62.

43. Buckner, R.L., F.M. Krienen, and B.T. Yeo, *Opportunities and limitations of intrinsic functional connectivity MRI.* Nat Neurosci, 2013. **16**(7): p. 832-7.

44. Fell, J., *Unraveling inner experiences during resting state.* Front Hum Neurosci, 2013. **7**: p. 409.

45. Levine, B., et al., *Aging and autobiographical memory: dissociating episodic from semantic retrieval.* Psychol Aging, 2002. **17**(4): p. 677-89.

46. Schacter, D.L., D.R. Addis, and R.L. Buckner, *Remembering the past to imagine the future: the prospective brain.* Nat Rev Neurosci, 2007. **8**(9): p. 657-61.

47. Addis, D.R., R.P. Roberts, and D.L. Schacter, *Age-related neural changes in autobiographical remembering and imagining.* Neuropsychologia, 2011. **49**(13): p. 3656-69.

48. Baird, B., J. Smallwood, and J.W. Schooler, *Back to the future: autobiographical planning and the functionality of mind-wandering.* Conscious Cogn, 2011. **20**(4): p. 1604-11.

49. Stawarczyk, D., et al., *Mind-wandering: phenomenology and function as assessed with a novel experience sampling method.* Acta Psychol (Amst), 2011. **136**(3): p. 370-81.

50. Addis, D.R., A.T. Wong, and D.L. Schacter, *Remembering the past and imagining the future: common and distinct neural substrates during event construction and elaboration.* Neuropsychologia, 2007. **45**(7): p. 1363-77.

51. Andrews-Hanna, J.R., et al., *Functional-anatomic fractionation of the brain's default network.* Neuron, 2010. **65**(4): p. 550-62.

52. Hurlburt, R.T., et al., *What goes on in the resting-state? A qualitative glimpse into resting-state experience in the scanner.* Frontiers in psychology, 2015. **6**: p. 1535.

53. Gorgolewski, K.J., et al., *A correspondence between individual differences in the brain's intrinsic functional architecture and the content and form of self-generated thoughts.* PLoS One, 2014. **9**(5): p. e97176.

54. Delamillieure, P., et al., *The resting state questionnaire: An introspective questionnaire for evaluation of inner experience during the conscious resting state.* Brain Res Bull, 2010. **81**(6): p. 565-73.

55. Diaz, B.A., et al., *The Amsterdam Resting-State Questionnaire reveals multiple phenotypes of resting-state cognition.* Front Hum Neurosci, 2013. **7**: p. 446.

56. Kuhn, S., et al., *Inner experience in the scanner: can high fidelity apprehensions of inner experience be integrated with fMRI?* Front Psychol, 2014. **5**: p. 1393.

57. Kucyi, A. and K.D. Davis, *Dynamic functional connectivity of the default mode network tracks daydreaming.* Neuroimage, 2014. **100**: p. 471-480.

58. Christoff, K., et al., *Experience sampling during fMRI reveals default network and executive system contributions to mind wandering.* Proc Natl Acad Sci U S A, 2009. **106**(21): p. 8719-24.

59. Kucyi, A., *Just a thought: how mind-wandering is represented in dynamic brain connectivity.* NeuroImage, 2017.

60. Fox, K.C., J.R. Andrews-Hanna, and K. Christoff, *The neurobiology of self-generated thought from cells to systems: Integrating evidence from lesion studies, human intracranial electrophysiology, neurochemistry, and neuroendocrinology.* Neuroscience, 2016. **335**: p. 134-50.

61. Chou, Y.H., et al., *Maintenance and Representation of Mind Wandering during Resting-State fMRI.* Sci Rep, 2017. **7**: p. 40722.

62. Andrews-Hanna, J.R., et al., *Evidence for the default network's role in spontaneous cognition.* J Neurophysiol, 2010. **104**(1): p. 322-35.

63. Mevel, K., et al., *Age effect on the default mode network, inner thoughts, and cognitive abilities.* Neurobiol Aging, 2013. **34**(4): p. 1292-301.

64. Doucet, G., et al., *Patterns of hemodynamic low-frequency oscillations in the brain are modulated by the nature of free thought during rest.* Neuroimage, 2012. **59**(4): p. 3194-200.

65. Chang, C. and G.H. Glover, *Time-frequency dynamics of resting-state brain connectivity measured with fMRI.* Neuroimage, 2010. **50**(1): p. 81-98.

66. Allen, E.A., et al., *Tracking whole-brain connectivity dynamics in the resting state.* Cereb Cortex, 2014. **24**(3): p. 663-76.

67. Hindriks, R., et al., *Can sliding-window correlations reveal dynamic functional connectivity in resting-state fMRI?* Neuroimage, 2016. **127**: p. 242-256.

68. Handwerker, D.A., et al., *Periodic changes in fMRI connectivity.* Neuroimage, 2012. **63**(3): p. 1712-9.

69. Leonardi, N. and D. Van De Ville, *On spurious and real fluctuations of dynamic functional connectivity during rest.* Neuroimage, 2015. **104**: p. 430-6.

70. Gonzalez-Castillo, J., et al., *Tracking ongoing cognition in individuals using brief, whole-brain functional connectivity patterns.* Proc Natl Acad Sci U S A, 2015. **112**(28): p. 8762-7.

71. Chang, C., et al., *EEG correlates of time-varying BOLD functional connectivity.* Neuroimage, 2013. **72**: p. 227-36.

72. Tagliazucchi, E., et al., *Dynamic BOLD functional connectivity in humans and its electrophysiological correlates.* Front Hum Neurosci, 2012. **6**: p. 339.

73. Damaraju, E., et al., *Dynamic functional connectivity analysis reveals transient states of dysconnectivity in schizophrenia.* Neuroimage Clin, 2014. **5**: p. 298-308.

74. Dickinson, P., et al. *Age-related dynamic functional connectivity states during sleep*. in *Organization for Human Brain Mapping*. 2014. Hamburg, Germany.

75. Faghiri, A., et al., *Changing brain connectivity dynamics: From early childhood to adulthood.* Hum Brain Mapp, 2018. **39**(3): p. 1108-1117.

76. Hutchison, R.M. and J.B. Morton, *Tracking the Brain's Functional Coupling Dynamics over Development.* J Neurosci, 2015. **35**(17): p. 6849-59.

77. Resnick, S.M., et al., *One-year age changes in MRI brain volumes in older adults.* Cereb Cortex, 2000. **10**(5): p. 464-72.

78. Preti, M.G., T.A. Bolton, and D. Van De Ville, *The dynamic functional connectome: State-of-the-art and perspectives.* Neuroimage, 2017. **160**: p. 41-54.

79. Raykov, Y.P., et al., *What to do when K-means clustering fails: a simple yet principled alternative algorithm.* PloS one, 2016. **11**(9): p. e0162259.

80. Ou, J., et al., *Characterizing and Differentiating Brain State Dynamics via Hidden Markov Models.* Brain Topogr, 2015. **28**(5): p. 666-679.

81. Yang, Z., et al., *Common intrinsic connectivity states among posteromedial cortex subdivisions: Insights from analysis of temporal dynamics.* Neuroimage, 2014. **93 Pt 1**: p. 124-37.

82. Geerligs, L., et al., *Challenges in measuring individual differences in functional connectivity using fMRI: The case of healthy aging.* Hum Brain Mapp, 2017. **38**(8): p. 4125-4156.

83. Amzica, F. and M. Steriade, *The functional significance of K-complexes.* Sleep Med Rev, 2002. **6**(2): p. 139-49.

84. Caporro, M., et al., *Functional MRI of sleep spindles and K-complexes.* Clin Neurophysiol, 2012. **123**(2): p. 303-9.

85. Fogel, S., et al., *NREM Sleep Oscillations and Brain Plasticity in Aging.* Front Neurol, 2012. **3**: p. 176.

86. Jan, J.E., et al., *The role of the thalamus in sleep, pineal melatonin production, and circadian rhythm sleep disorders.* J Pineal Res, 2009. **46**(1): p. 1-7.

87. Coulon, P., T. Budde, and H.C. Pape, *The sleep relay--the role of the thalamus in central and decentral sleep regulation.* Pflugers Arch, 2012. **463**(1): p. 53-71.

88. Holland, A.C., D.R. Addis, and E.A. Kensinger, *The neural correlates of specific versus general autobiographical memory construction and elaboration.* Neuropsychologia, 2011. **49**(12): p. 3164-77.

89. Waring, J.D., D.R. Addis, and E.A. Kensinger, *Effects of aging on neural connectivity underlying selective memory for emotional scenes.* Neurobiol Aging, 2013. **34**(2): p. 451-67.

90. Samann, P.G., et al., *Development of the brain's default mode network from wakefulness to slow wave sleep.* Cereb Cortex, 2011. **21**(9): p. 2082-93.

91. Czisch, M., et al., *Acoustic oddball during NREM sleep: a combined EEG/fMRI study.* PLoS One, 2009. **4**(8): p. e6749.

92. Portas, C.M., et al., *Auditory processing across the sleep-wake cycle: simultaneous EEG and fMRI monitoring in humans.* Neuron, 2000. **28**(3): p. 991-9.

93. Poudel, G.R., et al., *Losing the struggle to stay awake: divergent thalamic and cortical activity during microsleeps.* Hum Brain Mapp, 2014. **35**(1): p. 257-69.

94. Goldman, R.I., et al., *Simultaneous EEG and fMRI of the alpha rhythm.* Neuroreport, 2002. **13**(18): p. 2487-92.

95. Nooner, K.B., et al., *The NKI-Rockland Sample: A Model for Accelerating the Pace of Discovery Science in Psychiatry.* Front Neurosci, 2012. **6**: p. 152.

96. Enhanced Nathan Kline Institute Rockland Sample. Available from: http://fcon_1000.projects.nitrc.org/indi/enhanced/index.html.

97. Matthews, G., et al., *Validation of a comprehensive stress state questionnaire: Towards a state big three.* Personality psychology in Europe, 1999. **7**: p. 335-350.

98. Horne, J.A. and O. Ostberg, *A self-assessment questionnaire to determine morningness-eveningness in human circadian rhythms.* Int J Chronobiol, 1976. **4**(2): p. 97-110.

99. Johns, M.W., *A new method for measuring daytime sleepiness: the Epworth sleepiness scale.* Sleep, 1991. **14**(6): p. 540-5.

100. Buysse, D.J., et al., *The Pittsburgh Sleep Quality Index: a new instrument for psychiatric practice and research.* Psychiatry Res, 1989. **28**(2): p. 193-213.

101. Beck, A.T., et al., *An inventory for measuring clinical anxiety: psychometric properties.* J Consult Clin Psychol, 1988. **56**(6): p. 893-7.

102. Steer, R.A., et al., *Further evidence for the construct validity of the Beck depression Inventory-II with psychiatric outpatients.* Psychol Rep, 1997. **80**(2): p. 443-6.

103. Mullinger, K.J., W.X. Yan, and R. Bowtell, *Reducing the gradient artefact in simultaneous EEG-fMRI by adjusting the subject's axial position.* Neuroimage, 2011. **54**(3): p. 1942-50.

104. Allen, P.J., O. Josephs, and R. Turner, *A method for removing imaging artifact from continuous EEG recorded during functional MRI.* Neuroimage, 2000. **12**(2): p. 230-9.

105. Bellec, P., et al., *The pipeline system for Octave and Matlab (PSOM): a lightweight scripting framework and execution engine for scientific workflows.* Front Neuroinform, 2012. **6**: p. 7.

106. Montreal Neurological Instititue. Available from: http://bic-mni.github.io/.

107. Guillimin. Available from: http://www.calculquebec.ca/en/resources/compute-servers/guillimin.

108. Leclercq, Y., et al., *Rejection of pulse related artefact (PRA) from continuous electroencephalographic (EEG) time series recorded during functional magnetic resonance imaging (fMRI) using constraint independent component analysis (cICA).* Neuroimage, 2009. **44**(3): p. 679-91.

109. Brunner, D.P., et al., *Muscle artifacts in the sleep EEG: automated detection and effect on all-night EEG power spectra.* J Sleep Res, 1996. **5**(3): p. 155-64.

110. Silber, M.H., et al., *The visual scoring of sleep in adults.* J Clin Sleep Med, 2007. **3**(2): p. 121-31.

111. Carrier, J., et al., *Sleep slow wave changes during the middle years of life.* Eur J Neurosci, 2011. **33**(4): p. 758-66.

112. Lafortune, M., et al., *Reduced slow-wave rebound during daytime recovery sleep in middle-aged subjects.* PLoS One, 2012. **7**(8): p. e43224.

113. Massimini, M., et al., *The sleep slow oscillation as a traveling wave.* J Neurosci, 2004. **24**(31): p. 6862-70.

114. Collins, D.C.a.E., A.C., *Animal: Validation and Applications of Nonlinear Registration-Based Segmentation.* Int. J. Patt. Recogn. Artif. Intell., 1997. **11**(08): p. 1271-1294.

115. Fonov, V., et al., *Unbiased average age-appropriate atlases for pediatric studies.* Neuroimage, 2011. **54**(1): p. 313-27.

116. Zijdenbos, A.P., R. Forghani, and A.C. Evans, *Automatic "pipeline" analysis of 3-D MRI data for clinical trials: application to multiple sclerosis.* IEEE Trans Med Imaging, 2002. **21**(10): p. 1280-91.

117. Power, J.D., et al., *Spurious but systematic correlations in functional connectivity MRI networks arise from subject motion.* Neuroimage, 2012. **59**(3): p. 2142-54.

118. Giove, F., et al., *Images-based suppression of unwanted global signals in resting-state functional connectivity studies.* Magn Reson Imaging, 2009. **27**(8): p. 1058-64.

119. NIAK-preprocessing. Available from: http://niak.simexp-lab.org/pipe_preprocessing.html.

120. Urchs, S., et al., *MIST: A multi-resolution parcellation of functional brain networks.* MNI Open Research, 2017. **1**.

121. Bellec, P., et al., *Multi-level bootstrap analysis of stable clusters in resting-state fMRI.* Neuroimage, 2010. **51**(3): p. 1126-39.

122. Dadi, K., et al. *Comparing functional connectivity based predictive models across datasets*. in *Pattern Recognition in Neuroimaging (PRNI), 2016 International Workshop on Pattern Recognition in Neuroimaging*. <*hal-01319131*>. 2016. Trento, Italy.: IEEE.

123. Casella, G. and R.L. Berger, *Statistical inference*. 2001: Duxbury/Thomson Learning.

124. Power, J.D., B.L. Schlaggar, and S.E. Petersen, *Recent progress and outstanding issues in motion correction in resting state fMRI.* Neuroimage, 2015. **105**: p. 536-51.

125. Bellec, P., et al., *Impact of the resolution of brain parcels on connectome-wide association studies in fMRI.* Neuroimage, 2015. **123**: p. 212-28.

126. Benjamini, Y., et al., *Controlling the false discovery rate in behavior genetics research.* Behav Brain Res, 2001. **125**(1-2): p. 279-84.

127. Peck, R., C. Olsen, and J.L. Devore, *Introduction to statistics and data analysis*. Edition 5. ed. 2016, Boston, MA, USA: Cengage Learning. xxix, 809 pages.

128. Rowe, J.W. and R.L. Kahn, *Human aging: usual and successful*. Science, 1987. **237**(4811): p. 143-9.

129. Miquel, S., et al., *Poor cognitive ageing: Vulnerabilities, mechanisms and the impact of nutritional interventions.* Ageing Res Rev, 2018. **42**: p. 40-55.

130. Jannusch, K., et al., *A Complex Interplay of Vitamin B1 and B6 Metabolism with Cognition, Brain Structure, and Functional Connectivity in Older Adults.* Front Neurosci, 2017. **11**: p. 596.

131. Tucker, K.L., et al., *High homocysteine and low B vitamins predict cognitive decline in aging men: the Veterans Affairs Normative Aging Study.* Am J Clin Nutr, 2005. **82**(3): p. 627-35.

132. Chapman, S.B., et al., *Shorter term aerobic exercise improves brain, cognition, and cardiovascular fitness in aging.* Front Aging Neurosci, 2013. **5**: p. 75.

133. Colcombe, S.J., et al., *Cardiovascular fitness, cortical plasticity, and aging.* Proc Natl Acad Sci U S A, 2004. **101**(9): p. 3316-21.

134. Voss, M.W., et al., *Plasticity of brain networks in a randomized intervention trial of exercise training in older adults.* Front Aging Neurosci, 2010. **2**.

135. Sun, F.W., et al., *Youthful Brains in Older Adults: Preserved Neuroanatomy in the Default Mode and Salience Networks Contributes to Youthful Memory in Superaging.* J Neurosci, 2016. **36**(37): p. 9659-68.

136. Wang, X., et al., *Longitudinal Functional Brain Mapping in Supernormals.* Cereb Cortex, 2017: p. 1-11.

137. Zhang, J., et al., *Preserved functional connectivity in the default mode and salience networks is associated with youthful memory in superaging.* bioRxiv, 2018: p. 254193.

138. Dong, L., et al., *The heterogeneity of aging brain: altered functional connectivity in default mode network in older adults during verbal fluency tests.* Chin Med J (Engl), 2012. **125**(4): p. 604-10.

139. Eyler, L.T., et al., *A review of functional brain imaging correlates of successful cognitive aging.* Biol Psychiatry, 2011. **70**(2): p. 115-22.

140. Fleck, J.I., et al., *The Impact of Age and Cognitive Reserve on Resting-State Brain Connectivity.* Front Aging Neurosci, 2017. **9**: p. 392.

141. Katzman, R., et al., *Clinical, pathological, and neurochemical changes in dementia: a subgroup with preserved mental status and numerous neocortical plaques.* Ann Neurol, 1988. **23**(2): p. 138-44.

142. Franzmeier, N., et al., *Resting-state global functional connectivity as a biomarker of cognitive reserve in mild cognitive impairment.* Brain Imaging Behav, 2017. **11**(2): p. 368-382.

143. Martínez, J.H., et al., *Functional brain networks reveal the existence of cognitive reserve and the interplay between network topology and dynamics.* arXiv preprint arXiv:1712.00462, 2017.

144. Bastin, C., et al., *Cognitive reserve impacts on inter-individual variability in resting-state cerebral metabolism in normal aging.* Neuroimage, 2012. **63**(2): p. 713-22.

145. Stern, Y. and C. Habeck, *Deriving and Testing the Validity of Cognitive Reserve Candidates*, in *Biomarkers for Preclinical Alzheimer's Disease*. 2018, Springer. p. 63-70.

146. Marques, P., et al., *The functional connectome of cognitive reserve.* Hum Brain Mapp, 2016. **37**(9): p. 3310-22.

147. Wechsler, D., *Manual for the Wechsler abbreviated intelligence scale (WASI).* San Antonio, TX: The Psychological Corporation, 1999.

148. Li, W., et al., *Changes in regional cerebral blood flow and functional connectivity in the cholinergic pathway associated with cognitive performance in subjects with mild Alzheimer's disease after 12-week donepezil treatment.* Neuroimage, 2012. **60**(2): p. 1083-91.

149. Bierre, K.L., et al., *Cognitive Difficulty Intensifies Age-related Changes in Anterior Frontal Hemodynamics: Novel Evidence from Near-infrared Spectroscopy.* J Gerontol A Biol Sci Med Sci, 2017. **72**(2): p. 181-188.

150. Gauthier, C.J., et al., *Age dependence of hemodynamic response characteristics in human functional magnetic resonance imaging.* Neurobiol Aging, 2013. **34**(5): p. 1469-85.

151. Scarapicchia, V., et al., *Resting State BOLD Variability in Alzheimer's Disease: A Marker of Cognitive Decline or Cerebrovascular Status?* Front Aging Neurosci, 2018. **10**: p. 39.

152. Zhang, N., M.L. Gordon, and T.E. Goldberg, *Cerebral blood flow measured by arterial spin labeling MRI at resting state in normal aging and Alzheimer's disease.* Neurosci Biobehav Rev, 2017. **72**: p. 168-175.

153. Smith, J.C., et al., *Detecting changes in human cerebral blood flow after acute exercise using arterial spin labeling: implications for fMRI.* J Neurosci Methods, 2010. **191**(2): p. 258-62.

154. Tam, A., et al., *Consistent inter-protocol differences in resting-state functional connectomes between normal aging and mild cognitive impairment.* bioRxiv, 2015: p. 019646.

155. Jao, T., et al., *Volitional eyes opening perturbs brain dynamics and functional connectivity regardless of light input.* Neuroimage, 2013. **69**: p. 21-34.

156. McAvoy, M., et al., *Dissociated mean and functional connectivity BOLD signals in visual cortex during eyes closed and fixation.* J Neurophysiol, 2012. **108**(9): p. 2363-72.

157. Van Dijk, K.R., et al., *Intrinsic functional connectivity as a tool for human connectomics: theory, properties, and optimization.* J Neurophysiol, 2010. **103**(1): p. 297-321.

158. Zou, Q., et al., *Functional connectivity between the thalamus and visual cortex under eyes closed and eyes open conditions: a resting-state fMRI study.* Hum Brain Mapp, 2009. **30**(9): p. 3066-78.

159. Cunchillos, J.D. and I. De Andres, *Participation of the cerebellum in the regulation of the sleep-wakefulness cycle. Results in cerebellectomized cats.* Electroencephalogr Clin Neurophysiol, 1982. **53**(5): p. 549-58.

160. Canto, C.B., et al., *The Sleeping Cerebellum.* Trends Neurosci, 2017. **40**(5): p. 309-323.

161. Dang-Vu, T.T., et al., *Spontaneous neural activity during human slow wave sleep.* Proc Natl Acad Sci U S A, 2008. **105**(39): p. 15160-5.

162. Liu, X., et al., *Subcortical evidence for a contribution of arousal to fMRI studies of brain activity.* Nat Commun, 2018. **9**(1): p. 395.

163. Kaufmann, C., et al., *Brain activation and hypothalamic functional connectivity during human non-rapid eye movement sleep: an EEG/fMRI study.* Brain, 2006. **129**(Pt 3): p. 655-67.

164. Kaufmann, T., et al., *The brain functional connectome is robustly altered by lack of sleep.* Neuroimage, 2016. **127**: p. 324-32.

165. Catani, M., et al., *Occipito-temporal connections in the human brain.* Brain, 2003. **126**(Pt 9): p. 2093-107.

166. Bianciardi, M., et al., *Modulation of spontaneous fMRI activity in human visual cortex by behavioral state.* Neuroimage, 2009. **45**(1): p. 160-8.

167. Gomez-Ramirez, J., et al., *Eyes closed or Eyes open? Exploring the alpha desynchronization hypothesis in resting state functional connectivity networks with intracranial EEG.* bioRxiv, 2017: p. 118174.

168. Wang, C., et al., *Spontaneous eyelid closures link vigilance fluctuation with fMRI dynamic connectivity states.* Proc Natl Acad Sci U S A, 2016. **113**(34): p. 9653-8.

169. Murphy, K., et al., *The impact of global signal regression on resting state correlations: are anti-correlated networks introduced?* Neuroimage, 2009. **44**(3): p. 893-905.

170. Domhoff, G.W. and K.C. Fox, *Dreaming and the default network: A review, synthesis, and counterintuitive research proposal.* Conscious Cogn, 2015. **33**: p. 342-53.

171. Wechsler, D., *Wechsler memory scale.* 1945.

172. Stoyanova, S.Y., V. Giannouli, and T.K. Gergov, *Sentimentality and Nostalgia in Elderly People in Bulgaria and Greece - Cross-Validity of the Questionnaire SNEP and Cross-Cultural Comparison.* Eur J Psychol, 2017. **13**(1): p. 109-128.

173. Claassens, L., et al., *Development and validation of a questionnaire assessing the perceived control in health care among older adults with care needs in the Netherlands.* Qual Life Res, 2016. **25**(4): p. 859-70.

174. Benca, R.M., et al., *EEG alpha power and alpha power asymmetry in sleep and wakefulness.* Psychophysiology, 1999. **36**(4): p. 430-6.

175. Jovicich, J., et al., *Longitudinal reproducibility of default-mode network connectivity in healthy elderly participants: A multicentric resting-state fMRI study.* Neuroimage, 2016. **124**(Pt A): p. 442-454.

176. Dai, X.J., et al., *Long-term total sleep deprivation decreases the default spontaneous activity and connectivity pattern in healthy male subjects: a resting-state fMRI study.* Neuropsychiatr Dis Treat, 2015. **11**: p. 761-72.

177. Grady, C.L., et al., *Age-related changes in brain activity across the adult lifespan.* J Cogn Neurosci, 2006. **18**(2): p. 227-41.

178. Kennedy, K.M., et al., *Age trajectories of functional activation under conditions of low and high processing demands: an adult lifespan fMRI study of the aging brain.* Neuroimage, 2015. **104**: p. 21-34.

179. Gonzalez-Castillo, J. and P.A. Bandettini, *Task-based dynamic functional connectivity: Recent findings and open questions.* Neuroimage, 2017.

180. Genon, S., et al., *How to Characterize the Function of a Brain Region.* Trends in cognitive sciences, 2018.